

1988

Preparative, spectroscopic and structural studies of oxidative processes involving indium(I) and tin(II) halides.

Theodore James Allotey, Annan
University of Windsor

Follow this and additional works at: <http://scholar.uwindsor.ca/etd>

Recommended Citation

Annan, Theodore James Allotey, "Preparative, spectroscopic and structural studies of oxidative processes involving indium(I) and tin(II) halides." (1988). *Electronic Theses and Dissertations*. Paper 3178.

This online database contains the full-text of PhD dissertations and Masters' theses of University of Windsor students from 1954 forward. These documents are made available for personal study and research purposes only, in accordance with the Canadian Copyright Act and the Creative Commons license—CC BY-NC-ND (Attribution, Non-Commercial, No Derivative Works). Under this license, works must always be attributed to the copyright holder (original author), cannot be used for any commercial purposes, and may not be altered. Any other use would require the permission of the copyright holder. Students may inquire about withdrawing their dissertation and/or thesis from this database. For additional inquiries, please contact the repository administrator via email (scholarship@uwindsor.ca) or by telephone at 519-253-3000ext. 3208.



National Library
of Canada

Bibliothèque nationale
du Canada

Canadian Theses Service

Service des thèses canadiennes

Ottawa, Canada
K1A 0N4

NOTICE

The quality of this microform is heavily dependent upon the quality of the original thesis submitted for microfilming. Every effort has been made to ensure the highest quality of reproduction possible.

If pages are missing, contact the university which granted the degree.

Some pages may have indistinct print especially if the original pages were typed with a poor typewriter ribbon or if the university sent us an inferior photocopy.

Previously copyrighted materials (journal articles, published tests, etc.) are not filmed.

Reproduction in full or in part of this microform is governed by the Canadian Copyright Act, R.S.C. 1970, c. C-30.

AVIS

La qualité de cette microforme dépend grandement de la qualité de la thèse soumise au microfilmage. Nous avons tout fait pour assurer une qualité supérieure de reproduction.

S'il manque des pages, veuillez communiquer avec l'université qui a conféré le grade.

La qualité d'impression de certaines pages peut laisser à désirer, surtout si les pages originales ont été dactylographiées à l'aide d'un ruban usé ou si l'université nous a fait parvenir une photocopie de qualité inférieure.

Les documents qui font déjà l'objet d'un droit d'auteur (articles de revue, tests publiés, etc.) ne sont pas microfilmés.

La reproduction, même partielle, de cette microforme est soumise à la Loi canadienne sur le droit d'auteur, SRC 1970, c. C-30.

PREPARATIVE, SPECTROSCOPIC AND STRUCTURAL STUDIES

OF OXIDATIVE PROCESSES INVOLVING

INDIUM(II) AND TIN(II) HALIDES

by

THEODORE JAMES ALLOTEY ANNAN

A DISSERTATION

Submitted to the Faculty of Graduate Studies through the

Department of Chemistry and Biochemistry in

Partial Fulfillment of the Requirements for the

Degree of Doctor of Philosophy at the

University of Windsor

Windsor, Ontario, Canada

1988

Permission has been granted to the National Library of Canada to microfilm this thesis and to lend or sell copies of the film.

The author (copyright owner) has reserved other publication rights, and neither the thesis nor extensive extracts from it may be printed or otherwise reproduced without his/her written permission.

L'autorisation a été accordée à la Bibliothèque nationale du Canada de microfilmer cette thèse et de prêter ou de vendre des exemplaires du film.

L'auteur (titulaire du droit d'auteur) se réserve les autres droits de publication; ni la thèse ni de longs extraits de celle-ci ne doivent être imprimés ou autrement reproduits sans son autorisation écrite.

ISBN 0-315-43727-8

AKV 2258

© Theodore James Allotey Annan
All Rights Reserved

1988

ABSTRACT

PREPARATIVE, SPECTROSCOPIC AND STRUCTURAL STUDIES OF OXIDATIVE PROCESSES INVOLVING INDIUM(I) AND TIN(II) HALIDES

by

THEODORE JAMES ALLOTEY ANNAN

Indium(I) halides (InX) dissolve in aromatic solvents containing certain neutral donor ligands below ca. 0°C . The simplest solute species in InBr -toluene- N,N,N',N' -tetramethylethylenediamine (tmen) has been previously formulated as $\text{InBr} \cdot \text{tmen}$. Disproportionation of InX occurs above 0°C , yielding indium metal and In^{II} or In^{III} complexes, depending on X and the neutral ligand.

The present work has shown that InX ($\text{X} = \text{Cl}, \text{Br}, \text{I}$) can oxidatively insert into the Sn-Y bond of Ph_3SnY ($\text{Y} = \text{Cl}, \text{Br}, \text{I}, \text{OAc}$) in toluene-tmen solution to give neutral tmen adducts of $\text{Ph}_3\text{SnIn(Y)X}$. Vibrational and NMR spectroscopic studies suggest that the structures contain Sn-In metal bonds, parallel to earlier work in this laboratory involving the formation of In-In bonds. Attempts to synthesize compounds containing M-In ($\text{M} = \text{Ge}, \text{Pb}, \text{P}$) under identical conditions were not successful. Reaction of InBr with Ph_2BBr afforded a product which was formulated as $(\text{Ph}_2\text{BInBr})_n$ based on analytical and spectroscopic results. A general mechanism for the formation of these insertion products is proposed.

Oxidative addition reactions of tin(II) halides with substituted orthoquinones (A = halogeno substituted type, B = alkyl substituted type) were studied. The results show that with phen as the neutral donor ligand, the products are $\text{Y}_4\text{C}_6\text{O}_2\text{SnX}_2 \cdot \text{phen}$, ($\text{Y} = \text{Br}, \text{Cl}$; $\text{X} = \text{I}, \text{Br}, \text{Cl}$) with the type-A orthoquinone being converted to the corresponding catecholato anion. Reactions

in which phen is replaced by tmen are more complex and the products depend in part on the solvent. These products include $\text{Cl}_4\text{C}_6\text{O}_2\text{SnCl}_2\cdot\text{tmen}$ and products arising from solvation by ROH ($\text{R} = \text{CH}_3, \text{C}_2\text{H}_5$). An X-ray crystallographic study of $(\text{tmenH})_2[\text{Sn}(\text{O}_2\text{C}_6\text{Cl}_4)_3]$ shows that the anion contains a six-coordinate atom bonded to substituted catecholate anions. Reactions involving type-B orthoquinones were found to be slower and could be studied by ESR spectroscopy which showed that semiquinone derivatives are intermediates in these processes. A mechanism is proposed to explain satisfactorily both preparative and ESR results in terms of two successive one-electron transfer processes. The crystal structure of bis(3,5-di-t-butyl-catecholato)tin(IV).phen.2DMF has been determined by X-ray diffraction studies. In both structures, the average Sn-O distance (2.009 Å) is typical of tin(IV) compounds, and the average C-O distance (1.336 Å) confirms that the ligand is an aromatic diolate.

Indium monohalides also add oxidatively to both types of quinone. Reactions with type-A orthoquinones in the presence of a neutral donor ligand (e.g. tmen, phen or bipy) yielded products which were, exclusively, the catecholato complexes. Metallic indium also reacts with such quinones and phen or bipy in boiling toluene in the presence of iodine, diphenyl-diselenide or diphenyl-disulphide to form the indium(III) catecholato derivatives. All compounds were characterized by ^1H and ^{13}C NMR and vibrational spectroscopy which confirmed the formulation of the products as the phen or bipy adducts of a five-coordinate indium(III) catecholato complex. With tmen the products are ionic species with the coordination of indium varying from four ($\text{X} = \text{I}$) to six ($\text{X} = \text{Br}, \text{Cl}$). Conductivity measurements of these complexes confirm their formulation as 1:1 electrolytes. Variable temperature ^{13}C NMR study on the complex $(\text{Cl}_4\text{C}_6\text{O}_2)\text{InCl}(\text{tmen})$ lend an insight into the stereochemistry around the indium atom.

Reactions between type-B orthoquinones and indium monohalides give mixtures of indium(I) and indium(III) semiquinonato complexes. Typical indium(I) and indium(III) complexes were synthesized independently and studied by ESR spectroscopy. A mechanism is offered to explain the reaction pathway of this process. The structure of one compound, dibromoindium(III) semiquinonate.bis(γ -picoline) was confirmed by X-ray crystallography. The C-O bond distance (1.26 Å) is important in formulating this compound as a semiquinonate.

Preliminary results are also presented on the reactions of indium monohalides with some transition metal complexes. The products obtained were, generally, characterized as 1:1 adducts on the basis of spectroscopic and analytical results. These results are interesting and promising. For example, the product of the reaction of InCl with $(\text{Ph}_3\text{P})_2\text{NiCl}_2$ in a toluene/tmen, is $\text{Ni}_1\text{Cl}_2\text{InCl.tmen}$ but recrystallization of this compound gave a rearrangement product whose structure as revealed by X-ray crystallography is $\text{In}[\text{Ni}_3(\mu_3\text{-O})(\mu_3\text{-Cl})(\mu\text{-Cl})\text{tmen}]$.

ACKNOWLEDGEMENTS

I consider it a great privilege to have had the opportunity to study for a post-graduate degree at the University of Windsor, particularly in the Department of Chemistry and Biochemistry. The rich experience acquired academically and socially, I believe, will be of tremendous help in the successful establishment of my future career.

Working under the guidance and supervision of Professor D.G. Tuck has not only been an honour but a worthy experience. His patience and encouragement throughout all the different stages of this work is duly acknowledged.

Special thanks to members of my committee, Drs. R.C. Rumpfolt, B.A. Keay, B.R. McGarvey, G.W.F. Drake and my external examiner Dr. J.P. Oliver (Wayne State University) for their reading and comments on this dissertation.

Past and present members of Room 362 Essex Hall are particularly thanked for their contributions in different ways to the outcome of this research project. Those of special mention are Dr. R. Kumar for valuable discussions and Ms. Cassie Watson for conducting part of the experiments in Chapter 3.

Dr. R.K. Chadha (University of Manitoba) is sincerely thanked for help in solving most of the X-ray crystallographic structures. Dr. D.W. Stephan is also thanked in this regard.

A special mention of gratitude to Drs. P.E. Doan, B.R. McGarvey and A. Ozarowski for their helpful discussions on the ESR-related work. Mr. D.H. McConville is also thanked for his experimental contribution to part of the ESR work in Chapter 6.

I am also grateful to faculty members, technical and secretarial staff and my fellow graduate students for various assistance rendered me and for their friendship during the course of my stay in the Department. Special mention of thanks to Miss Maeve Doyle for her patience and help in the preparation of this dissertation.

Outside the University community, the support and friendship of Mr. and Mrs. Harry Annan, Mrs. Irene MacKew and Mr. and Mrs. Julius Nathoo and their families is gratefully acknowledged. To my friends Alex B. Darko (Dartford, England), Akwasi A. Boateng (University of Guyana) and Mr. and Mrs. Vic Persaud (also of Guyana) I say thanks for the confidence placed in me.

Finally, I would like to thank my family, especially my sister Captain Eunice A. Annan (Ghana Armed Forces) for being so understanding and supportive.

DEDICATION

This dissertation is dedicated to
the everlasting memory of my mother
Susannah Ewuraba Stephens
and to my uncle and mentor
Daniel Ofohiquaye Annan.

TABLE OF CONTENTS

	Page
ABSTRACT	ii
ACKNOWLEDGEMENTS	v
DEDICATION	vii
LIST OF TABLES	xii
LIST OF FIGURES	xv
LIST OF ABBREVIATIONS	xvii
CHAPTER	
1 GENERAL CONSIDERATIONS	1
1.1 Introduction	1
1.1.1 Compounds of Indium(I)	1
1.1.1.1 Reactions with donor ligands	2
1.1.2 Compounds of Indium(II)	4
1.1.3 Oxidative-Addition Reactions	6
1.2 Present Work	9
1.3 Experimental Techniques	10
1.3.1 Starting Materials	10
1.3.2 Characterization of Products	11
1.3.3 X-Ray Crystallography	12
1.3.3.1 Data Collection	12
1.3.3.2 Solution and Refinement of the Structure	14
2 THE REACTION BETWEEN InX AND Ph_3SnY : THE PREPARATION OF Sn-In BONDED COMPOUNDS.	16
2.1 Introduction	16
2.2 Experimental	20
2.2.1 The Reaction of InX with Triphenyltin Compounds	20
2.2.2 Reaction of $\text{Ph}_3\text{SnInBr}_2$ with 1,2-dibromoethane	22
2.2.3 Other Systems	25

2.3 Results and Discussion	28
2.3.1 Reaction Pathway	28
2.3.2 The Structure of $\text{Ph}_3\text{SnIn(X)Y.tmen}$ Compounds	31
2.3.3 The Structure of $\text{Ph}_3\text{SnIn(OAc)X.tmen}$ Compounds	32
2.3.4 The Structure of $\text{Ph}_2\text{BinBr.tmen}$	35
2.3.5 The Reaction of $\text{Ph}_3\text{SnInBr}_2$ with $1,2\text{-C}_2\text{H}_4\text{Br}_2$: The Reactivity of Sn-In bonded compound	36
3 THE REACTION BETWEEN SnX_2 AND TETRA-HALOGENO- ORTHOQUINONES FORMATION OF Sn(IV) CATECHOLATES	
3.1 Introduction	38
3.2 Experimental	41
3.2.1 The Formation of $\text{Y}_4\text{C}_6\text{O}_2\text{SnX}_2$	41
3.3 Results and Discussion	47
3.3.1 Preparative	47
3.3.2 Spectroscopic Results	50
3.4 X-Ray Studies: The Molecular and Crystal Structure of $(\text{tmenH})_2[\text{Sn}(\text{O}_2\text{C}_6\text{Cl}_4)_3]$	55
3.4.1 Description and Discussion of the Structure	58
4 THE REACTION OF SnX_2 (X = Cl, Br, I) WITH 3,5-DI-TERT-BUTYL- 1,2-BENZOQUINONE AND 9,10-PHENANTHROQUINONE: EVIDENCE OF ONE ELECTRON TRANSFER	67
4.1 Introduction	67
4.1.1 Electron Spin Resonance Spectroscopy	68
4.2 Experimental	73
4.2.1 Preparation of Adducts of Sn^{IV} -Catecholato Compounds	73
4.2.2 Crystallographic Studies	76
4.2.3 Electron Spin Resonance Spectroscopy	88
4.3 Results and Discussion	90
4.3.1 Preparative	90
4.3.1.1 Electron Spin Resonance Spectroscopic Studies	99
4.3.2 Structural Studies	109

5 THE REACTION OF In(I) HALIDES WITH TETRAHALOGENO- ORTHOQUINONES: FORMATION OF In(III) CATECHOLATES	111
5.1 Introduction	111
5.2 Experimental	114
5.2.1 The Reaction of InX (X = Cl, Br, I) with Y ₄ C ₆ O ₂ (Y = Cl, Br)	114
5.2.2 The Reaction of InCl with Cl ₄ C ₆ O ₂ : Kinetic Studies	118
5.3 Results and Discussion	127
5.3.1 Preparative	127
5.3.2 Spectroscopy	133
5.3.3 The Reaction Mechanism	143
6 THE REACTION OF In(I) HALIDES WITH 3,5-DI-TERT- BUTYL-1,2-BENZOQUINONE AND 9,10-PHENANTHROQUINONE: FORMATION OF INDIUM(I) AND INDIUM(III) SEMIQUINONES	145
6.1 Introduction	145
6.2 Experimental	146
6.2.1 Reactions of InX (X = Cl, Br, I) with 9,10-phenanthroquinone	150
6.2.3 The Reaction of Indium Metal with 3,5-di-tert-butyl 1,2-benzoquinone: Solubility Studies	151
6.2.3.1 Oxidation by Iodine	153
6.3 Results and Discussion	153
6.3.1 Preparative	153
6.3.2 Reaction of Indium(III) Halides with TBC	155
6.3.3 Reaction of Metallic Indium with TBQ: Solubility Studies	156
6.3.4 Spectroscopic Results	160
6.4 X-ray Studies	178
6.4.1 Description and Discussion of the Structure	189
6.4.2 Mechanism	192

7 THE REACTIONS OF InX (X = Cl, Br, I) WITH SOME TRANSITION METAL COMPLEXES. THE CRYSTAL STRUCTURE OF In[Ni ₃ (μ ₃ -O)(μ ₃ -Cl)(μ-Cl) ₃ .tmen ₃]	195
7.1 Introduction	191
7.2 Experimental	196
7.2.1 The Reaction of InX (X = Cl, Br, I) with Some Transition Metal Complexes	196
7.3 Results and Discussion	196
7.3.1 Preparative	196
7.4 The Crystal and Molecular Structure of In[Ni ₃ (μ ₃ -O)(μ ₃ -Cl)(μ-Cl) ₃ .tmen ₃]	205
REFERENCES	220
VITA AUCTORIS	235

LIST OF TABLES

<u>Table</u>	<u>Title</u>	<u>Page</u>
2.1	Yield, Melting Points and Analytical Results for $\text{Ph}_3\text{Sn}(\text{X})\text{Y}$ Tmen Compounds	21
2.2	^1H NMR Spectra of $\text{Ph}_3\text{SnIn}(\text{X})\text{Y}$ Compounds	23
2.3	Far Infrared Spectra of $\text{Ph}_3\text{SnInX}_2$ Compounds	33
2.4	Raman Emissions Assigned as $\nu(\text{Sn-In})$ in Tmen Adducts of $\text{Ph}_3\text{SnIn}(\text{Y})\text{X}$	34
3.1	Analytical Results	42
3.2	^1H NMR Spectra of Tin(IV) Derivatives of $o\text{-Cl}_4\text{C}_6\text{O}_2$	44
3.3	Diagnostic IR Absorptions of Adducts of Sn(IV) Catecholates	51
3.4	^{13}C NMR Spectra of Tin(IV) Derivatives of $o\text{-Cl}_4\text{C}_6\text{O}_2$	53
3.5	Summary of Crystal Intensity Data Collection and Structural Refinement	56
3.6	Final Fractional Coordinates and Isotropic Thermal Parameters for Non-Hydrogen Atoms of $(\text{tmenH})_2[\text{Sn}(\text{O}_2\text{C}_6\text{O}_2)_3]$ With Standard Deviations in Parentheses	59
3.7	Interatomic Distances (Å) and Angles ($^\circ$) for $(\text{tmenH})_2[\text{Sn}(\text{O}_2\text{C}_6\text{O}_2)_3]$	61
4.1	Analytical Data for Products of SnX_2 (X = Cl, Br, I/TBQ (OR) PQ) Reactions	74
4.2	Summary of Crystal Data, Intensity Collection and Structure Refinement for $(\text{Bu}^t_2\text{C}_6\text{H}_2\text{O}_2)\text{Sn}.\text{Phen}.2\text{dmf}$	77
4.3	Final Fractional Coordinates and Isotropic Thermal Parameters ($\text{Å}^2 \times 10^{-3}$) For Non-Hydrogen Atoms of $(\text{Bu}^t_2\text{C}_6\text{H}_2\text{O}_2)\text{Sn}.\text{Phen}.2\text{dmf}$	80
4.4	Bond Lengths (Å) and Angles (Deg) for $(\text{Bu}^t_2\text{C}_6\text{H}_2\text{O}_2)\text{Sn}.\text{Phen}.2\text{dmf}$	83
4.5	Diagnostic IR Absorptions of $(\text{TBC})\text{SnCl}_2.\text{L}$ and $(\text{PD})\text{SnCl}_2$ (L = Bipy, Phen)	92
4.6	^1H NMR Spectra for Products On SnX_2	

	(X = Cl, Br, I)/TBQ/PQ Reactions	93
4.7	^{13}C NMR Spectra of Tin(IV) Derivatives of $o\text{-Cl}_4\text{C}_6\text{O}_2$	96
4.8a	ESR Parameters of Sn(IV) Semiquinone Complexes at 298 K	103
4.8b	ESR Parameters of the Biradical Formed From the Reaction of TBQ with SnCl_2 In THF at 77 K	103
5.1	Analytical Results for In(III) Catecholate	116
5.2	^{13}C NMR Spectra of Indium(III) Derivatives of $o\text{-Cl}_4\text{C}_6\text{O}_2$	123
5.3	Far Infrared Spectra of Some In(III) Catecholates	136
5.4	^1H NMR Spectra of Indium(III) Derivatives of $o\text{-Y}_4\text{C}_6\text{O}_2$ (Y = Cl, Br)	137
6.1	Analytical Data on-Indium Semiquinonates	147
6.2	Data on Solubility Studies of Indium with TBQ	152
6.3	Infrared Spectra of Indium Semiquinonates	161
6.4	Far Infrared Spectra of Some Indium Semiquinonates	164
6.5	ESR Parameters of Indium Semiquinonate Complexes	168
6.6	Summary of Crystal Data, Intensity Collection, and Structural Refinement 3,5-Bis- <i>t</i> -butyl-1,2-benzosemiquinone) $\text{InBr}_2(\nu\text{-Pic})_2$	179
6.7	Final Fractional Coordinates and Isotropic Thermal Parameters (A^2) for Non-Hydrogen Atoms of 3,5-Bis- <i>t</i> -butyl-1,2-benzosemiquinone)	183
6.8	Interatomic Distances (A) and Angles with ESD's in Parentheses for 3,5-Bis- <i>t</i> -butyl-1,2-benzosemiquinone)	185
6.9	Chelate Ring Bond Lengths (A) for Semiquinone Complexes Characterized Crystallographically	191
7.1	The Synthesis of Transition Metal-Indium Complexes	197
7.2	Analytical Data	198
7.3	Summary of Crystal Data, Intensity Collection, and Structural Refinement for $\text{In}^{3+}[\text{Ni}_3(\mu_3\text{-O})(\mu_3\text{-Cl})(\mu\text{-Cl})_3\text{tmen}_3]^{3-} \cdot \text{CHCl}_3$	206
7.4	Final Fractional Coordinates and Isotropic Thermal Parameters for Non-Hydrogen Atoms of	

	$\text{In}^{3+}[\text{Ni}_3(\mu_3\text{-O})(\mu_3\text{-Cl})(\mu\text{-Cl})_3\text{men}_3]^{3-} \cdot \text{CHCl}_3$ with Standard Deviations in Parentheses	209
7.5	Some Important Interatomic Distances (Å) and Angles (°) for $\text{In}^{3+}[\text{Ni}_3(\mu_3\text{-O})(\mu_3\text{-Cl})(\mu\text{-Cl})_3\text{men}_3]^{3-} \cdot \text{CHCl}_3$ with Standard Deviation in Parentheses	211

LIST OF FIGURES

<u>Figure</u>	<u>Title</u>	<u>Page</u>
3.1	ORTEP Diagram of $[\text{Sn}(\text{O}_2\text{C}_6\text{Cl}_4)_3]^{2-}$	63
3.2	Crystal Packing Diagram of $(\text{tmenH})_2[\text{Sn}(\text{O}_2\text{C}_6\text{Cl}_4)_3]$	64
4.1a	The Effects of Zero-Field Splitting on the Expected ESR Transitions	71
4.2	ORTEP Diagram of Bis(3,5-Di-tert-butylcatecholato)tin(IV)-1,10 Phenanthroline	86
4.3	Unit Cell Packing of Bis(3,5-Di-tert-butylcatecholato)tin(IV)-1,10 Phenanthroline	87
4.4	Diagram of Apparatus Used in Preparation of Solutions for ESR Spectroscopy	89
4.5	ESR Spectrum of the SnCl_2/TBQ Reaction in THF	100
4.6	ESR Spectrum of a Frozen THF Solution of SnCl_2/TBQ Reaction	102
5.1	Electronic Absorption Spectra of (A) Tetrachloro-1,2-benzoquinone and (B) The Reaction Between Tetrachloro-1,2-benzoquinone and indium chloride both in tmen/toluene solution	119
5.2a	Electronic Absorption Spectra of (A) Tetrachloro-1,2-Benzoquinone and (B) The Reaction Between Tetrachloro-1,2-benzoquinone and Indium(I) Chloride in THF	120
5.2b	Electronic Absorption Spectra of the Reaction Between InCl and Tetrachloro Orthobenzoquinone in THF Showing the Disappearance of Transition Due to $\text{C}=\text{O}$	121
5.3	Plot of Absorbance and Log of Absorbance Against Time	122
5.4	The Infrared Spectra of KBR Pellets of (A) $\text{Br}_4\text{C}_6\text{O}_2$ (B) $\text{Br}_4\text{C}_6\text{O}_2\text{InCl.phen}$ (C) $\text{Br}_4\text{C}_6(\text{OH})_2$	135
5.5	The ESR Spectrum of the Reaction $\text{In}/\text{Cl}_4\text{C}_6\text{O}_2^{1/2} \text{I}_2$ in Toluene (A) Experimental (B) A + Pyridine (C) Calculated	142
6.1	Plot of % Reacted Indium Against Molar Ratio of TBQ to Indium	158

6.2	Plot of Concentration of Reacted Indium Against the Molar Ratio of TBG to Indium	159
6.3	IR Spectrum of (A) TBG (B) (TBSQ)InCl ₂ .phen	166
6.4	ESR Spectra of (PSQ)InCl ₂ .tmen in Toluene: (A) Experimental (B) Calculated	169
6.5	ESR Spectra of (TBSQ)InCl ₂ .tmen (A) In Toluene (B) In CH ₂ Cl ₂ (C) Calculated Spectrum of B	170
6.6	ESR Spectrum of the System inCl/TBG/Py In Toluene (A) Experimental (B) Calculated	171
6.7	ESR Spectra of (TBSQ)InCl ₂ .2py in THF (A) First Derivative on 100G Scan Range (B) Expanded Portion of the Right Hand Spectrum of A (C) Second Derivative of B	172
6.8	ESR Spectra of (TBSQ)InCl ₂ .2py In Toluene (A) Experimental (B) Calculated	173
6.9	ORTEP Plot of the Molecule (C ₁₄ H ₂₀ O ₂)InBr ₂ .2γ-pic	187
6.10	The Unit Cell of (C ₁₄ H ₂₀ O ₂)InBr ₂ .2γ-pic	188
7.1	ORTEP Plot of the Molecule In[Ni ₃ (μ ₃ -O)(μ ₃ -Cl)(μ-Cl) ₃ .tmen ₃]	214
7.2	Unit Cell Contents of the Molecule In[Ni ₃ (μ ₃ -O)(μ ₃ -Cl)(μ-Cl) ₃ .tmen ₃]	215

LIST OF ABBREVIATIONS

acac	acetylacetonate
anil	aniline
bipy	2,2'-bipyridine
br	broad
Cat	catecholato anion
CNDO	complete neglect of differential overlap
Cp	cyclopentadienyl
DMF or dmf	N,N'-dimethylformamide
DMSO or dmsO	dimethylsulphoxide
DPPH	diphenyl picrylhydrazyl
ESR	electron spin resonance
FD	field desorption
G	gauss
ir	infrared
m	medium
Me	methyl
morph	morpholine
NMR	nuclear magnetic resonance
OAc	acetate
PD	phenanthro-9,10-diolato anion
Ph	phenyl
phen	1,10-phenanthroline
ppm	parts per million
PQ	9,10-phenanthroquinone
PSQ	9,10-phenanthrosemiquinone

γ -Pic	γ -picoline (4-methylpyridine)
R	Raman
R-X	alkyl halides
s	strong
sh	shoulder
TBC	3,5-di-tert-butyl-1,2-catecholato anion
TBQ	3,5-di-tert-butyl-1,2-benzoquinone
TBSQ	3,5-di-tert-butyl-1,2-benzosemiquinone
tBu	tertiary butyl
terpy	2,2',2''-terpyridine
THF	tetrahydrofuran
tmen	N,N,N',N'-tetramethylethylenediamine
TMS	tetramethylsilane
Tol	toluene
triene	trimethyltetramine
UV	ultra-violet
vs	very strong
vw	very weak
w	weak

CHAPTER 1

GENERAL CONSIDERATIONS

1.1 Introduction

Indium is a group III element, atomic number 49, with the outer electronic configuration $5s^2 5p^1$, and like its congeners gallium and thallium can form compounds in the +3, +2 and +1 oxidation states. Similarly, tin which is a group IV element with atomic number 50, has the outer electronic configuration $5s^2 5p^2$ and is known to form compounds in the +4, +3 and +2 oxidation states. The work presented in this dissertation involves studies of the low oxidation state of both indium and tin, with emphasis on the former as far as the nature and reactivity of its compounds are concerned, due in the main to recent developments in our laboratory concerning the solubility of indium(I) halides.

The chemistry of indium(III) and tin(IV) will not be discussed in this Introduction, since competent authors have reviewed their inorganic^{1,2} and organometallic chemistry^{3,4} elsewhere.

1.1.1 Compounds of indium(I)

Simple inorganic compounds of indium(I) In_2O ,^{5,6} In_2S ,⁷ In_2Se ,⁵ In_2Te ,⁵ and InX ($\text{X} = \text{Cl}$,⁸ Br ,⁷ I ⁸) have been known for many years. The best characterized of these are the monohalides, which are easily prepared but are insoluble and intractable materials which readily undergo hydrolysis and disproportionation. Their crystal structures have, nonetheless, been determined ($\text{X} = \text{Cl}$,⁹ Br ,¹⁰ I ¹¹).

The only known organoindium(I) compounds are the cyclopentadienyl¹² and methylcyclopentadienyl¹³ derivatives, and the former has proven a useful starting point for some synthetic work.

1.1.1.1 Reactions with donor ligands

Tin dihalides (SnX_2) form a number of 1:1 adducts with monodentate ligands,^{14,15} consistent with the fact that SnX_2 compounds with six valence level electrons are expected to be electron pair acceptors. Similarly, such compounds are known to be electron pair donors.^{16,17} Indium(I) halides with four valence shell electrons are also expected to have Lewis acid character but adducts with neutral ligands have been obtained in very few cases and are poorly characterized.

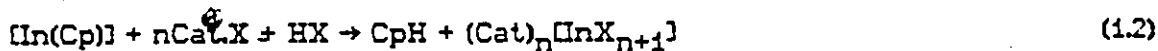
The neutral adducts of InBr and InI with ammonia, $\text{InX} \cdot n\text{NH}_3$ ($n = 1,2$) are reported to be black insoluble substances which disproportionate in air or in the presence of moisture.¹⁸ The thermal decomposition of $\text{InX} \cdot 2\text{NH}_3$ is represented by eqn. (1.1); unfortunately, no structural details were published.



Some unusual species are reported to be formed in the reaction of InX ($X = \text{Cl}, \text{Br}, \text{I}$) with morpholine and aniline.¹⁹ The halides are fairly insoluble in these solvents, but the bulked products of several reactions, which involve long refluxing analyzed as $[\text{In}(\text{anil})_4]\text{X}$ and $[\text{In}(\text{morph})_2]\text{X}$ which are 1:1 electrolytes in nitrobenzene. Attempts to repeat this work in our laboratory by C. Pèppe were unsuccessful.

Anionic halide complexes of indium(I) have been prepared by refluxing a suspension of InX with a methanolic solution of N,N' -dimethyl-4,4'-bipyridinium halide.²⁰ The vibrational spectra of the resultant $[\text{InX}_3]^{2-}$ anions have been assigned on the basis of C_{3v} molecular symmetry as in the case of the isoelectronic $[\text{SnX}_3]^-$ molecule. Force constant calculations have been carried out, and the primary stretching-force constants compared with those of related

molecules.²¹ Similarly anionic complexes involving InCp have been made by treating a benzene solution of InCp with an ethanolic solution of Et₄NX and HX.²²



It was reported that when X=I and Cat = 1,2-bis(methyldiphenylphosphino)-ethane the product from reaction 1.2 is [Me₂dppe][InI₃]. However, when the cation was Et₄N⁺ the products for X = Cl, Br or I were the salts [Et₄N][InX₂]. Vibrational spectroscopy demonstrated that the InX₂⁻ anions are isostructural with tin(II) halides. [Et₄N][InI₂] could also be prepared by the electrolytic oxidation of indium metal in a benzene-methanol solution of Et₄NI and I₂.²³ The salt [Me₂dppe][InI₃] could also be obtained by this technique.

Further reactions showed that these anions could undergo metathetical reactions to give the pseudohalogeno compounds.²³ For example, tetraethylammonium dichloroindate(I) reacted with 2 mol of sodium cyanate in ethanol to yield [NEt₄][In(NCO)₂]. Analogous reactions gave [NEt₄][In(NCS)₂] and [Me₂dppe][In(NCS)₃].

An interesting new development which should help in the development of indium(I) chemistry is the finding that the monohalides InX (X = Cl, Br, I) dissolve in mixtures of aromatic solvents and organic bases.²⁴ These solutions are relatively stable at low temperature (-20°C, and below), and the dependence of solubility on temperature concentration suggests that in the case of InBr or InI, the solute species is InX₃ in dilute solution, although addition of petroleum ether to the cold solution precipitates InX_{0.5} in. The synthetic usefulness of such solutions is discussed below.

Adduct formation has also been observed with cyclopentadienyl indium in its reaction with boron compounds²⁵ as shown in eqn. (1.3)



Few indium(I)- β -ketoenolates have been prepared, and this has been attributed to the lack of suitable starting materials. Cyclopentadienylium(I) reacts in Et₂O/benzene mixtures with 4,4,4-trifluoro-1-(thien-2'-yl)butane-1,3-dionate (= ttaH) to give the extremely hygroscopic In(tta). Similar derivatives of other bidentate ligands have been obtained by this same process.²⁶ The reactions of the analogues In(oxine) (oxine = 8-hydroxyquinoline anion) shows that such InL species are easily oxidized to indium(III) complexes.

1.1.2 Compounds of indium(II)

The existence of compounds with the stoichiometry InX₂ has been established for many years, since the first compound of this type, InCl₂, was initially prepared in 1888.⁸ The simplest method of preparation involves heating for example InCl₃ with a calculated excess of indium metal, but the reactions of indium with gaseous hydrogen chloride, or of InCl₃ with a mixture of hydrogen and hydrogen chloride, also provide a route to these species. Such methods have been used to prepare InCl₂,²⁷⁻²⁹ InBr₂,^{30,31} and InI₂.^{30,32} Indium(II) fluoride was reported by Hannebohn and Klemm,³³ and indium(II) cyanide has been obtained by the reaction of indium metal with mixtures of hydrogen and hydrogen cyanide gas.³⁴ An unexpected and apparently atypical compound is In(OAc)₂ (OAc = acetate anion) which was produced when crystals of indium metal, freshly deposited by electrolysis in almost anhydrous acetic acid, were allowed to react with the electrolyte solution.³⁵

5

Neutral adducts of the indium dihalides are known with both mono- and bidentate nitrogen ligands. Condensation of ligand onto InX_2 ($\text{X} = \text{Cl}, \text{Br}, \text{I}$) cooled in liquid nitrogen gave InX_2L ($\text{L} = \text{piperidine}, \text{piperazine}$ and morpholine). Raman emissions at ca. 173 (Cl), 143 (Br) or 105 (I) cm^{-1} were assigned as $\nu(\text{In-In})$, leading to the formulation of these compounds as $\text{X}_2(\text{L}_2)\text{InIn}(\text{L}_2)\text{X}_2$, with the bases acting as monodentate ligands at five coordinate indium(II).³⁶ The reaction between InX_2 ($\text{X} = \text{Br}, \text{I}$) and various ligands in benzene³⁷ yielded adducts only with tmen and Et_3P ; other ligands, and all reactions involving InCl_2 , lead to disproportionation, either to $\text{In}^0 + \text{InX}_3$ or to $\text{InX} + \text{InX}_3$. A later X-ray crystallographic investigation³⁸ confirmed both the In-In structure of $\text{In}_2\text{Br}_3\cdot 2\text{tmen}$, for which $r(\text{In-In}) = 2.775(2)\text{\AA}$, and five-coordination at indium.

Condensation of pyridine onto InX_2 gave the In-In bonded compounds $\text{In}_2\text{X}_4\text{py}_4$ ($\text{X} = \text{Br}, \text{I}$), but $\text{X} = \text{Cl}$ products could not be obtained by this or other methods.³⁸ Adducts of InI_2 with $\text{EtNH}_2(\text{In}_2\text{I}_4\text{L}_6)$, and EtNH_2 and bipy($\text{In}_2\text{I}_4\cdot 2\text{bipy}\cdot 4\text{EtNH}_2$; $\text{In}_2\text{I}_4\cdot \text{Et}\cdot \text{bipy}\cdot \text{bipy}\cdot 8\text{EtNH}_2$; $\text{In}_2\text{I}_4\cdot \text{Et}_4\cdot \text{bipy}\cdot \text{bipy}\cdot 8\text{NH}_3$) have also been reported,³⁹ but unfortunately no structural information is available on these unusual compounds.

The solid state structure of In_2I_4 has been shown to be $\text{In}^+[\text{InI}_4]^-$ by X-ray crystallography,^{40,41} isostructural with GaCl_2 .⁴² Structural work on InBr_2 indicates a similar structure,⁴³ and confirms previous assignments based on vibrational spectroscopy⁴⁴ for both InBr_2 and InI_2 .

The anionic species $\text{In}_2\text{X}_6^{2-}$ ($\text{X} = \text{Cl}, \text{Br}, \text{I}$), prepared via InX_2 ,⁴⁵ are apparently isostructural with the corresponding gallium(II) anions. In non-aqueous solution, ^{115}In NMR studies⁴⁶ show that these molecules disproportionate to $\text{InX}_2^- + \text{InX}_4^-$. Recent studies from our laboratory of the InX/InY_3 reaction⁴⁷

cast some light on these matters, and it appears that kinetic factors, and specifically intramolecular halide transfer, are at least as important as thermodynamic effects in the stability of both $\text{In}_2\text{X}_4\text{L}_2$ and $\text{In}_2\text{X}_6^{2-}$ species. The importance of phase is shown by the fact that the gas phase above molten InX_2 contains InX , InX_3 and In_2X_6 molecules.³⁴

The research reported in the different chapters in this dissertation falls under the general description of oxidative addition, and therefore it is appropriate to review the theoretical aspects of this process.

1.1.3 Oxidative-Addition Reactions

Of all the reactions of In(I) compounds, one of the most interesting is the oxidative addition process.

From a theoretical standpoint, the term oxidative addition⁴⁸ is usually used to describe a process whereby a complex L_yM^n behaves simultaneously as a Lewis acid and a Lewis base. This is generally written as



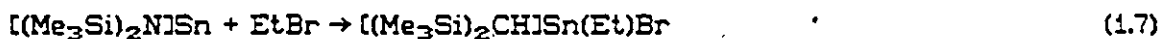
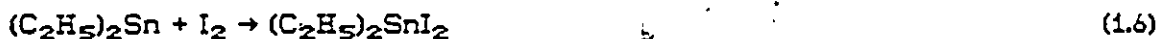
For an addition reaction to proceed one must have:

- (i) non-bonding electron density on the metal M
- (ii) two vacant coordination sites on the complex L_yM to allow formation of two new bonds to X and Y; and
- (iii) a metal M with oxidation states separated by two units.

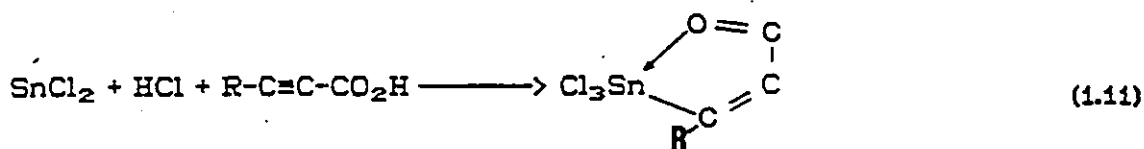
The above criteria have been identified in the chemistry of SnX_2 compounds. The general reaction scheme is presented in (1.5)



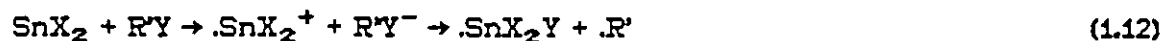
The atoms Y and Z may be identical as in halogens,⁴⁹⁻⁵¹ in disulphanes,⁵² elemental sulphur,⁵³ and polynuclear transition metal compounds,⁵⁴⁻⁵⁷ or they can be different as in organic halides,^{49,58-63} hydrogen halides,⁴⁹ transition metal halides.^{49,56,64-67} Some representative examples of reaction (1.5) are listed below



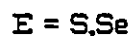
Many of these reactions are of great synthetic importance as they provide facile routes to functionally substituted tin(IV) compounds. One procedure, which is of great industrial interest, is the addition of HCl to SnCl₂ forming the intermediate HSnCl₃ which reacts with C=C bonds, as in eq. (1.11).⁶⁸



Mechanistic studies on the reaction of stable stannylenes with organic halides have been performed by M.F. Lappert and his group.⁶¹⁻⁶³ On the basis of ESR spectroscopic data they proposed a radical pathway for these reactions. Initially, one electron of the stannylene is transferred to the organic halide the halogen of which is then added to the tin atom according to eq. (1.12) (Y = halogen, X = bulky organic group).



The development of the redox chemistry of indium(I) compounds has been slow for the reasons given in Section 1.1.1. Nonetheless, there has been limited success in reactions involving oxidative addition; typical examples include reactions with alkyl halides,⁶⁹⁻⁷³ S-S,⁷⁴⁻⁷⁶ Se-Se⁷⁶ and O-O⁷⁷ bonded species as well as some M-M⁷⁸⁻⁸¹ bonded transition metal carbonyls. Some of the reactions are presented in (1.13) through (1.15).



After the discovery of the solubility of indium monohalides (see 1.1.1) most of these reactions were reinvestigated, and the results showed improved yield of the products. The first structurally determined In-In bonded compound was made by this new method, by the reaction of InX ($\text{X} = \text{Br}, \text{I}$) with InY_2 ($\text{Y} = \text{Cl}, \text{Br}, \text{I}$). There was, therefore, no doubt, as to the synthetic usefulness of this new indium(I) halide system and the solutions in question can also be regarded as powerful reducing agents for a large variety of substrates. They may become of interest not only to experimental chemists but to material scientists, electronic engineers and chemical engineers since current trends in electrical conductor, semiconductor and superconductor technologies are responsible for a growing demand for ultra high purity metals. It is known,⁸² for example, that in the electrolytic production of high purity gallium, a solution of a gallium(II) complex of the type $\text{Ga}(\text{GaX}_4)$ ($\text{X} = \text{Cl}, \text{Br}$) in an aromatic solvent (e.g. benzene, toluene, xylene) is used as electrolyte. The electrolyte is obtained by extraction of the gallium complex compound with this solvent. Liquid gallium is thus obtained by conducting the electrolysis with a current density ≥ 200 amp/sq. dm., and powdered gallium is obtained by using a cathode current density < 200 amp/sq. dm. The unusual solubility behaviour of the indium(I) halides may well be significant for new purification processes involving redistribution and extraction in non-aqueous solvents.

1.2. Present Work

The research which is described in this dissertation can be considered in part as an extension of work involving the reactions of indium monohalides in mixtures of aromatic solvents containing neutral ligands. The usefulness of this system is judged from the number of applications in this laboratory since its discovery. Chapter 2 describes how this method has been utilized in the

synthesis of compounds containing Sn-In bonds. Subsequent chapters take a look at efforts made to establish a mechanistic route to formation of Sn(IV) and In(III) compounds from their respective low valent compounds. The substrates used in these reactions are substituted orthoquinones and with the aid of electron spin resonance spectroscopy it has been established that, contrary to the assumed transfer of pairs of electrons in oxidative addition processes, the actual process in fact, is a two-step one electron transfer process.

The last chapter revisits some oxidative insertion reactions, this time with transition metal halides, both inorganic and organometallic.

1.3. Experimental Techniques

1.3.1 Starting Materials

Indium trichloride and tribromide were prepared by the action of a stream of nitrogen containing the corresponding molecular halogen over molten metallic indium.⁸³

Indium triiodide was prepared by refluxing indium metal and I₂ in xylenes⁸⁴ or toluene.

Indium monohalides (InX; X = Cl, Br, I) were prepared by reacting the correspondent trihalide with two equivalents in indium metal in a sealed tube at 350°C (X = Cl, Br) and 450°C (X = I) for 24 hours.⁸⁵

Due to the sensitive nature of indium mono- and trihalides to air, all reactions and operations were carried out in an atmosphere of dry nitrogen using a glove bag or a dry box.

The solvents (ACS grade) were dried and distilled before use according to standard procedures. Aromatic solvents (benzene, toluene, xylenes), petroleum

ether (40-60°C), tetrahydrofuran, and diethyl ether were refluxed with sodium and benzophenone and distilled from the blue ketyl formed.

Acetonitrile and methylene chloride were refluxed with calcium hydride (or P_2O_5) and distilled before use.

Liquid ligands were dried over molecular sieves. All other reagents were used as supplied.

1.3.2 Characterization of Products

(i) Elemental Analysis:

Halide: the Volhard method was used for halide analysis. Samples (~ 50-100 mg) were added to a known excess of standard silver nitrate. The excess silver nitrate was then titrated with standard potassium thiocyanate in the presence of small amounts (2 mL) of nitrobenzene and ferric ammonium sulfate as the indicator.

Tin and Indium: indium and tin analyses were by atomic absorption using a 1L 251 Atomic Absorption Spectrophotometer. Samples (50-100 mg) were destroyed in HNO_3 and diluted appropriately in order to give concentrations of 20-50 mg L^{-1} for analysis. Standard solutions were prepared by dissolving 1 g of the pure metal in 20 mL of HNO_3 and diluting it to 1000 mL, with distilled water. Subsequent appropriate dilutions were used for the actual measurement.

Carbon, hydrogen and nitrogen: analyses were by Guelph Chemical Laboratories Limited, Guelph, Ontario.

(ii) Spectroscopic:

NMR Spectra: 1H NMR spectra were recorded on a Varian EM 360 or Bruker AC 300L instrument. ^{13}C NMR spectra were recorded on a Bruker AC 300L.

IR Spectra: Infrared spectra in the region $4000-400\text{ cm}^{-1}$ were obtained on the Perkin Elmer 180 or Nicolet 5DX instrument with emulsions of the solid sample in Nujol, between polyethylene plates or as KBr discs. Far infrared spectra in the region $500-50\text{ cm}^{-1}$ were run on the Perkin-Elmer 180. Samples were run as Nujol mulls between polyethylene plates.

Raman spectra were obtained with the solid samples sealed in capillary glass tubes in the Spectraphysics 700 instrument equipped with a Spectraphysics 265 exciter, or with a Ramanor U-1000 instrument interfaced with an IBM/PC microcomputer.

Electronic spectra were taken on a Shimadzu UV-240 spectrophotometer. Conductivity measurement was done using a YSI model 31 conductivity bridge with cell constants of 1.0 cm^{-1} , calibrated with aq KNO_3 .

All ESR samples were run in degassed solvents in 2 mm quartz tubes on a Varian E-12 ESR Spectrometer operating in the X-band frequency range. The field sweeps were calibrated using a proton NMR magnetometer. The cyclotron frequency was calculated from the position of the DPPH (diphenylpicrylhydrazyl) signal measured with proton NMR.

1.3.3 X-ray crystallography

1.3.3.1 Data Collection

For data collection, air stable materials were handled on glass fibers and the air sensitive crystals sealed in thin glass capillary tubes. Data were collected on a Syntex P2₁ four-cycle automated diffractometer controlled by a Nova 1200 computer. The diffractometer, at a take off angle of 6.1° , was equipped with a molybdenum X-ray tube and a highly oriented graphite monochromator ($\lambda = 0.71069\text{ \AA}$, $2\theta_m = 12.2^\circ$) and was operated at 50 kV and 20 mA.

The determination of the unit cell parameters was accomplished by the following procedure:

(i) A random-orientation photograph was taken with $2\theta = \omega = \chi = 0^\circ$ and the θ axis rotating at $2.34^\circ/\text{min}$. The x,y film coordinates for 7-10 reflections were entered for a centering reflections routine. The program searches for a particular reflection by calculating 2θ and χ , assuming $\omega = 0$. The value of θ was determined by rotating around θ at low speed until a peak with intensity greater than 10^3 counts/s was found. The centering program found the refined values of 2θ , χ and ω angles and these values were used in the subsequent autoindexing program, which produce a list of axial vectors and the angles between these vectors from which the unit cell dimensions were selected according to the standard symmetry rules. Mirror symmetry of the axis were checked by axial photographs.

(ii) After establishing the initial cell parameters, preliminary data were collected in the shell defined by $15^\circ < 2\theta < 25^\circ$. From the data, 15 strong reflections widely separated in the reciprocal space were selected. Their refined angular values were used in the least squares refinement program, which gives the final cell constants and the orientation matrix for data collection.

(iii) Intensity data were then collected via a θ (crystal) - 2θ (counter) scan in 96 steps using bisecting geometry with the scan from $[2\theta (\text{Mo K}\alpha_1) - 1.0]^\circ$ to $[2\theta (\text{Mo K}\alpha_2) + 1.0]^\circ$. Backgrounds (B_1 and B_2) were measured at the beginning and the end of the scan, each for 25% of the time of the scan. The stability of the system and the crystal was monitored by measuring three strong reflections every 197 data. In some cases, we observed a decrease in the intensity of the monitor reflections and this was corrected by the application of

were calculated from equations (1.16) and (1.17).

$$I = SC - \tau(B_1 + B_2) \quad (1.16)$$

$$\sigma(I) = (SC + (B_1 + B_2) + p^2 I^2)^{1/2} \quad (1.17)$$

where SC = count during the scan.

τ = ratio of scan time to background time (= 2 for all the compounds in the present study)

p = ignorance factor (= 0.05 in the present study)

From the intensity of the reflections the structure factors $|F_o|$ were calculated according to equation (1.18) and its

$$|F_o| = (I/Lp)^{1/2} \quad (1.18)$$

standard deviation $\sigma(F_o)$ given by equation (1.19).

$$\sigma(F_o) = \sigma(I)/2|F_o|Lp \quad (1.19)$$

The Lp factor for a monochromator in the equatorial mode is given by equation (1.20); the equation assumes that

$$Lp = \frac{0.5}{\sin 2\theta} \frac{1 + (\cos^2 2\theta_m)(\cos^2 2\theta)}{1 + \cos^2 2\theta_m} + \frac{1 + [\cos 2\theta_m] \cos^2 2\theta}{1 + [\cos 2\theta_m]} \quad (1.20)$$

The graphite monochromator is 50% mosaic and 50% perfect. The monochromator angle $2\theta_m$ is 12.2° for Mo $K\alpha$ radiation. The examination of the data for systematic absences lead to the determination of the corresponding space groups.

1.3.3.2 Solution and Refinement of the Structure

Programs used during the structural analysis include local versions of CHECK (check reflections), PROC (data reduction), ABSORB (analytical absorption correction), SHELX 77 (full matrix least square refinement and Fourier Synthesis),

correction), SHELX 77 (full matrix least square refinement and Fourier Synthesis), XANADU (librational analysis and medium plane calculations) and ORTEP (thermal ellipsoid plotting program).

All the anomalous scattering factors for Sn, In, Ni, Br and I atoms were taken from reference 86.

All the structures were solved by the heavy atom method. The position of the heavy atom(s) was determined from a sharpened three-dimensional Patterson synthesis, and the position of the remaining non-hydrogen atoms determined by subsequent difference Fourier synthesis. The structures were then anisotropically refined by full matrix least squares methods. The function minimized during the refinement was $\sum w(|F_o| - |F_c|)^2$. In the initial stages of refinement unit weights (w) were used, and in the final stages a weighting scheme of the form $w = (1/\sigma^2[F_o] + p F_o^2)$ was employed. At this stage the difference Fourier map normally showed electron density in plausible hydrogen atom locations, and these hydrogen atoms were included in idealized positions (except when stated otherwise) with C-H = 0.95Å. The discrepancy indexes used in the text are defined in equations (1.21) and (1.22).

$$R = \frac{\sum(|F_o| - |F_c|)}{\sum|F_o|} \quad (1.21)$$

$$R_w = \frac{\sum w(|F_o| - |F_c|)^2}{\sum w|F_o|^2}^{1/2} \quad (1.22)$$

CHAPTER 2

THE REACTION BETWEEN InX AND Ph_3SnY :

THE PREPARATION OF Sn-In BONDED COMPOUNDS

2.1 Introduction

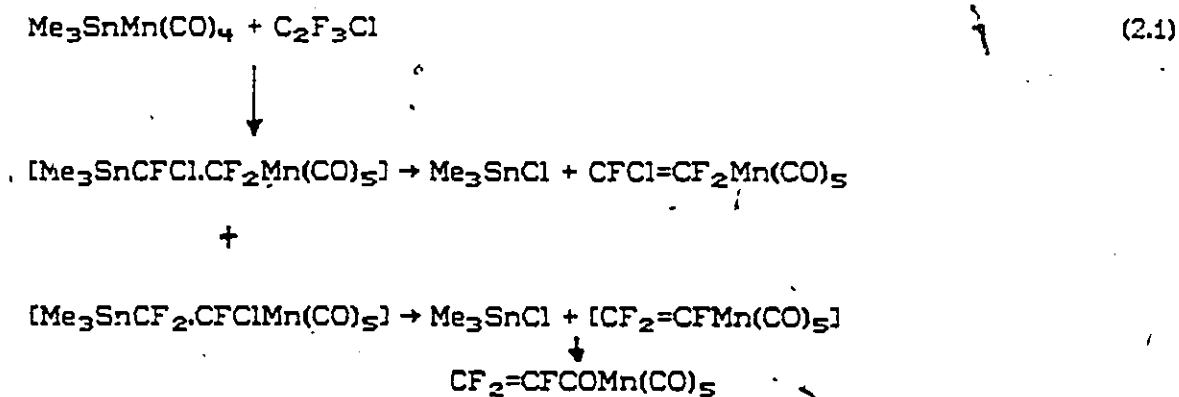
This chapter deals with work done in the preparation and isolation of compounds containing Sn-In bonds as well as attempts made at synthesizing related compounds. The principle underlying these reactions is the oxidative insertion of InX into Sn-X bonds. The recent discovery in our laboratory of the solubility of InX in mixtures of aromatic hydrocarbons and organic bases (see Chapter 1) was an important experimental factor in this work.

Organometallic and inorganic compounds containing metal-metal bonds have been the subject of a very large number of studies, most of which have focused on their preparation and chemical properties.⁸⁷⁻⁹³ The reactions of such compounds are particularly interesting, largely because of the potentially wide application in catalysis. For example, metal-metal bonded compounds ought to show special reactivity features as a result of cooperation between adjacent metals and so could function as homogeneous catalysts,⁹⁴⁻⁹⁶ and clusters containing three or more metal atoms may also function as "storehouses" for the release and take-up of catalytically active fragments. Such clusters are also being used to model the bonding reactions of substrates on metal surfaces.⁹⁷⁻⁹⁹ Di- and polynuclear compounds have also proven to be useful precursors for the preparation of several heterogeneous catalysts. For example, trichlorotin derivatives of platinum have been used as homogeneous catalysts in the reduction of acetylenes or short chain olefins to paraffins under mild conditions,¹⁰⁰ in the hydrogenation of polyenes to dienes or monoenes, and in

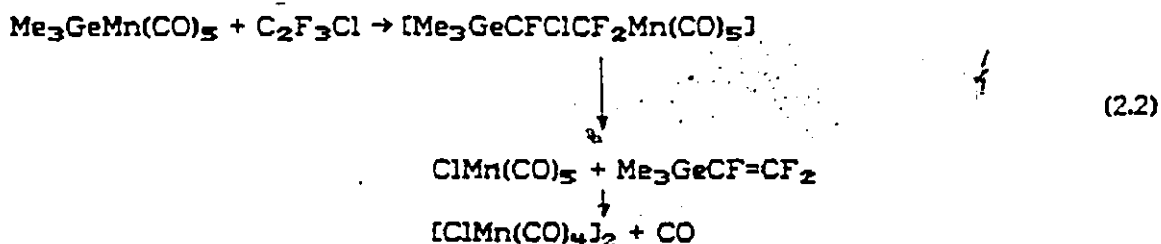
the isomerization of olefins.^{101,102}

Heteronuclear (or mixed-metal) compounds involving Main Group metals may be expected to show unique reactivity features as a result of combining the different properties of the constituent metals. Evidence of this was obtained from dipole measurements¹⁰³ on compounds of the type $R_3M-Mn(CO)_5$ ($M = Si, Ge, Sn, Pb$) since the results imply a small bond polarity $M^{\delta-}-Mn^{\delta+}$. A positive polarity for the transition element is indicated by cleavage reactions on many species. Substituent changes on either metal produce relatively large changes in the bond moment, leading to the conclusion that the metal-metal bonds are highly polarizable.

To demonstrate the difference in reactivity of complexes, one could consider the reactions between tin-manganese¹⁰⁴ and germanium-manganese¹⁰⁵ complexes with fluoro-olefins. Products isolated from the $Me_3SnMn(CO)_5$ reaction with chlorotrifluoroethylene suggest that insertion of $CF_2 = CFCI$ can occur in one of two ways, although the principal pathway gives $Me_3SnCF_2CFCIMn(CO)_5$. The reaction scheme is presented below in eqn. (2.1)



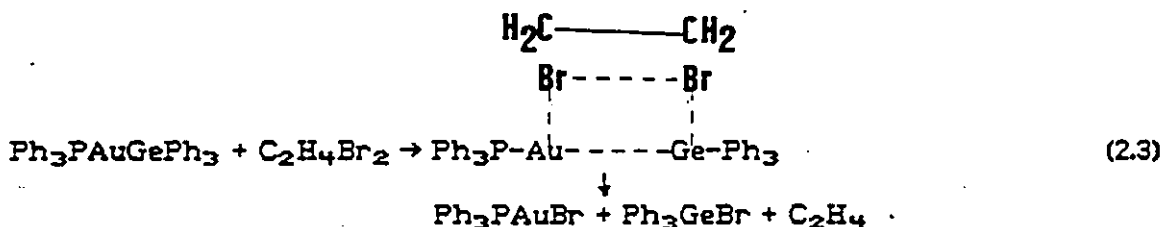
The difference in the reaction of the germanium analogue appears to be in the extent of the specific insertion to form the intermediate $\text{Me}_3\text{GeCFClCF}_2\text{Mn}(\text{CO})_5$, but neither product was isolated. See eqn. (2.2).



The difference in reactivity may also be accounted for by a slight difference in the polarity of the metal-metal bonds.

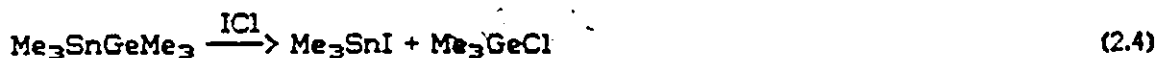
Generally, metal-metal bonds are cleaved by halogens, halogen acid and a variety of organic and inorganic halides including RI , CHCl_3 , CCl_4 , MgI_2 and HgCl_2 .

The cleavage of metal-metal bonds by 1,2-dibromoethane is believed to proceed through a multicentre activated complex, and has been suggested as a quantitative test for these structures.¹⁰⁶ A typical example of such a reaction is shown in eqn. (2.3).

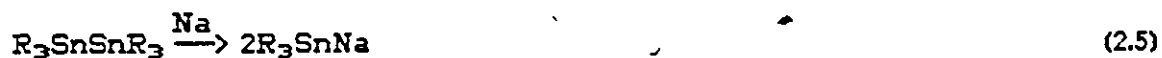


Similar reactions have been observed with Sn-Mn containing compounds.

Another type of cleavage involving unsymmetrical compounds has been noted in the reaction of ICl with $\text{Me}_3\text{MM}'\text{Me}_3$ ($\text{M} \neq \text{M}' = \text{Si, Ge, or Sn}$)¹⁰⁷ carried out in a sealed tube which lead to the products predicted by the hard-acid, soft-base generalization, as in eqn. 2.4.



A further reaction which shows the lability of the Sn-Sn bond is the reaction of hexaalkylditins in liquid ammonia with excess sodium¹⁴ eqn. (2.5).



The alkali metal derivatives R_3SnM form yellow or red solutions in liquid ammonia, and these are important reagents in organotin chemistry.

The above-mentioned method has been used in preparing Sn-M (M = Al, Ga, In, Tl) bonded compounds¹⁰⁸ which was identified by nmr spectroscopy, and were obtained by the reaction of trimethylstannyl-lithium of the Group III trimethyl, Me_3M , in dimethoxyethane and were formulated as $\text{Li}(\text{Me}_3\text{SnMMe}_3)$. Unfortunately, stable solids were not obtained.

As mentioned in Chapter 1, In-In bonded compounds were made by the oxidative insertion reaction of InX into InX_3 (X = Br, I) using such solutions. A similar reaction of InX with SnX_4 or GeX_4 , however, did not give the expected results, but instead an insoluble compound of analytical composition $\text{InMI}_{5.25}$ was isolated.¹⁰⁹ This failure to obtain the desired product suggested the choice of R_3SnX (R-aryl) for our studies, since the insertion reaction could occur easily as there will be only one Sn-X bond to attack; the aryl groups are electron withdrawing, and this could assist in weakening the Sn-X bond and hence facilitate the insertion reaction. An attempt was also made in this work to synthesize compounds containing In-B, In-Ge, In-Pb and In-P bonds. As our results show, we were unable to obtain satisfactory results on the remaining systems other than In-B.

Unlike the Group IV elements, where heteronuclear diatomic molecules are known,⁹³ the analogues among Group III elements are as of now very few in

number.¹¹⁰ There are some excellent reviews^{111,112} in the literature on the chemistry of metal-boron containing compounds. The established routes to synthesizing these complexes are:

1. the reaction of a metal hydride derivative and a boron halide with the elimination of hydrogen halide.¹¹³
2. the reaction between a metal anion and a boron halide with the elimination of an alkali metal salt.^{114,115}
3. the insertion of a metal into a boron-halogen bond by oxidative addition of a boron halide to a metal complex.¹¹⁶

The third method was the most compatible to our studies and hence was used.

2.2 Experimental

2.2.1 The Reaction of InX with Triphenyltin Compounds

(i) $\text{Ph}_3\text{SnIn(X)Y.tmen}$. The same experimental method was used throughout this part of the work. Equimolar quantities (ca. 2-3 mmol) of InX (X=Cl,Br,I) and Ph_3SnY (Y=Cl,Br,I,OAc) were placed in a flask and 50 mL of toluene added. The suspension was cooled with stirring to -20°C , at which point tmen (0.3 g, 2.6 mmol) was syringed into the mixture. Stirring was continued for about 1 h, after which the cooling bath was removed and the mixture allowed to reach room temperature (ca. 20°C) over a period of 1-2 h.

The mixture was filtered, and the suspended solid collected, washed with toluene and dried *in vacuo* at room temperature. This material was shown to be $\text{Ph}_3\text{SnIn(X)Y.tmen}$. Table 2.1 shows percentage yield, melting points and analytical results from these compounds. The products are insoluble in most common organic solvents, but $\text{Ph}_3\text{SnIn(OAc)I.tmen}$ could be recrystallized from

TABLE 2.1

YIELD, MELTING POINTS AND ANALYTICAL RESULTS FOR $\text{Ph}_3\text{SnIn}(X)\text{Y.tmen}$ COMPOUNDS

Compound	Yield (%)	Mpt ($^{\circ}\text{C}$)	C	H	N	In	Sn	X
$\text{Ph}_3\text{SnInCl}_2\text{.tmen}$	96	>150 (dec)	44.10 (44.21)	4.66 (4.76)	4.19 (4.30)	17.6 (17.6)	18.1 (18.2)	10.5 (10.6)
$\text{Ph}_3\text{SnInBr}_2\text{.tmen}$	94	>150 (dec)	38.91 (38.90)	4.15 (4.18)	3.75 (3.78)	15.4 (15.4)	15.9 (16.0)	21.5 (21.6)
$\text{Ph}_3\text{SnInI}_2\text{.tmen}$	97	>200 (dec)	34.50 (34.52)	3.70 (3.72)	3.35 (3.36)	13.6 (13.7)	14.0 (14.2)	30.5 (30.4)
$\text{Ph}_3\text{SnIn}(\text{OAc})\text{Cl.tmen}$	94	90	-	-	-	17.0 (17.0)	17.4 (17.5)	5.4 (5.3)
$\text{Ph}_3\text{SnIn}(\text{OAc})\text{Br.tmen}$	98	95	-	-	-	15.9 (16.0)	16.3 (16.5)	11.2 (11.1)
$\text{Ph}_3\text{SnIn}(\text{OAc})\text{I.tmen}$	92	110	-	-	-	15.0 (15.0)	15.5 (15.5)	16.5 (16.6)
$\text{Et}_4\text{N}^+[\text{Ph}_3\text{SnInCl}_3]^-$	98	>150 (dec)	-	-	-	16.5 (16.4)	16.9 (16.9)	15.4 (15.2)

1:1 mixtures of tetrahydrofuran and methanol.

The ^1H NMR spectra of these products are presented in Table 2.2.

(ii) $\text{Et}_4\text{N}[\text{Ph}_3\text{SnInCl}_3]$. Equimolar quantities (ca. 0.5 mmol) of Et_4NCl and $\text{Ph}_3\text{SnInCl}_2 \cdot \text{tmen}$ were suspended in toluene and the mixture stirred together for 10 h. Filtration yielded a greyish white product which was washed with toluene and dried *in vacuo*. The yield was quantitative. The molar conductivity in nitromethane (4×10^{-4} mol L^{-1}) was $88 \text{ ohm}^{-1}\text{cm}^2\text{mol}^{-1}$, which falls in the reported range of $75\text{--}95 \text{ ohm}^{-1}\text{cm}^2\text{mol}^{-1}$ for 1:1 electrolytes in this solvent.¹⁰¹ The ^1H NMR spectrum in $\text{dms}\text{-d}_6$ had resonances at 7.9–7.4 m (15H) (aromatic protons), and 3.2 q (8H), 1.3 t (12H) assigned to methyl and methylene protons of Et_4N^+ .

2.2.2 Reaction of $\text{Ph}_3\text{SnInBr}_2 \cdot \text{tmen}$ with 1,2-dibromoethane

This experiment was conducted in order to test the reactivity of the Sn-In containing compound (see 2.1).

0.3 g (0.4 mmol) of $\text{Ph}_3\text{SnInBr}_2 \cdot \text{tmen}$ was treated with 20 mL of 1,2- $\text{C}_2\text{H}_4\text{Br}_2$, and the resultant suspension stirred at room temperature for 3 h, after which the solid was collected by filtration, washed with toluene and dried overnight *in vacuo*. The solid was analyzed as $\text{InBr}_3 \cdot 1.5\text{tmen}$. Found: In = 21.8%, Br = 45.6%. Calc: In = 21.7%, Br = 45.3%. The ^1H NMR in $\text{dms}\text{-d}_6$ had resonances at 2.6(s), 2.8(s) ppm confirming the presence of the tmen ligand. The infrared spectrum had bands at ca. 2900 cm^{-1} which were assigned to alkyl C-H stretching and also a broad band at ca. 1400 cm^{-1} due to the C-N vibration of the ligand.

TABLE 2.2

 ^1H NMR SPECTRA OF $\text{Ph}_3\text{SnIn(X)Y}$ COMPOUNDS (PPM FROM Me_4Si)

Compound	Solvent	Resonances (ppm) ^a	Assignment
$\text{Ph}_3\text{SnInCl}_2 \cdot \text{tmen}$	$\text{CD}_3\text{OD}/\text{CDCl}_3$	7.4-7.8(m,15H)	$\text{Sn}-(\text{C}_6\text{H}_5)_3$
		2.9 (s,4H)	N- CH_2
		2.6 (s,12H)	N- CH_3
$\text{Ph}_3\text{SnInBr}_2 \cdot \text{tmen}$	$\text{CD}_3\text{OD}/\text{CDCl}_3$	7.4-7.7 (m,15H)	$\text{Sn}-(\text{C}_6\text{H}_5)_3$
		2.8 (s,4H)	N- CH_2
		2.5 (s,12H)	N- CH_3
$\text{Ph}_3\text{SnInI}_2 \cdot \text{tmen}$	$\text{CD}_3\text{OD}/\text{CDCl}_3$	7.2-7.7 (m,15H)	$\text{Sn}-(\text{C}_6\text{H}_5)_3$
		2.8 (s,4H)	N- CH_2
		2.6 (s,12H)	N- CH_3
$\text{Ph}_3\text{SnIn}(\text{OAc})\text{Cl} \cdot \text{tmen}$	CDCl_3	7.2-7.7 (m,15H)	$\text{Sn}-(\text{C}_6\text{H}_5)_3$
		2.8 (s,4H)	N- CH_2
		2.7 (s,12H)	N- CH_3
		2.1 (s,3H)	$\text{O}_2\text{C}-\text{CH}_3$
$\text{Ph}_3\text{SnIn}(\text{OAc})\text{Br} \cdot \text{tmen}$	CDCl_3	7.2-7.7 (m,15H)	$\text{Sn}-(\text{C}_6\text{H}_5)_3$
		2.8 (s,4H)	N- CH_2
		2.6 (s,12H)	N- CH_3
		2.1 (s,3H)	$\text{O}_2\text{C}-\text{CH}_3$
$\text{Ph}_3\text{SnIn}(\text{OAc})\text{I} \cdot \text{tmen}$	CDCl_3	7.3-7.9 (m,15H)	$\text{Sn}-(\text{C}_6\text{H}_5)_3$
		2.7 (s,4H)	N- CH_2
		2.6 (s,12H)	N- CH_3
		2.1 (s,3H)	$\text{O}_2\text{C}-\text{CH}_3$

$\text{Et}_4\text{N}[\text{Ph}_3\text{SnInCl}_3]$	$(\text{CD}_3)_2\text{SO}$	7.4-7.9 (m, 15H)	$\text{Sn}-(\text{C}_6\text{H}_5)_3$
		3.2 (q, 8H)	N- CH_2
		1.3 (t, 12H)	N- CH_3

(a) m = multiplet; q = quartet; s = singlet; t = triplet. Integrated intensities in parentheses.

Excess 1,2-C₂H₄Br₂ was removed from the filtrate by evaporation *in vacuo* to leave a colourless solid identified as Ph₃SnBr. The ¹H NMR (dmsO-d₆) showed resonances between 7.3-7.7 ppm due to the phenyl ring. This was supported by the infrared spectrum which had bands between 3100 and 3000 cm⁻¹ assigned to the aromatic C-H stretching vibration. Another diagnostic band in the infrared spectrum was in region between 800 and 650 cm⁻¹, with a strong band appearing at 697 cm⁻¹ confirming the presence of a monosubstituted benzene ring. The mass spectrum in the FD mode has a molecular ion peak (plus a manifold of isotopic peaks). There were minor peaks at m/e 352 corresponding to m-77, and at m/e = 257 (m-144). Analysis Found: Sn = 27.9%, Br = 19.0%, Calc: Sn = 27.6%, Br = 18.6%.

2.2.3 Other Systems

(i) Reaction of InBr with Ph₂BBr: 0.59 g of InBr (3.0 mmol) was suspended in 25 mL of toluene. The suspension was cooled with stirring to -20°C, at which point tmen (2 mL, 13 mmol) was syringed in, producing a reddish solution; 0.74 g of Ph₂BBr (3.0 mmol) in 25 mL of toluene was then added dropwise to the solution over a period of 1 h. The solution has a yellowish tinge at this stage, and stirring was continued for another hour after which the cooling bath was slowly removed. As the solution warmed up deposition of a greyish white product began. Stirring was continued at room temperature for a further 2 h, and the greyish white precipitate was then filtered, washed twice with 10 mL portions of benzene and dried *in vacuo* overnight.

The ^1H NMR of the precipitate in dmsO-d_6 showed resonances between 7.2-7.5 ppm (m, 10H) which were assigned to the aromatic protons, and singlets at 2.9 ppm (4H) and 2.7 ppm (12H) due respectively to the methylene and methyl protons of the tmen ligand. These assignments were supported by the infrared spectrum where vibrations due to both aromatic C-H and alkyl C-H were observed in the 3100-2800 cm^{-1} region. A strong band at 1420 cm^{-1} was assigned to the C-N vibration of the tmen ligand. Based on the spectroscopic evidence and the analytical data, the product obtained was formulated as $(\text{Ph}_2\text{BInBr.tmen})_n$. (See discussion below.) Analysis Found: C = 45.61%, H = 5.88%, N = 5.87%, In = 24.45%, Br = 16.94%. Calc: C = 45.44%, H = 5.51%, N = 5.88%, In = 24.13%, Br = 16.80%.

(ii) Reactions of InX (X = Cl, Br, I) with Me_3SnCl , Ph_3SnH , Ph_3GeCl , Ph_3PbCl : Equimolar quantities (ca. 3 mmol) of InX and each of the substrates were suspended at ca. -40°C in 50 mL of toluene. Excess tmen (2 mL, 13 mmol) was syringed into the reaction mixture. A reddish colour was observed as the InX was gradually drawn into solution. Stirring was continued at this temperature for 1 h, and the cooling bath then slowly removed. As the solution began to warm up deposition of metallic indium began to occur. Stirring was continued at room temperature for another hour, and the greyish black precipitate collected by filtration. In the reaction with Ph_3PbCl the precipitate was found to contain 37% Pb and 10% In. In all other cases, the precipitates were found to contain almost 100% indium, which is indicative of the fact that the indium monohalide has undergone disproportionation yielding metallic indium and indium trihalide (see Chapter 4). Under the circumstances, the desired product could not have been formed and as a result no attempt was made to work on the filtrate.

(iii) Reaction of InCl with Ph₂PCl: 0.45 g of InCl (3 mmol) was suspended in 25 mL of toluene and cooled to ca. -80°C. Excess tmen (2 mL, 13 mmol) was syringed into the reaction mixture to obtain the characteristic red solution. 0.66 g of Ph₂PCl (3 mmol) in 25 mL of toluene was added dropwise over a period of 1 h. The resultant yellow solution was stirred at -80°C for another hour and the cooling bath slowly removed. As the solution warmed up metallic indium was thrown out of the solution. Stirring was continued at room temperature for another hour and the precipitate filtered. The filtrate was left standing in an opened round bottom flask. Colourless crystals began to grow from the filtrate after a day. These were collected, washed with 10 mL of toluene, and dried *in vacuo* overnight. Analyses on indium and chlorine showed them to be absent. The crystals were also found to be soluble in polar solvents. The ¹H NMR in CD₃CN had resonance signals between 7.2-7.7 ppm (m, 20H), at 2.9 ppm (s, 4H) and 2.4 ppm (s, 12H). The last two signals are attributed respectively to the methylene and methyl protons of tmen and the former to aromatic protons. This observation was supported by data from the infrared spectrum where besides the characteristic bands easily assigned to the above described groups there was also a broad band between 2500 and 1800 cm⁻¹ diagnostic of a P-OH vibration. The ³¹P NMR at room temperature showed a broad signal at 17.4 ppm. This signal sharpened to form a singlet at 250°K at 16.5 ppm, pointing to the fact that the molecule exhibited some fluxional behaviour. Despite all this information it is still not easy to propose one particular structure for this molecule. The analytical data found C = 58.32%, H = 6.35% and N = 3.34% gives a ratio of C:H:N as 20.4: 26.4: 1 or ca. 41: 53: 2. Integration of the ¹H NMR signals (see above) gives a total of 36 hydrogen atoms, 20 of which belong to 4 aromatic rings and hence to 24 carbons and 16 to the tmen ligand which has 6 carbon

atoms. By this assessment, we arrive at the following empirical formula $C_{30}H_{36}N_2$. It was uncertain at this point as to what the structure of this unusual compound was. Evidently more work needs to be done to gain a better understanding of this system.

2.3 Results and Discussion

2.3.1 Reaction Pathway

The results demonstrate that there is an efficient reaction between InX ($X = Cl, Br, I$) and Ph_3SnY ($Y = Cl, Br, I, OAc$) to give the corresponding $Ph_3SnIn(X)Y$ compounds, which were isolated as their tmen adducts. The structure of these compounds is discussed below; the main conclusion at this point is that the reaction (2.6)

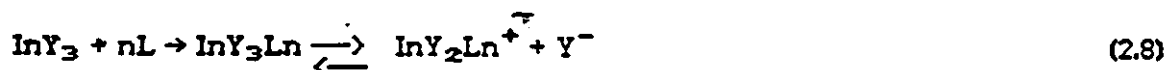


corresponds formally to the oxidative addition of $In^I X$ across the $Sn-Y$ bond.

In discussing the possible reaction pathway for the formation of $Ph_3SnIn(X)Y$ compounds, it is appropriate to draw an analogy from the reaction of InX ($X = Br, I$) with InY_3 ($Y = Cl, Br, I$) which was mentioned in Chapter 1. The stoichiometry of this reaction corresponds formally to the insertion of In^I into an $In^{III}-Y$ bond, eqn. (2.7)



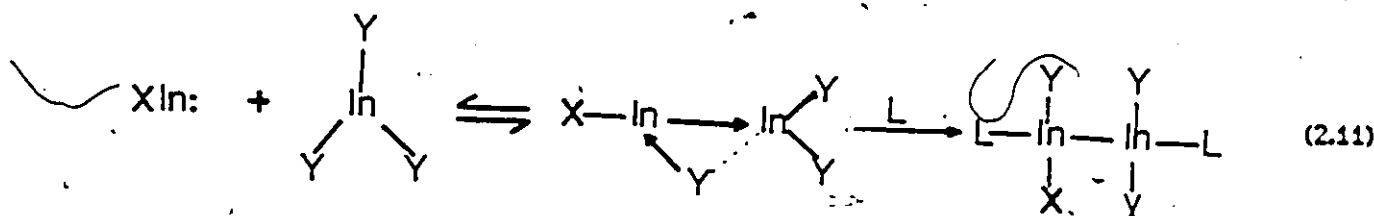
At least two possible pathways can be proposed for the overall reaction. The first of these involves the base-catalyzed dissociation of InY_3 , followed by halide ion transfer to InX , followed by recombination.





The chemical evidence for eqn. (2.8) is that non-aqueous solutions of adducts of indium trihalides do show a significant conductivity, which has been explained in terms of ionization of the type shown,¹¹⁷ while eqn. (2.9) which implies that InX molecules are Lewis acids, is supported by the known existence of InX_2^- anions (X = Cl, Br, I, NCS).

The second pathway depends on the ability of In^{I} species to function as mentioned earlier as both electron pair donors and acceptors. The importance of a lone pair in the structure of cyclopentadienylindium has been demonstrated by calculation¹¹⁸ and it is reasonable to assume a similar feature in indium(I) halides. The alternative description of eqn. (2.7) is then via a concerted process in which donation from InX into the In-Y bond of InY_3 is accompanied by donation from a halide ligand of InY_3 to InX.



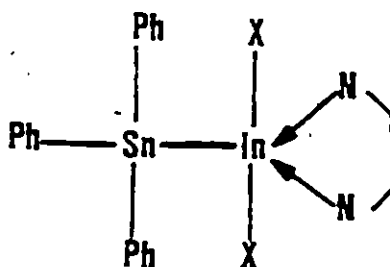
A similar reaction pathway has been proposed to account for the insertion of InX into various symmetric M-M bonded molecules. The postulated pathway, therefore, for the $\text{InX}/\text{Ph}_3\text{SnY}$ system is

compound result in the formation of Ph_3Pb^+ and InCl_2^+ ; the former could then go to Pb^0 with the reaction of InCl_2^+ and unreacted InCl yielding In^0 .

2.3.2 The Structure of $\text{Ph}_3\text{SnIn(X)Y.tmen}$ compounds

It is clear that the products of the reaction of Ph_3SnY with InX in toluene/tmen solution are the $\text{Ph}_3\text{SnIn(Y)X.tmen}$ adducts, which are readily formulated as having an Sn-In bond:

The proposed structure of one of these products, when $X = Y = \text{Cl, Br, I}$ can be represented as follows



The compounds described above can be regarded formally as intermediate between Ph_6Sn_2 and $\text{In}_2\text{X}_4.2\text{tmen}$, both of which are M-M bonded, and the analysis of the vibrational spectra relies on published information on these systems.^{93,120}

The vibrational spectroscopic data and Raman data are presented in Tables 2.3 and 2.4. In each of the $\text{Ph}_3\text{SnIn(Y)X.tmen}$ compounds, there are weak bands in the $400\text{--}500\text{ cm}^{-1}$ region in the infrared assigned to $\nu(\text{In-N})$ modes, although exact identification is hindered by the dominant Sn-Ph band at $\sim 445\text{ cm}^{-1}$ (vs). The $\nu(\text{In-X}_2)$ vibrations are then identified at $296s + 275sh$ (Cl), $212s + 195sh$ (213,189 Ra) (Br) and $165m + 158m$ (cm^{-1}) (I), all in good agreement with the spectra of $\text{In}_2\text{X}_4.2\text{tmen}$. In the salt $\text{Et}_4\text{N}(\text{Ph}_3\text{SnInCl}_3)$, the $\nu(\text{In-Cl})$ modes are identified at $330m + 302m$ (cm^{-1}), higher than in the $\text{In}_2\text{Cl}_6^{2-}$ anion which appear at $292s + 284sh$ (cm^{-1}), but close to the values of $330s + 320sh$ (cm^{-1}) reported

for InCl_3Br^- .¹²¹ The various Sn-Ph modes in these compounds are little changed from those in the parent Ph_3SnX compounds. The Raman spectra of some of these compounds (see Table 2.4) had a strong emission at ca. 148 cm^{-1} which has been assigned to $\nu(\text{Sn-In})$.

The molar conductivities of these compounds are close to zero, so that the formulation as neutral Sn-In bonded species is supported. Tin is four-coordinated, while indium is five-coordinate with an InSnX_2N_2 kernel, analogous to the coordination in $\text{In}_2\text{X}_4\cdot 2\text{tmen}$ ($\text{InIn}^1\text{X}_2\text{N}_2$). The compounds therefore formally involve tin(III) and indium(II).

2.3.3 The Structure of $\text{Ph}_3\text{SnIn}(\text{OAc})\text{X}\cdot\text{tmen}$ Compounds

The spectra and structure of the acetato compounds $\text{Ph}_3\text{SnIn}(\text{X})\text{OAc}\cdot\text{tmen}$ are best discussed in terms of Ph_3SnOAc and Me_2InOAc . The $\nu(\text{C-O})$ vibrations in these compounds are at $1544\text{vs} + 1428\text{vs cm}^{-1}$ and $1530\text{s} + 1445\text{s cm}^{-1}$, respectively, and in the latter case crystallographic studies have shown that acetate ligand is bidentate.¹²² The present compounds typically show these same vibrations at $1550\text{vs} + 1430\text{vs}$, so that bidentate acetate is present. Weak bands at $300\text{-}320\text{ cm}^{-1}$ are then reasonably assigned to $\nu(\text{In-O})$. The $\nu(\text{In-X})$ modes are at 297w (Cl) and 205m cm^{-1} (Br; 209 cm^{-1}); but no $\nu(\text{In-I})$ mode could be detected. The remaining features of the spectra are essentially identical to those discussed above, except that the $\nu(\text{In-N})$ region is effectively blanked by strong bands at 450 and 570 cm^{-1} . The molar conductivity of the iodo derivative in both dmf ($67\text{ ohm}^{-1}\text{cm}^2\text{mol}^{-1}$) and nitromethane ($70\text{ ohm}^{-1}\text{cm}^2\text{mol}^{-1}$) shows that the compound is a 1:1 electrolyte in these solvents. The absence of the $\nu(\text{In-I})$ band in the infrared spectrum suggests that the correct formulation for both solid and solution states is:

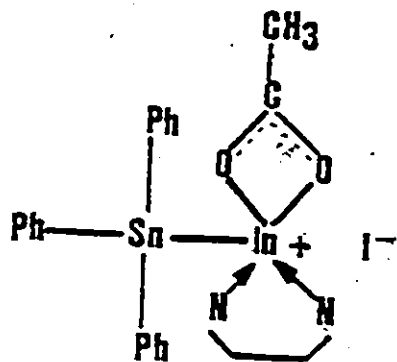
TABLE 2.3

FAR INFRARED SPECTRA OF $\text{Ph}_3\text{SnInX}_2$ COMPOUNDS (cm^{-1})

Compound	$\nu(\text{Sn-Ph})$	$\nu(\text{In-X})$	$\nu(\text{In-N})$	$\nu(\text{Sn-In})$
$\text{Ph}_3\text{SnInCl}_2 \cdot \text{tmen}$	446(s)	295(s)	495(m)	145
	442(sh)		468(m)	
	258(s)		455(m)	
$\text{Ph}_3\text{SnInBr}_2 \cdot \text{tmen}$	450(s)	210(s)	492(m)	153
	442(sh)	(213)	465(m)	
	258(s)	196(sh)		
		(189)		
$\text{Ph}_3\text{SnInI}_2 \cdot \text{tmen}$	445(s)	165(m,br)	500(m,br)	-
	258(s)			
$\text{Ph}_3\text{SnIn(OAc)Cl} \cdot \text{tmen}$	430(s)	297(s,br)	482(m)	-
	260(s)		384(m)	
$\text{Ph}_3\text{SnIn(OAc)Br} \cdot \text{tmen}$	448(s)	206(s)	484(m)	-
	249(s)	(209)	385(m)	
$\text{Ph}_3\text{SnIn(OAc)I} \cdot \text{tmen}$	446(s)	-	500(m)	
	272		382(m)	
$\text{Et}_4\text{N[Ph}_3\text{SnInCl}_3]$	448(s)	392(s,br)	498(m)	
	260(s)		381(m)	

TABLE 2.4
RAMAN EMISSIONS ASSIGNED AS $\nu(\text{Sn-In})$ IN TMEN
ADDUCTS OF $\text{Ph}_3\text{SnIn}(\text{Y})\text{X}$ (cm^{-1})

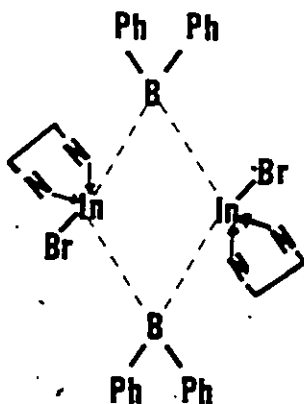
Compound	Sn-In
$\text{Ph}_3\text{SnInCl}_2$	147
$\text{Ph}_3\text{SnInBr}_2$	148
$\text{Ph}_3\text{SnInI}_2$	148
$\text{Ph}_3\text{SnIn}(\text{OAc})\text{Cl}$	149
$\text{Ph}_3\text{SnIn}(\text{OAc})\text{Br}$	149



In contrast, the chloro compound is a non-conductor in dmf (Λ_0 10 $\text{ohm}^{-1}\text{cm}^2\text{mol}^{-1}$), while the bromo analogue undergoes some dissociation in polar solvents (Λ_0 27 $\text{ohm}^{-1}\text{cm}^2\text{mol}^{-1}$ in dmf, 34 $\text{ohm}^{-1}\text{cm}^2\text{mol}^{-1}$ in MeNO_2) so that both these compounds can be formulated as neutral species in the solid state. The difference between the iodo compounds, and the chloro- or bromo-acetato species, probably lies in the difficulty of accommodating the larger iodine atom in the coordination kernel of $\text{SnInO}_2\text{N}_2\text{X}$.

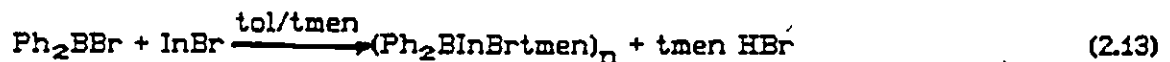
2.3.4 The Structure of $\text{Ph}_2\text{BInBr.tmen}$

The product obtained from the reaction of InBr with Ph_2BBr was formulated as $(\text{Ph}_2\text{BInBr.tmen})_n$ and a proposed structure as below.



where $n = 2$, although higher values for n cannot be excluded. An identical structure has been proposed for $[(\text{Ph}_3\text{P})_2\text{NiBPh}_2 \cdot \frac{1}{2}\text{Et}_2\text{O}]_2$ which was obtained together with $[(\text{Ph}_3\text{P})_2\text{NiBr}]_2$ by the reaction of Ph_2BBr with $(\text{Ph}_3\text{P})_2\text{NiC}_2\text{H}_4$.¹²³

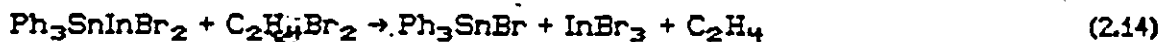
The proposed structure for the indium analogue seems justified on the basis of the analytical and spectroscopic data. The infrared spectrum for example, does not contain any bands near 800 cm^{-1} from the B-Br group but does not contain absorptions between 3000 and 2800 cm^{-1} arising from the C-H vibrations from the Ph_2B group and the tmen ligand. Due to the low solubility of the complex we were unable to obtain a concentrated solution to do ^{11}B NMR studies. The overall reaction could therefore be presented as



The fate of the Br^- could be to form a salt with the tmenH^+ after first being converted to HBr by moisture from an incompletely dried solvent.

2.3.5 The reaction of $\text{Ph}_3\text{SnInBr}_2$ with $1,2\text{-C}_2\text{H}_4\text{Br}_2$: The reactivity of Sn-In bonded compound

This reaction, as mentioned earlier, was used to test the reactivity of the complex. As our results showed this reaction (eqn. 2.13) led to the homolytic cleavage of the Sn-In bond.



Similar cleavage of related metal-metal bonded complexes has been observed.¹²⁴ It appears, therefore, that reaction 2.14 is a general one and may be useful in an analytical sense.

In the context of the present discussion, homolytic cleavage of the Sn-In bond implied disruption such that each metal centre received one of the

electrons from the electron pair that constituted the metal-metal bond. As a result tin(III) was oxidized to tin(IV) and indium(II) to indium(III).

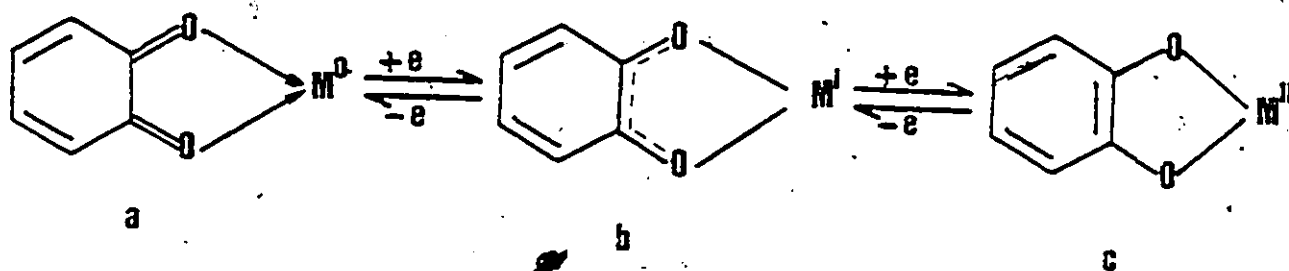
Results presented in this chapter show that indium monohalides oxidatively insert into metal-halogen bonds of some Main Group organometallic compounds. Following earlier work in our laboratory involving the InX/InX_3 systems one can draw some similarities as far as the mechanism of the formation of the insertion products are concerned. It will also be of interest to revisit some of the failed systems in our work with some modifications. The synthetic usefulness of the $\text{InX}/\text{toluene}/\text{tmen}$ system has been mentioned in Chapter 1 and has featured prominently in work in the various chapters of this dissertation. It is worthy to reiterate the fact that temperature plays a critical role in this system as instant disproportionation of the indium monohalide easily occurs at temperatures higher than the stipulated values.¹⁰⁹ This is also a signal as to whether a reaction is proceeding favourably or not. This observation renders the $\text{InX}/\text{toluene}/\text{tmen}$ system very labile and one could consider using different neutral donor ligands like 1,10-phenanthroline or 2,2'-bipyridine which due to their size may help in stabilizing the resultant product.

CHAPTER 3

THE REACTION BETWEEN SnX_2 AND TETRA-HALOGENO-ORTHO-QUINONES FORMATION OF Sn(IV) CATECHOLATES

3.1. Introduction

As mentioned in the previous chapter, a useful method for the synthesis of metal complexes in which the metal is in a high oxidation state is the process of oxidative addition with compounds with the metal in a low oxidation state. The use of orthoquinones as a substrate in these studies is particularly attractive since orthoquinones show redox behaviour at easily accessible and chemically useful potentials. They are also able to fix substrate molecules by donor-acceptor complexation.^{125,126} The metal-quinone interaction can be viewed in terms of three isoelectronic forms related by the distribution of formal charge over chelated ligand and metal ion (see below).



where (a) is the unreduced quinone¹²⁷ (b) the semiquinone¹²⁸ (partially reduced) and (c) the catecholate¹²⁹ (fully reduced) forms.

As shown above, the various bonding descriptions can be induced either chemically or electrochemically by the addition or removal of charge from ligand localized electronic levels by interaction with some external species.

To date, most of the studies in this area has been on the transition metals. There has been several reports of the addition of orthoquinones to transition metals with formal d^{10} ,¹³⁰⁻¹³⁴ d^8 ,^{130,131,135} d^6 ,^{135,136} d^4 ,¹³⁷ and d^2 ,¹³⁸ electron configurations. In all these cases it was established that these complexes undergo a number of well defined, one-electron transfer reactions. In particular, complexes obtained from tetrahalogeno-ortho-quinones undergo one-electron oxidation to give complexes whose properties are indicative of the presence of coordinated semiquinone radicals. These oxidations have been detected by cyclic voltammetry which reveals that electron transfer in each case is reversible.¹³⁹ There is a thorough review of this subject covering all aspects of the chemistry of transition metal-quinone complexes.¹⁴⁰

In the Main Group area there has been very limited work on the elements of groups III and IV in their low oxidation states.¹⁴¹⁻¹⁴⁴ The lack of soluble indium(I) compounds could be considered as a factor, but the same cannot be said of tin(II) halides. Most of the benzoquinone complexes of these two Main Group elements as well as that of their congeners have been made by the reaction of the metal halides, organometallic halides,¹⁴⁵ with an alkali metal salt of the fully reduced quinone (i.e., the dianion of the catechol). This method of synthesis has the advantage of using relatively stable starting materials which are readily soluble in common organic solvents. So for the purpose of the further studies of the coordination chemistry of these elements this method of synthesis or any other method which does not involve the use of the low valent state of the element appears satisfactory. On the other hand there is much to be

gained from kinetic and mechanistic studies which should give an understanding of the behaviour of Main Group elements in their lower oxidation states. In general terms the chemistry of the Main Group metals is marked by the existence of oxidation states which differ by the addition or removal of pairs of electrons (e.g. Tl^I/Tl^{III} ; Sn^II/Sn^{IV} ; Bi^{III}/Bi^V ; Po^{II}/Po^{VI}), this has led to a general assumption, in the absence of evidence to the contrary, that redox reactions involve two-electron transfers. This approach has provided a satisfactory although simplified model for processes such as oxidative addition as exemplified by work presented in Chapter 2. In order to establish a mechanistic pathway for the formation of tin(IV) and indium(III) compounds by this process, we have undertaken a series of studies of the redox reaction of InX and SnX_2 .

This Chapter and Chapter 4 deal with the reaction of SnX_2 with some substituted orthoquinones. Our results confirm the difference in the reactivity of these quinones, depending upon the type of substituent on the quinone ring. The halogeno-substituted quinones were found to have a high reactivity, and a higher redox potential, attributed to the electron withdrawing effect of the halogens on the ring. The electron donating effect brought about by the alkyl substitution on other quinones lead to lower reactivity, compatible with a lower redox potential. This difference in reactivity of these quinones has been fully exploited in the course of our work, and will be discussed in detail later.

3.2 Experimental

3.2.1 The formation of $Y_4C_6O_2SnX_2$

(i) A solution of $SnCl_2$ (0.39 g, 2 mmol) and tetrachloro-o-quinone (0.50 g, 2 mmol) in acetone (50 mL) was stirred mechanically for 1 h at room temperature to give a yellow-orange solution. Addition of phen (0.31 g, 2 mmol) precipitated $Cl_4C_6O_2SnCl_2$.phen in quantitative yield. Later work showed that the synthesis is more conveniently carried out by refluxing equimolar quantities of $SnCl_2$, $Cl_4C_6O_2$ (or $Br_4C_6O_2$) and phen in acetone for 1 h, and this technique was used in the preparation of the analogous compounds listed in Table 3.1, since the direct reaction at room temperature is unsatisfactory with $SnBr_2$ or SnI_2 . The yellow-orange solids were collected, washed successively with acetone (2 x 20 mL) and n-pentane (20 mL), and dried *in vacuo*.

(ii) $Cl_4C_6O_2SnI_2$.phen can also be prepared by refluxing tin metal (0.4g, 2.4 mmol), iodine (0.86g, 3.4 mmol calculated as I_2) and $Cl_4C_6O_2$ (0.83g, 3.4 mmol) in toluene (50 mL) for 3 h, by which time the tin had dissolved to give a light green solution. An equimolar quantity of phen was then added, and refluxing stopped. The mixture was stirred for 1 h as it cooled; the orange solid which formed was then collected and washed as described above.

(iii) $SnCl_2$ (0.39 g, 2 mmol) was suspended in toluene (50 mL) containing an equimolar quantity of $Cl_4C_6O_2$ (0.5 g), and tmen (0.35 g, 3 mmol) added to the red solution. The mixture was stirred at room temp. for 16 h, and then filtered, to give an off-white solid which was washed with toluene and then n-pentane, and dried *in vacuo*. This solid was identified as $Cl_4C_6O_2SnCl_2$.tmen.

TABLE 3.1
ANALYTICAL RESULTS

Compound	Found/Calcd (%)				Molar mass
	Sn	C	H	N	
$\text{Cl}_4\text{C}_6\text{O}_2\text{SnCl}_2\cdot\text{phen}$	19.0(19.3)	36.0(35.1)	1.69(1.3)	4.6(4.6)	616
$\text{Cl}_4\text{C}_6\text{O}_2\text{SnBr}_2\cdot\text{phen}$	14.4(15.0)	27.7(27.2)	1.2(1.0)	3.3(3.5)	704
$\text{Cl}_4\text{C}_6\text{O}_2\text{SnI}_2\cdot\text{phen}$	16.9(16.8)	-	-	-	-
$\text{Br}_4\text{C}_6\text{O}_2\text{SnCl}_2\cdot\text{phen}$	13.7(13.5)	-	-	-	794
$\text{Br}_4\text{C}_6\text{O}_2\text{SnBr}_2\cdot\text{phen}$	15.0(14.9)	-	-	-	-
$\text{Br}_4\text{C}_6\text{O}_2\text{SnI}_2\cdot\text{phen}$	11.8(12.2)	-	-	-	-
$\text{Cl}_4\text{C}_6\text{O}_2\text{SnCl}_2\cdot\text{tmen}$	21.3(21.5)	-	-	-	552
$\text{Cl}_4\text{C}_6\text{O}_2\text{SnCl}_2\cdot\text{tmen}\cdot 2\text{CH}_3\text{OH}$	18.8(19.3)	-	-	-	-
$\text{Cl}_4\text{C}_6\text{O}_2\text{Sn}(\text{OCH}_3)_2$	27.6(27.8)	-	-	-	-
$\text{Cl}_4\text{C}_6\text{O}_2\text{SnCl}_2\cdot\text{tmen}\cdot\text{C}_2\text{H}_5\text{OH}$	19.8(19.9)	-	-	-	-
$\text{Cl}_4\text{C}_6\text{O}_2\text{Sn}(\text{OC}_2\text{H}_5)_2$	25.9(26.1)	-	-	-	-
$(\text{tmenE})_2[\text{Sn}(\text{O}_2\text{C}_6\text{Cl}_4)_3]$	10.6(10.9)	32.3(33.0)	3.3(3.1)	5.1(5.1)	-

on the basis of metal analysis, infrared and ^1H nmr spectroscopy. Repetition of this procedure with $\text{Br}_4\text{C}_6\text{O}_2$ in place of the tetrachloro-o-quinone gave as the final insoluble product a beige-coloured solid which contained tmen and the $\text{Br}_4\text{C}_6\text{O}_2^{2-}$ ligand, but did not correspond analytically to $\text{Br}_4\text{C}_6\text{O}_2\text{SnCl}_2\cdot\text{tmen}$ (Calc'd Sn 16.3%. Found Sn 24.7%). ^1H NMR, singlets at 2.72 and 3.33 ppm from Me_4Si , in d_6 -dmsO.

(iv) A mixture of SnCl_2 and $\text{Cl}_4\text{C}_6\text{O}_2$ (quantities as in (c)) was dissolved in acetone, and tmen (0.35 g, 3 mmol) added; the solution darkened in colour, and a slight cloudiness developed. After 1 h, the now pale yellow solution was filtered to remove a white solid, and the solution evaporated *in vacuo* to yield crystals of $\text{Cl}_4\text{C}_6\text{O}_2\text{SnCl}_2\cdot\text{tmen}$. The white solid collected by filtration contained Sn (32%) and $\text{Cl}_4\text{C}_6\text{O}_2$, but no tmen. This material analytically corresponds to $(\text{Cl}_4\text{C}_6\text{O}_2\text{Sn})_n$.

(v) Stannous chloride (0.56 g, 3.0 mmol) was dissolved in dry methanol (50 mL), and tmen (0.35 g, 3.0 mmol) added dropwise to the stirred solution. The slight cloudiness disappeared on warming the solution. A methanol solution of $\text{Cl}_4\text{C}_6\text{O}_2$ (0.73 g, 3.0 mmol in 50 mL) was added dropwise over 1 h. Some slight precipitation was obvious at this point, and on refluxing over 4 h considerable quantities of solid were thrown down. This solid was collected, washed with hot methanol (2 x 20 mL) and dried *in vacuo*. This material was identified as $\text{Cl}_4\text{C}_6\text{O}_2\text{SnCl}_2\cdot\text{tmen}\cdot 2\text{CH}_3\text{OH}$ (A) on the basis of metal analysis (Table 3.1), infrared and ^1H nmr spectroscopy (Table 3.2). Yield 0.87 g. No spectroscopic or weight changes were detected after heating the substance *in vacuo* (60° , 6h).

TABLE 3.2

 ^1H NMR SPECTRA OF TIN(IV) DERIVATIVES OF $\text{p-Cl}_4\text{C}_6\text{O}_2$ (PPM, RELATIVE TO Me_4Si)

Compound (a)	Chemical Shift	Assignment
1,10-phenanthroline (b)	9.2, (m,2H)	C2,C9 (phen)
	7.7 (m,2H)	C3,C8
	8.4 (m,2H)	C4,C7
	7.9 (m,2H)	C5,C6
$\text{Cl}_4\text{C}_6\text{O}_2\text{SnCl}_2\cdot\text{phen}$	9.25 (m,2H)	C2,C9 (phen)
	8.00 (m,2H)	C3,C8
	8.70 (m,2H)	C4,C7
	8.25 (m,2H)	C5,C6
$\text{Br}_4\text{C}_6\text{O}_2\text{SnCl}_2\cdot\text{phen}$	9.25 (m,2H)	C2,C9 (phen)
	8.20 (m,2H)	C3,C8
	8.75 (m,2H)	C4,C7
	8.55 (m,2H)	C5,C6
$\text{Cl}_4\text{C}_6\text{O}_2\text{SnCl}_2\cdot\text{tmen}$	2.93(s,1H)	CH_2 tmen
	2.50 (s,3H)	CH_3
$\text{Cl}_4\text{C}_6\text{O}_2\text{SnCl}_2\cdot\text{tmen}\cdot 2\text{CH}_3\text{OH}$	6.35 (br,2H)	CH_3OH
	3.20 (s,6H)	CH_3OH
	2.95 (s,4H)	CH_2
	2.60 (s,12H)	CH_3 tmen
$\text{Cl}_4\text{C}_6\text{O}_2\text{SnCl}_2(\text{OCH}_3)_2$	3.25 s	CH_3

$\text{Cl}_4\text{C}_6\text{O}_2\text{SnCl}_2 \cdot \text{tmen} \cdot \text{C}_2\text{H}_5\text{OH}$	6.15 (br, 1H)	$\text{C}_2\text{H}_5\text{OH}$
	3.45 (q, 2H)	$\text{CH}_3\text{CH}_2\text{OH}$
	2.90 (s, 4H)	CH_2 tmen
	2.55 (s, 12H)	CH_3
	1.05 (t, 3H)	$\text{CH}_3\text{CH}_2\text{OH}$
$(\text{tmenH})_2[\text{Sn}(\text{O}_2\text{C}_6\text{Cl}_4)_3]$	2.90 (s, 2H)	CH_2N
	3.60 (t, 2H)	CH_2N^+
	2.45 (s, 6H)	CH_3N
	3.20 (s, 6H)	CH_2N^+
	5.50 (br, 1H)	N-H

(a) All compounds run in d_6 -dmsO solution.

(b) In d_6 -acetone; results from ref. 146.

The filtrate from this reaction was taken to dryness *in vacuo*, giving a mixture of colourless and yellow powders. The former was found to be insoluble in most common organic solvents, and the compounds were separated by treatment with hot acetonitrile. The insoluble colourless solid (weight 0.24 g) was identified as the salt $(\text{tmenH}_2)\text{Cl}_2$ (B) (Analysis Found Cl 37.4, calc'd 37.5%). ^1H nmr in D_2O showed singlets at 3.7 (4H) and 3.0 (12H) ppm from internal sodium 3-(trimethylsilyl)propionate. The molar conductivity of a mmol solution in H_2O was $209 \text{ ohm}^{-1} \text{ mol}^{-1} \text{ cm}^2$, slightly less than the classical value of $240 \text{ ohm}^{-1} \text{ mol}^{-1} \text{ cm}^2$ for 2:1 electrolytes.

*The acetonitrile extract of the above solid mixture was subsequently taken to dryness *in vacuo*. Analysis and spectroscopy showed that this compound is $\text{Cl}_4\text{C}_6\text{O}_2\text{Sn}(\text{OCH}_3)_2$ (C).

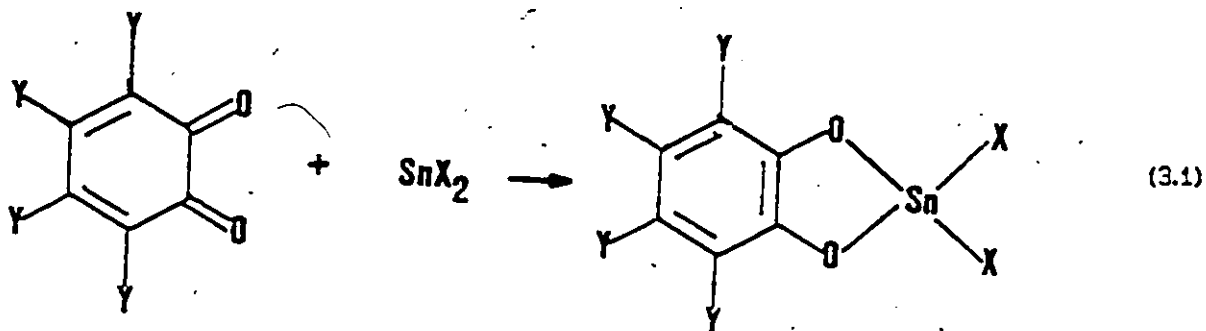
The total mass of products A, B and C was 1.72 g, to be compared with the 1.64 g of reactants used. After making appropriate allowance for the MeOH and MeO incorporated into A and C, the mass balance accounts for 94% of the starting materials.

(vi) Stannous chloride (0.50 g, 2.6 mmol) and $\text{Cl}_4\text{C}_6\text{O}_2$ (0.65 g, 2.6 mmol) were dissolved in dry ethanol (50 mL), and 0.4 mL (2.6 mmol) of tmen added to the pale yellow solution. An instant opalescence was followed by the formation of a white precipitate. The mixture was refluxed for 12 h under nitrogen, after which the precipitate was collected by filtration, washed with hot ethanol (2 x 20 mL) and dried overnight *in vacuo*. This solid is $\text{Cl}_4\text{C}_6\text{O}_2\text{SnCl}_2 \cdot \text{tmen} \cdot \text{C}_2\text{H}_5\text{OH}$. The filtrate was treated by the method described above for the methanol solution, and the products identified were $(\text{tmeOH}_2)\text{Cl}_2$ and $\text{Cl}_4\text{C}_6\text{O}_2\text{Sn}(\text{OC}_2\text{H}_5)_2$.

3.3 Results and Discussion

3.3.1 Preparative

The six compounds $Y_4C_6O_2SnX_2 \cdot phen$ ($X=Cl, Br, I$; $Y = Cl, Br$) are the result of adduct formation by the dihalogenotin(IV)catecholates species, which are themselves generated by the redox reaction



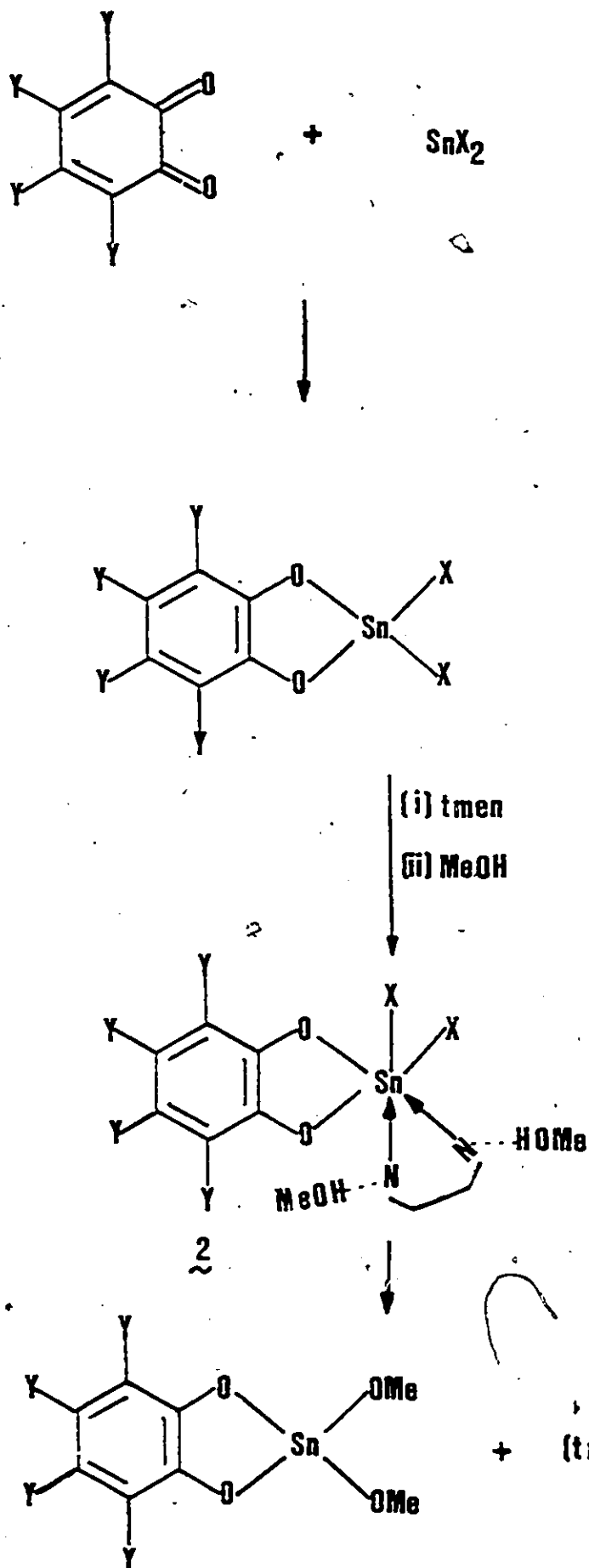
Reaction 3.1 is formally equivalent to oxidative addition. Given our results on indium(I) systems (see chapter 5), and the work on transition metals such as the copper complexes of semiquinones, it seems very probable that reaction 3.1 actually proceeds via successive one-electron transfers. Due to the instantaneous nature of the reactions being discussed in this chapter, we were not able to conduct a detailed study by ESR spectroscopy. It is clear that the mechanism proposed to account for the insertion of InX into $M-M$ and $M-X$ bonds cannot apply in the case of eqn. 3.1, since neither the ground state nor any readily accessible excited state of the quinone can act as an electron pair acceptor, detailed discussion of this point is given in later Chapters.

The $Y_4C_6O_2SnX_2$ molecules identified as the primary product in eqn. 3.1 are clearly Lewis acids, in keeping with the presumption that the coordination

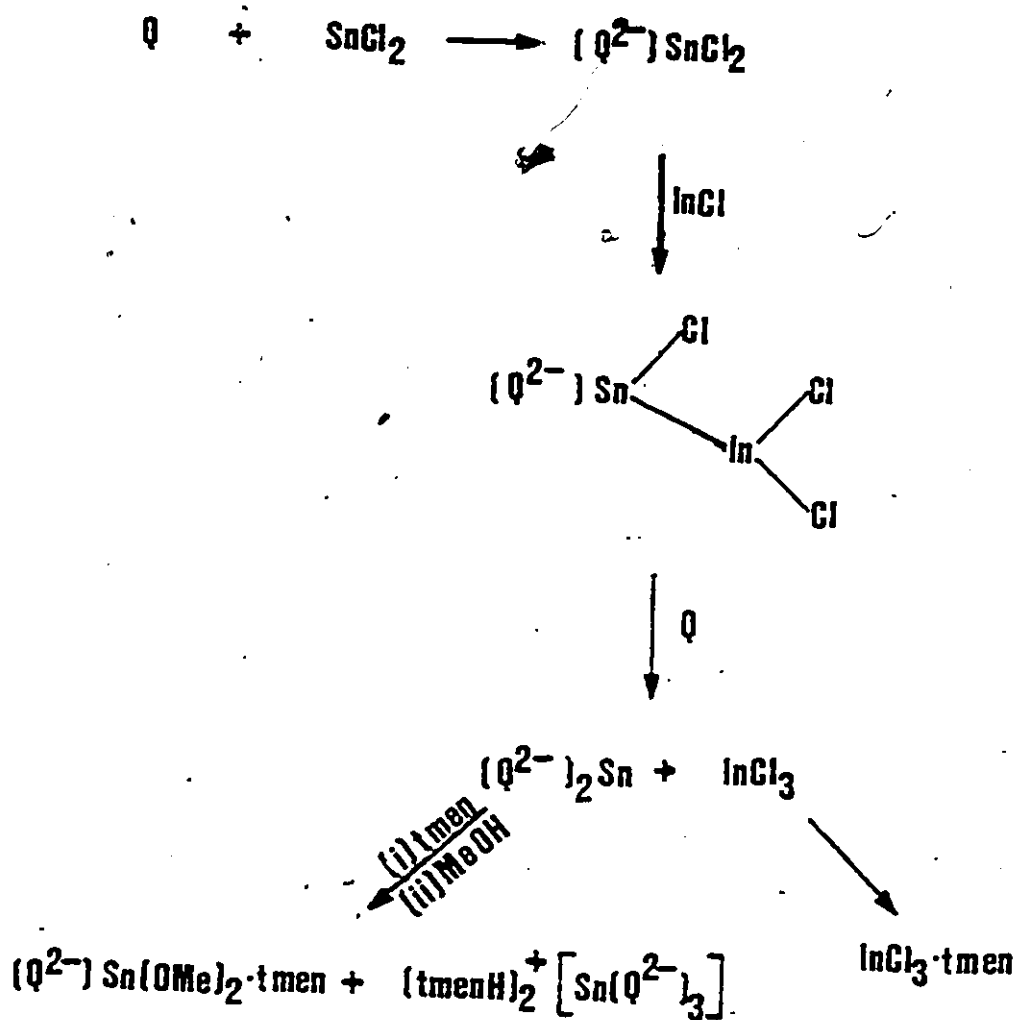
number at tin is four. The adducts formed with 1,10-phenanthroline are thermally stable, and only slightly soluble in most common organic solvents. The tmen derivatives of $\text{Cl}_4\text{C}_6\text{O}_2\text{SnCl}_2$ are more labile, and the reactions leading to these compounds merit some discussion. The preparations in either toluene or acetone give the expected 1:1 adduct, but in methanol or ethanol the product is solvated by strongly bound ROH which is probably hydrogen-bonded either to a chloride ligand or to an oxygen atom of the catecholate ligand. The other products obtained from this reaction mixture are the salt $(\text{tmenH}_2)\text{Cl}_2$ and the tin alkoxide derivatives $\text{Cl}_4\text{C}_6\text{O}_2\text{Sn}(\text{OR})_2$. On the basis of the experimental evidence, we suggest the reaction sequence presented in Scheme 1.

This sequence implies that the difference between CH_3OH and $\text{C}_2\text{H}_5\text{OH}$ resides in the composition of the solvate 2 formed in the second step. The formation of such solvates, and the subsequent intramolecular reaction, are common features of tin(IV) chemistry. The products $\text{Cl}_4\text{C}_6\text{O}_2\text{Sn}(\text{OR})_2$ may be stabilized by intermolecular Sn...O bonding.

The unexpected formation of the $[\text{Sn}(\text{O}_2\text{C}_6\text{Cl}_4)_3]^{2-}$ anion took place during experiments designed to investigate the insertion of InCl into the Sn-Cl bond of $\text{Cl}_4\text{C}_6\text{O}_2\text{SnCl}_2$, following earlier work on such insertion reactions between InX and Ph_3SnX (Chapter 2). The following sequence is in keeping with the known reactions of SnX_2 and $\text{Cl}_4\text{C}_6\text{O}_2$ (= Q), as demonstrated in this work, and of InX and InX_3 :



SCHEME 1



3.3.2 Spectroscopic Results

The most informative region of the infrared spectra is the $\nu(C=O)$ mode, which occurs at ca. 1700 cm^{-1} (vs) in both tetrahalogeno-quinones. (See Table 3.3.) This band is conspicuously absent in all the tin compounds prepared in this work. This band is replaced by $\nu(C=O)$ vibrations at $1430m + 1240s\text{ cm}^{-1}$, indicating the presence of the $o\text{-Cl}_4\text{C}_6\text{O}_2^{2-}$ ligand. The phenanthroline adducts exhibited multiple bands in the region between 1640 and 1520 cm^{-1} and they could be assigned to the C=C stretching vibrations from the catecholato ring

TABLE 3.3

DIAGNOSTIC IR ABSORPTIONS OF ADDUCTS OF Sn(IV) CATECHOLATES

<u>Compound</u>	<u>Absorptions</u>	<u>Assignment</u>
$Y_4C_6O_2$	1673(s)	C=O
	1591(s)	C=C
$Y_4C_6O_2SnX_2.phen$	3100 (m,w)	C-H (phen)
	1440 (s,br), 1244(m,s)	C-O
$Y_4C_6O_2SnX_2.tmen$	2990 (m,br)	C-H(tmen)
	1450 (s,br), 1250 (m,s)	C-O
Y = Cl, Br		
X = Cl, Br, I		

and from the phenanthroline. An aromatic C-H vibration could also be assigned to the band at 3100 cm^{-1} . The tmen adduct, beside the characteristic C-O vibration, had medium bands between 3000 and 2800 cm^{-1} assigned to the alkyl C-H vibration. The $\nu(\text{C}=\text{C})$ vibrations were obscured by the broadness of the strong band at 1440 cm^{-1} which again could be a combination of the $\nu(\text{C}-\text{N})$ vibration of the tmen ligand the $\nu(\text{C}-\text{O})$ of the catecholato ligand.

The ^1H NMR spectra have been noted in the Experimental section and are tabulated in Table 3.1. The symmetric nature of the resonances show that the catecholato ligands are symmetrically bonded to the tin atom, and this symmetry has been confirmed by the ^{13}C NMR spectral data. These are summarized in Table 3.4; each signal recorded appears as a sharp singlet. There are significant changes in the ^{13}C resonance spectrum of $\text{Cl}_4\text{C}_6\text{O}_2$ following reduction from the quinone to the catechol form, and these same changes are apparent in the spectra of the neutral adducts with tmen or phen, and in the $[\text{Sn}(\text{O}_2\text{C}_2\text{Cl}_4)_3]^{2-}$ anion, again confirming the presence of the reduced form in each of these species. Smaller changes are observed in the spectrum of tmen or phen upon coordination, or on formation of the protonated species. It is rather surprising that tmenH⁺ cation shows two sets of resonances, and it appears that the hydrogen-bonding identified in the solid state (Fig. 3.1) persists in solution, thus removing the degeneracy observed in the spectrum of the free ligand.



TABLE 3.4

 ^{13}C NMR SPECTRA OF TIN(IV) DERIVATIVES OF $\text{p-Cl}_4\text{C}_6\text{O}_2$ (PPM, RELATIVE TO Me_4Si)

Compound	Solvent	$\text{Cl}_4\text{C}_6\text{O}_2$	tmen	phen	other
$\text{p-Cl}_4\text{C}_6\text{O}_2$	CDCl_3	131.9	C4,C5		
		143.7	C3,C6		
		168.8	C1,C2		
$\text{p-Cl}_4\text{C}_6(\text{OH})_2^{(a)}$	$(\text{CD}_3)_2\text{CO}$	119.5	C4,C5		
		122.5	C3,C6		
		143.0	C1,C2		
tmen	neat		45.2	CH_2	
			57.6	CH_3	
phen	dmsO-d_6			123.0	C5,C6
				126.4	C4a,C6a
				128.1	C4,C7
				135.3	C3,C8
				145.4	C4b,C6b
				149.7	C2,C9
$\text{Cl}_4\text{C}_6\text{O}_2\text{SnCl}_2\text{.phen}$	dmsO-d_6	113.9	C4,C5	124.1	C5,C6
		115.0	C3,C6	126.1	C4a,C6a
		146.7	C1,C2	128.1	C4,C7
				137.5	C3,C8

						139.7	C4b, C6b
						145.0	C2,C9
$\text{Cl}_4\text{C}_6\text{O}_2\text{SnCl}_2 \cdot \text{tmen} \cdot \text{EtOH}$	dms o-d_6	115.6	C4,C5	42.9	CH_2	18.0	$\text{CH}_3\text{CH}_2\text{OH}$
		117.0	C3,C6	50.9	CH_3	56.1	$\text{CH}_3\text{CH}_2\text{OH}$
		148.5	C1,C2				
$(\text{tmenH})_2[\text{Sn}(\text{O}_2\text{C}_6\text{Cl}_4)_3]$	dms o-d_6	115.9	C4,C5	44.0	CH_2^+N		
		117.2	C3,C6	47.4	CH_2N		
		149.0	C1,C2	53.7	CH_3N^+		
				54.9	CH_3N		

(a) Results from ref. 147.

3.4 X-Ray Studies: The molecular and crystal structure of $(tmenH)_2[Sn(O_2C_6Cl_4)_3]$

A single crystal of $(tmenH)_2[Sn(O_2C_6Cl_4)_3]$ (1) was mounted along the largest dimension, and the cell parameters obtained from 15 strong reflections with $15 < 2\theta < 30^\circ$. Data were collected on a Syntex P2₁ diffractometer following the procedure described in Chapter 1. The intensities of three monitored reflections did not change significantly during data collection. The data were corrected for Lorentz and polarization effects, no absorption correction was deemed necessary because of the low absorption coefficient. Details of the X-ray data collection are given in Table 3.5.

The systematic absences (hkl , $h + k = 2n + 1$; $h 0 l$, $l = 2n + 1$) indicated the space groups C2/c or Cc. The former was used and later assumed to be correct because of the successful refinement of the structure. The position of the tin atom was obtained from a sharpened Patterson synthesis using SHELX, 1976, and was found to be on a twofold axis. The positions of remaining non-hydrogen atoms were determined from a difference Fourier map. The structure was refined anisotropically using full-matrix least squares methods and, the refinement converged at $R = (\sum ||F_o| - |F_c||) / \sum |F_o| = 0.0369$. Hydrogen atoms were included in subsequent refinement in ideal positions (C-H 0.95 Å and CCH 109.5°), leading to the final values $R = 0.0324$ and $R_w = [E_w \Delta^2 / \sum_w F_o^2]^{1/2} = 0.0378$. The function $(|F_o| - |F_c|)^2$ was minimized during least squares refinement; in the final cycles, a weighting scheme of the form $w = 1/[\sigma^2(F) + pF]^2$ was employed, with a final p value of 0.0011. No evidence of secondary extinction was found.

TABLE 3.5

SUMMARY OF CRYSTAL INTENSITY DATA, COLLECTION, AND STRUCTURAL
REFINEMENT FOR $(\text{tmen H})_2[\text{Sn}(\text{O}_2\text{C}_6\text{Cl}_4)_3]$

Cell constants	$\underline{a} = 20.501(8)\text{\AA}$, $\underline{b} = 12.607(3)\text{\AA}$ $c = 17.357(7)\text{\AA}$; $\beta = 113.53(5)^\circ$
Cell volume (\AA^3)	4113(4)
Crystal system	monoclinic
space group	C2/c
Mol. wt.	1090.6
Z, F(000)	4, 2168
ρ_c, ρ_o (g cm^{-3})	1.76, 1.80
Cryst dimens (mm)	0.21 x 0.27 x 0.28
Abs coeff, μ (cm^{-1})	13.33
Radiation	$\text{MoK}\alpha$, $\lambda = 0.71069\text{\AA}$
Monochromator	highly oriented graphite
Temp ($^\circ\text{C}$)	24
2θ angle ($^\circ$)	45
Scan type	coupled θ (crystal)/ 2θ (counter)
Scan width	$K_{\alpha_1} - 1^\circ$ to $K_{\alpha_2} + 1^\circ$
Scan speed ($^\circ\text{min}^{-1}$)	variable, 2.02-4.88
Bkgd time/scan time	0.5
Total reflcns measd	4133 [$+h, +k, \pm l$]
Unique data used	2901 [$I > 3\sigma(I)$]
No. of parameters (NP)	240

$R = (\sum F_o - F_c) / \sum F_o $	0.0324
$R = [\sum w(F_o - F_c)^2 / \sum w F_o ^2]^{1/2}$	0.0378
$\Delta P_{\max} (e\text{\AA}^{-3})$	0.6
Shift: error (max)	0.01

Sources of scattering factors and computer programs have been given in Chapter 1. The final atomic coordinates for non-hydrogen atoms are given in Table 3.6 and important distances and angles in Table 3.7. List of structure factors, anisotropic thermal parameters, and fractional coordinates for hydrogen atoms are available as Deposited Material. The structure of the $[\text{Sn}(\text{O}_2\text{C}_6\text{Cl}_4)_3]^{2-}$ anion is shown in Fig. 3.1, and the crystal packing of $(\text{tmenH})_2[\text{Sn}(\text{O}_2\text{C}_6\text{Cl}_4)_3]$ in the unit cell in Fig. 3.2.

3.4.1 Description and discussion of the structure

The crystal structure of 1 confirms the presence of the anionic tris-catecholato complex of tin(IV). The tmenH^+ cations show no unusual stereochemical features except that there is clear evidence of hydrogen-bonding at Cl(1) of two $\text{Cl}_4\text{C}_6\text{O}_2^{2-}$ ligands, with $\text{Cl}(1)\cdots\text{H}-\text{N} = 2.626 \text{ \AA}$, and $\text{N}(2)-\text{H}\cdots\text{Cl}(1) = 144.8^\circ$ (Fig. 3.1). There are no significant non-bonded distances involving the hydrogen atoms of the cation ($\text{Cl}(1)-\text{H}(12\text{A}) = 2.936 \text{ \AA}$; $\text{Cl}(2)-\text{H}(13\text{A}) = 2.908 \text{ \AA}$; $\text{Cl}(4) - \text{H}(13\text{B}) = 2.953 \text{ \AA}$; $\text{Cl}(5) - \text{H}(11) = 3.052 \text{ \AA}$; $\text{Cl}(5) - \text{H}(13\text{A}) = 2.901 \text{ \AA}$; $\text{Cl}(6) - \text{H}(16\text{A}) = 2.943 \text{ \AA}$). It seems reasonable to conclude that the hydrogen-bonding is responsible in part for the stability of the crystals isolated.

The bond distances observed in the $[\text{Sn}(\text{O}_2\text{C}_6\text{Cl}_4)_3]^{2-}$ anion (Table 3.5) are typical of those reported for other tin(IV) complexes. The average Sn-O bond length is $2.062(3) \text{ \AA}$ in good agreement with the values reported for CF_3CO_2^- ligands coordinated to octahedral tin(IV) in the complex $[\text{Sn}^{\text{II}}\text{Sn}^{\text{IV}}\text{O}(\text{O}_2\text{CCF}_3)_4]_2$ (range $2.040(6) - 2.070(7) \text{ \AA}$).¹⁴⁸ Some older results include $\text{Sn}(\text{OCCH}_3)_4$ (mean $r(\text{Sn}-\text{O}) = 2.22$, range $2.13 - 2.29 \text{ \AA}$)¹⁴⁹ and $[\text{Sn}^{\text{II}}\text{Sn}^{\text{IV}}(\text{O}_2\text{CC}_6\text{H}_4\text{NO}_2\text{-o})_2]\cdot\text{THF}_2$ (mean $r(\text{Sn}-\text{O})$ at octahedral tin(IV) = 2.059 , range $2.047(6) - 2.067(7) \text{ \AA}$);¹⁵⁰ the latter paper

TABLE 3.6

FINAL FRACTIONAL COORDINATES AND ISOTROPIC THERMAL PARAMETERS FOR
NON-HYDROGEN ATOMS OF (tmen H)₂[Sn(O₂C₆Cl₄)₃] WITH STANDARD DEVIATIONS
IN PARENTHESES

	\bar{x}	\bar{y}	\bar{z}	U_{eq}^* (Å ² × 10 ³)
Sn	0.0	0.10175(3)	0.25000	33.1(2)
Cl(1)	0.0225(1)	0.1369(1)	0.5487(1)	57(1)
Cl(2)	0.1415(1)	0.2992(1)	0.6501(1)	66(1)
Cl(3)	0.2310(1)	0.4124(1)	0.5629(1)	56(1)
Cl(4)	0.1990(1)	0.3598(1)	0.3741(1)	50(1)
Cl(5)	-0.1628(1)	-0.2073(1)	0.1420(1)	73(1)
Cl(6)	-0.0827(1)	-0.4257(1)	0.1960(1)	104(1)
O(1)	0.0820(1)	0.2084(2)	0.2976(2)	42(2)
O(2)	-0.0011(1)	0.1209(2)	0.3685(2)	39(1)
O(3)	-0.0707(1)	-0.0221(2)	0.2089(2)	28(1)
N(1)	0.1453(2)	0.1180(3)	0.1330(2)	48(2)
N(2)	0.0850(2)	0.3319(3)	0.0781(2)	51(2)
C(1)	0.0958(2)	0.2315(3)	0.3777(2)	35(2)
C(2)	0.0537(2)	0.1831(3)	0.4161(2)	34(2)
C(3)	0.0699(2)	0.2032(3)	0.4999(2)	41(2)
C(4)	0.1239(2)	0.2736(4)	0.5459(2)	42(2)
C(5)	0.1641(2)	0.3242(3)	0.5078(3)	42(2)
C(6)	0.1497(2)	0.3014(3)	0.4234(2)	38(2)
C(7)	-0.0378(2)	-0.1149(3)	0.2269(2)	43(2)
C(8)	-0.0729(3)	-0.2112(4)	0.2023(3)	56(3)
C(9)	-0.0368(3)	-0.3073(4)	0.2262(3)	66(3)
C(11)	0.1594(3)	0.0893(5)	0.0574(3)	76(3)
C(12)	0.1709(3)	0.0319(4)	0.1966(3)	64(3)

C(13)	0.1800(2)	0.2196(4)	0.1745(3)	59(3)
C(14)	0.1602(2)	0.3130(4)	0.1158(3)	63(3)
C(15)	0.0604(3)	0.3895(4)	0.1343(3)	65(3)
C(16)	0.0634(3)	0.3870(4)	-0.0011(3)	71(3)

U_{eq}^* is calculated from the refined anisotropic thermal parameter

$$U_{eq} = \frac{1}{3} \sum_i \sum_j U_{ij} a_i^* a_j^* a_i \cdot a_j$$

TABLE 3.7

INTERATOMIC DISTANCES (Å) AND ANGLES (°) FOR $(tmenH)_2[Sn(O_2C_6Cl_4)_2]$

Sn-O(1)	2.051(3)	O(1)-Sn-O(1)'	98.1(2)
Sn-O(2)	2.079(3)	O(1)-Sn-O(2)	81.7(1)
Sn-O(3)	2.055(3)	O(1)-Sn-O(3)	171.5(1)
Cl(1)-C(3)	1.737(4)	O(2)-Sn-O(3)	98.5(1)
Cl(2)-C(4)	1.729(4)	O(3)-Sn-O(3)'	81.1(2)
Cl(3)-C(5)	1.728(4)	Sn-O(1)-C(1)	111.2(2)
Cl(4)-C(6)	1.729(4)	Sn-O(2)-C(2)	109.8(2)
Cl(5)-C(8)	1.719(5)	Sn-O(3)-C(7)	111.5(2)
Cl(6)-C(9)	1.731(5)	C(11)-N(1)-C(12)	109.9(4)
O(1)-C(1)	1.335(4)	C(11)-N(1)-C(13)	114.1(4)
O(2)-C(2)	1.349(5)	C(12)-N(1)-C(13)	107.8(4)
O(3)-C(7)	1.324(5)	C(14)-N(2)-C(15)	111.9(4)
N(1)-C(11)	1.494(6)	C(14)-N(2)-C(16)	112.2(4)
N(1)-C(12)	1.487(6)	C(15)-N(2)-C(16)	110.0(4)
N(1)-C(13)	1.502(6)	O(1)-C(1)-C(2)	118.5(3)
N(2)-C(14)	1.434(6)	O(1)-C(1)-C(6)	121.6(3)
N(2)-C(15)	1.457(6)		
N(2)-C(16)	1.443(6)	O(2)-C(2)-C(1)	118.4(3)
<u>Ring C(1)-C(6)*</u>		O(2)-C(2)-C(3)	118.6(4)
mean C-C	1.398(8)	Cl(1)-C(3)-C(2)	118.6(3)
mean C-C-C	120.0(6)	Cl(1)-C(3)-C(4)	119.9(3)

<u>Ring C(7)-C(9), C(7)'-C(9)'</u>		C1(2)-C(4)-C(3)	120.3(3)
mean C-C	1.400(9)	C1(2)-C(4)-C(5)	119.5(3)
mean C-C-C	120.0(7)	C1(3)-C(5)-C(4)	121.3(3)
		C1(3)-C(5)-C(6)	120.0(3)
N(2)-H...C1(4)	2.626	C1(4)-C(6)-C(1)	118.4(3)
		C1(4)-C(6)-C(5)	120.5(3)
		O(3)-C(7)-C(8)	123.1(4)
		O(3)-C(7)-C(7)'	117.9(4)
		C1(5)-C(8)-C(7)	117.4(4)
		C1(5)-C(8)-C(9)	121.2(4)
		C1(6)-C(9)-C(8)	120.0(4)
		C1(6)-C(9)-C(9)'	120.4(4)
		N(1)-C(13)-C(14)	113.2(4)
		N(2)-C(14)-C(13)	113.0(4)
		N(2)-H...C1(4)	144.8

Symmetry equivalent position: ' is $-x, y, 0.5-z$.

* E.S.D.'s on mean values have been calculated with the use of the scatter formula.

$$\sigma = [\sum(d_i - \bar{d})^2 / (N-1)]^{1/2}$$

where d_i is the i th and \bar{d} is the mean of N equal measurements.

FIGURE 3.1

ORTEP DIAGRAM OF $[\text{Sn}(\text{O}_2\text{C}_6\text{Cl}_4)_3]^{2-}$: THERMAL ELLIPSOIDS ARE DRAWN AT 50%
PROBABILITY LEVELS

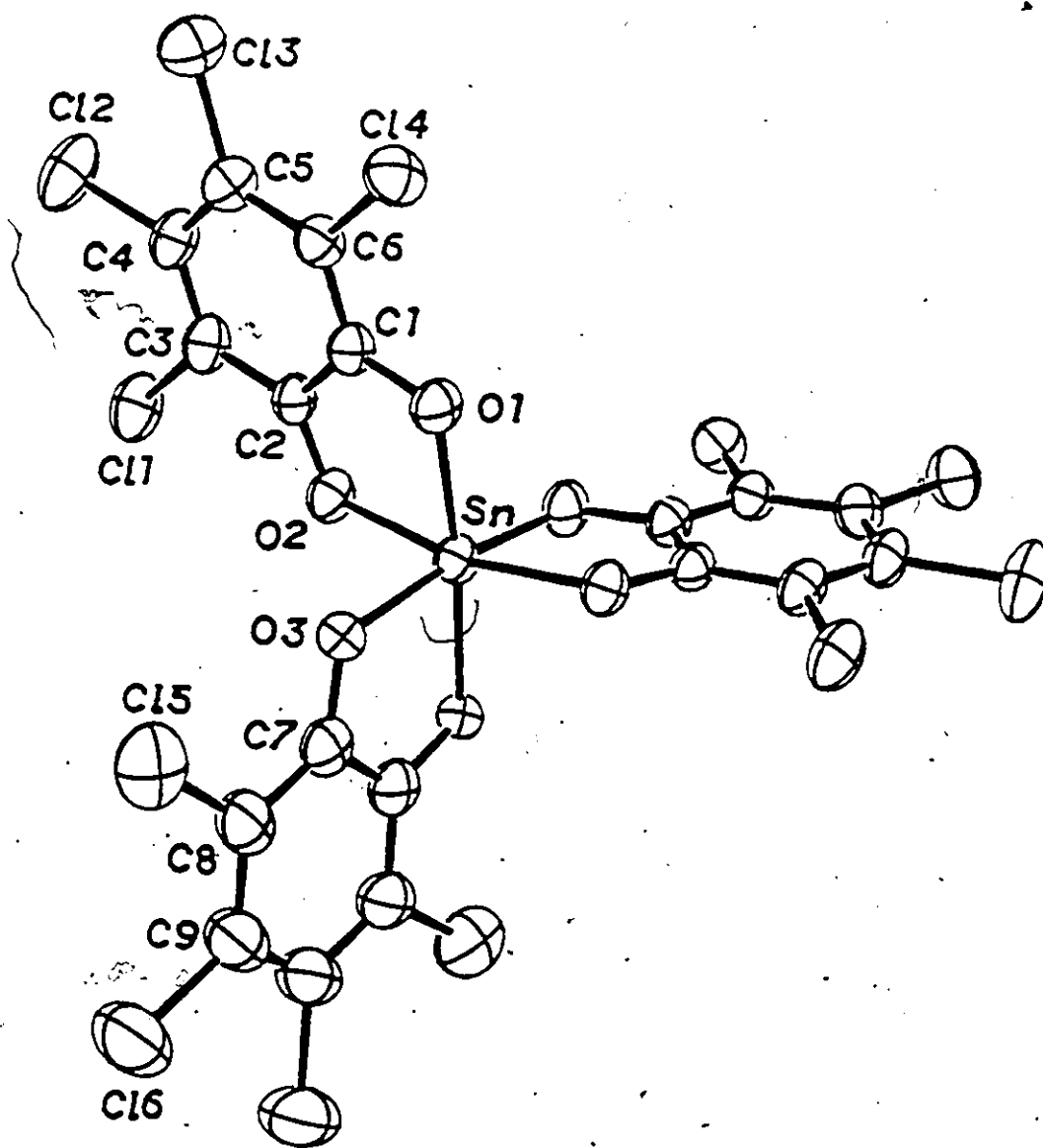
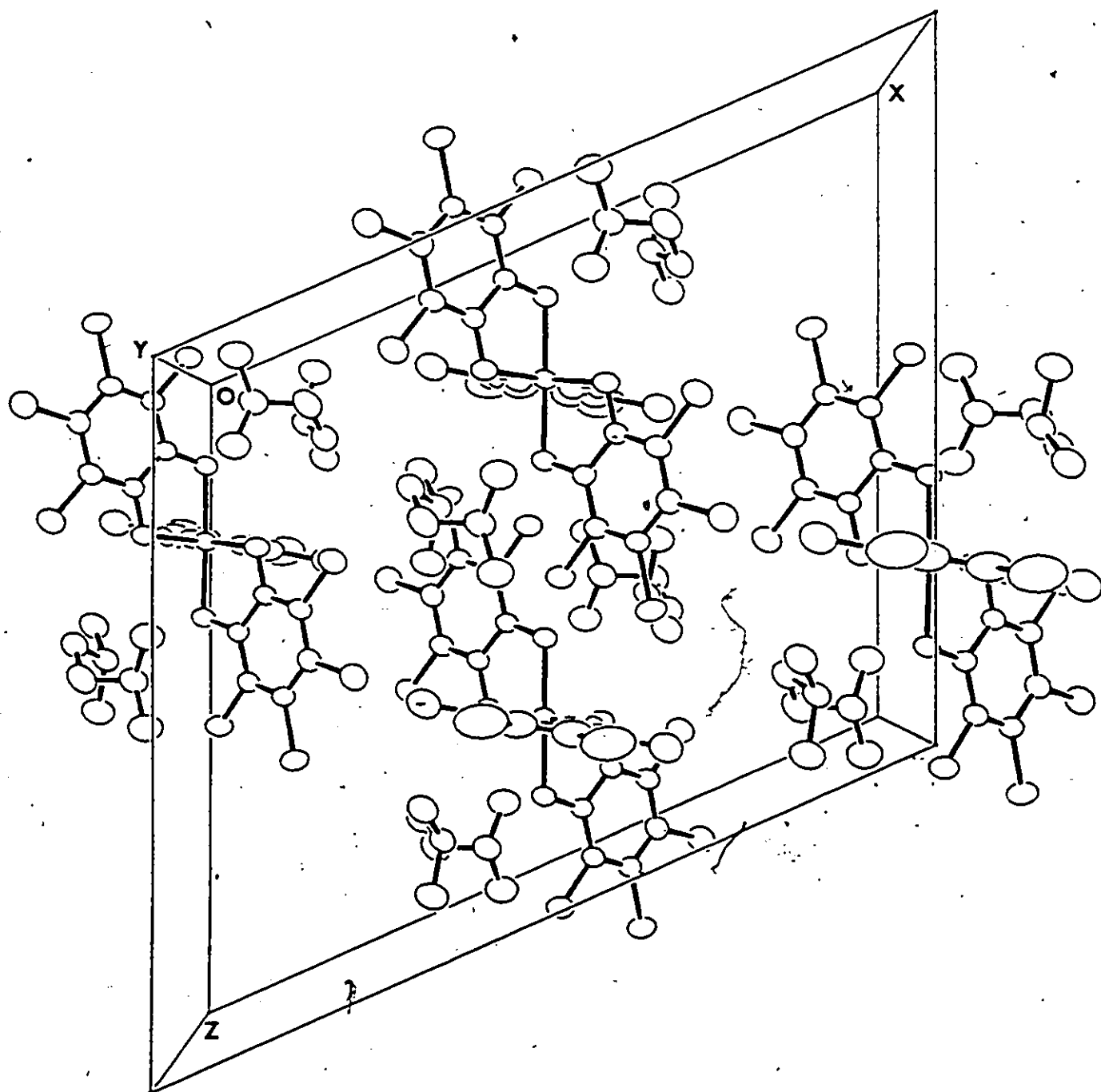


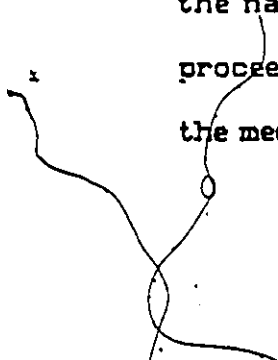
FIGURE 3.2

CRYSTAL PACKING DIAGRAM OF $(\text{tmenH})_2[\text{Sn}(\text{O}_2\text{C}_6\text{Cl}_4)_3]$ 

reviews earlier results for $\text{Sn}^{\text{IV}}\text{-O}$ bonds in a variety of stereochemistries. In the present structure, the Sn-O_6 kernel is distorted octahedral, with the average O-Sn-O bite angle = $81.5(2)^\circ$.

The coordinated $\text{Cl}_4\text{C}_6\text{O}_2$ ligands are aromatic, with planar hexagonal C_6 rings, with $r(\text{C-C})(\text{av}) = 1.400(9) \text{ \AA}$, and $\text{C-C-C}(\text{av}) = 120.0(7)^\circ$. The C-Cl distances are typical of those in aromatic compounds, as are the C-O values, but these bonds (av. $1.336(5) \text{ \AA}$) are significantly longer than the average of 1.29 \AA found in a variety of transition metal complexes of the 3,5-di-tert-butyl-o-semiquinone ligand^{139,151} thus confirming that the reduction of the $\text{Cl}_4\text{C}_6\text{O}_2$ ligand has indeed proceeded beyond the semiquinone state to the dianion. In summary, there is ample confirmation from the crystallographic results that the reaction product in this case is a tin(IV)-catecholate derivative. The remaining features of the structure do not call for any comment.

The work presented in this chapter has unambiguously gone to confirm that the oxidative addition reactions involving tin(II) halides and tetrahalogeno-orthoquinones proceed in a manner by which the tin(IV) catecholates are formed. The mechanism by which these products were formed could not be fully investigated due to the instantaneous nature of the reaction. This was also found to be the case of the reactions of tetrachloro 1,2-benzoquinone with some low valent state transition metals.^{132,152} The use of quinones with bulky substituents with tin(II) halides will be looked at in the next chapter. Due to the nature of the substituent on the quinones those reactions were found to proceed more slowly so ESR spectroscopy was used to provide an insight into the mechanism of the formation of tin(IV) catecholate.



In general, we conclude that the spectroscopic evidence is exactly congruent with that from X-ray crystallography, and shows clearly that the reaction of SnX_2 with the tetrahalogeno-o-quinones is an oxidative addition process to give the appropriate tin(IV) catecholate species.

CHAPTER 4

THE REACTION OF SnX_2 ($\text{X} = \text{Cl}, \text{Br}, \text{I}$) WITH 3,5-DI-TERT-BUTYL-1,2-BENZOQUINONE AND 9,10-PHENANTHROQUINONE: EVIDENCE OF ONE-ELECTRON TRANSFER

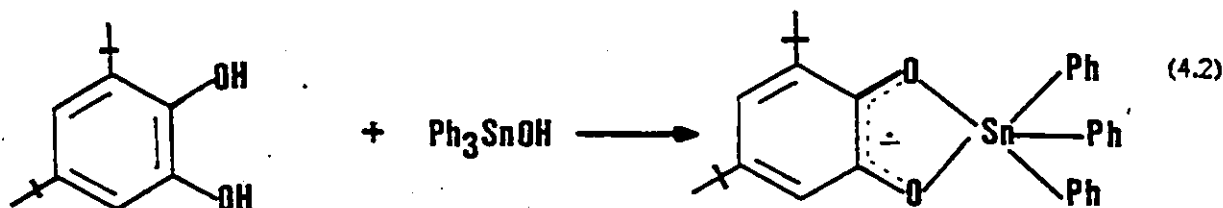
4.1 Introduction

As a continuation of work described in Chapter 3, we extended our studies to cover the reactions of tin(II) halides with quinones having bulky substituents, namely 3,5-di-tert-butyl-1,2-benzoquinone and 9,10-phenanthroquinone. The great advantage in this particular study is that the rates are such to permit us to monitor the reaction with the help of electron spin resonance (ESR) spectroscopy. In this way, we obtained considerable insight into the reaction mechanism.

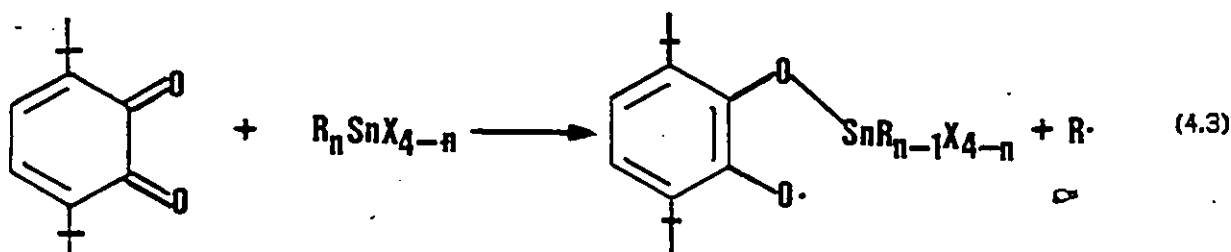
The existence of stable Sn(IV) semiquinone complexes has been reported in a number of publications. One characteristic feature of all these reports is that these semiquinone complexes are made from inorganic or organometallic Sn(IV) compounds. For example, when a frozen solution of hexamethylditin and 9,10-phenanthroquinone (PQ) in benzene, prepared¹⁵³ at -150°C in the dark, was allowed to warm up in the cavity of an ESR spectrometer, an intense ESR spectrum of the adduct $\text{Me}_3\text{Sn-PQ}^\cdot$ was observed.



Similarly when triphenyltin hydroxide reacted with 3,5-di-tert-butyl catechol, a stable tin-semiquinone complex was formed. This was confirmed with the aid of ESR.¹⁵⁴



Davies et al.¹⁵⁵ carried out an ESR study of the organotin(IV) derivatives of 3,6-di-*tert*-butyl 1,2-benzosemiquinone prepared by eqn. 4.3



Variable temperature studies on these systems with the aid of ESR allowed them to assign different structures to the products of these reactions, depending on the nature of R.

Our work has shown that stable tin(IV) catecholates can be made with these quinones and tin(II) halides through a two step one-electron transfer process. The first transfer of electrons then allowed us to identify a semiquinone intermediate which immediately gets converted to the tin(IV) catecholate in the presence of a neutral donor ligand.

In the course of this work, we obtained crystals of the 1,10-phenanthroline adduct of bis(3,5-di-*tert*-butyl-catecholato)tin(IV), and the crystal structure of this compound has been established by X-ray crystallography.

4.1.1 Electron Spin Resonance Spectroscopy¹⁵⁶⁻¹⁵⁸

It is incumbent at this point to define some of the terms used in discussing the work described in this section, and in the next two chapters which also depend quite extensively on spectral data obtained from ESR studies.

(i) The *g*-value: The energy separation between the two spin states for a free electron in a magnetic field *H* is $g_e \beta H$, where β is the Bohr magneton, and g_e is the *g*-value for the free electron - a dimensionless proportionality constant, of value 2.0023. The condition for the absorption of radiation of

frequency ν by the system is thus:

$$\Delta E = g_e \beta H = h\nu \quad (4.4)$$

For a fixed frequency ν , the g -value for a given radical governs the magnetic field H at which absorption takes place. The g -values for most organic radicals lie close to that of the unpaired electron, but small changes result from interaction between the spin angular momentum of the electron and its orbital angular momentum, and such changes are sometimes diagnostic of the exact structure of the radical.

(ii) Hyperfine splitting: Hyperfine splittings arise from the interaction between the electron's magnetic moment and the magnetic moments of neighbouring nuclei in the radical. In general, a set of n equivalent nuclei of spin I will produce $2nI + 1$ lines in the ESR spectrum. For a radical containing q different sets of nuclei:

$$\text{Number of lines} = \prod_{q=0}^q (2n_q I_q + 1) \quad (4.5)$$

where each factor in the product is the number of lines arising from the q th set of equivalent nuclei and n_q is the number of nuclei (of spin I_q) in the set. The hyperfine splitting constant (or coupling constant) of the q th set of nuclei is simply the separation between the individual lines of the splitting pattern arising from that set.

Radicals in solids give rise to broad spectra because the electron-nucleus dipole-dipole interaction varies with the orientation of the radical in the magnetic field. Interelectronic interaction also causes broadening. However, when a radical tumbles freely in a low viscosity solvent, this interaction is averaged

to zero and sharp lines exhibiting isotropic splittings are observed.

(iii) Line widths: As the term resonance implies, ESR is a dynamic effect involving rapid energy exchanges between the spin system and the incident radiation. Now, in the magnetic field, the lower energy spin-state is more heavily populated than the upper, the equilibrium ratio being given by the Boltzmann distribution:

$$\frac{n_u}{n_e} = e^{-\Delta E/KT} = e^{-g\beta H/KT} \quad (4.6)$$

When radiation of the exact energy difference ($\Delta E = h\nu$) is absorbed, transitions in the upward and downward directions are induced with equal probability. The net result is an energy absorption only so long as the population excess is maintained in the lower state. Spin-lattice relaxation, which is essentially the rapid energy exchange between the spins and the surrounding molecules, tends to depopulate the upper level and hence ensures that this situation is maintained. Otherwise, when $n_u = n_l$, the system would be saturated and no net absorption could be detected.

In practice, the absorption in an ESR spectrum has a finite width, being spread over a small range of field. This line broadening results because processes take place which create an uncertainty in the energy difference (ΔE) between the spin states.

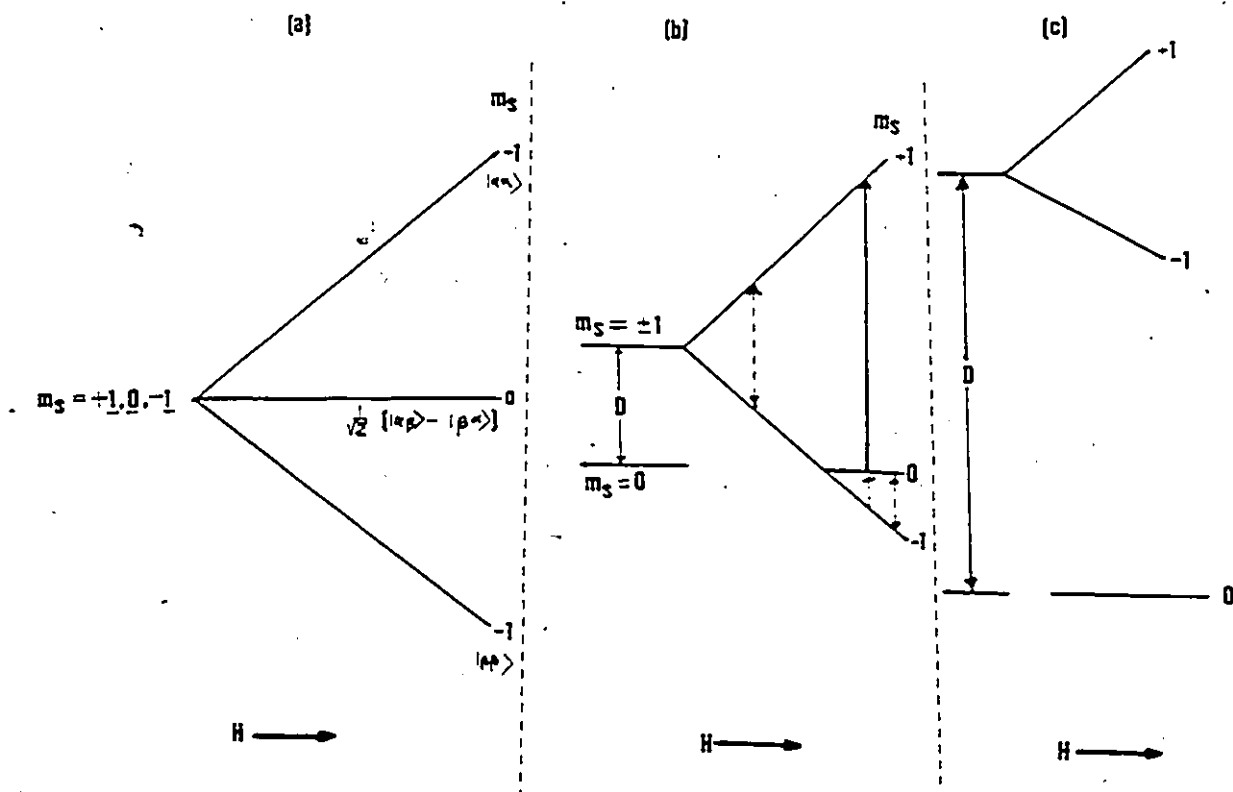
(iv) The ESR of Triplet State: When two molecular orbitals are closer in energy than the difference between exchange and repulsive energies, a stable triplet state arises. For the triplet state $S = 1$ and $M_S = 1, 0, -1$. If only exchange and electrostatic interactions existed in the molecules, the three configurations $M_S = 1, 0$, and -1 would be degenerate in the absence of a magnetic field. A magnetic field would remove this degeneracy, as shown in Fig. 4.1a, and only

FIGURE 4.1

THE EFFECTS OF ZERO-FIELD SPLITTING ON THE EXPECTED ESR TRANSITIONS

- (a) No zero-field effects
- (b) Moderate zero-field splittings. The dashed arrows show the fixed frequency result, and the solid arrows show the fixed field result.
- (c) Large zero-field effects.

The magnetic field is assumed to be parallel to the dipolar axis in the molecule.



a single transition would be observed. However, magnetic dipole-dipole interaction between the two unpaired electrons remove the degeneracy of the M_S components of $S = 1$ even in the absence of an external field as shown in Fig. 4.1b. This removal of the degeneracy in the absence of the field is called zero-field splitting. When a magnetic field is applied, the levels are split so that two $\Delta M_S = \pm 1$ transitions can be detected (see Fig. 4.1b). Two of the three peaks usually observed are the $\Delta M_S = \pm 1$ transition, and the third is the $\Delta M_S = \pm 2$ transition, which becomes allowed when the magnetic field is not aligned with the z-axis. When the zero-field splitting is very large, as in Fig. 4.1c, the M_S values become valid quantum numbers and the energies for the $\Delta M_S = \pm 1$ allowed transitions become too large to be observed in the microwave region; accordingly no spectrum is observed.

Since the electron-electron interaction is dipolar, it is expected to be described by a symmetric tensor, the so-called zero-field splitting tensor.

$$\hat{H}_D = \hat{S} \cdot D \cdot \hat{S} \quad (4.7)$$

where \hat{S} is the total spin operator, and D is a second rank tensor with a trace of zero. Since the trace of D is zero, only two independent parameters are required, and these are designated as D and E , defined as

$$D = -3Z/2 \quad (4.8a)$$

$$E = -1/2(X-Y) \quad (4.8b)$$

Both D and E depend on the distance between two electrons with parallel spins in a simple model.

$$D = \frac{3}{4}g^2\beta^2 \left\langle \frac{r^2 - 3z^2}{r^5} \right\rangle \quad (4.9a)$$

$$E = \frac{3}{4}g^2\beta^2 \left\langle \frac{y^2 - x^2}{r^5} \right\rangle \quad (4.9b)$$

where the angular brackets imply an average over the electron wave function. Experimental values of D and E can provide information on the mean separation between the two electrons if the averages in eqns. 4.9a,b can be calculated. This procedure is valid only if the interaction is predominantly dipolar in nature, which means there is not a significant contribution from spin-orbit coupling to the zero-field splitting.

4.2 Experimental

4.2.1 Preparation of adducts of Sn^{IV}-catecholato compounds

In experiments involving SnCl₂, 0.57 g (3 mmol) of solid was dissolved in acetonitrile (25 mL), and a solution of either TBQ or PQ in the same solvent (3 mmol in 25 mL) added slowly over a period of 1 h. This mixture was heated to 50° for 3 h, at which point phen or bipy (3 mmol) was added, either in acetonitrile solution or as the solid. The pale yellow solution became brick-red, and a red precipitate formed. This was collected by filtration, washed with petroleum ether (2 x 10 mL) and dried *in vacuo* at room temperature. Yield of (e.g.) dichloro(3,5-di-tert-butylcatecholato)tin(IV), 1,10-phenanthroline was quantitative. Analytical results are given in Table 4.1. In that Table, as in the text, we use ~~the~~ nomenclature TBQ $\xrightarrow{e^-}$ TBSQ \cdot $\xrightarrow{e^-}$ TBC, and PQ $\xrightarrow{e^-}$ PSQ \cdot \rightarrow PD for the o-quinone, o-semiquinone anion and o-diolato dianion respectively.

TABLE 4.1
ANALYTICAL DATA FOR PRODUCTS OF
SnX₂ (X = Cl, Br, I) / TBQ (or PQ) REACTIONS

Compound	Found/Calc. (%)				
	Sn	C	H	N	X=Cl, Br, I
(TBC)SnCl ₂ .bpy	20.9(21.0)	-	-	-	12.5(12.5)
(TBC)SnCl ₂ .phen	20.2(20.1)	53.3(52.9)	5.50(4.78)	4.43(4.75)	12.2(12.0)
(TBC)SnBr ₂ .bpy	18.2(18.1)	-	-	-	24.5(24.4)
(TBC)SnBr ₂ .phen	17.6(17.5)	-	-	-	23.0(23.5)
(TBC) ₂ Sn.phen.1 ^{1/2} /2dmf	14.1(14.0)	62.3(62.8)	6.56(6.93)	5.65(5.76)	-
(FD)SnCl ₂ .bpy	21.3(21.4)	-	-	-	12.6(12.8)
(FD)SnBr ₂ .bpy	18.6(18.5)	-	-	-	21.9(22.3)
(FD)SnI ₂ .phen	15.5(15.6)	40.6(41.0)	2.38(2.12)	3.68(3.68)	33.5(33.4)

When SnBr_2 was used under the above conditions, no precipitation occurred on addition of bpy or phen. The brown solution was filtered after cooling to room temperature to remove any suspended material; addition of diethyl ether (50 mL) to this filtrate gave a brown solid which was collected, washed and dried. This solid is $(\text{TBC})\text{SnBr}_2 \cdot \text{L}$ (L = bpy, phen).

Stannous iodide was dissolved in 2:1 (v/v) mixture of acetonitrile and dimethylformamide (dmf), since it is only slightly soluble in acetonitrile. The solution resulting from reaction with TBQ and phen was concentrated by reducing the volume by approx. 60%. No solid appeared at this point, but after several days at room temp. under nitrogen, red crystals of bis(3,5-tert-butylcatecholato)tin(IV), 1,10-phenanthroline, sesqui-dimethylformamide solvate appeared. This compound loses dmf on standing, as is easily shown by following the intensity of the $\nu(\text{C}=\text{O})$ band of dmf at 1677 cm^{-1} . The crystal used in the X-ray crystallographic study proved to be the bis-dimethylformamide solvate (see below).

In an attempt to establish the mode of formation of $(\text{TBC})_2\text{Sn} \cdot \text{phen}$, we performed the reaction under different conditions. Stannous iodide (1.2 g, 3.2 mmol) was suspended in toluene (25 mL) and a solution of TBQ (0.71 g, 3.2 mmol) in the same solvent (25 mL) added dropwise. The quinone solution changed colour from red to light brown on contact with the suspension. After addition of all the TBQ, the mixture was refluxed for 4 h, after which a wine-red solution was obtained; 2,2'-bipyridine (0.50 g, 3.2 mmol) was then added, producing a red-orange precipitate. Refluxing was continued for a further hour, after which the mixture was cooled, and the product collected by filtration washed with petroleum ether (3 x 20 mL) and dried *in vacuo*. Yield 0.58 g (0.74 mmol) of $\text{SnI}_4 \cdot \text{bpy}$. IR spectrum establishes presence of bpy. Found: Sn, 15.8; I, 64.5. $\text{C}_{10}\text{H}_8\text{N}_2\text{SnI}_4$

requires Sn, 15.2; I, 64.9%. We were unable to identify an oily product which was obtained from the filtrate after removing the solvent by evaporation.

The procedures with phenanthrene-9,10-quinone were similar. For example, stannous iodide (0.80 g, 2.15 mmol) was suspended in a solution of PQ (0.45 g, 2.15 mmol) in toluene (mL), and the mixture refluxed gently for 5 h. On addition of 1,10-phenanthroline (0.39 g, 2.15 mmol) to the deep red solution, a purple precipitate was thrown down. Refluxing was continued for 1 h, after which the mixture was cooled to room temperature and the precipitate collected, washed with petroleum ether (3 x 20 mL) and dried *in vacuo*. Yield of (PD)SnI₂-phen was quantitative.

4.2.2 Crystallographic Studies

A suitable crystal of bis(3,5-di-tert-butylcatecholato)tin(IV)-1,10-phenanthroline bisdimethylformamide solvate (2) was sealed in a capillary. (See Table 4.2 for crystal size and other relevant parameters.) Diffraction results were collected using a Syntex P2₁ diffractometer following the procedures described Chapter 1. The unit cell dimensions were determined from 55 strong reflections in the range $15 < 2\theta < 25^\circ$. The intensities of three monitored reflections changed by 34% during the period of 150 h required for data collection, and the appropriate decay corrections were applied. Corrections were also applied for Lorentz and polarization effects, but no absorption correction was necessary because of the low absorption coefficient.

TABLE 4.2

SUMMARY OF CRYSTAL DATA, INTENSITY COLLECTION, AND STRUCTURE
REFINEMENT FOR $(\text{Bu}^t_2\text{C}_6\text{H}_2\text{O}_2)_2\text{Sn.phen.2dmf}$

cell constants	10.761(2), 14.357(3), 15.361(4) Å
	93.5(3), 95.8(2), 94.8(3)
cell volume (Å ³)	2330(1)
crystal system	triclinic
space group	$\bar{P}1$
mol. wt.	884.7
Z,F(000)	2,928
pc,ρo(g cm ⁻³)	1.26, 1.20
cryst dimens (mm)	0.10 x 0.20 x 0.50
abs coeff, μ(cm ⁻¹)	5.25
radiation	MoKα, λ=0.71069 Å
monochromator	highly oriented graphite
temp (°C)	20
2θ angle (°C)	4-45
scan type	coupledθ (crystal)/2θ (counter)
scan width	$K_{\alpha_1} - 1^\circ$ to $K_{\alpha_2} + 1^\circ$
scan speed (° min ⁻¹)	variable, 2.02-4.88
bkgd time/scan time	0.5
total reflcns measd	4596 (+h,±k,±l)
unique data used	3005 [I>2σ(I)]
no. of parameters (NP)	347 (two blocks of 172 and 175 parameters)

$$R = (\sum |F_o| - |F_c| / \sum |F_o|^2)^{1/2} \quad 0.0699$$

$$R_w = (\sum w(|F_o| - |F_c|)^2 / \sum w |F_o|^2)^{1/2} \quad 0.0719$$

$$\Delta \rho_{\max} (e\text{\AA}^{-3}) \quad 0.72$$

$$\text{shift: error (max)} \quad 0.05$$

There were no systematic absences, and the space group $P\bar{1}$ was therefore used and later assumed to be correct in view of the successful refinement of the structure. The position of the tin atom was determined by the heavy atom method, and the remaining non-hydrogen atoms were located from a difference Fourier map. The structure was refined using a blocked matrix least squares method, with Sn and O(1) in both blocks; one block also contained O(2)-O(3), N(1)-N(2) and C(1)-C(12), and the other C(21)-C(66), O(4), O(5) and N(3)-N(4). The atoms Sn, O(1), O(2), N(1), N(2) and C(1)-C(12) were refined anisotropically, and the remainder isotropically. Hydrogen atoms were included in later cycles in ideal positions (C-H = 0.95Å, and CCH = 109.5 or 120° as appropriate). The convergence minimized the function $\sum w(|F_o| - |F_c|)^2$, and in the final cycles the weighting scheme $w = 1/[\sigma^2(F) + pF]^2$ was employed, with $p = 0.0001$. No evidence was found of secondary extinction. Sources of scattering factors and computer programmes were those given in Chapter 1.

The refinement converged at $R = 0.0699$. The final atomic coordinates for non-hydrogen atoms are given in Table 4.3, and important interatomic distances and angles in Table 4.4. Tables of observed and calculated structure factors, anisotropic thermal parameters, fractional coordinates for hydrogen atoms, and equations of important planes, are available as supplementary material. Fig. 4.2 shows the molecular structure of 2, and Fig. 4.3 the unit cell packing with the dmf molecules are shown. There is some evidence of disorder in one of these dmf molecules (C(66)) from the thermal parameters.

TABLE 4.3

FINAL FRACTIONAL COORDINATES AND ISOTROPICAL THERMAL PARAMETERS (\AA^2
 $\times 10^3$) FOR NON-HYDROGEN ATOMS OF $(\text{Bu}^t_2\text{C}_6\text{H}_2\text{O}_2)_2\text{Sn}$ PHEN.2DMF;
 $(\text{C}_{34}\text{H}_{42}\text{N}_4\text{O}_4\text{Sn})$ WITH STANDARD DEVIATIONS IN PARENTHESES

	x	y	z	U_{eq}^a/U
Sn	0.1305(1)	0.2610(1)	0.3166(1)	51.8(6)
O(1)	0.2727(7)	0.1843(5)	0.3659(5)	59(5)
O(2)	0.1612(8)	0.1672(6)	0.2226(5)	70(6)
O(3)	-0.0176(7)	0.3354(5)	0.2707(5)	60(5)
O(4)	0.2216(7)	0.3735(5)	0.2714(5)	54(5)
O(5)	0.2381(24)	0.8814(17)	0.7697(16)	276(11)
O(6)	0.2536(18)	0.6093(14)	0.5038(13)	207(7)
N(1)	-0.0032(9)	0.1671(8)	0.3936(7)	68(8)
N(2)	0.0924(10)	0.3190(8)	0.4506(7)	63(8)
N(3)	0.3442(20)	0.7963(16)	0.8530(13)	157(7)
N(4)	0.3926(18)	0.6549(12)	0.5750(12)	134(6)
C(1)	-0.0530(15)	0.0948(10)	0.3632(11)	88(11)
C(2)	-0.1314(14)	0.0390(11)	0.4230(16)	107(14)
C(3)	-0.1609(17)	0.0571(15)	0.5082(14)	111(15)
C(4)	-0.1083(14)	0.1316(13)	0.5378(13)	86(13)
C(5)	-0.0319(12)	0.1878(10)	0.4789(10)	66(10)
C(6)	0.0214(13)	0.2667(9)	0.5099(10)	63(10)
C(7)	-0.0101(17)	0.2894(14)	0.6005(10)	92(13)
C(8)	0.0378(17)	0.3691(15)	0.6229(11)	96(14)
C(9)	0.1067(15)	0.4237(13)	0.5621(13)	98(14)
C(10)	0.1348(12)	0.3969(11)	0.4736(9)	73(10)
C(11)	-0.1324(17)	0.1554(18)	0.6269(14)	114(17)
C(12)	-0.0853(18)	0.2302(17)	0.6577(12)	111(15)

C(21)	0.3079(10)	0.1062(8)	0.3188(7)	47(3)
C(22)	0.3995(10)	0.0400(8)	0.3429(7)	51(3)
C(23)	0.4351(11)	-0.0398(8)	0.2950(7)	54(3)
C(24)	0.3738(11)	-0.0451(9)	0.2217(8)	62(4)
C(25)	0.2827(11)	0.0178(9)	0.1927(8)	56(3)
C(26)	0.2486(10)	0.0984(8)	0.2430(7)	54(3)
C(27)	0.5355(13)	-0.1122(10)	0.3219(9)	77(4)
C(28)	0.6588(17)	-0.1044(14)	0.2646(13)	154(8)
C(29)	0.4936(18)	-0.2082(13)	0.3190(13)	148(8)
C(30)	0.5835(16)	-0.0996(13)	0.4082(11)	126(6)
C(31)	0.2154(14)	0.0069(10)	0.1078(9)	81(4)
C(32)	0.2441(16)	0.0869(12)	0.0407(11)	128(6)
C(33)	0.0799(16)	0.0112(13)	0.1242(12)	133(7)
C(34)	0.2557(17)	-0.0852(12)	0.0690(12)	136(7)
C(41)	0.0169(11)	0.4176(8)	0.2314(7)	52(3)
C(42)	-0.0653(11)	0.4799(8)	0.1914(7)	55(3)
C(43)	-0.0271(11)	0.5626(9)	0.1481(8)	59(4)
C(44)	0.0972(11)	0.5800(9)	0.1474(7)	55(3)
C(45)	0.1836(10)	0.5219(8)	0.1895(7)	49(3)
C(46)	0.1448(10)	0.4392(8)	0.2314(7)	51(3)
C(47)	-0.1194(14)	0.6311(10)	0.1036(9)	80(4)
C(48)	-0.0869(20)	0.6320(16)	0.0078(14)	180(9)
C(49)	-0.1150(18)	0.7291(14)	0.1281(14)	157(8)
C(50)	-0.2572(24)	0.6162(20)	0.1254(18)	244(14)

C(51)	0.3233(12)	0.5457(9)	0.1881(8)	65(4)
C(52)	0.4090(12)	0.4690(10)	0.1419(9)	87(5)
C(53)	0.3478(15)	0.6404(10)	0.1386(10)	105(5)
C(54)	0.3619(13)	0.5504(10)	0.2795(9)	90(5)
C(61)	0.2593(24)	0.7321(18)	0.8815(17)	203(11)
C(62)	0.4571(23)	0.7783(19)	0.8993(17)	215(12)
C(63)	0.3350(47)	0.8604(34)	0.8113(28)	357(26)
C(64)	0.4985(33)	0.6871(25)	0.5865(22)	326(20)
C(65)	0.3221(44)	0.6387(34)	0.6458(31)	603(45)
C(66A)	0.2764(53)	0.6690(38)	0.5527(37)	179(19)
C(66B)	0.4050(63)	0.5933(48)	0.5072(45)	240(27)

TABLE 4.4

BOND LENGTHS (Å) AND ANGLES (DEG) FOR $(\text{Bu}^t_2\text{C}_6\text{H}_2\text{O}_2)_2\text{Sn}$ phen.2dmf;
 $\text{C}_{34}\text{H}_{42}\text{N}_4\text{O}_4\text{Sn}$ with standard deviations in parentheses.

Sn-O(1)	1.995(8)	O(1)-Sn-O(2)	82.6(3)
Sn-O(2)	2.019(8)	O(1)-Sn-O(3)	177.6(3)
Sn-O(3)	2.008(7)	O(2)-Sn-O(3)	97.9(3)
Sn-O(4)	2.010(7)	O(1)-Sn-O(4)	98.5(3)
		O(2)-Sn-O(4)	106.6(3)
		O(3)-Sn-O(4)	83.6(3)
Sn-N(1)	2.25(1)	O(1)-Sn-N(1)	89.2(3)
		O(1)-Sn-N(1)	89.2(3)
		O(2)-Sn-N(1)	89.8(4)
		O(3)-Sn-N(1)	88.5(3)
		O(4)-Sn-N(1)	162.6(3)
Sn-N(2)	2.26(1)	O(1)-Sn-N(2)	85.5(3)
		O(2)-Sn-N(2)	160.0(4)
		O(3)-Sn-N(2)	93.4(3)
		O(4)-Sn-N(2)	91.0(4)
		N(1)-Sn-N(2)	74.0(4)
O(1)-C(21)	1.38(1)	Sn-O(1)-C(21)	111.3(7)
O(2)-C(26)	1.35(1)	Sn-O(2)-C(26)	111.2(7)
O(3)-C(41)	1.35(1)	Sn-O(3)-C(41)	110.4(7)
O(4)-C(46)	1.36(1)	Sn-O(3)-C(41)	110.4(7)
O(4)-C(46)	1.36(1)	Sn-O(4)-C(46)	111.4(7)
N(1)-C(1)	1.34(2)	Sn-N(1)-C(1)	126(1)

N(1)-C(5)	1.36(2)	Sn-N(1)-C(5)	115(1)
		C(1)-N(1)-C(5)	119(1)
N(2)-C(6)	1.36(2)	Sn-N(2)-C(6)	115(1)
N(2)-C(10)	1.32(2)	Sn-N(2)-C(10)	125(1)
		C(6)-N(2)-C(10)	120(1)
§			
<u>Rings 1,10-phenanthroline</u>			
mean C-C ^a	1.40(5)	C(23)-C(27)	1.51(2)
mean C-C-C/N-C-C	120(5)	C(25)-C(31)	1.58(2)
<u>Ring C(21)-C(26)</u>			
mean C-C	1.39(5)	O(1)-C(21)-C(22)	122(1)
mean C-C-C	120(6)	O(1)-C(21)-C(26)	117(1)
		O(2)-C(26)-C(21)	118(1)
		O(2)-C(25)-C(21)	124(1)
<u>Ring C(41)-C(46)</u>			
mean C-C	1.39(4)	C(22)-C(23)-C(27)	122(1)
mean C-C-C	120(4)	C(24)-C(25)-C(31)	124(1)
		C(26)-C(25)-C(31)	119(1)
<u>t-butyl group C(27)-C(30)</u>			
mean C-C	1.51(3)	C(43)-C(47)	1.52(2)
mean C-C-C	110(2)	C(45)-C(51)	1.57(2)
		O(3)-C(41)-C(42)	122(1)
		O(3)-C(41)-C(46)	118(1)
<u>t-butyl group C(31)-C(34)</u>			
mean C-C	1.49(3)	O(4)-C(46)-C(41)	116(1)
mean C-C-C	109(2)	O(4)-C(46)-C(45)	124(1)
		C(42)-C(43)-C(47)	121(1)
		C(44)-C(43)-C(47)	121(1)
<u>t-butyl group C(47)-C(50)</u>			
mean C-C	1.49(3)	C(44)-C(45)-C(51)	122(1)
mean C-C-C	109(5)	C(46)-C(45)-C(51)	120(1)

t-butyl group C(51)-C(54)

mean C-C 1.53(2)

mean C-C-C 110(2)

a Esd's on mean values have been calculated with the use of the scatter formula $\sigma = [\sum(D_i - \bar{d})^2 / (N-1)]^{1/2}$, where d_i is the i th and \bar{d} is the mean of N equal measurements.

FIGURE 4.2

ORTEP DIAGRAM OF BIS(3,5-DI-TERT-BUTYL-CATECHOLATO)TIN(IV),
1,10-PHENANTHROLINE (1) WITH ATOMS SHOWN AS 30% PROBABILITY ELLIPSOIDS

Hydrogen atoms are omitted for clarity. Those atoms only identified by
numbers are carbons.

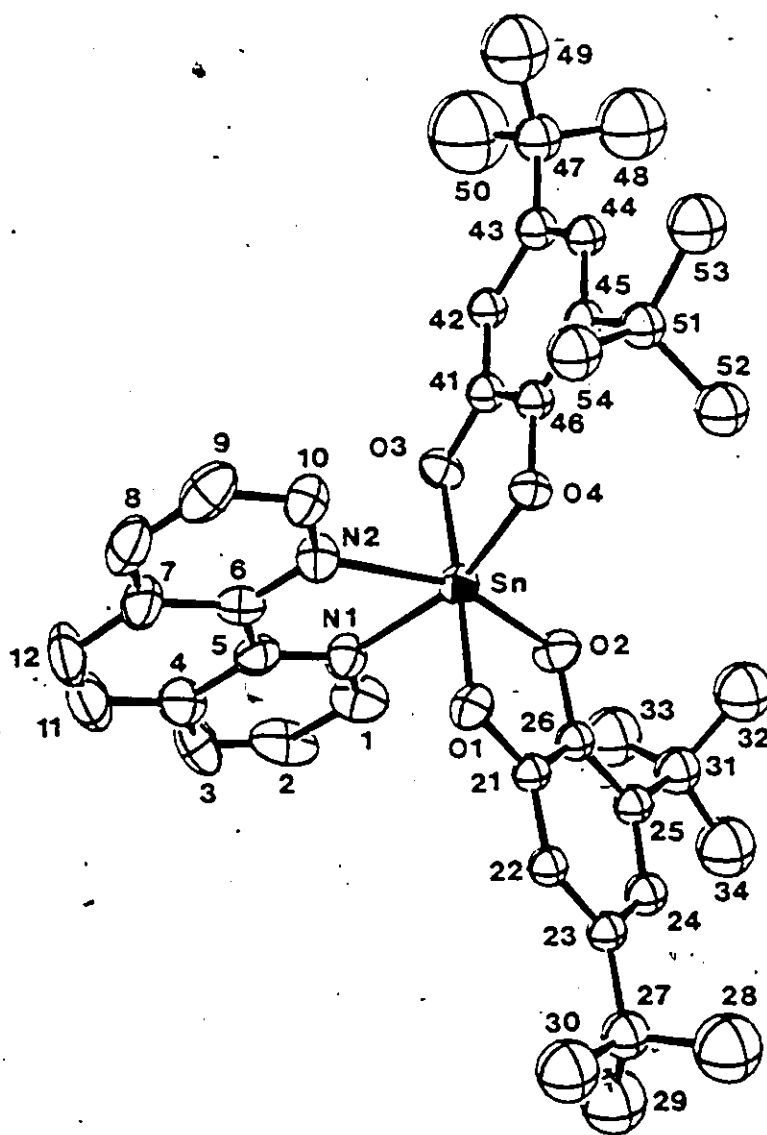
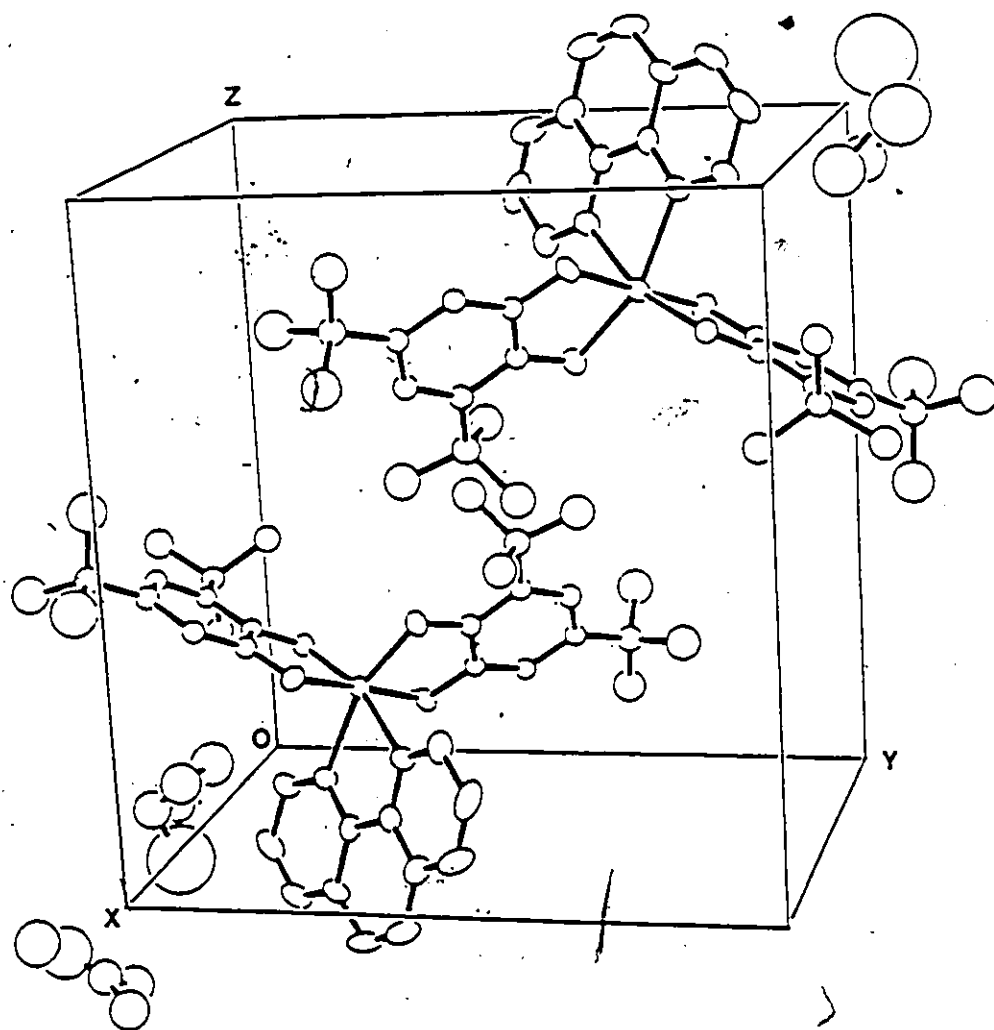


FIGURE 4.3

UNIT CELL PACKING OF 2

Also showing the position of the dimethylformamide molecules, drawn about $\frac{1}{2}, \frac{1}{2}, \frac{1}{2}$. Atoms are drawn as 20% probability ellipsoids.



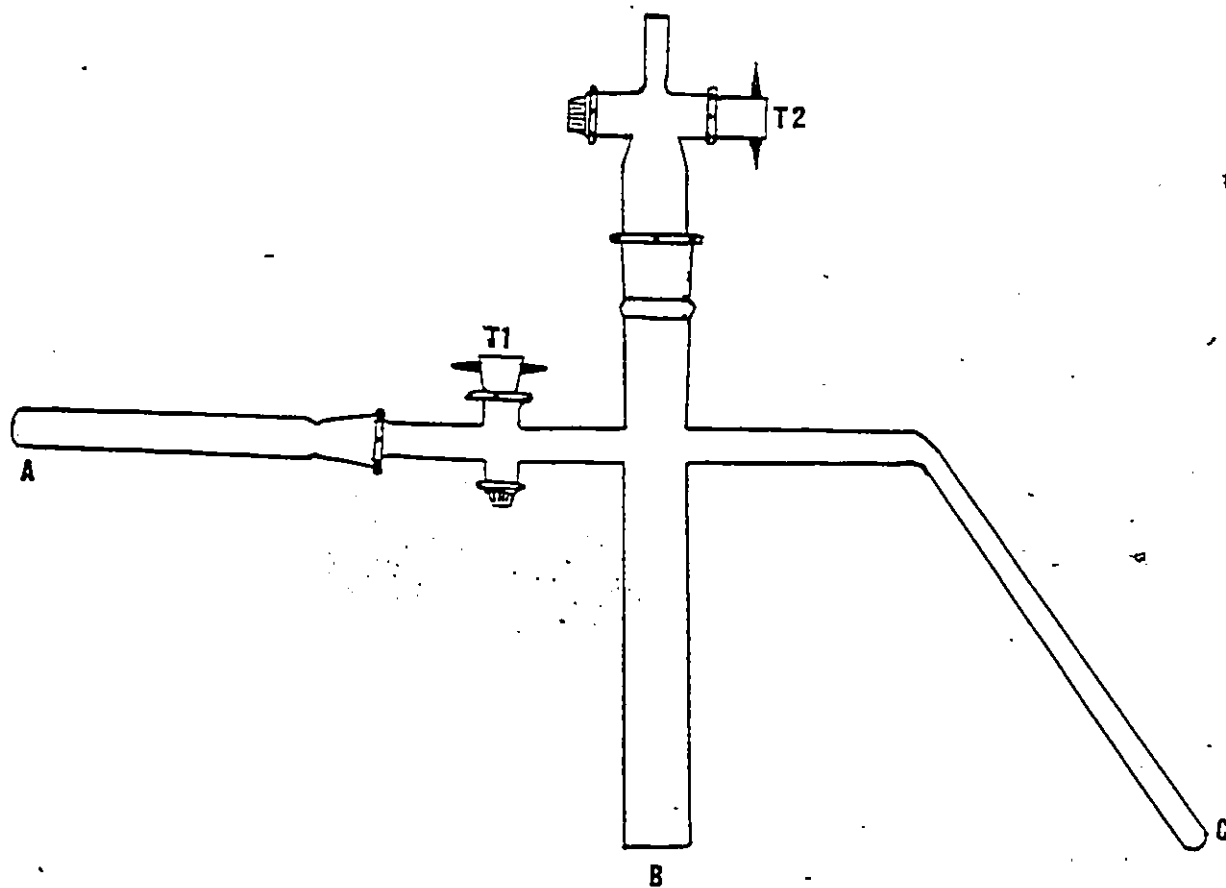
4.23 Electron Spin Resonance Spectroscopy

Spectra were recorded on a Varian E12 spectrometer which was calibrated with an NMR gaussmeter. The klystron frequency was determined from the ESR spectrum of diphenylpicrylhydrazyl. Spectra run at 77 K involved solids frozen on a liquid nitrogen cold finger Dewar vessel. The Varian cooling system was used in the variable temperature studies.

Solutions for ESR spectroscopy were prepared in the apparatus shown in Fig. 4.4. The chamber A was charged with a solution of SnX_2 (1 mg) in dry tetrahydrofuran (THF) (5 mL), and the solution thoroughly degassed by a series of freezing, evacuating and thawing cycles (3 x). The final solution *in vacuo* was isolated by closing stopcock T1, and an equimolar quantity of the *o*-quinones in 5 mL thf placed in chamber B, where it too was degassed. Reaction was initiated by opening T1 and tilting the apparatus to allow the solutions to mix in chamber B. After mild agitation, part of the reaction mixture was allowed to flow into the chamber C. This chamber could then be inserted into the cavity of the ESR spectrometer.

FIGURE 4.4

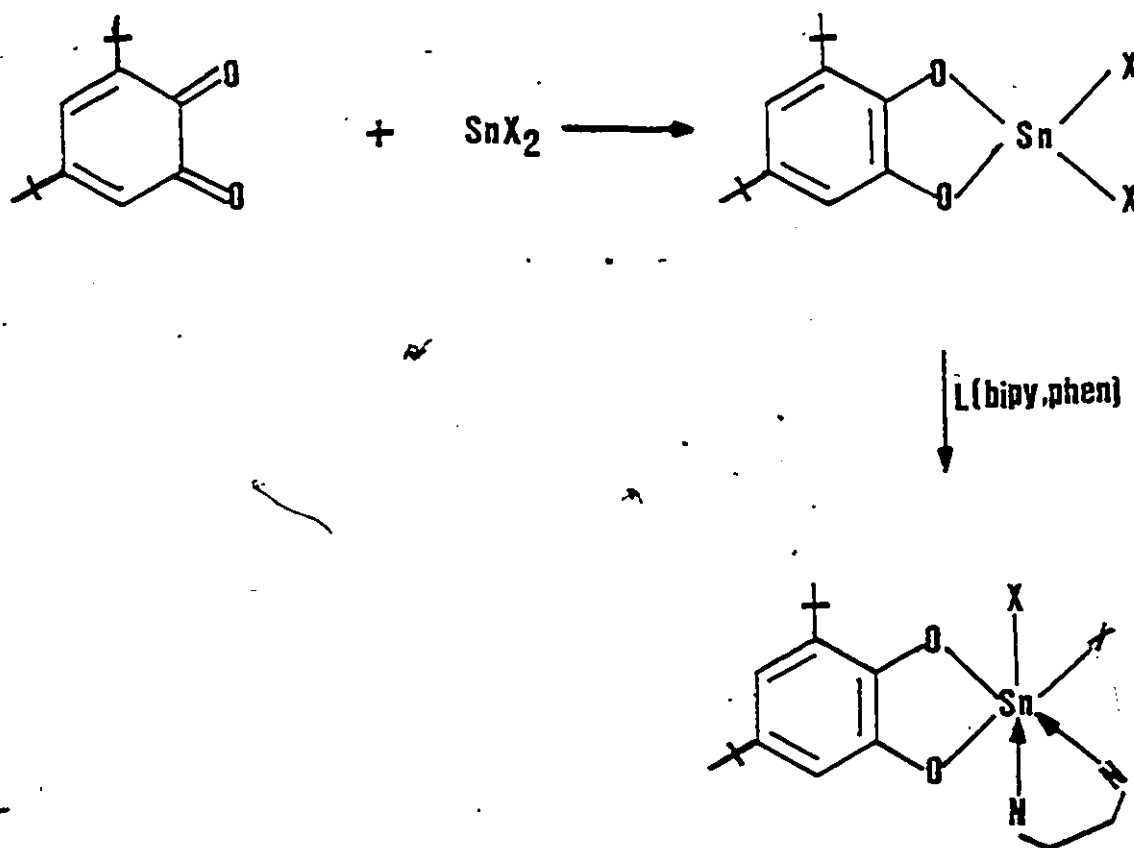
DIAGRAM OF APPARATUS USED IN PREPARATION OF SOLUTIONS FOR ESR SPECTROSCOPY



4.3 Results and Discussion

4.3.1 Preparative

The compounds listed in Table 4.1 are evidently the result of adduct formation by the dihalogeno(catecholato)tin(IV) species, whose genesis must lie in the overall oxidative addition reaction:



To this extent, the reactions are identical to those identified in the SnX_2 /tetrahalogeno-orthoquinone system (see Chapter 3), although the ESR studies reveal important features in the present reaction sequence not observable in the earlier work. (See below.)

In addition to the crystallographic evidence discussed below, the vibrational and NMR spectra confirm the formulation of these products as catecholato-tin(IV) species. The most significant feature of the infrared spectra is the absence of $\nu(\text{C}=\text{O})$. This mode is observed at $1661 \text{ s} + 1662 \text{ sh}$ in TBQ, and at $1673 \text{ s} + 1648 \text{ sh}$ in PQ; in the corresponding o-diolato derivatives, these vibrations are absent, and $\nu(\text{C}-\text{O})$ modes appear at $1468 \text{ s} + 1414 \text{ s}$ in $\text{TBC}^{2-}/\text{SnX}_2$, and at $1453 \text{ s} + 1443 \text{ s}$ for $\text{PD}^{2-}/\text{SnX}_2$. The infrared spectra also demonstrate the presence of coordinated bpy or phen in the adducts. (See Table 4.5.)

The ^1H NMR spectra equally confirm the presence of the appropriate o-diolato and bidentate nitrogen ligands. The results are summarized in Table 4.6. The assignments for bpy and phen are based on the previous work of Castellano, Gunther and Ebersole¹⁵⁹ and Dove and Hallett¹⁶⁰ respectively, and those for the anionic ligands by comparison with the spectra of the relevant quinone and diol. For TBQ, in $(\text{CD}_3)_2\text{SO}$ solution we found ^1H resonances at 6.97 m, 1H (assigned as H4): 6.13, m, 1H (H6): and 1.18, s, 18H ($t\text{-C}_4\text{H}_9$); for the corresponding diol, in the same solvent, the values are 8.00, br, 2H (OH): 6.74, m, 2H (H4,H6): 1.32, s, 9H ($t\text{-C}_4\text{H}_9$ at C5): and 1.21, s, 9H ($t\text{-C}_4\text{H}_9$ at C3). The resonances for PQ are at 8.31 m, 8.05 m, 7.75 m and 7.45 m, each 2H; the corresponding lines in the spectra of PD complexes could not be individually integrated or assigned. Finally, the ^{13}C NMR spectra of the products clearly

TABLE 4.5

DIAGNOSTIC IR ABSORPTIONS OF $(TBC)SnCl_2 \cdot L$ AND $(PD)SnCl_2 \cdot L$ ($L = BPY, PHEN$)

COMPOUND	ABSORPTION	ASSIGNMENT
$(TBC)SnCl_2 \cdot bipy$	3074 (w,s)	C-H bipy
	2958 (vs,br)	C-H-butyl
	1621 (s)	C=C(bipy)
	1459 (vs,br), 1240(s)	C-O
$(TBC)SnCl_2 \cdot phen$	3054 (w,s)	C-H phen
	2951 (vs,br)	C-H-butyl
	1624 (s)	C=C
	1471 (vs), 1230 (s)	C-O
$(PD)SnCl_2 \cdot bipy$	3064 (w,s)	C-H bipy, PD
	1615 (s,s)	C=C
	1453 (s,br)	C-O
$(PD)SnCl_2 \cdot phen$	3068 (w,s)	C-H bipy,PD
	1620 (s,s)	C=C
	1457 (s,br)	C-O

TABLE 4.6

 ^1H NMR SPECTRA FOR PRODUCTS ON SnX_2 ($\text{X} = \text{Cl}, \text{Br}, \text{I}$)/TBQ/PQ REACTIONS

COMPOUNDS ^(a)	CHEMICAL SHIFT ^(b)	ASSIGNMENT
(TBC)SnCl ₂ .bipy/	8.8 (m,2H)	bipy H3,H3'
	8.6 (m,2H)	bipy H4,H4'
	8.2 (m,2H)	bipy H5,H5'
	7.7 (m,2H)	bipy H6,H6'
	6.6 (m,2H)	TBC H3,H5
	1.4 (s,9H)	TBC C4,H9
	1.2 (s,9H)	TBC C4,H9
(TBC)SnCl ₂ .phen	9.2 (m,2H)	phen H2,H9
	8.8 (m,2H)	phen H4,H7
	8.6 (m,2H)	phen H4,H7
	8.2 (m,2H)	phen H5,H6
	6.6 (m,2H)	TBC H3,H5
	1.4 (s,9H)	TBC C4,H9
	1.2 (s,9H)	TBC C4,H9
(TBC)SnBr ₂ .bipy ^(c)		
(TBC)SnBr ₂ .phen ^(c)		
(PD)SnCl ₂ .bipy ^(d)		

(PD)SnBr₂.bipy^(c,d)

9.1-7.1

(PD)SnI₂.phen^(c,d)

- (a) TBC = 3,5-di-tert-butyl-catecholato anion. PD = phenanthro-9,10-diolato anion.
- (b) Solutions in dmsO-d₆. Values in ppm relative to Me₄Si.
- (c) Spectrum essentially identical to that of corresponding chloro compound.
- (d) Individual integration not possible.

demonstrate the presence of aromatic rather than quinonoid ring system. The spectra of the starting materials, the corresponding o-diols, the neutral ligands, and certain typical products are shown in Table 4.7. The values for phen are taken from Table 3.4. While some of the assignments are tentative, there is no doubt that the high field resonances identified as >C=O of TBQ and PQ disappear on the formation of the tin(IV) species, and that these same changes are observed on comparing TBQ and TBC(OH)₂. In summary, the spectroscopic evidence shows unambiguously that the final products are tin(IV) derivatives of aromatic o-diolato ligands.

We note finally that there are significant differences in the solubility of the adducts of (TBC)SnX₂, with the chloride precipitating spontaneously from the reaction mixture, and bromide requiring addition of diethyl ether. The iodo derivative is the most soluble, and apparently undergoes the rearrangement reaction



The existence of such an equilibrium is demonstrated by the identification of (TBC)₂Sn.phen and SnI₄.bipy as the products of two similar reactions (see experimental). Such rearrangements are a common feature of tin(IV) solution chemistry. It seems probable that the detailed course of the reaction between TBQ and SnI₂ is solvent and temperature dependent, but we have not investigated this point in detail.

TABLE 4.7

^{13}C NMR SPECTRA OF TBN(IV) DERIVATIVES OF $\text{O}-\text{Cl}_4\text{C}_6\text{O}_2$ IN $(\text{CD}_3)_2\text{SO}$; VALUES
IN PPM, RELATIVE TO Me_4Si

Compound ^(a)	TBQ,TBC,PQ,PD	bipy	phen
TBQ	180.5(C 2),179.7(C 1) 162.5(C 3),148.9(C 5) 133.4(C 4),121.7(C 6) 35.7(C 7),35.0(C 8) 29.0(C 9), 27.5(C 10)		
TBC(OH) ₂	144.3(C 2),141.4(C 1) 140.0(C 3), 134.5(C 5) 113.1(C 4), 110.2(C 6) 34.4(C 7),33.8(C 8) 31.5(C 9),29.5(C 10)		
bipy		155.2(C 3),149.2(C 1) 137.2(C 4),124.1(C 6) 120.4(C 5)	

phen

149.7(C 2,C 9)
 145.4(C 4b,C 6b)
 135.3(C 3,C 8)
 128.1(C 4,C 7)
 126.4(C 4a,C 6a)
 123.0(C 5,C 6)

(TBC)SnCl ₂ -bipy	148.3(C 1,C 2)	150.4(C 3)
	112.6(C 3,C 5)	147.6(C 1)
	110.9(C 4,C 6)	140.6(C 4)
	34.4(C 7),33.8(C 8)	126.0(C 6)
	31.7(C 9),29.6(C 10)	122.4(C 5)

(TBC)SnBr ₂ -phen	149.4(C 1,C 2)	144.7(C 2,C 9)
	110.0(C 3,C 5)	141.6(C 4b,C 6b)
	109.8(C 4,C 6)	139.0(C 3,C 8)
	35.0(C 7),34.7(C 8)	128.2(C 4,C 7)
	31.8(C 9),29.8(C 10)	127.0(C 4a,C 6a)
		125.0(C 5,C 6)

PQ	179.0(C 9,C 10)
	135.5(C 11,C 14)
	135.3(C 12,C 13)
	131.2(C 1,C 8)
	129.3(C 4,C 5)

	129.1(C 3,C 6)		
	124.4(C 2,C 7)		
<hr/>			
(PD)SnCl ₂ .bipy	145.5 (C 9,C 10)	154.9(C 3)	
	139.1(C 11,C 14)	149.1(C 1)	
	129.2(C 12,C 13)	137.5(C 4)	
	126.9(C 1,C 8)	122.5(C 6)	
	125.8(C 4,C 5)	120.7(C 5)	
	124.3(C 3,C 6)		
	121.5(C 2,C 7)		
<hr/>			
(PD)SnI ₂ .phen	147.25(C 9,C 10)	141.7(C 2,C 9)	
	138.9(C 11,C 14)	137.11(C 4,C 6)	
	128.8(C 12,C 13)	129.3(C 3,C 8)	
	128.2(C 1,C 8)	127.3(C 4,C 7)	
	125.7(C 4,C 5)	124.1(C 49,C 69)	
	124.11(C 3,C 6)	122.5(C 5,C 6)	
	121.3(C 2,C 7)		
<hr/>			

(a) Abbreviations as in Table 4.2.

4.3.1.1 Electron Spin Resonance Spectroscopic Studies

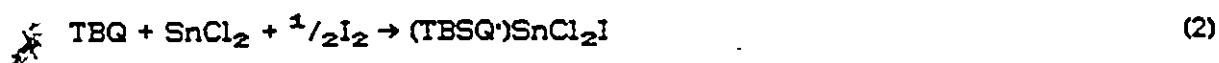
Fig. 4.5 shows the ESR spectrum of a THF solution prepared by reacting SnX_2 ($\text{X}=\text{Cl}$) with TBQ at room temperature. Although the spectrum is not well resolved, the most obvious feature is the presence of the recognizable spectrum of the orthosemiquinone (TBSQ \cdot). The splitting due to one aromatic hydrogen atom is clearly observed, as is that due to the magnetic isotopes of tin, but the resonances due to ^{117}Sn and ^{119}Sn could not be separated because of the large line-width ($\nu^{1/2} = 1.34\text{G}$). The coupling constants, $a_{\text{H}} = 3.4\text{G}$ and $a_{\text{Sn}} = 10.3\text{G}$ allowed the spectrum to be computer-simulated to a satisfactory agreement. (See Table 4.8a.) These values are similar to those reported by Davies and Hawari⁹ for the semiquinone-tin radical $\text{X}_3\text{SnO}_2\text{C}_6\text{H}_2(\text{tBu})_2$ formed by the reaction of RSnX_3 ($\text{R} = \text{Me, Bu, Cp}$) and 3,6-di-tert-butyl-1,2-benzoquinone. They are also close to those found for the InX/TBQ system,² (see Chapter 6) and indicate a similar distribution of the unpaired electron density on the aromatic ring of all these semiquinone systems. The coupling constant for indium in $\text{In}^{\text{III}}\text{Br}_2(\text{TBSQ}\cdot)\cdot 2\text{py}$ ($\text{py} = \text{pyridine}$) is 5.16 G, so that the ratio $a_{\text{Sn}}/a_{\text{In}} = 2$, which is close to the ratio of the Fermi contact terms ($= 2.18$)¹⁶¹, implying that the appropriate metal orbitals contribute equally to the bonding orbital in the two $\text{M}(\text{TBSQ}\cdot)$ systems.

A significant result was obtained by running the ESR spectrum of a solution obtained from heating $\text{TBQ} + \text{SnCl}_2 + \frac{1}{2}\text{I}_2$ in refluxing toluene until total discharge of iodine colour (4 hrs). The spectrum of this solution was notably

FIGURE 4.5

ESR SPECTRUM OF THE SnCl_2 /TBQ REACTION IN THF

sharper than those discussed above, and the derived coupling constants were $a_H = 3.4$ G, $a_{Sn} = 8.6$ G. This spectrum is undoubtedly that of (TBSQ') $SnCl_2I$, formed by



and is essentially identical to those reported by Davies and Hawari.¹⁵⁵

The ESR spectrum of a frozen solution at 77K is shown in Fig. 4.8a. In addition to the spectrum of the (TBSQ') SnX_n species, we observe a pair of spin-triplet features, indicating the presence of two biradical species. These would not be observed in the solution spectra because of the averaging effect of molecular motion. Although the amplitude of the first derivative spectrum of these biradicals are in total about twenty times smaller than that of the semiquinone species, the signal from the latter is isotropic and only a few gauss wide, while the highly anisotropic biradical spectra are spread over about 500 G. We estimate that the total concentration of these biradicals is of the same order as that of (TBSQ') SnX_2 ; it was not possible to integrate the spectra to establish this ratio exactly. The ESR parameters of the two biradicals are presented in Table 4.8b. The zero-field splitting parameters D and E may be assumed in the present system to arise uniquely from the magnetic dipole-dipole interactions between the two unpaired electrons, and the D parameter in particular may be used to estimate the effective distance between the two electrons, using the formula.¹⁶²

$$D_{dipole} = -(3/2)g^2\beta^2/r^3 \quad (3)$$

The above results give distances of 4.9Å for A, and 7.4Å for B, although some error may arise when the electrons are highly delocalized. The addition of iodine to a solution of (TBSQ') SnX_2 , followed by freezing, causes the ESR spectrum

FIGURE 4.6

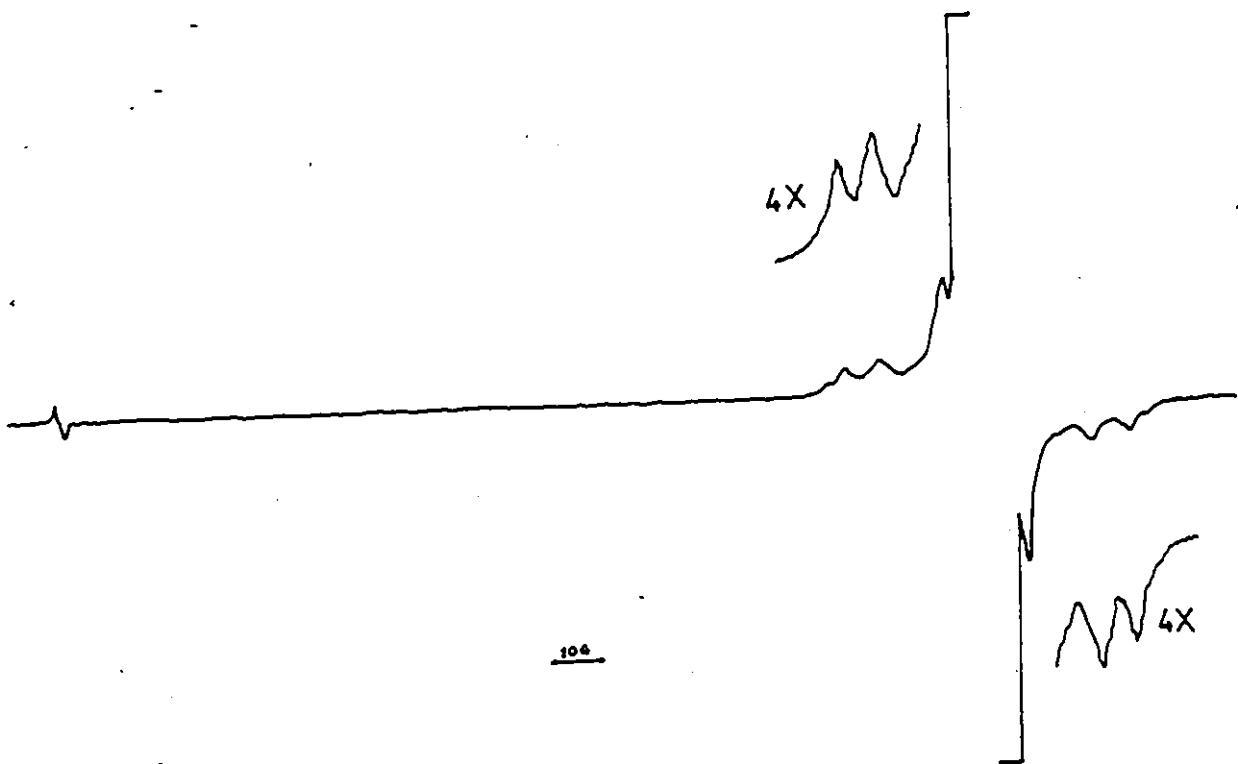
ESR SPECTRUM OF A FROZEN THF SOLUTION OF SnCl_2 /TBQ REACTION

TABLE 4.8a
ESR PARAMETERS OF Sn(IV) SEMIQUINONE COMPLEXES AT 298 K

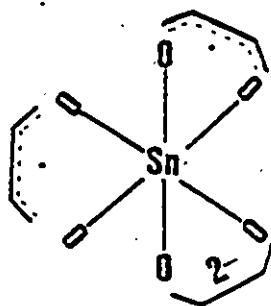
COMPOUND	SOLVENT	HYPERFINE CONSTANTS IN GAUSS	
		a_{Sn}	a_{H}
(TBSQ)SnCl ₃	THF	10.3	3.4
(TBSQ)SnBr ₃	THF	9.5	3.5
(TBSQ)SnI ₃	THF	8.0	3.5
(TBSQ)SnCl ₂ I	THF	8.6	3.4
(PSQ)SnCl ₃	THF		
(PSQ)SnBr ₃	THF	Broad unresolved spectra with $g \approx 2.0023$	
(PSQ)SnI ₃	THF		

TABLE 4.8b
ESR PARAMETERS OF THE BIRADICAL FORMED FROM THE REACTION OF TBQ
WITH SnCl₂ IN THF AT 77 K

TYPE	$g_x(\text{G})$	$g_y(\text{G})$	$g_z(\text{G})$	$D(\text{cm}^{-1})$	$E(\text{cm}^{-1})$
A	-	2.0037	2.0037	0.0228	0.0035
B	-	-	2.0037	0.0065	-

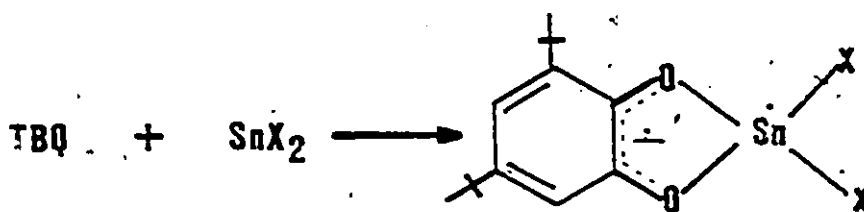
identified as A to disappear while that of B is unaffected.

The reaction of tin (dissolved in mercury) with 3,6-di-tert-butylorthoquinone (DBQ) has also been studied by ESR spectroscopy.¹⁶³ In addition to lines identifying the semiquinone ligand bonded to tin, the spectra also reveal the presence of biradicals in the frozen solution, and these have been assigned by Prokof'ev et al. to structure



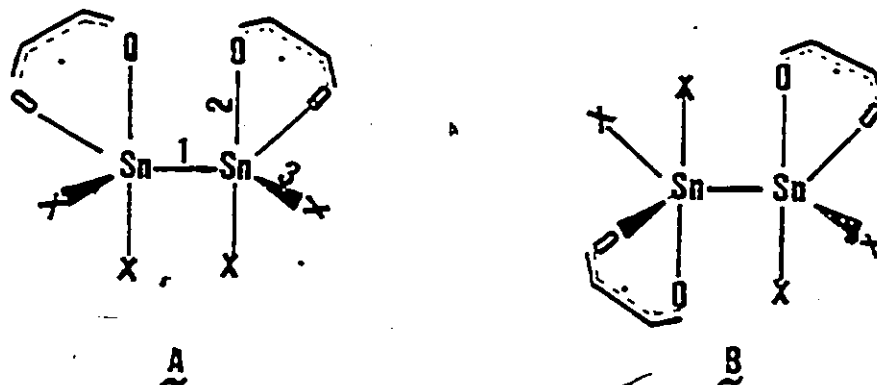
identified as a six-coordinate tin(IV) complex, and reduction of this biradical with tin amalgam is reported.

We offer a different interpretation for the present results. The first step in the reaction between TBQ and SnX_2 is believed to be



in which the product has two unpaired electrons, one delocalized on the semiquinone bidentate ligand, and the other on the tin atom. Tin-centred radicals have been reported for a number of $\text{Sn}^{\cdot}\text{R}_3$ species by Lappert et al.,^{164,165} who find that the hyperfine coupling constants are extremely large. A similar conclusion applies to SnCl_3^{\cdot} .¹⁶⁵ If this is also the case for $(\text{TBSQ})\text{SnX}_2$, the resultant components of the ESR spectrum arising from ^{119}Sn will appear at the magnetic field of about 5000 G which we did not observe.

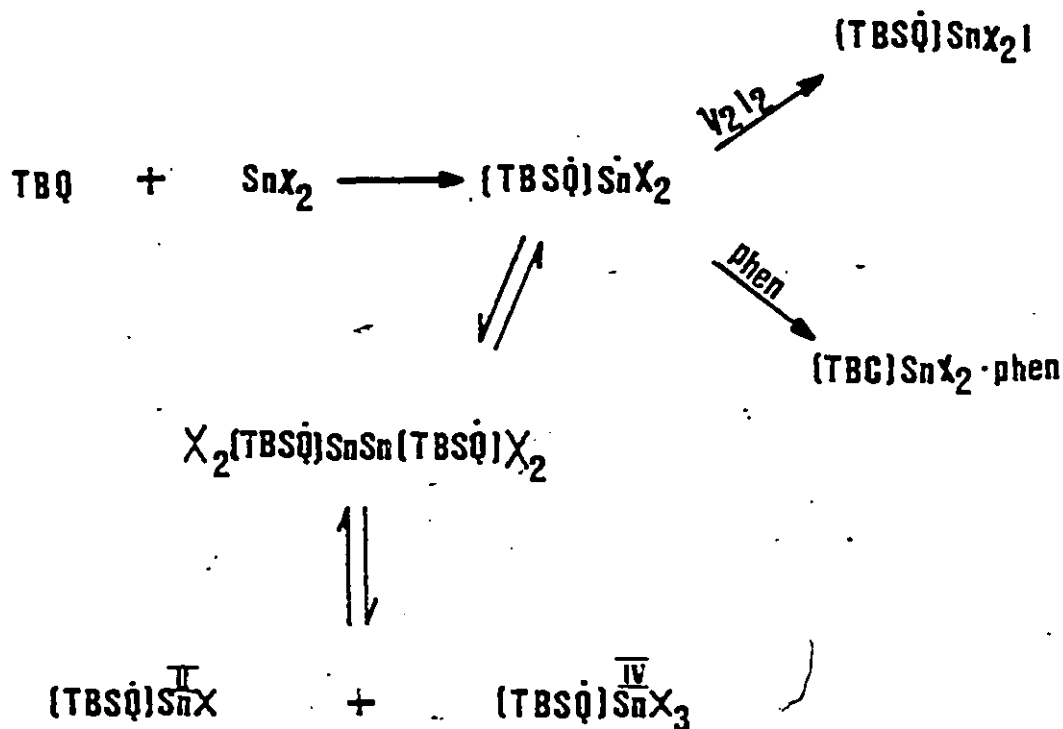
The spectra observed are therefore those of species derived from $(\text{TBSQ}^{\cdot})\text{Sn}\cdot\text{X}_2$. This species can be oxidized by $^{1/2}\text{I}_2$ to $(\text{TBSQ}^{\cdot})\text{SnX}_2\text{I}$, but in the absence of this equivalent of oxidant, the proposed fate of the diradical is to dimerize by Sn-Sn bonding to give the diradical $\text{X}_2(\text{TBSQ}^{\cdot})\text{SnSn}(\text{TBSQ}^{\cdot})\text{X}_2$. This latter species would require tin to be five-coordinate and would therefore give rise to two isomers if the coordination is essentially trigonal bipyramidal



where 1,2,3 as presented below, are typical bond distances (\AA) of Sn-Sn,¹⁶⁶ Sn-O,¹⁶⁷ and Sn-X (X = Cl)¹⁶⁸ respectively; 1 = 2.77 \AA , 2 = 2.05 \AA , 3 = 2.11 \AA .

We identify these as the A and B species whose ESR parameters are given in Table 4.8b. Of these, the interelectronic distances, estimated from models using reasonable bond lengths and angles, are 5.5 \AA in A and 7.1 \AA in B, in remarkably good agreement with the distances estimated from the spectral data. The more rapid (5 min) reaction of A with I_2 appears to be keeping with the openness of this structure in terms of the polar transition state proposed for the attack of I_2 at the Sn-Sn bond of organometallic compounds.¹⁶⁹

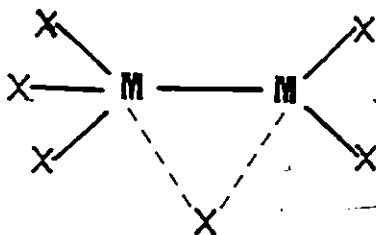
The overall scheme is then



Scheme 2

Under the conditions used, the only species whose ESR spectrum would be observed with solutions of TBQ + SnX₂ are (TBSQ)Sn^{II}X and (TBSQ)SnX₃. Although the ESR spectrum of the former has not been reported, it seems reasonable to assume that it might be very similar to that for (TBSQ)SnX₃, since the spectra of the series of such molecules studied by Davies and Hawari¹⁵⁹ are only slightly dependent on the nature of the other group attached to tin, insofar as the spectrum of the TBSQ moiety is concerned. We also note that the *a*_H values for TBSQ complexed to either indium(III) or indium(I) (see Chapter 6) are similar to those for the tin(IV) radicals, again supporting the close identity proposed for (TBSQ)SnX and (TBSQ)SnX₃.

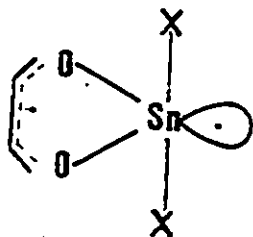
The disproportionation of the proposed Sn-Sn dimer is in keeping with the behaviour of Sn_2Cl_6 , which above -65°C goes to SnCl_2 and SnCl_4 .⁹³ There are similar processes in the chemistry of indium(II), both in terms of the interaction of InX and InX_3 ,⁷⁶ and the disproportionation of $\text{In}_2\text{X}_6^{2-}$ anions to InX_2^- and InX_4^- .⁴⁶ All of these processes can be accommodated within a mechanism of halide transfer, in which the intermediate is;



the detailed arguments for this process have been given elsewhere.^{46,47}

Two final points should be made about the mechanism proposed in Scheme 2. Firstly, as already noted, the addition of 0.5 I_2 converts $(\text{TBSQ}')\text{SnX}_2$ to $(\text{TBSQ}')\text{SnX}_2\text{I}$, thus oxidizing $\text{Sn}^{\text{III}} \rightarrow \text{Sn}^{\text{IV}}$, rather than affecting the TBSQ' ligand. This $(\text{TBSQ}')\text{SnX}_2\text{I}$ species is sufficiently stable in solution to permit ESR investigation, and does not spontaneously convert to the corresponding TBC derivative. Secondly, the preparative results show that when neutral bidentate donors are present in the reaction mixture, the products are derivatives of $(\text{TBC})\text{SnX}_2$, so that under these conditions the final product is an adduct of $(\text{TBC})\text{SnX}_2$, or a rearrangement product of the latter depending on the conditions (see Experimental).

The effect of coordination of the neutral ligand can be understood in the following way. If the unpaired electron on tin in $(\text{TBSQ}')\text{SnX}_2$ is in a localized orbital, the structure can be written as the five-coordinate species C;



c

the question of whether this is trigonal bipyramidal or square pyramidal is not important at this stage. Coordination transfers negative charge to the tin, thereby favouring transfer of the unpaired electron to the TBSQ ligand to give the corresponding catecholate. Furthermore, the adduct $(\text{TBSQ})\text{SnX}_2\text{bipy}$ can only retain the localized electron by being seven-coordinate, whereas transfer to the dioxo ligand yields the six-coordinate complex, a stereochemistry of established stability in tin(IV) chemistry.

It also follows from this argument that the essential difference in the behaviour of TBQ (and by analogy PQ) and the tetrahalogeno-*o*-quinones studied in Chapter 3 lies in the redox properties of the two pairs of quinones. It is clear from measurements of the half-wave potentials^{170,171} that the tetrahalogeno species are more easily reduced than the compounds used in the present work. In keeping with this, we observed a faster reaction in the earlier work, (see Chapter 3) with no evidence of stable semiquinone species as intermediates in the reaction.

Although the reaction of SnX_2 with PQ appears to proceed in an identical fashion to that with TBQ, the discernible features seen in the ESR spectrum of the latter are not observed with this quinone. Instead, we observed a broad unresolved spectrum in THF both at room temperature and in liquid nitrogen (77 K) with $g \approx 2.0023$.

4.3.2 Structural Studies

The structure of the compound 2 confirms the conclusions reached from the NMR and vibrational spectroscopic studies, namely that the isolated products are o-diolato derivatives of tin(IV). The SnO_4N_2 kernel has a strongly distorted octahedral geometry, due in part to the bite of the ligands being far from 90° .

The bond distances in 2 are typical of those reported for other tin(IV) complexes. The average Sn-O bond distance is 2.008 \AA which is slightly less than the value of $2.062(3) \text{ \AA}$ found in $[\text{Sn}(\text{O}_2\text{C}_6\text{Cl}_4)_3]^{2-}$ anion ($\text{O}_2\text{C}_6\text{Cl}_4$) $^{2-}$ = tetrachlorocatecholate anion (Chapter 3), and the average value of $2.049(4) \text{ \AA}$ in the closely related $(\text{TBC}^{2-})\text{Sn}(\text{OCF}_3)_2\cdot\text{CH}_3\text{OH}$ studied by Butters, Scheffler, Stegmann, Weber and Winter.¹⁶⁷ These distances are at the low end of the range reported for other tin(IV)-oxoligand species. The O-C distances in the TBC^{2-} ligand (av. 1.36 \AA) are typical of those in phenolates, and intermediate between the comparable values for $[\text{Sn}(\text{O}_2\text{C}_6\text{Cl}_4)_3]^{2-}$ (av. $1.336(5) \text{ \AA}$) and $(\text{TBC}^{2-})\text{Sn}(\text{OCF}_3)_2\cdot\text{CH}_3\text{OH}$ (av. $1.374(7) \text{ \AA}$).¹⁷² More importantly, the bonds are significantly longer than the average (1.29 \AA) found for a variety of transition metal complexes of the 3,5-di-tert-butyl-o-semiquinonato ligand.^{150,151} The diolato ligand is essentially planar as far as the C_6O_2 atoms are concerned, and the C_6 ring is clearly aromatic, as evidenced by the C-C-C bond lengths and angles. The bite angle of the ligand (i.e. O-Sn-O) is 83.1° (av), slightly larger than that reported for $[\text{Sn}(\text{O}_2\text{C}_6\text{Cl}_4)_3]^{2-}$ (O-Sn-O = 81.5° (av)). (See Chapter 3.)

The Sn-N bond distance in 2 is 2.26 \AA (av), within the range for $\text{Sn}^{\text{IV}}\text{-N}$ bonds in a variety of organotin compounds,¹⁷³ and slightly less than the average value in $\text{Sn}(\text{SPh})_4\cdot\text{bipy}$ (2.331 \AA (av)).¹⁷⁴ The bite of the ligand is $74.0(4)^\circ$, again

in agreement with previous values, and the phen ligand is essentially planar.

Our work in this chapter has served to confirm that oxidative addition reactions involving metals in their low oxidation state proceed by a series of one electron transfers an important conclusion in Main Group Element Chemistry. Subsequent chapters cover related work involving low oxidation state indium compounds.

CHAPTER 5

THE REACTION OF In(I) HALIDES WITH TETRAHALOGENO-ORTHO-QUINONES: FORMATION OF In(III) CATECHOLATES

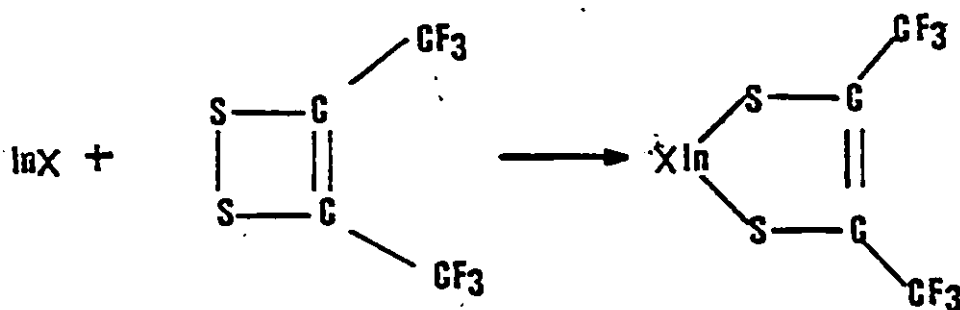
5.1 Introduction

In Chapters 3 and 4, we examined the reactions of tin(II) halides with two sets of orthoquinones, each of which reacts differently with the substrate, and this difference was exploited in deriving a mechanistic pathway to their respective end-products. The present chapter examines similar reactions with indium(I) halides. Although the synthetic route in these reactions had to be modified as our studies progressed, full advantage was taken again of the solubility of indium(I) halides in a mixture of an aromatic solvent and an organic base at low temperature, as described in Chapter 2.

Indium compounds containing metal-oxygen bonds have been of some interest over the years, particularly because of the information they provide on the coordination chemistry of indium. Perhaps the most widely studied are the β -ketoenolates, which bear some resemblance to the indium catecholates since both have two oxygen atoms directly bonded to the metal. The well-characterized tris (pentane-1,2-dionato)-indium(III), $\text{In}(\text{acac})_3$,¹⁷⁵ is a good representative of this group of complexes. It was first prepared in 1921 by the reaction of Hacac with freshly precipitated $\text{In}(\text{OH})_3$. A direct route involving the electrochemical oxidation of indium metal in a solution of Hacac in methanol has also been established.¹⁷⁶ The infrared^{177,178} and Raman¹⁷⁹ spectra of $\text{In}(\text{acac})_3$ have been reported and its proton NMR has been discussed by a number of authors.¹⁸⁰⁻¹⁸³ The diamagnetism allows a clear interpretation in terms of delocalized electron density in the (OCCCCO) system, but it is not clear whether

this bonding extends to the metal itself. The planarity and the InO_6 kernel implicit in these results have been confirmed by X-ray crystallography.^{24,184} Diketonates of indium(III) are thermodynamically stable complexes in non-aqueous solution,¹⁸⁵ and are sufficiently robust to allow polarographic studies which demonstrated one-electron reductions to the (formally) indium(II) and indium(I) compounds.¹⁸⁶

Another set of related compounds are the indium dithiolates. There have been several reports of different synthetic routes to their formation, one of which is the reaction of indium(I) halides with 1,2-bis(trifluoromethyl) dithiete⁷⁵ or R_2S_2 ⁷⁶ in non-aqueous solution. This reaction proceeds by insertion of indium into the S-S bond of the dithiete to give polymeric products containing an InS_2C_2 ring. A similar reaction has been found to occur when the dithiete reacts with cyclopentadienylindium.⁷⁵



Complexes with anionic dithiolene ligands have been prepared^{186,187} by the reaction of InCl_3 with the sodium salt of the appropriate ligand such as MNT^{2-} (= maleonitrile-dithiolate), TDT^{2-} (= toluene-3,4-dithiolate) or $i\text{-MNT}^{2-}$ (= 1,1-dicyanoethylene-2,2-dithiolate), and these products can also be reduced polarographically. The crystal structure of $(\text{Et}_4\text{N})_3[\text{In}(\text{MNT})_3]$ established the planarity of the InS_2C_2 ring system.^{187,188}

Indium catecholates have been prepared¹⁸⁹ in aqueous media by Bevillard in aqueous media, and were characterized as anionic complexes e.g. $[\text{In}(\text{O}_2\text{C}_6\text{H}_5)_3]^{3-}$. Physico-chemical investigations by Srivastava and Mohan¹⁹⁰ on solutions made by mixing 10 mL of 0.01 M indium nitrate solutions showed that depending on the pH of the medium, one can isolate indium catecholates in which the ratio of indium to catechol corresponds to 1:1, 1:2 or 1:3.

Work presented in this chapter involves the oxidative addition of indium(I) compounds to halogeno-substituted orthoquinones. In contrast with related reactions carried out with other quinones which gave stable indium(III) semiquinonato products (see Chapter 6), the products obtained in this case were characterized as indium(III) catecholato complexes. Due to the instantaneous nature of the reactions we were unable to monitor the electron transfer processes with the aid of ESR spectroscopy, as was also the case with identical reactions with tin(II) halides (see Chapter 3). Direct reaction of metallic indium with these quinones by refluxing in toluene in the presence of half molar quantities of iodine, diphenyldiselenide or diphenyldisulphide has led to the isolation of derivatives of indium(III) catecholates. In the course of the latter reaction, a blue solution was formed when only part of the indium had been consumed, and this solution exhibited a strong ESR signal suggesting the formation of a semiquinonato complex. An interpretation of the ESR spectra is offered, as well as a mechanism relating to the electron transfer processes in these reactions. A brief kinetic study was conducted with the aid of absorption spectroscopy.

5.2 Experimental

5.2.1 The reaction of InX (X = Cl, Br, I) with Y₄C₆O₂ (Y = Cl, Br)

(i) With tmen: The same general method was used for all the reactions with isolation procedures which varied depending on the particular system. In a typical experiment, 3 mmol of InX (X = Cl, Br, I) was suspended in 25 mL of toluene/methylene chloride mixture (1:1, v/v). This was then cooled to about -40°C and tmen (ca 2 mL 13 mmol) syringed into the mixture, when the characteristic reddish colour of solutions of InX in such mixtures was observed. With the temperature still at about -40°C, an equimolar amount of tetrachloro-orthoquinone in 25 mL of toluene/methylene chloride mixture (1:1, v/v) was added dropwise over a period of 1 h. Stirring was continued at this temperature for an hour and then the solution allowed to warm up slowly to room temperature. Further stirring at room temperature for another 1 h followed. The resultant clear red-wine solution was filtered and the volume of the filtrate reduced by $\frac{2}{3}$ *in vacuo*, addition of diethyl ether or petroleum ether then afforded a light-brown precipitate when X = Cl, or Br. When X = I an oily material was obtained, and a solid product was formed only after lengthy trituration with cold petroleum ether. All products were washed twice with 20 mL portions of either petroleum ether or diethyl ether, and then dried *in vacuo*. These products analyzed as Cl₄C₆O₂InX.n tmen (n = 1 $\frac{1}{2}$, 2). It was quite apparent from our analytical data that due to the excess amount of tmen used, the products did not correspond to the 1:1 adduct. A strategy to eliminate this problem is described in the next paragraph.

(ii) A 3 mmol amount of InX (X = Cl, Br, I) was stirred with the tetrahalogeno orthoquinone (3 mmol) in 50 mL of a tol/methylene chloride mixture (1:1, v/v)

at room temperature. The red colour of the quinone was discharged after stirring for ca. 6 h with the complete consumption of the indium monohalide. At this stage, tmen (0.45 mL, 3 mmol) was syringed into the reaction mixture. Stirring was continued for another hour. The now light yellow solution was filtered to remove any solid impurities. The isolation procedure was as described above. Analytical results are presented in Table 5.1.

(iii) With phen: We were able to synthesize the indium(III) catecholates (InXCat) by reacting equimolar amounts (ca 3 mmol) of InX with tetrahalogeno-orthoquinones (Q) in methylene chloride at room temperature. Complete reaction occurs over a period of 4 to 6 h. Addition of an equimolar amount of 1,10-phenanthroline quantitatively precipitated the adduct of the target compound InXCatL_n . See Table 5.1 for analytical data.

(iv) The reaction of metallic indium with $\text{Y}_4\text{C}_6\text{O}_2$ ($\text{Y} = \text{Cl, Br}$) in the presence of I_2 or Ph_2Se_2 or Ph_2S_2 . Finely cut indium (0.5 g, 4.4 mmol) was refluxed with an equimolar amount of the tetrahalogeno-orthoquinone and a half-molar quantity of iodine, diphenyldiselenide or diphenyldisulphide in toluene. Reactions involving iodine or diphenyldiselenide were complete within 6 h, but with diphenyldisulphide a period of 24 h was needed. In each case, a blue solution formed half way through the reaction, and this solution was found to be ESR active. The end of the reaction was signified by the formation of a clear solution

TABLE 5.1
ANALYTICAL RESULTS FOR In(III) CATECHOLATES

Compound	Method	In(%) ^a	C(%)	H(%)	N(%)
Cl ₄ C ₆ O ₂ InCl ₂ tmen. ¹ / ₂ Et ₂ O	i	17.3(17.3)	35.6(36.1)	6.0(5.9)	8.6(8.4)
Cl ₄ C ₆ O ₂ InBr ₂ tmen	i	17.0(17.1)	32.3(32.1)	4.9(4.8)	8.1(8.3)
Cl ₄ C ₆ O ₂ InL ₁ ¹ / ₂ tmen.	i	17.4(17.4)	27.9(27.2)	4.1(4.0)	6.5(6.4)
Cl ₄ C ₆ O ₂ InCl.tmen	ii	22.0(22.4)	-	-	-
Cl ₄ C ₆ O ₂ InBr.tmen	ii	21.0(20.6)	-	-	-
Cl ₄ C ₆ O ₂ InL.tmen	ii	18.7(19.0)	-	-	-
Br ₄ C ₆ O ₂ InCl.tmen	ii	16.6(16.6)	-	-	-
Br ₄ C ₆ O ₂ InBr.tmen	ii	15.7(15.6)	-	-	-
Br ₄ C ₆ O ₂ InL.tmen	ii	14.45(14.7)	-	-	-
Cl ₄ C ₆ O ₂ InCl.phen	iii	19.9(19.9)	-	-	-
Cl ₄ C ₆ O ₂ InBr.phen	iii	18.4(18.5)	-	-	-
Cl ₄ C ₆ O ₂ InL.phen	iii,iv	17.2(17.2)	32.5(32.4)	1.42(1.2)	4.0(4.2)
Cl ₄ C ₆ O ₂ InL.phen.DMF	iv	15.9(15.5)	34.1(34.2)	2.04(2.3)	5.7(5.6)
Br ₄ C ₆ O ₂ InCl.phen	ii	15.2(15.2)	-	-	-
Br ₄ C ₆ O ₂ InBr.phen	iii	14.4(14.4)	-	-	-
Br ₄ C ₆ O ₂ InL.phen	iii	13.6(13.6)	-	-	-

$\text{Cl}_4\text{C}_6\text{O}_2\text{In}(\text{SPh})_2\text{phen}$	iv	17.8(17.7)	-	-	-
$\text{Cl}_4\text{C}_6\text{O}_2\text{In}(\text{SPh})_2\gamma\text{-pic}$	iv	17.4(17.5)	-	-	-
$\text{Br}_4\text{C}_6\text{O}_2\text{In}(\text{SPh})_2\text{phen}$	iv	14.0(13.9)	-	-	-
$\text{Cl}_4\text{C}_6\text{O}_2\text{In}(\text{SePh})_2\text{phen}^{1/4}\text{ Tol}$	iv	16.4(16.5)	42.6(43.0)	2.3(2.1)	4.4(3.9)
$\text{Cl}_4\text{C}_6\text{O}_2\text{In}(\text{SePh})_2\gamma\text{-pic}$	iv	16.4(16.3)	39.2(41.0)	2.9(2.7)	4.0(4.0)
$\text{Cl}_4\text{C}_6\text{O}_2\text{In}(\text{SePh})_2\text{tmen}$	iv	18.2(18.1)	-	-	-
$\text{Br}_4\text{C}_6\text{O}_2\text{In}(\text{SePh})_2\text{phen}$	iv	13.4(13.1)	-	-	-

a. As described in experimental section.

and by total consumption of the metallic indium. Addition of an equimolar amount of 1,10-phenanthroline afforded a light brown precipitate. However, when excess γ -picoline was used in place of phen, a light yellow solution was obtained. This was allowed to cool down to ambient temperature and addition of 20 mL of petroleum ether gave a light yellow precipitate. In both cases stirring was continued at room temperature for an hour. The precipitate was then filtered and washed twice with 20 mL portions of petroleum ether and then dried *in vacuo*. Analytical and spectroscopic data are presented in Tables 5.1 and 5.2-5.3 respectively.

5.2.2 The Reaction of InCl with $\text{Cl}_4\text{C}_6\text{O}_2$: Kinetic Studies

InCl (ca 0.1 g, 0.6 mmol) was suspended in toluene in 1 mL cuvette. A drop of tmen was added, the septum was sealed and then shaken. $\text{Cl}_4\text{C}_6\text{O}_2$ (ca 2.0 mg, 8 μmol) was added, the mixture again shaken and the cuvette quickly placed in the spectrophotometer. An overlay scan of absorbance against wavelength at a 2 minute time interval was run. The plot obtained was presented in Fig. 5.1. The above procedure was repeated in tetrahydrofuran in the absence of tmen. Figs. 5.2a and b show the plots obtained.

It is quite evident that the second experiment was much slower, and the results were convenient for the kinetic analysis. Plots of absorbance and log of absorbance against time are presented in Figs 5.3a and 5.3b.

When the above reaction was repeated in toluene in the absence of tmen, there was no significant change in the absorption band intensity over the same period of time as the experiments described above.

FIGURE 5.1

ELECTRONIC ABSORPTION SPECTRA OF (A) TETRACHLORO-1,2-BENZOQUINONE AND
(B) THE REACTION BETWEEN TETRACHLORO-1,2-BENZOQUINONE AND INDIUM(II)
CHLORIDE BOTH IN TMEN/TOLUENE SOLUTION

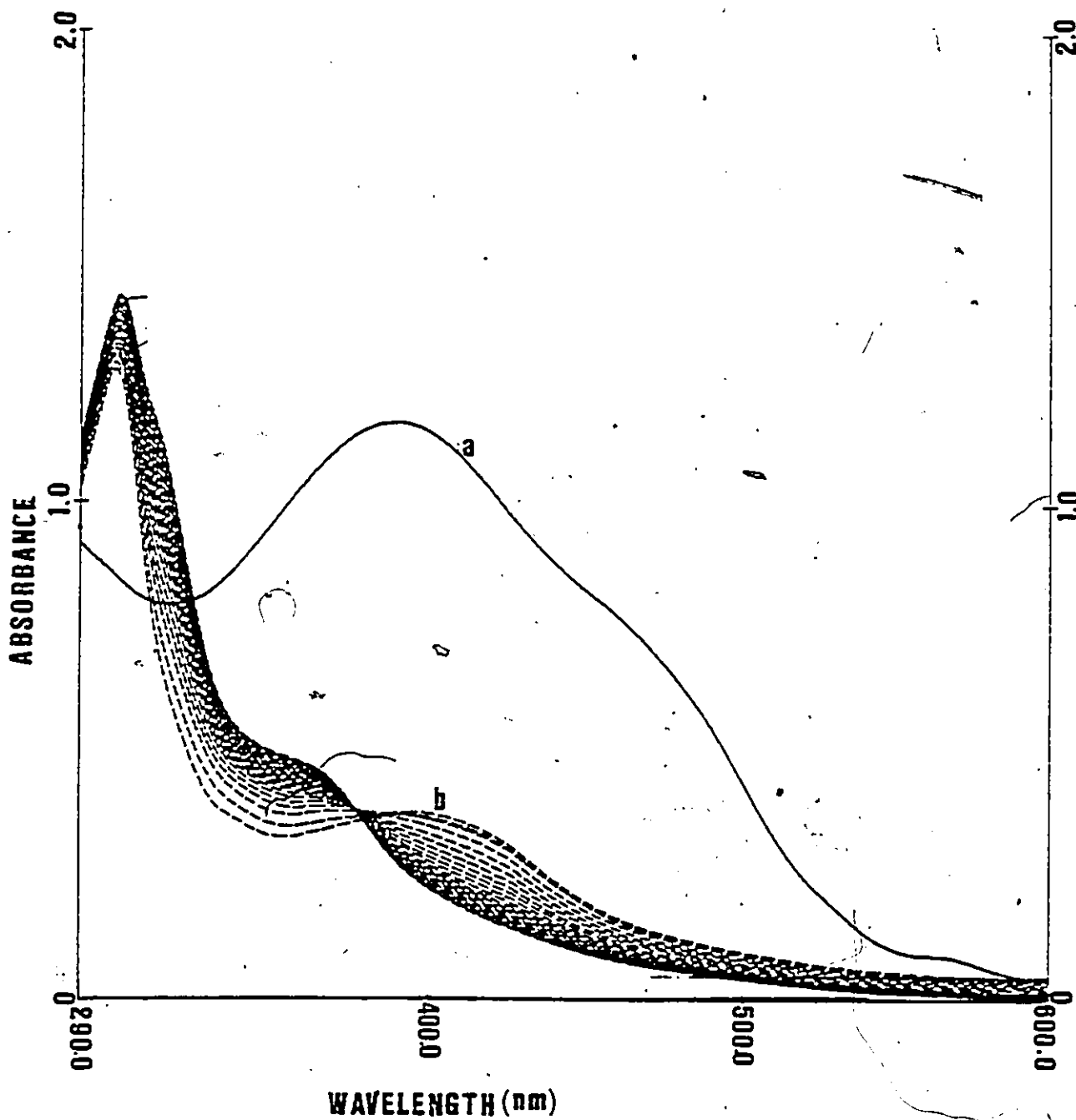


FIGURE 5.2a

ELECTRONIC ABSORPTION SPECTRA OF (A) TETRACHLORO-1,2-BENZOQUINONE AND
(B) THE REACTION BETWEEN TETRACHLORO-1,2-BENZOQUINONE AND INDIUM(II)
CHLORIDE IN THF

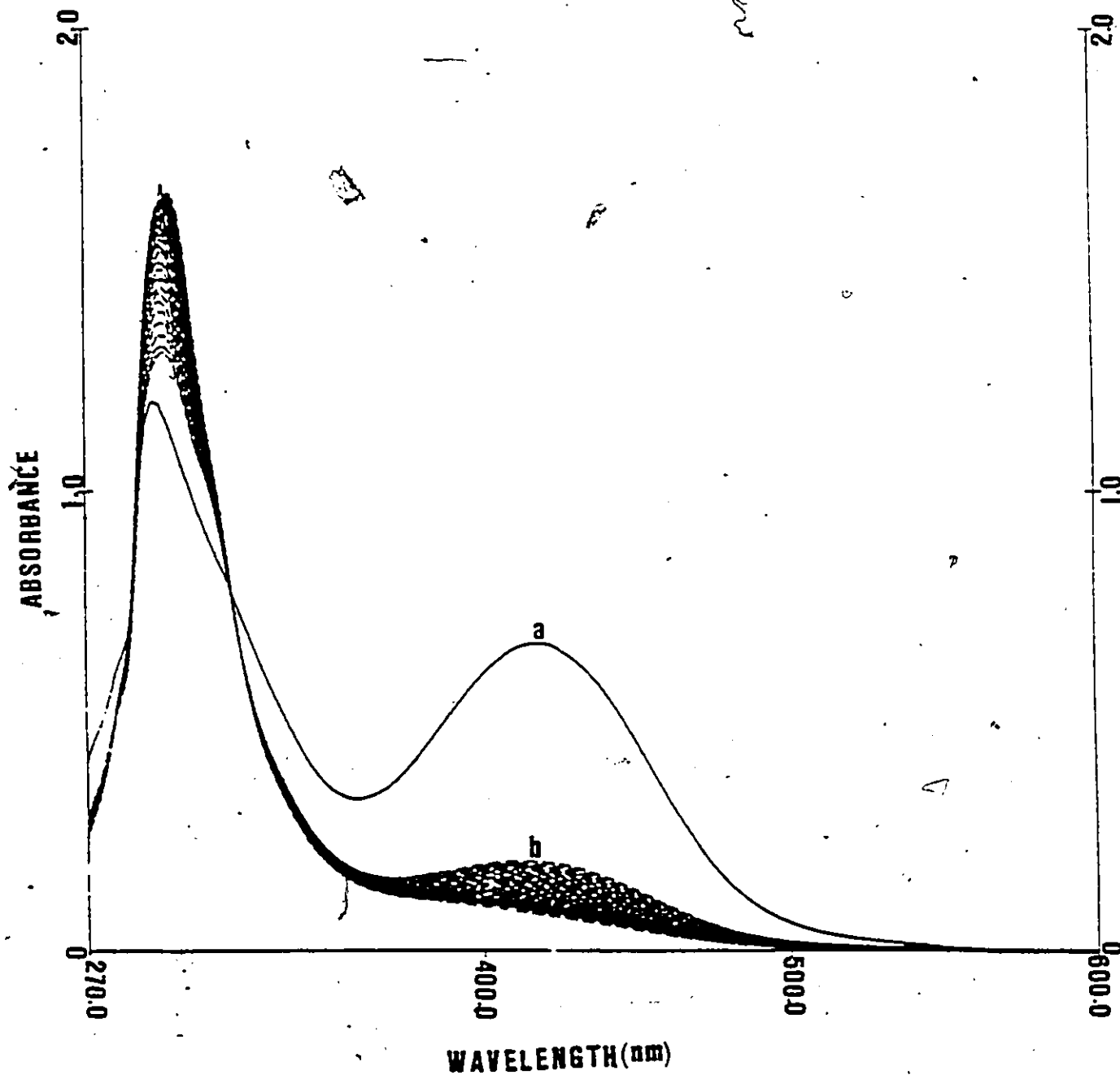


FIGURE 5.2b

ELECTRONIC ABSORPTION SPECTRA OF THE REACTION BETWEEN InCl AND
TETRACHLORO ORTHOBENZOQUINONE IN THF SHOWING THE DISAPPEARANCE OF
TRANSITION DUE TO C=O

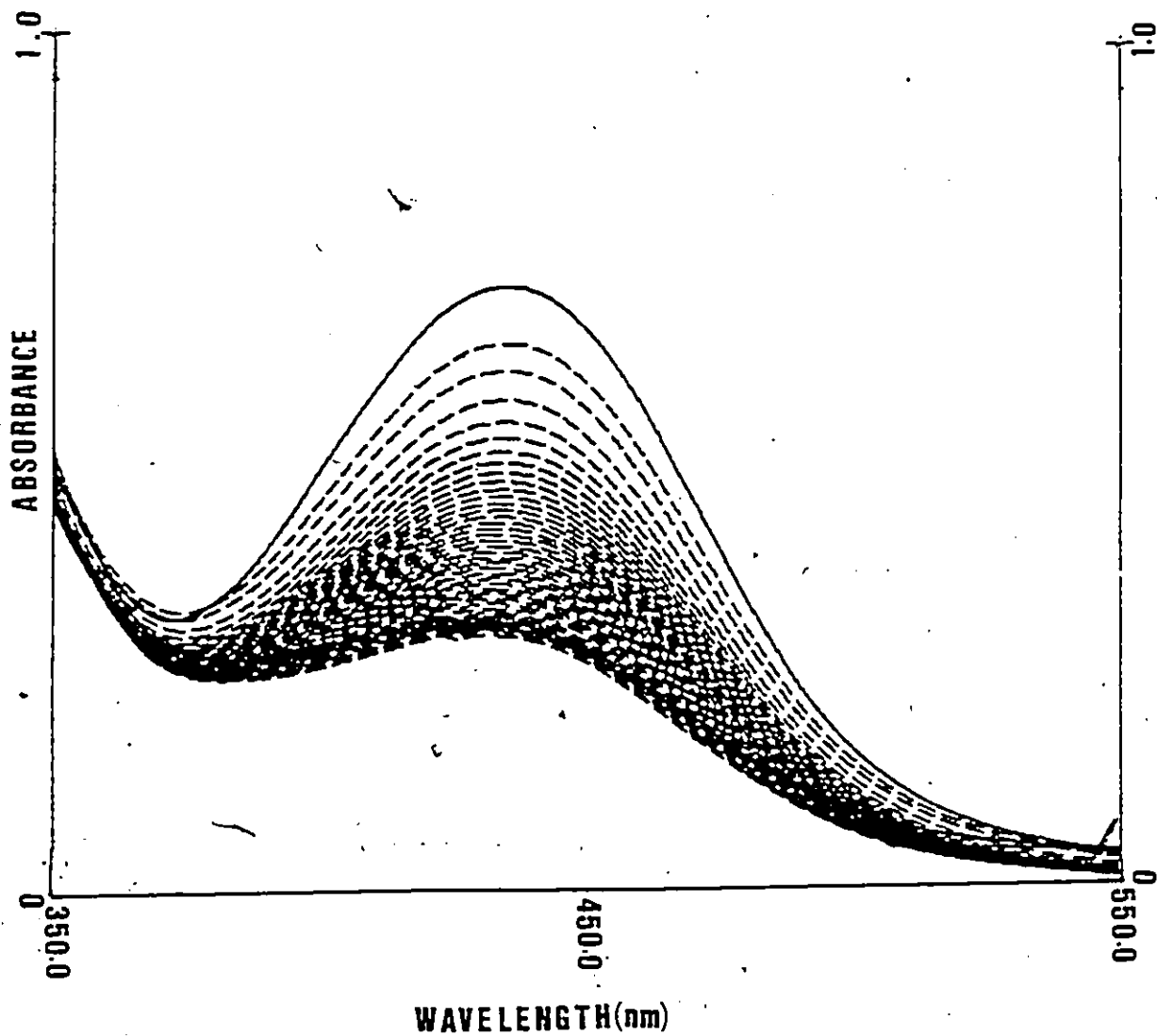


FIGURE 5.3

PLOT OF (A) ABSORBANCE AND (B) LOG OF ABSORBANCE AGAINST TIME BASED
ON FIG. 5.2b

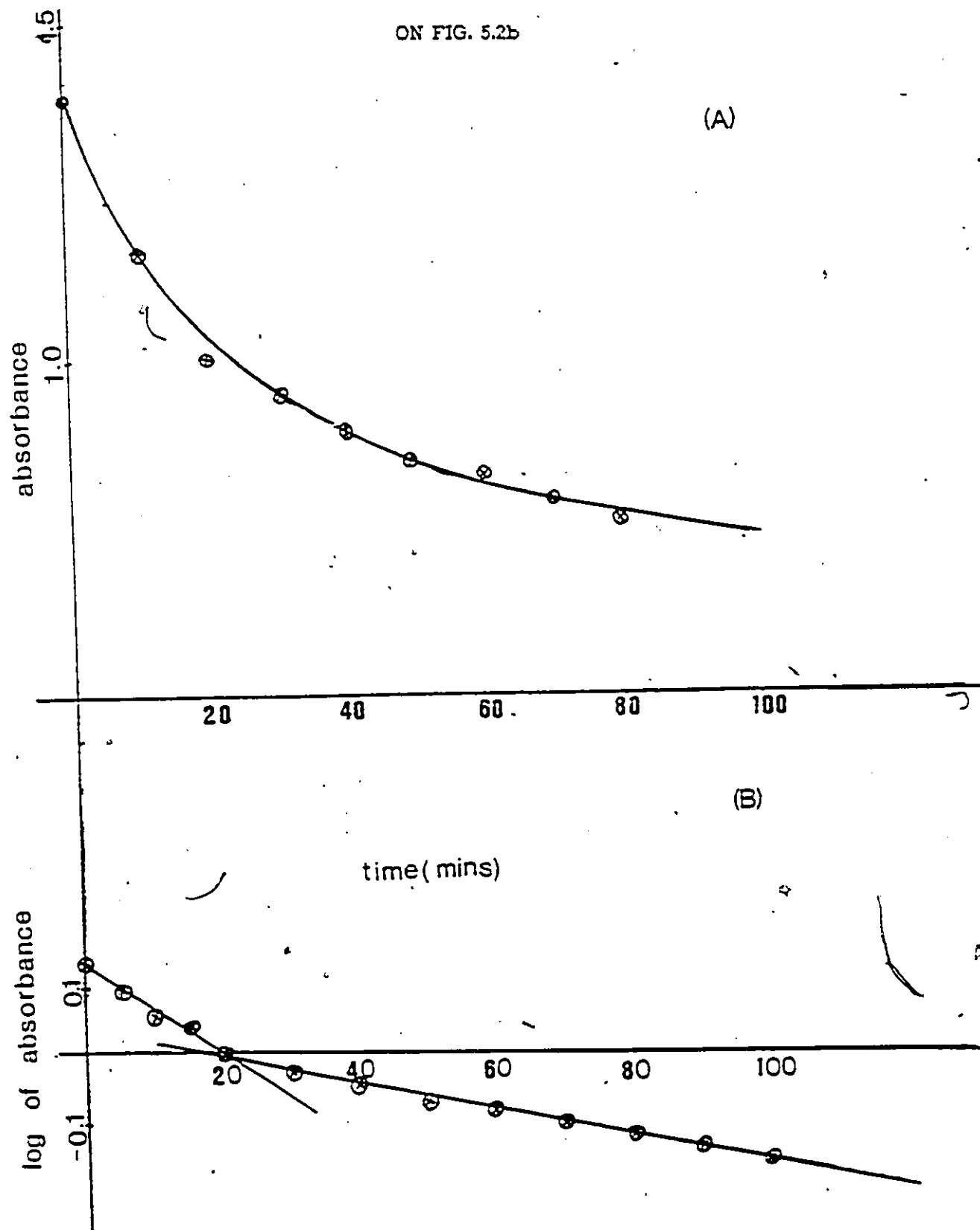


TABLE 5.2

^{13}C NMR SPECTRA OF INDIUM(III) DERIVATIVES OF $\text{o-Cl}_4\text{C}_6\text{O}_2$ (PPM RELATIVE TO Me_4Si)

Compound	Solvent	Chemical Shift	Assignment
$\text{o-Cl}_4\text{C}_6\text{O}_2$	CDCl_3	131.95	C4,C5
		143.71	C3,C6
$\text{o-Cl}_4\text{C}_6(\text{OH})_2$	$(\text{CD}_3)_2\text{CO}$	119.54	C4,C5
		122.43	C3,C6
		143.01	C1,C2
tmen	neat	45.23	CH_3
		57.64	CH_2
Phen	$(\text{CD}_3)_2\text{SO}$	123.00	C5,C6
		126.43	C4a,C6a
		128.12	C4,C7
		135.32	C3,C8
		145.39	C4b,C6b
γ -picoline	neat	149.68	C2,C9
		24.95	CH_3
		129.27	C4
		151.24	C3,C3'
		154.36	C2,C2'

$\text{Cl}_4\text{C}_6\text{O}_2\text{InCl}_2\text{tmen} \cdot \frac{1}{2}\text{Et}_2\text{O}$	$(\text{CD}_3)_2\text{SO}$	113.99	C4,C5	
		114.84	C3,C6	
		152.36	C1,C2	
		43.83,47.11	tmen	$\text{N}(\text{CH}_3)_2$
		53.45,54.09		$\text{N}(\text{C}_2\text{H}_4)\text{N}$
		22.04	Et ₂ O	$(\text{CH}_3-\text{CH}_2)_2\text{O}$
		63.54		$(\text{CH}_3-\text{CH}_2)_2\text{O}$
		$\text{Cl}_4\text{C}_6\text{O}_2\text{InI} \cdot \frac{1}{2}\text{tmen}$	$(\text{CD}_3)_2\text{SO}$	112.62
114.04	C3,C6			
153.20	C1,C2			
43.70,47.14	tmen			$\text{N}(\text{CH}_3)_2$
53.12,54.67				$\text{N}(\text{C}_2\text{H}_4)\text{N}$
$\text{Cl}_4\text{C}_6\text{O}_2\text{InI.phen}$	$(\text{CD}_3)_2\text{SO}$			114.53
		115.62	C3,C6	
		152.19	C1,C2	
		126.22	C5,C6	
		127.64	C4a,C6a	
		129.33	C4,C7	
		135.59	C3,C8	
		141.32	C4b,C6b	
		147.88	C2,C9	

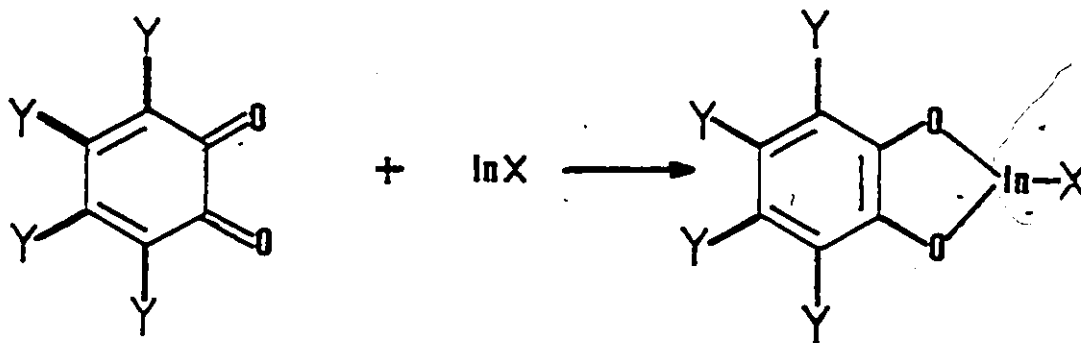
$\text{Cl}_4\text{C}_6\text{O}_2\text{In}(\text{SePh})\text{tmen}$	$(\text{CD}_3)_2\text{SO}$	113.49	C4,C5	
		114.90	C3,C6	
		152.99	C1,C2	
		43.81,46.55	tmen	(CH ₃) ₂ N
		53.61,54.15		N(C ₂ H ₄)N
		124.30	SePh	
		125.16		
		127.87		
		139.27		
		$\text{Cl}_4\text{C}_6\text{O}_2\text{In}(\text{SePh})_2\text{pic}$	$(\text{CD}_3)_2\text{SO}$	113.99
115.17	C3,C6			
152.82	C1,C2			
20.54	pic			CH ₃
125.10				C4
135.99				C3,C3'
148.64				C2,C2'
124.30	Se-Ph			
127.83				
128.84				
139.30				
$\text{Cl}_4\text{C}_6\text{O}_2\text{In}(\text{SPh})_2\text{pic}$	$(\text{CD}_3)_2\text{SO}$	114.00	C4,C5	
		115.19	C3,C6	
		152.25	C1,C2	
		20.55	pic	CH ₃
		125.08		C4
		127.82		C3,C3'

		148.52	C2,C2'	
		118.99	SPh	
		133.22		
		133.95		
		139.15		
		114.22		C4,C5
Cl ₄ C ₆ O ₂ In(S _e Ph).phen. ² / ₄ tol	(CD ₃) ₂ SO	115.59	C3,C6	
		152.76	C1,C2	
		126.90	C5,C6	
		127.99	C4a,C6a	
		129.28	C4,C7	
		137.51	C3,C8	
		140.44	C4b,C6b	
		148.25	C2,C9	
			tol	124.55
				128.72
				130.30
				135.46

5.3 Results and Discussion

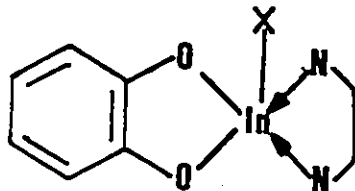
5.3.1 Preparative

(i) The $\text{InX}/\text{Y}_4\text{C}_6\text{O}_2$ reaction. Our results show that the reaction of InX ($\text{X} = \text{Cl}, \text{Br}, \text{I}$) with the halogeno substituted orthoquinones yields the corresponding indium(III) catecholato complex, by a reaction which can be regarded formally as an oxidative addition process:



The initial purpose of the neutral ligand was to solubilize the indium monohalides, as in the case of *tmen* discussed in Chapter 2, but it has also been suggested that the presence of these neutral ligands enhances the availability of the lone pair of InX and consequently increase the possibility of reaction. This point of view was supported by comparing the rate at which reactions occur in the presence of a donor ligand (see section 5.2.2) with the slower reaction in the absence of donor ligands.

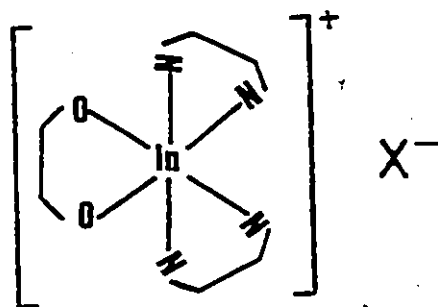
(ii) The structure of $\text{Y}_4\text{C}_6\text{O}_2\text{InX.L}$ compounds ($\text{L} = \text{tmen}, \text{phen}$ or $\gamma\text{-pic}$). Generally, most of the products obtained analyzed satisfactorily as adducts of indium(III) catecholates, whose proposed structure is



Compounds with the indium atom in a five coordinate (trigonal bipyramidal) environment have been noted in $\text{Ph}_3\text{SnInX}_2 \cdot \text{tmen}$ (see Chapter 2), $(\text{R}_2\text{E})_2\text{InX} \cdot \text{L}_2$ ($\text{E} = \text{S, Se}$),⁷⁶ $\text{EtInX}_2 \cdot \text{tmen}$,¹⁹¹ L_2InX ($\text{L} = 2\text{-}[(\text{dimethyl-amino})\text{methyl}]\text{-phenyl}$ ligand)^{192,193} and $\text{In}^{\text{III}}(\text{dthz})$ ($\text{dthz} = \text{dithizone}$).¹⁹⁴ X-ray structure determination has confirmed the trigonal bipyramidal geometry around the indium atom.^{191,193}

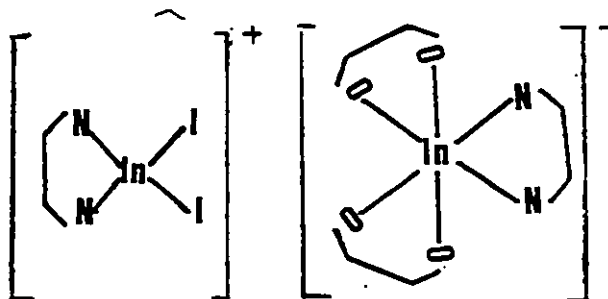
(iii) The structure(s) of $\text{Cl}_4\text{C}_6\text{O}_2\text{InX} \cdot \text{tmen}$ ($n = 1\frac{1}{2}, 2$) compounds. The coordination chemistry of indium is dominated by compounds with tetrahedral (four coordinate) or octahedral (six coordinate) environments around the indium atom. (See Chapter 1).

The compounds obtained with excess tmen had molar conductivities which allows them to be formulated as ionic species. A 3 mmol solution in nitrobenzene gave values of $35 \text{ ohm}^{-1}\text{cm}^2\text{mol}^{-1}$ for $\text{Cl}_4\text{C}_6\text{O}_2\text{InCl} \cdot 2\text{tmen}$, $29 \text{ ohm}^{-1}\text{cm}^2\text{mol}^{-1}$ for $\text{Cl}_4\text{C}_6\text{O}_2\text{InBr} \cdot 2\text{tmen}$ and $34 \text{ ohm}^{-1}\text{cm}^2\text{mol}^{-1}$ for $\text{Cl}_4\text{C}_6\text{O}_2\text{InL} \cdot 1\frac{1}{2} \text{ tmen}$. These values fall in the range of 20 to $40 \text{ ohm}^{-1}\text{cm}^2\text{mol}^{-1}$ determined for 1:1 electrolyte in this solvent. The formulation was also supported by the absence of $\nu(\text{In-X})$ in the far ir spectra of $\text{Cl}_4\text{C}_6\text{O}_2\text{InX} \cdot 2\text{tmen}$ ($\text{X} = \text{Cl, Br}$). Their proposed structure therefore is



where the indium attains its highest coordination number of six.

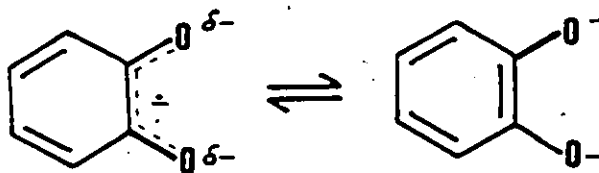
The compound $\text{Cl}_4\text{C}_6\text{O}_2\text{In}.1\frac{1}{2}\text{tmn}$ has two bands in the far i.r. spectrum at 177 and 152 cm^{-1} assignable to $\nu_{\text{as}}(\text{In}-\text{I})$ and $\nu_{\text{s}}(\text{In}-\text{I})$. These values are in good agreement with that of 176 and 158 cm^{-1} obtained from the i.r. of the complex $[\text{Pr}_4\text{N}]\text{I}_2\text{In}(\text{SPh})_2$ ⁷⁶. On this basis, we propose the following structure for the compound $\text{Cl}_4\text{C}_6\text{O}_2\text{In}.1\frac{1}{2}\text{tmn}$.



Similar structures have been proposed for $\text{InX}_3.1\frac{1}{2}\text{bipy}$ ¹⁹⁵ based on conductivity and infrared studies. The fact that the iodo complex differs in our studies from the bromo and chloro analogues is in keeping with the known behaviour of coordination compounds of indium. It has been mentioned elsewhere for example,¹⁹⁶ that indium(III) halides from which six-coordinate products were typically obtained with electronegative δ -donor ligands, whereas lower coordination numbers have been found when either the halogen or the donor ligand or both had low electronegativities.

Efforts are being made to obtain single crystals for X-ray diffraction studies, which should help in confirming the proposed structures.

(iv) Reaction of InCl with Cl₄C₆O₂: Kinetic Studies. The interpretation of the results obtained here will be treated semi-quantitatively since the nature of the reaction did not permit accurate monitoring of the reaction rate. The data for the plots presented in Fig. 5.3 were obtained by measuring the decrease in intensity of the absorption band at 424 nm. This low intensity band has been assigned to the $n \rightarrow \pi^*$ transition¹⁹⁷ of C=O. The eventual disappearance of this band also supports this assignment, since the $\pi \rightarrow \pi^*$ transition of C=O does not occur in this region. The complete reduction of C=O of the quinone has, therefore, been brought about by electron transfer from the indium monohalide which was used in excess. The absorption spectrum in Fig. 5.2 clearly illustrates the disappearance of the band in question. The spectrum in Fig. 5.1 shows the same effect but the distinct band which is seen in Fig. 5.2 is conspicuously absent for the toluene systems, and in its place we observe an isosbestic point at 380 nm indicating that two absorbing species exist in solution. It is reasonable to assume that these species could be the semiquinone and the catecholate.



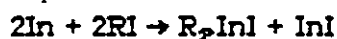
- The plots in Fig. 5.3 reveals the characteristic rate of decrease in concentration typical for first order reactions. In the plot of the log of absorbance against time, however, we obtained two separate curves (see Fig. 5.3b). In our opinion

the first plot (1) represents the first reduction step to the quinone to the semiquinone. The second plot (2) then will be the conversion of the semiquinone to the catecholate which presumably is a slower process as evidenced by the difference in slopes of the two curves.

An identical study conducted with toluene in the absence of a donor ligand did not show any change in the intensity of the absorption band of the quinone implying absence of reactions. This is not surprising since indium(I) halides are insoluble in aromatic solvents. This observation also emphasizes the importance of donor ligands like tmen in such medium in facilitating the solubility of indium monohalides.

(ii) The In/Y₄C₆O₂/E-E reaction (E-E = I₂, Ph₂Se₂, Ph₂S₂). Refluxing metallic indium with the quinone in the presence of a half molar quantity of iodine, diphenyldiselenide or diphenyldisulphide provided another route for synthesizing indium(III) catecholate derivatives with I₂R or SeR bonded to In.

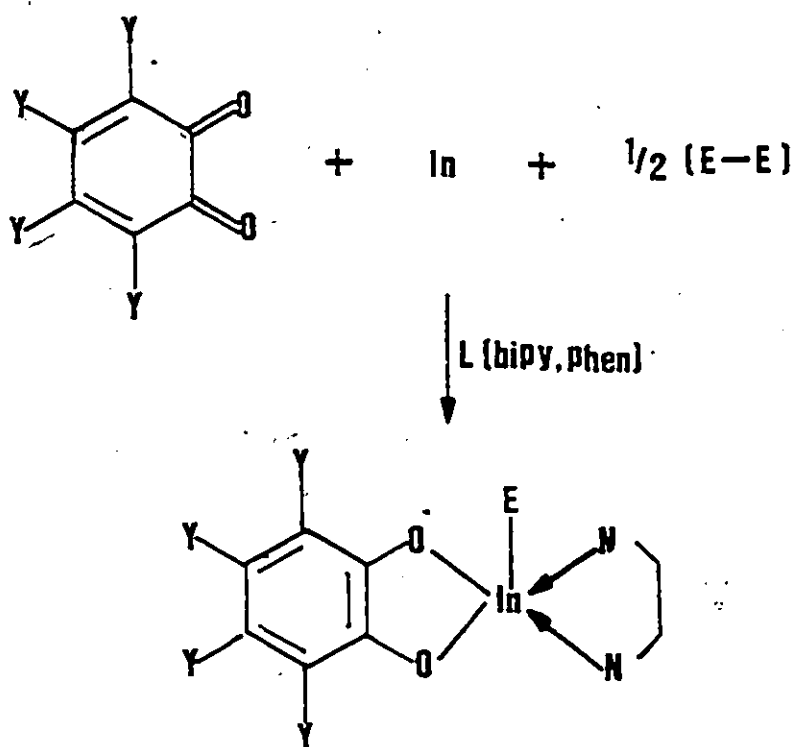
The use of indium metal in the direct synthesis of indium(III) compounds is well-established. Worrall and coworkers¹⁹⁸ reported the slow direct reaction of indium metal with alkyl halides to give products which were mixtures of R₂InX and RInX. Other researchers¹⁹⁹ improved on this method by using activated metal obtained by the reduction of indium trichloride with metallic sodium or potassium. By this means the reaction time was considerably reduced and only the diorgano product was obtained:



Recent reports from our laboratory²⁰⁰ also show that metallic indium reacts in boiling toluene with R₂E₂ substrates to yield In(ER)₃ compounds in quantitative yield and high purity, as for example:



The point here, therefore, is that for synthetic purposes metallic indium is a useful reagent. In these one-pot syntheses, the reaction of metallic indium with stoichiometric amounts of the orthoquinone and half molar quantities of iodine, diphenyldiselenide or diphenyldisulphide provides the respective derivatives of indium(II) catecholates. The reaction is represented as follows.



The end of the reaction is indicated by the solution clearing, with the complete dissolution of the indium metal. Addition of 1,10-phenanthroline or 2,2'-bipyridine to the solution precipitates the desired products in high yield. Spectroscopic results are presented in Tables 5.2, 5.3 and 5.4 and are discussed below.

As the reaction proceeded, a deep blue solution was formed after ca. 2h, with visible signs of unreacted indium metal in the flask, suggesting that the reaction was only half complete. The ESR spectrum of this solution was recorded (see discussion below). Eventually, the blue colour was discharged with the formation of a light brown solution when E = SPh and a light yellow solution when E = SePh with complete dissolution of the indium metal and formation of the products reported.

5.3.2 Spectroscopy

(i) Infrared Spectra: Fig. 5.4 compares the mid-region of the IR spectrum of a typical catecholato complex ($\text{Br}_4\text{C}_6\text{O}_2\text{InCl.phen}$) with the spectrum of the tetrabromo-orthoquinone from which it was derived. Fig. 5.4c is a spectrum of the corresponding diol. Prominent features of the spectra on these complexes above 1000 cm^{-1} include an intense band near 1240 cm^{-1} and a strong broad band near 1430 cm^{-1} . Similar bands have been identified in catecholato complexes of vanadium²⁰¹ and cobalt²⁰² as the C-O stretching vibration of the catechol ligand. These two prominent and characteristic bands are present with only slight variations in their positions in all cases studied, and their occurrence provides good evidence for the presence of a coordinated catecholate.

The vibrational spectra in the far infrared region are presented in Table 5.3. The tmen adducts have weak to medium bands between 450 and 520 cm^{-1} , readily assigned to $\nu(\text{In-N})$ from earlier work (see Chapter 2). The $\nu(\text{In-N})$ of the phenanthroline adducts are in good agreement with reported values for $\text{InX}_3\text{.phen 1.5}$ ($X = \text{Cl, Br, I}$)²⁰³⁻²⁰⁶ which fall in the range $270-220\text{ cm}^{-1}$. The assignment of $\nu(\text{In-X})$ and $\nu(\text{In-O})$ was aided by comparing the spectra with that of $\text{InX}_2(\text{acac})\text{L}_2$ ($X = \text{Cl, Br, I}$, $L = \text{phen, py}$).²⁰⁴ The values are in general

agreement with those reported for $\nu(\text{In-X})$ in adducts of indium halides.²⁰⁷ The identification of $\nu(\text{In-O})$ has been the subject of debate^{204,207} with frequencies between 450 cm^{-1} and 180 cm^{-1} being proposed. The $\nu(\text{In-O})$ absorption in the Raman spectrum of $\text{In}(\text{acac})_3$ has been assigned to a band at 444 cm^{-1} .²⁰³ In the present work, the band at ca. 420 cm^{-1} is observed in all the compounds prepared and is therefore tentatively assigned as $\nu(\text{In-O})$. The assignment of M-S stretching modes has been a matter of some discussion. For $\nu(\text{Cd-S})$ frequencies in the range $160\text{--}400 \text{ cm}^{-1}$ were proposed;²⁰⁸ $\nu(\text{In-S})$ has been assigned at $370\text{--}380 \text{ cm}^{-1}$ in a series of toluene-3,4-dithiol derivatives of indium,¹⁸⁶ at $319\text{--}339 \text{ cm}^{-1}$ for $\text{InX}_3 \cdot 2\text{Et}_2\text{S}$ ($\text{X} = \text{Cl, Br}$) complexes,²⁰⁹ and at $342\text{--}300 \text{ cm}^{-1}$ for $\text{XIn}(\text{SPh})_2 \cdot 2\text{py}$ ($\text{X} = \text{Cl, Br}$).⁷⁶ Analogous modes in the polymeric compounds $\text{M}(\text{SR})_2$ ($\text{M} = \text{Zn, Cd, Hg}$; $\text{R} = \text{nB}_u, \text{tB}_u, \text{Ph}$) have been identified²¹⁰ in the range $300\text{--}350 \text{ cm}^{-1}$. On the basis of these results, we assign the broad band centred at 350 cm^{-1} as $\nu(\text{In-S})$ for the compounds $\text{Y}_4\text{C}_6\text{O}_2\text{In}(\text{SPh})\cdot\text{phen}$. The assignment of $\nu(\text{In-Se})$ for $\text{Y}_4\text{C}_6\text{O}_2\text{In}(\text{SePh})\cdot\text{phen}$ is in good agreement with the compounds $\text{XIn}(\text{SePh})_2 \cdot 2\text{py}$ ($\text{X} = \text{Cl, Br, I}$), where it occurs at $211\text{--}256 \text{ cm}^{-1}$.⁷⁶ Due to the high fluorescence of these compounds, we could not obtain any Raman spectra.

(ii) NMR Spectra. The ^1H NMR spectra as presented in Table 5.4 are useful in confirming the presence of the coordinated bidentate ligand, and also confirmed that the species under study are diamagnetic. The resolution of the spectra of the phenanthroline adducts were hampered by their low solubility in dimethyl sulphoxide, but shifts of the appropriate proton signals due to complexation are obvious, as the data in the table depict.

FIGURE 5.4

THE INFRARED SPECTRA OF KBr PELLETS OF (A) $\text{Br}_4\text{C}_6\text{O}_2$ (B) $\text{Br}_4\text{C}_6\text{O}_2\text{InCl.phen}$
(C) $\text{Br}_4\text{C}_6(\text{OH})_2$

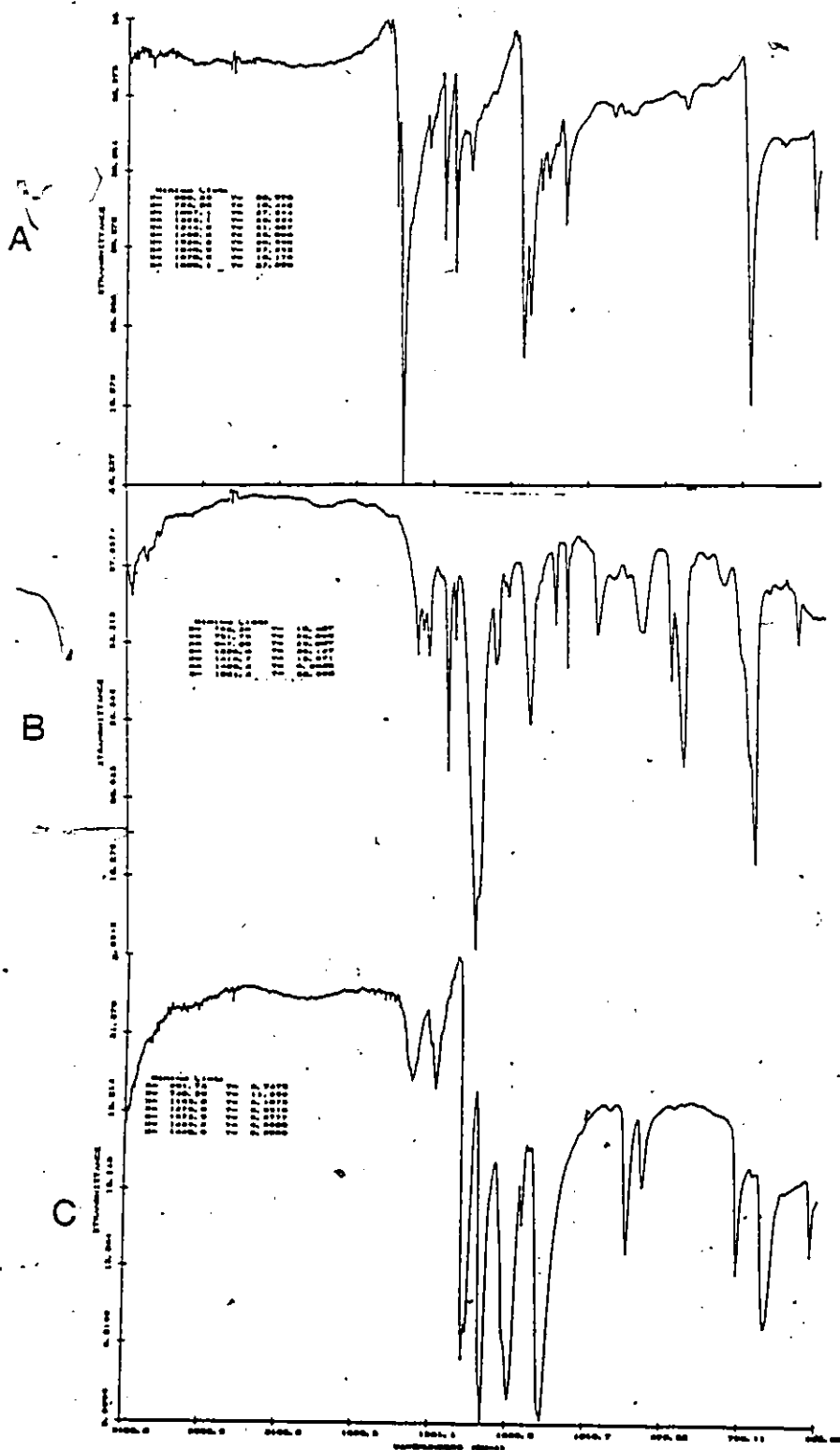


TABLE 5.3

FAR INFRARED SPECTRA OF SOME In(III) CATECHOLATES (IN CM^{-1})

Compound	$\nu(\text{In-N})$	$\nu(\text{In-O})$	$\nu(\text{In-X})$	$\nu(\text{In-E})$ E = S,Se
$\text{Cl}_4\text{C}_6\text{O}_2\text{InCl.tmen}$	480(m) 454(m)	400(w)	270 (s,br)	-
$\text{Cl}_4\text{C}_6\text{O}_2\text{InCl.2tmen}$	476(m) 458(m)	426(m)	-	-
$\text{Cl}_4\text{C}_6\text{O}_2\text{InL.1}^{1/2}\text{tmen}$	482(m) (454(m))	428(m)	177(s,br)	-
$\text{Cl}_4\text{C}_6\text{O}_2\text{InCl.phen}$	(a)	424(m)	290 (s,br)	-
$\text{Cl}_4\text{C}_6\text{O}_2\text{InBr.phen}$	288(m)	422(m)	208(s,br)	-
$\text{Cl}_4\text{C}_6\text{O}_2\text{InL.phen}$	290(m)	424(m)	175(s,br)	-
$\text{Cl}_4\text{C}_6\text{O}_2\text{In(SPh).2pic}$	286(s,br)	400(w)	-	350(m)
$\text{Cl}_4\text{C}_6\text{O}_2\text{In(SePh).phen}$	288(s)	422(s)	-	238(s)
$\text{Br}_4\text{C}_6\text{O}_2\text{InL.phen}$	290(s)	424(s)	185(s)	-

a) $\nu(\text{In-N})$ obscured by broad In-Cl band

TABLE 5.4

^1H NMR SPECTRA OF INDIUM(III) DERIVATIVES OF $\text{O}-\text{Y}_4\text{C}_6\text{O}_2$ ($\text{Y} = \text{Cl, Br}$) (PPM,
RELATIVE TO Me_4Si)

Compound ^(a)	Chemical Shift	Assign
γ -picoline	2.04(s,3H)	H5
	6.92(d,2H)	H2,2'
	8.42(d,2H)	H3,3'
$\text{Y}_4\text{C}_6\text{O}_2\text{InX.tmen}$	2.50(s,12H)	$(\text{CH}_3)_2\text{N}$
	2.86 (s,4H)	$\text{HC}_2\text{H}_4\text{N}$
X = Cl, Br, I		
Y = Cl, Br		
$\text{Cl}_4\text{C}_6\text{O}_2\text{InCl.tmen.}^{\frac{1}{2}}\text{Et}_2\text{O}$	2.48(s,48H)	$(\text{CH}_3)_2\text{N}$
	2.87(s,16H)	$\text{NC}_2\text{H}_4\text{N}$
	1.20(t,3H)	
	3.64(q,2H)	$(\text{CH}_3\text{CH}_2)_2\text{O}$
$\text{Y}_4\text{C}_6\text{O}_2\text{InL.phen}$	9.24(m,2H)	C2,C9 (phen)
	7.90(m,2H)	C3,C8
	8.60(m,2H)	C4,C7
	8.15(m,2H)	C5,C6

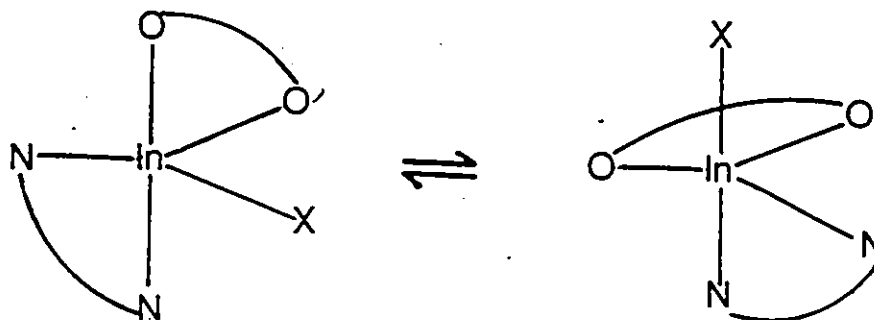
$Y_4C_6O_2In(SPh).2pic$	2.31(s,6H)	H-5
	7.27(d,4H)	H-2,2'
	8.44(d,4H)	H-3,3'
	6.98-7.54(m,5H)	S-Ph
<hr/>		
$Cl_4C_6O_2In(SePh).phen.^{1/4}tol$	8.97(m,8H)	C2,C9(phen)
	8.00(m,8H)	C3,C8
	8.66(m,8H)	C4,C7
	8.02(m,8H)	C5,C6
	6.98-7.52(m,20H)	Se-Ph
	7.20(s,5H)	
	Tol	
	2.15(s,3H)	
<hr/>		
$Y_4C_6O_2In(SePh).2pic$	2.35(s,6H)	H-5
	7.27(d,4H)	H-2,2'
	8.54(d,4H)	H-3,3'
	6.99-7.47(m,5H)	Se-Ph
<hr/>		

Good diagnostic use was made of ^{13}C NMR spectroscopic results. There was a considerable shift of the signal due to $\text{C}=\text{O}$ from ca. 170 ppm to ca. 150 ppm, indicating a reduction from $\text{C}=\text{O}$ to $\text{C}-\text{O}$. The spectra of the corresponding selenolate and thiolate derivatives, as shown in Table 5.3 agree with these assignments. These results also show that the catecholato ligands are symmetrically bound to the metal, hence rendering all the appropriate pairs of carbon atoms equivalent. The chemical shifts of the ligand due to adduct formation are similar to those reported in Chapter 3.

The assignment of the chemical shifts to the respective carbon atoms in the phen and bipy adducts of the indium(III) catecholates prepared in this work was reasonably straightforward. The tmen adducts, on the other hand, were found to be more complicated and as a result a variable temperature study was conducted, the discussion of which is undertaken in the next paragraph.

(iii) Variable Temperature ^{13}C NMR Spectroscopic Study. This study was undertaken in an attempt to gain a better understanding as to the nature of the product obtained by the reaction of InX with $\text{Cl}_4\text{C}_6\text{O}_2$ in toluene/tmen. The room temperature spectrum of the tmen adduct of $\text{Cl}_4\text{C}_6\text{O}_2\text{InCl}$ in $\text{dms}-d_6$ showed doubled resonance signals for the three pairs of the carbons on the catecholato ring. As the solution warmed up, these signals began to coalesce. At 353 K, the signals coalesced forming three sharp singlets at 158.51, 120.34 and 119.07 ppm from their original paired values of 158.35 + 157.70, 120.40 + 120.27, and 119.36 + 118.94 ppm. The chemical shifts of the resultant signals represent approximate average values of the initial paired values. These results imply that the molecule has an essentially trigonal bipyramidal geometry, with the possibility of undergoing "Berry pseudorotation" analogous to that seen in the temperature dependence of the ^{19}F NMR of PF_5 . On this basis, the two possible structures

are proposed



The carbons on the catecholato ring will then be in a different chemical environment due to loss of symmetry. The rate of exchange between these two structures, at room temperature is such that each carbon becomes distinguishable and hence different resonance are observed. At higher temperatures, the exchange becomes so fast that the different chemical shifts average out, and we therefore see singlets for each pair of carbon atoms. This process was found to be reversible, as on cooling the solution back to room temperature the initial spectrum was reproduced. It is interesting to note that similar observation was made on the tmen part of the spectrum. At room temperature, one observes two singlets for the methylene carbons at 60.34 and 59.44 ppm, and two signals for the methyl carbons at 51.87 and 49.43 ppm. At 353 K two singlets are observed at 60.47 and 51.09 ppm respectively. It is quite clear then that the equilibration process involves the whole molecule.

Further work is needed in this area to confirm the absolute configuration of these compounds by single crystal X-ray diffraction studies. Our attempts to grow suitable crystals have not so far been successful.

(iv) ESR Spectra. Fig. 5.5a shows a typical room temperature ESR spectrum of the blue solution obtained the reaction of indium metal with tetrachlorobenzoquinone in the presence of iodine. (See Experimental.) The

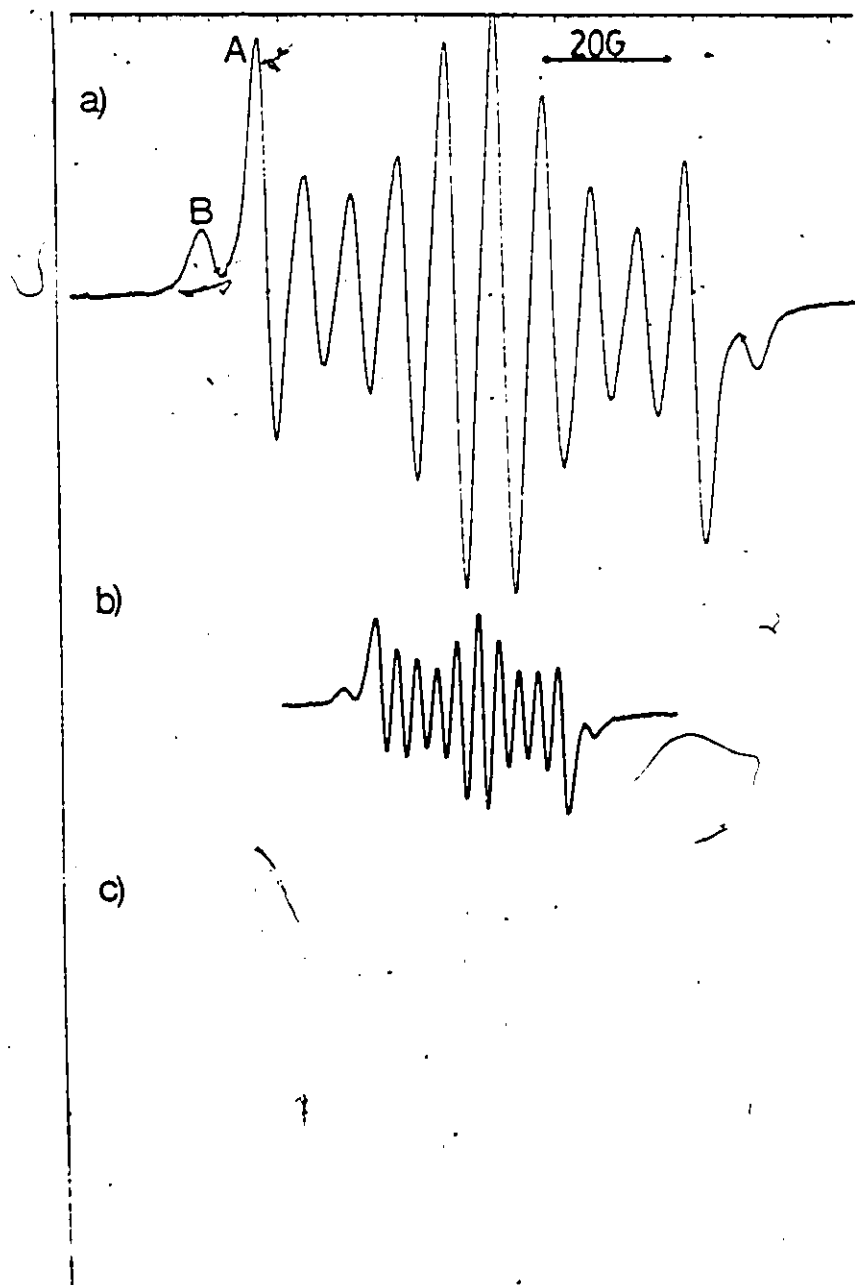
spectrum is made up of two components marked A and B. Each of these is made up of 10 lines due to coupling of an unpaired electron to the $I = 9/2$ ^{115}In nucleus. The magnitude of the coupling of A is 7.8 G which is comparable to the value of 7.1 G reported by Felix and Sealy for an In^{3+} benzosemiquinonate prepared by UV photolysis of aqueous solutions of catechol in the presence of indium(III) chloride at around neutral pH; B has a coupled constant of 9.2 G and is assigned to an In^{+2} benzosemiquinonate (see Chapter 6). Using these two values, a computer simulated spectrum was generated, and the good agreement between experimental and calculated spectra (see Fig. 5.5c) suggested that both In(III) and In(I) species do exist in this solution. From the relative intensities of the two spectra, we deduce that the two species in the ratio $\text{In(III)}/\text{In(I)}$ 7:1 at the stage of the reaction which we happened to study.

A helpful study which could provide better insight into the reaction scheme is by monitoring the reaction over the whole time with the aid of ESR.

We also found that addition of a nitrogen donor ligand to the blue solution does not facilitate the final transfer of the electron, as was observed in the case of the reaction of SnX_2 with TBQ (see Chapter 4). Fig. 5.5b shows a spectrum obtained on addition of excess pyridine to the solution whose spectrum is presented in Fig. 5.5a. We instead observed a change in the hyperfine constants from 9.2G and 7.2G to 2.0G and 1.6G respectively. This suggests that on adduct formation, the electron density on the indium metal becomes more delocalized.

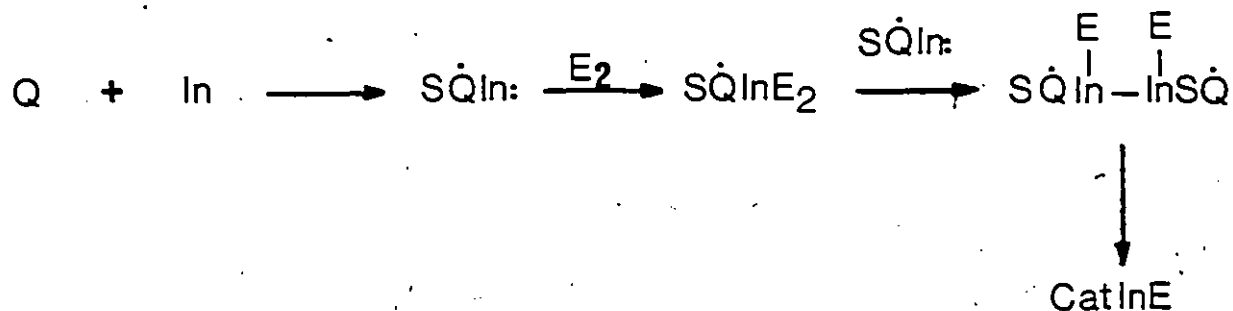
FIGURE 5.5

THE ESR SPECTRA OF THE REACTION $\text{In}/\text{Cl}_4\text{C}_6\text{O}_2/\text{I}_2$ IN TOLUENE (A)
EXPERIMENTAL (B) A + PYRIDINE (C) CALCULATED



5.3.3 The reaction mechanism

Reactions leading to the formation of catecholato complexes as presented in this work and elsewhere involve the successive transfer of electrons from the metal centre to the substrate (quinon). The reaction scheme presented in Chapters 3 and 4, therefore appear to be general. Below is the scheme of the reactions described in section 5.2.1 (iv).



The first step of the reaction is presumably the transfer of an electron from indium to the quinone to form an indium(I) semiquinonate, evidence of which is derived from the ESR spectra (see Fig. 5.5). Indium(I) complexes are expected to be nucleophiles since they are believed to have a lone pair of electrons. For cyclopentadienylindium(I) the existence of this lone pair has been supported by CNDO calculations and confirmed by dipole moment measurements.¹¹⁸ In keeping with this, the next step in our reaction sequence is the oxidative insertion of the indium(I) complex into the E-E bond of the substrate. Under the condition of our reaction the formation of the indium(I) species is a slow process as evidenced by the presence of metallic indium at the bottom of the reaction vessel and from the ratio of In(I):In(III) in the ESR spectra (see Fig. 5.5). This reaction rate, therefore, favours a further attack of the indium(I)

specie on the indium(III) specie to form a dimeric In-In bonded complex. Although we did not do a low temperature ESR study to confirm the presence of this complex as in the case of the reaction with tin (see Chapter 4). Our proposed scheme is consistent with results presented in the various chapters of this dissertation. The final step in this sequence involves an internal electron transfer leading to the formation of the catecholato complex. Mention must also be made of the fact that the ease with which these electron transfer processes take place is dictated by redox potential of the quinone involved. This is considered in detail in the next chapter.

Results presented in this chapter suggest that the reaction of the tetrahalogeno orthoquinones with indium halides leads to the formation of indium(III) catecholates. It is quite clear that the transfer of electrons in these reactions proceed in a two step process instead of the originally proposed mechanism in which both electrons are transferred simultaneously.

CHAPTER 6

THE REACTION OF In(I) HALIDES WITH 3,5-DI-TERT-BUTYL 1,2-BENZOQUINONE AND 9,10-PHENANTHROQUINONE. FORMATION OF INDIUM(I) AND INDIUM(III) SEMIQUINONES

6.1 Introduction

The reactions of orthoquinones with metals in their low oxidation states described in Chapters 3, 4 and 5 suggest that this oxidation reaction proceeds in two one-electron transfer steps with a semiquinone intermediate, rather than a single two electron-transfer step. It has also been quite clear from our work and that of others that the nature of the products is dependent on the type of substituent on the quinone, as well as the properties of the metal. To date no compound of a Main Group Metal directly bonded to a semiquinone ligand has been isolated, although the existence of such complexes has been inferred from ESR spectroscopic data. For example, UV photolysis of aqueous solutions of catechol in the presence of a Main Group III metal ion at pH ~ 7 lead to the detection of an ESR signal attributable to hyperfine of an unpaired electron to the metal coupling between the metal ion in the metal complex of the o-benosemiquinone.²¹³

Results presented in this chapter demonstrate the formation of stable In(III) semiquinone complexes. Single crystals were obtained in one case and the structure was confirmed unambiguously by X-ray crystallographic studies. ESR studies has shown that the reaction of In(I) halides with the quinones in question leads to the formation of a product made up of a mixture of In(I) and In(III) semiquinone complexes. Further work had to be carried on to confirm this claim and we prepared both In(I) and In(III) semiquinone complexes. On this basis, we

can propose a satisfactory mechanism to explain the formation of these complexes.

6.2 Experimental

6.2.1 Reactions of InX (X = Cl, Br, I) with 3,5 di-tert-butyl 1,2-benzoquinone (TBQ)

(i) A 3.3 mmol amount of InX (X = Cl, Br, I) was suspended in 25 mL of toluene and cooled to about -40°C . Tmen (2 mL, 13.2 mmol) was syringed into the mixture to obtain the reddish solution characteristic of solutions of indium(I) halides in such media. At this stage, an equimolar amount of 3,5-di-tert-butyl 1,2-benzoquinone in toluene (25 mL) was added dropwise over a period of 1 h. Stirring was continued at this temperature for another hour, when a green solution was obtained. The cold bath was slowly removed until room temperature was attained. Any solid impurities at this point were removed by filtration, and the volume of the filtrate was reduced by half. Addition of petroleum ether (25 mL) afforded a light greenish precipitate when X = Cl or Br and a light brown precipitate when X = I. These materials analyzed as $\text{C}_{14}\text{H}_{20}\text{O}_2\text{InX}_2\cdot\text{tmen}$. Analytical results are presented in Table 6.1. Identical results were obtained when toluene and tmen were replaced by THF and pyridine. Table 6.1 gives analytical results.

(ii) InX (X = Cl, Br) (4 mmol) was refluxed with an equimolar amount of TBQ in toluene followed by the addition of excess pyridine (2 mL, 24 mmol). The green solution which was obtained after ca. 2h was filtered and on slow evaporation of the filtrate, a fine crystalline product was obtained. This was identified (elemental analysis, infrared spectroscopy) as $\text{C}_{14}\text{H}_{20}\text{O}_2\text{InX}_2\cdot 2\text{py}$. The ESR spectrum of the toluene solution is discussed below.

TABLE 6.1
ANALYTICAL DATA ON INDIUM SEMIQUINONATES

Compound	Method	In	C	H	N	X=Cl,Br,I
(TBSQ)InCl ₂ .tmen	i	21.45(21.98)	46.75(45.99)	7.65(6.95)	5.45(5.36)	13.72(13.58)
(TBSQ)InBr ₂ .tmen	i	18.50(18.78)	-	-	-	26.28(26.15)
(TBSQ)InI ₂ .tmen	i	16.39(16.28)	-	-	-	36.17(35.99)
(TBSQ)InCl ₂ 2py	ii	21.79(21.71)	-	-	-	6.31(6.71)
(TBSQ)InBr ₂ 2py	ii	20.58(20.03)	50.01(50.29)	5.43(5.27)	4.75(4.89)	14.10(13.95)
(TBSQ)InCl ₂ 2py. ¹ / ₂ thf	ii	19.00(19.12)	-	-	-	11.65(11.83)
(TBSQ)InBr ₂ 2py. ¹ / ₂ thf	ii	16.73(16.66)	45.43(45.31)	5.12(4.97)	3.76(4.07)	23.00(23.19)
(TBSQ)InCl ₂ 2pic	v	19.16(19.38)	-	-	-	12.06(11.99)
(TBSQ)InBr ₂ 2pic. ¹ / ₂ dmf	v	15.94(16.00)	45.26(46.02)	5.04(5.27)	4.87(4.88)	22.31(22.27)
(TBSQ)InI ₂ .phen	iii	14.62(14.93)	-	-	-	33.10(32.99)
(TBSQ)In(SePh) ₂ .phen. ¹ / ₂ tol	iv	13.10(13.14)	57.43(57.07)	5.10(4.85)	4.15(3.21)	-
(TBSQ)In(SePh) ₂ 2pic. ¹ / ₂ tol	iv	13.16(13.05)	56.65(56.67)	5.99(5.50)	3.79(3.19)	-
(TBSQ)In(SPh) ₂ .phen	iv	15.72(15.65)	-	-	-	-
(TBSQ)In(SPh) ₂ 2pic	iv	15.49(15.53)	-	-	-	-
(PSQ)InCl.tmen	i	24.30(24.19)	50.42(50.55)	5.35(5.06)	5.16(5.89)	7.45(7.48)
(PSQ)InBr.tmen	i	22.31(22.12)	-	-	-	15.49(15.39)
(PSQ)InI.tmen	i	20.72(20.28)	-	-	-	22.53(22.42)

(TBSQ)In.phen.1 ¹ / ₂ Et ₂ O	iv	18.74(18.33)	60.93(61.36)	6.21(6.92)	4.48(4.47)	-
(TBSQ)In.phen	iv	22.46(22.28)	58.22(60.60)	5.67(5.48)	5.25(5.44)	-
TBQ(TBSQ)In.phen	iv	15.79(15.61)	65.71(65.31)	6.68(6.58)	4.11(3.81)	-

When the above reaction was repeated in THF, the product was $C_{14}H_{20}O_2InX_2 \cdot 2py \cdot THF$ with a solvating THF molecule (see Table 6.1 for analytical data).

(iii) Finely cut indium metal (0.25 g, 2.2 mmol) was refluxed with TBQ (0.48 g, 2.2 mmol) and iodine (0.55 g, 4.4 mmol) as I_2 in toluene (50 mL). The metal was consumed in 2 h with a total discharge of the colour of iodine. An addition of equimolar amount of 1,10-phenanthroline afforded a light brown precipitate. Refluxing was stopped at this stage and stirring continued until the mixture attained ambient temperature, when 20 mL of petroleum ether was added and stirring continued for another hour followed by filtration. The solid product was washed twice with 10 mL portions of petroleum ether and then dried *in vacuo*. Yield was quantitative and the product analyzed as $C_{14}H_{20}O_2InI_2 \cdot Phen$.

(iv) Diphenyldiselenide (0.69 g, 2.2 mmol) or diphenyldisulphide (0.48 g, 2.2 mmol) was refluxed with finely cut indium metal (0.25 g, 2.2 mmol) and TBQ (0.48 g, 2.2 mmol) in toluene (50 mL). In the case of the diselenide, the metal was consumed in a matter of 3 h, while ca. 18 h was required in the case of the disulphide. Addition of equimolar amount of 1,10-phenanthroline or γ -picoline to the resultant clear solution afforded a light brown precipitate. Isolation procedure was as described in (iii). The products analyzed satisfactorily (see Table 6.1) as $C_{14}H_{20}O_2In(EPh)_2 \cdot L$ where E = Se, S and L = phen or 2-pic.

(v) 3,5-Di-tert-butyl catechol (2 g, 4.5 mmol) was reacted with sodium hydride (0.11 g, 4.5 mmol) in benzene to give a blue solution of sodium benzosemiquinonate with evolution of hydrogen gas. The mixture was stirred until evolution of hydrogen stopped (30 min). At this stage, indium tribromide (1.59 g, 4.5 mmol) or indium trichloride (1 g, 4.5 mmol) in 25 mL of benzene or toluene was added

dropwise to the reaction mixture. Instant reaction commenced with the blue solution starting to clear up forming a light green solution. After addition of the indium halide solution, the flask was fitted with a condenser and the mixture refluxed for an hour. The NaX ($\text{X} = \text{Cl, Br}$) was collected and weighed ($\text{X} = \text{Cl}$, Found 0.19 g, Calc. 0.23 g; $\text{X} = \text{Br}$, Found 0.40 g, Calc 0.46 g).

A 2-fold excess of γ -picoline or pyridine was added to the filtrate and the mixture stirred at room temperature for 1 h. The volume was then reduced by half. Slow evaporation afforded greenish crystals which were collected and dried *in vacuo*; the yield was quantitative. This solid analyzed satisfactorily as $\text{C}_{14}\text{H}_{20}\text{O}_2\text{InX}_2 \cdot 2\text{L}$ ($\text{L} = \gamma$ -picoline or pyridine). Recrystallization of the γ -picoline adduct of this complex in DMF gave solvated X-ray quality crystals. (See Table 6.1 for analytical data.)

6.2.2 Reactions of InX ($\text{X} = \text{Cl, Br, I}$) with 9,10-phenanthroquinone

InX ($\text{X} = \text{Cl, Br, I}$) (3.3 mmol) and 9,10-phenanthroquinone (3.3 mmol) were suspended in toluene. The mixture was cooled to -40°C and tmen (2 mL 13.3 mmol) syringed into the mixture. Stirring was continued at this temperature until the indium(I) halide dissolved completely, and the cooling bath was then slowly removed. As the solution warmed up it became cloudy and at room temperature there was a substantial amount of solid deposit, which was collected, washed twice with 20 mL portions of benzene and dried *in vacuo*. The product analyzed (elemental analysis and infrared spectroscopy) as $\text{C}_{14}\text{H}_8\text{O}_2\text{InX} \cdot \text{tmen}$ which is soluble in methylene chloride and tetrahydrofuran. The ESR spectrum of this in the latter solvent is discussed below.

6.23 The Reaction of Indium Metal with 3,5-Di-tert-butyl 1,2-Benzoquinone:
Solubility Studies

It was apparent from our work involving the reaction of InX with TBQ, that the products obtained could be formulated either as a dimer or as a mixture of In(I) and In(III) species. (See below.) It has since been shown in Section 6.22 (v) that the indium species could be made by reacting In(III) halide with the sodium salt of TBQ. In order to obtain the In(I) species, we refluxed metallic indium with the quinone. By varying the amount of the quinone with respect to the indium we were able to determine the quantity of quinone required to dissolve the indium completely.

All reactions were carried out at constant temperature (100°C), time (24 h), amount of indium (0.18 g, 1.6 mmol), and volume of toluene (50 mL). Finely cut indium metal was refluxed with varying amounts of the quinone in toluene. At the end of the period the mixture was filtered hot and the unreacted metal was weighed (See Table 6.2).

The filtrate was taken to dryness and the residue redissolved in 20 mL of petroleum ether or diethyl ether to afford a greenish solution. Addition of equimolar amounts of 1,10-phenanthroline gave a brownish precipitate. The mixture was stirred for about 2 h at room temperature, filtered and then dried *in vacuo*. The yield of solid, shown by analysis to be adducts of indium(I) semiquinonates (see Table 6.1) was quantitative, based on the amount of indium consumed. In cases where the ratio of the quinone to indium exceeded two, the excess quinone was recovered from the filtrate by backing off the solvent, to afford reddish crystals whose infrared spectrum and melting point were identical to those of an authentic sample of the quinone.

TABLE 6.2

DATA ON SOLUBILITY STUDIES OF INDIUM WITH TBQ

Wt of In (g)	Wt of TBQ (g)	[In]:[TBQ] mole:mole	Wt of Reacted In (g)	% Reacted In	[In] ^(a) mol L ⁻¹
0.182	0.349	1:1.00	0.116	64	1.01×10^{-3}
0.182	0.437	1:1.25	0.134	74	1.20×10^{-3}
0.182	0.524	1:1.50	0.145	80	1.3×10^{-3}
0.182	0.698	1:2.00	0.172	94.5	1.5×10^{-3}
0.182	0.786	1:2.25	0.181	99.5	1.6×10^{-3}
0.182	0.873	1:2.50	0.182	100	1.6×10^{-3}

(a) Concentration of all indium species in filtrate.

The above reaction was repeated adding pyridine to the reaction mixture at the initial stage in a bid to enhance the solubility of metallic indium. Under conditions identical to those described above, equimolar amounts of metallic indium and TBQ were refluxed in toluene in the presence of 2 molar equivalent of pyridine. After 24 h, only 65% of the indium had reacted, and this did not change on using excess pyridine.

6.2.3.1 Oxidation by iodine

Each of the indium(I)-semiquinone products from the above reaction underwent oxidation to form the indium(III) semiquinolone complex on reacting with equimolar amount of molecular iodine.

In a typical experiment, equimolar amounts (0.4 mmol) of iodine and indium(I) semiquinonate complex (TBSQ In(I).phen) were stirred at room temperature in 20 mL of methylene chloride. The colour of iodine was discharged in an hour producing a yellow solution. Stirring was continued for an hour and then 50 mL of petroleum ether added to precipitate a yellowish powder in quantitative yield. Analysis found: In 15.1%; I 32.7%; calc. In 14.9%, I 33.0% for (TBSQ)InI₂.phen. The ESR and infrared spectra were similar to an identical compound prepared differently (see Section 6.2.1 (iii)) and will be discussed later (see discussion).

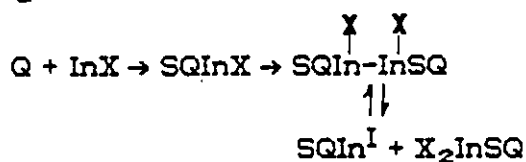
6.3 Results and Discussion

6.3.1 Preparative

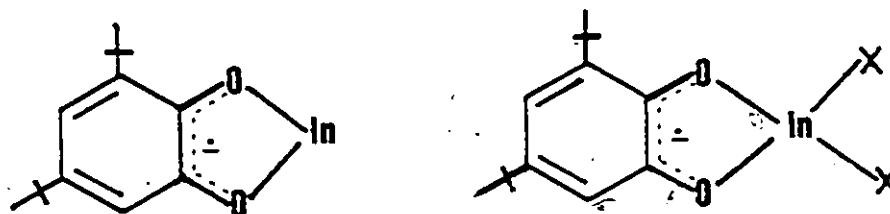
The oxidative addition reaction between tetrahalogeno orthoquinones and indium(I) halides lead to the formation of indium(III) catecholates as we saw in Chapter 5. The reaction between InX with TBQ or PQ on the other hand yields a stable semiquinone complex as the product. It is clear from ESR studies (see below) that these complexes are formed as a result of one-electron reduction

of the parent quinone. The stability of these complexes is presumably enhanced by the bulky substituents on the *o*-benzoquinone ring. The nature as well as the structure, of these complexes is considered below.

(i) InX/TBQ/L (L = nitrogen donor ligand). With the aid of ESR spectroscopy discussed later, we were first able to confirm that all the products obtained in this reaction were semiquinonato complexes. Secondly, we were able to infer the presence of both In(I) and In(III) species and this was confirmed by the analytical data on these complexes (see Table 6.1). As a result the reaction scheme was considered as involving the formation of an indium(II) semiquinone as a first step by the transfer of one electron from the indium(I) halide to the substrate. The first product, then is essentially a biradical which then dimerizes as shown below in the scheme. The dimer then undergoes disproportionation yielding the indium(I) and indium(III) semiquinonates.

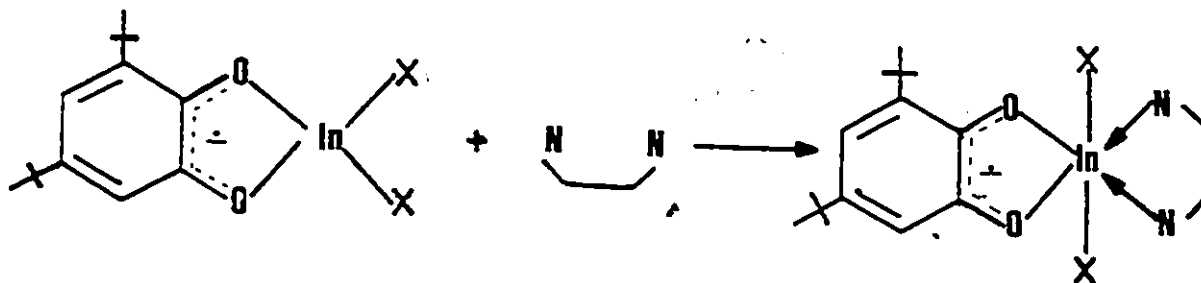


The structure of the complexes are then considered as



where the unpaired electron is located largely on the semiquinonato ring. Evidence to support this is derived from the coupling constants of the protons on the ring (see below).

It is justifiable at this point to advance arguments regarding the stability of the semiquinonates of indium. From Chapter 4, we found that in the presence of a donor ligand, the semiquinonates of tin(IV) can be converted to the corresponding catecholates. Using a similar argument, it can be inferred that in the presence of a donor ligand, the indium attains a stable coordination state of six in the case of indium(III).

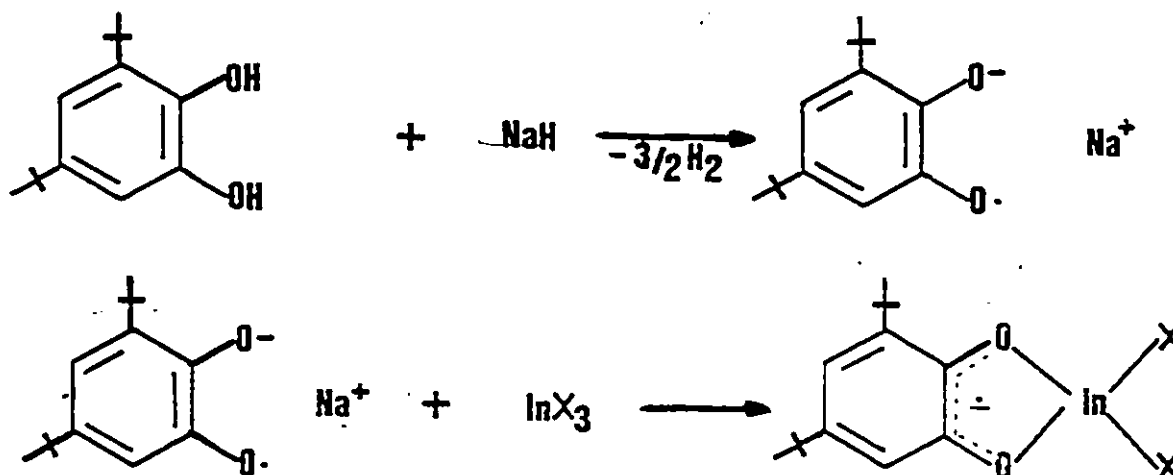


X-ray diffraction studies has confirmed the structure of the indium(III) semiquinonates, and we are still attempting to grow suitable crystals of the indium(I) complex. This is the first ever structurally determined semiquinonate of a Main Group Element.

Other experiments were conducted to aid the further understanding of the apparent disproportionation reaction which occurred in the reaction of InX_3 with TBQ leading to the formation of the different species. These experiments are described below.

6.3.2 Reaction of Indium(III) Halides with TBC

To generate one of the species mentioned above, we reacted InX_3 (X - Cl, Br) with sodium benzo-semiquinonate (see experimental) by the following scheme:



The products from these reactions were exclusively indium(III) semiquinonates. The ESR parameters (Table 6.3) and the analytical results agree satisfactorily with those of the species obtained in a reaction involving InX/TBQ (see Table 6.3). The structure of one of the products was determined by X-ray diffraction studies. (see Section 6.4)

6.3.3 Reaction of Metallic Indium with TBQ: Solubility Studies

This reaction was run primarily to confirm the earlier assumption that one of the species in the InX/TBQ system is indeed an indium(I) semiquinonate. Refluxing metallic indium with an equimolar amount of TBQ in toluene gave ca. 70% yield of a product which was subsequently isolated as the phenanthroline adduct and characterized as the indium(I) complex SQIn^IL. (See Table 6.1.) These studies were extended to include the studies of the solubility of metallic indium in solution of varying TBQ concentrations under reflux. The results obtained are presented in Table 6.2. Plots of percentage consumption of indium and the concentration of reacted indium against the molar ratio of TBQ to In are presented in Figs. 6.1 and 6.2 respectively. It is evident from the first graph that the amount of indium reacting approaches 100% close to a molar ratio

of 2:1. This suggests the formation of a stable four-coordinate indium compound in solution. The addition of an equimolar amount of phenanthroline precipitates the presumably six-coordinate stable indium(I) complex. The nature of the ligands was confirmed by infrared spectroscopy (see below).

The second plot shows the limiting solubility of indium(I) complexes in such a medium. A value of 1.6×10^{-3} mol is obtained from the graph, a value which differs by a factor of 10 from that reported in parallel studies conducted in our laboratory involving the InBr/toluene/tmen system at -20°C .²⁴ This difference could be due in part to the fact that the products obtained in the present work are more stable.

All the indium (I) complexes obtained in this work undergo oxidation by an equimolar amount of iodine by the reaction



which is typical of indium compounds in a low oxidation state. One point of interest in this particular reaction is the fact that the attack of the iodine was specifically at the metal centre without any effect on the bonded semiquinone ligand. This, in a way, points to how strongly bonded the ligand is to the metal. A similar effect was observed in Chapter 4 when we reacted iodine with the dimeric tin(IV) specie in our ESR studies.

FIGURE 6.1

PLOT OF % REACTED INDIUM AGAINST MOLAR RATIO OF TBQ TO INDIUM

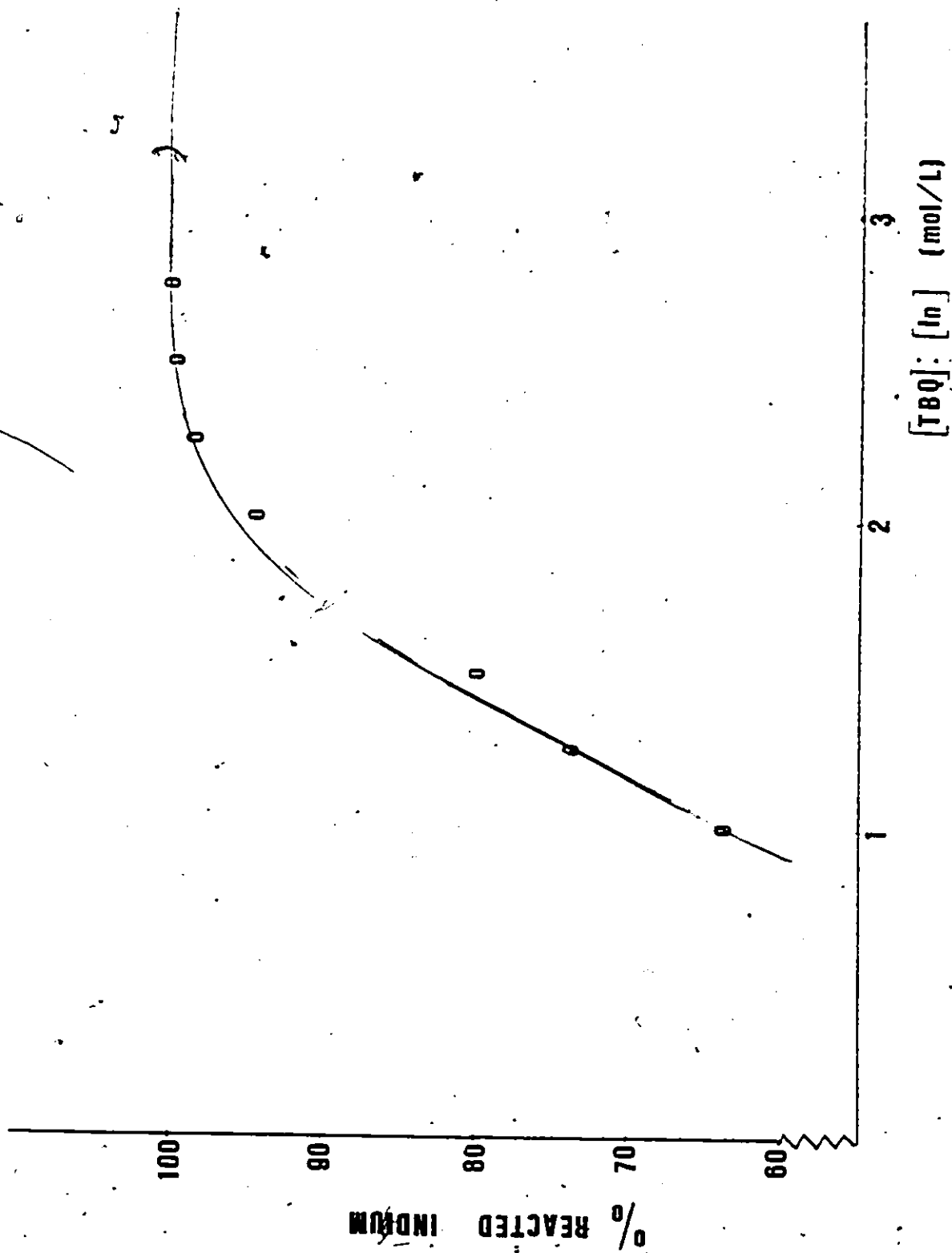
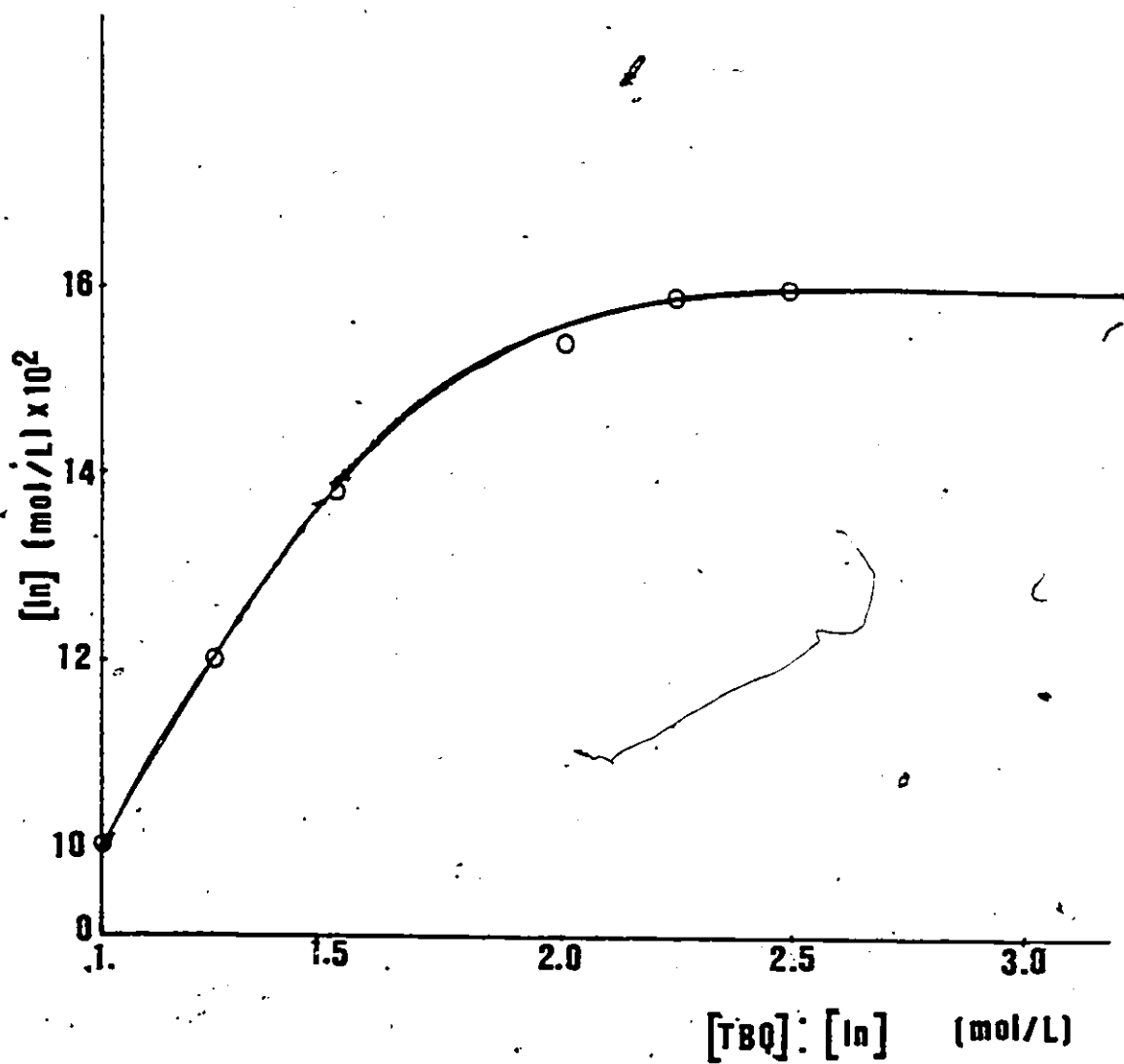
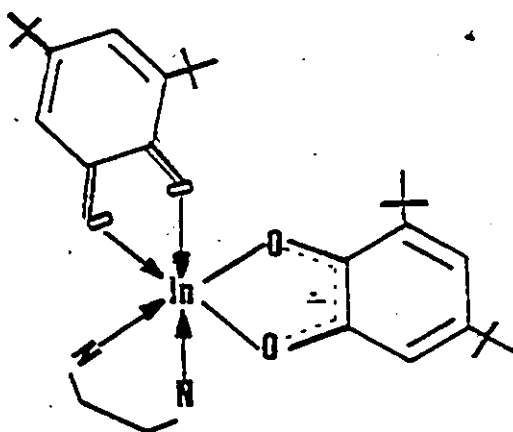


FIGURE 6.2

PLOT OF CONCENTRATION OF REACTED INDIUM AGAINST THE MOLAR RATIO OF
TBQ TO INDIUM



Complexes obtained when the molar ratio of TBQ:In was ≥ 2 were formulated as $(C_{14}H_{20}O_2)_2In.phen$, or as presented in the Tables as TBQ(TBSQ)In.phen. One of the quinones in this case acts as a bidentate neutral ligand (see vibrational spectroscopy) the other binds as a semiquinone ligand. Analytical data also support this formulation. The proposed structure is



6.3.4 Spectroscopic Results

(i) Vibrational Spectroscopy

The infrared spectra of the semiquinonato complexes in the mid and far regions are presented in Tables 6.4 and 6.5 respectively.

In the mid region, we concentrate on the vibrations between 1200 and 1700 cm^{-1} (see Fig. 6.3 for a typical spectrum). Each complex has strong band centred around 1480 cm^{-1} which can be resolved into at least three separate bands, plus an intense band near 1250 cm^{-1} . These bands are identical to that found in the semiquinone complexes $Cr(Cl_4SQ)_3$,²⁰¹ $[Co(trien)(TBSQ)]Cl_2$,²¹³ and $Cr(TBSQ)_3$.²¹⁴ These bands have been assigned to the stretching vibration of the partially reduced carbonyl bond.

TABLE 6.3

INFRARED SPECTRA OF INDIUM SEMIQUINONATES IN THE MID-REGION (cm^{-1})

Compound	Absorption	Assignment
(TBSQ)InX ₂ .tmen	3060 (w,s)	C-H (TBSQ)
	2954 (s,br)	C-H (TBSQ + tmen)
	1474 (vs), 1446 (vs), 1418 (vs)	C=O (TBSQ)
(TBSQ)InX ₂ .2py	3066 (w,s)	C-H (TBSQ + Py)
	2949 (s,br)	C-H (TBSQ)
	1605 (s,s)	C=C (py)
	1470 (vs), 1448 (vs), 1418 (vs)	C=O (TBSQ)
(TBSQ)InX ₂ .2pic. ¹ / ₂ dmf	1250 (s,br)	
	3058 (w,s)	C-H (TBSQ + pic)
	2957 (s,br)	C-H (TBSQ + pic)
	1681 (s,s)	C=O (dmf)
	1621 (s,s)	C=C (pic)
(TBSQ)In(SPh) ₂ .phen	1482 (vs), 1474 (vs), 1459 (vs)	C=O (TBSQ)
	3054 (w,s)	C-H (TBSQ + phen + SPh)
	2948 (s,br)	C-H (TBSQ)
	1586 (s,s)	C=C (phen)
(TBSQ)In(SPh) ₂ .phen	1475 (vs), 1430 (vs), 1416 (vs)	C=O (TBSQ)
	1254 (s,br)	
	3053 (w,s)	C-H (TBSQ + phen + SPh)
(TBSQ)In(SePh) ₂ .phen	2947 (s,br)	C-H (TBSQ)

PAGE 162 IS OMITTED.

PAGE 162 NON INCLUS DANS LA PAGINATION.

	1586 (s,s)	C=C (phen)
	1474 (vs), 1437 (vs), 1415 (vs)	C=O (TBSQ)
	1255	
(TBSQ)In.phen	3058	C-H (TBSQ + phen)
	2950	C-H (TBSQ)
	1585	C=C (Phen)
	1485 (vs), 1423 (vs), 1414 (vs)	C=O (TBSQ)
	1243	
(TBSQ)In.phen	3058	C-H (TBSQ + phen)
	2950	C-H (TBSQ)
	1585	C=C (phen)
	1485 (vs), 1432 (vs), 1414 (vs)	C=O (TBSQ)
	1243	
TBQ(TBSQ)In.phen	3056 (w,s)	C-H (TBSQ + phen)
	2951 (s,br)	C-H (TBSQ)
	1624 (s,s)	C=O (TBQ)
	1471 (vs), 1441 (vs), 1417 (vs)	C=O (TBSQ)
	1260 (s,br)	

TABLE 6.4

FAR INFRARED SPECTRA OF SOME INDIUM SEMIQUINONATES (IN CM^{-1})

Compound	$\nu(\text{In-N})$	$\nu(\text{In-O})$	$\nu(\text{In-X})$	$\nu(\text{In-Ef})$ E = S, Se
(TBSQ)InCl ₂ .phen	282(s)	428(s)	305(s,br)	
(TBSQ)InBr ₂ .phen	280(m)	420(s)	219(s) 200(s)	-
(TBSQ)InI ₂ .phen	290(s)	422(s)	182(s,br)	-
(TBSQ)InBr ₂ .2pic	274(s)	432(s)	224(s,br) 170(s,br)	-
(TBSQ)InBr ₂ .2py	292(s)	420(s)	188(s,br)	-
(TBSQ)In(SPh) ₂ .phen	288(m)	420(s)	-	330(s,br)
(TBSQ)In(SePh) ₂ .phen	282(m)	420(s)	-	212(s,br)
(TBSQ)In.phen	285(m)	422(s)	-	-

The DMF complex shows in addition to the above bands a strong absorption at 1681 cm^{-1} due to $\nu(\text{C}=\text{O})$. This value is identical with that of the $\text{C}=\text{O}$ band in pure DMF, which suggests that the DMF is not coordinated in the complex but rather is present as solvent of crystallization in the lattice.

The spectrum of $\text{TBQ}(\text{TBSQ})\cdot\text{M}(\text{phen})$ has a strong band at 1624 cm^{-1} which is assigned to a coordinated $\text{C}=\text{O}$ group, showing that the quinone is indeed, acting as a bidentate ligand. This constitutes a shift of ca. 50 cm^{-1} from the parent quinone consistent with observations made on the i.r. spectra of products prepared from the reaction of some metal halides with phenanthroquinone, e.g. $\text{InBr}_3\cdot\text{PQ}$.¹²⁷

The spectra in the far infrared region are presented in Table 6.4. The bands observed were identical to those of the indium (III) catecholates, and assignments were essentially based on those spectra (see Chapter 5).

(ii) ESR Spectroscopy

For the purpose of our discussion under this section, the following numbering system will be used:

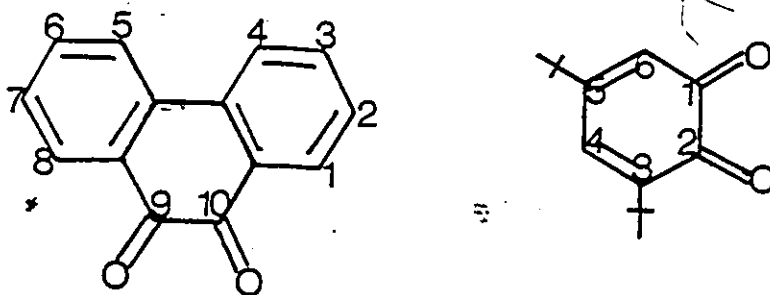
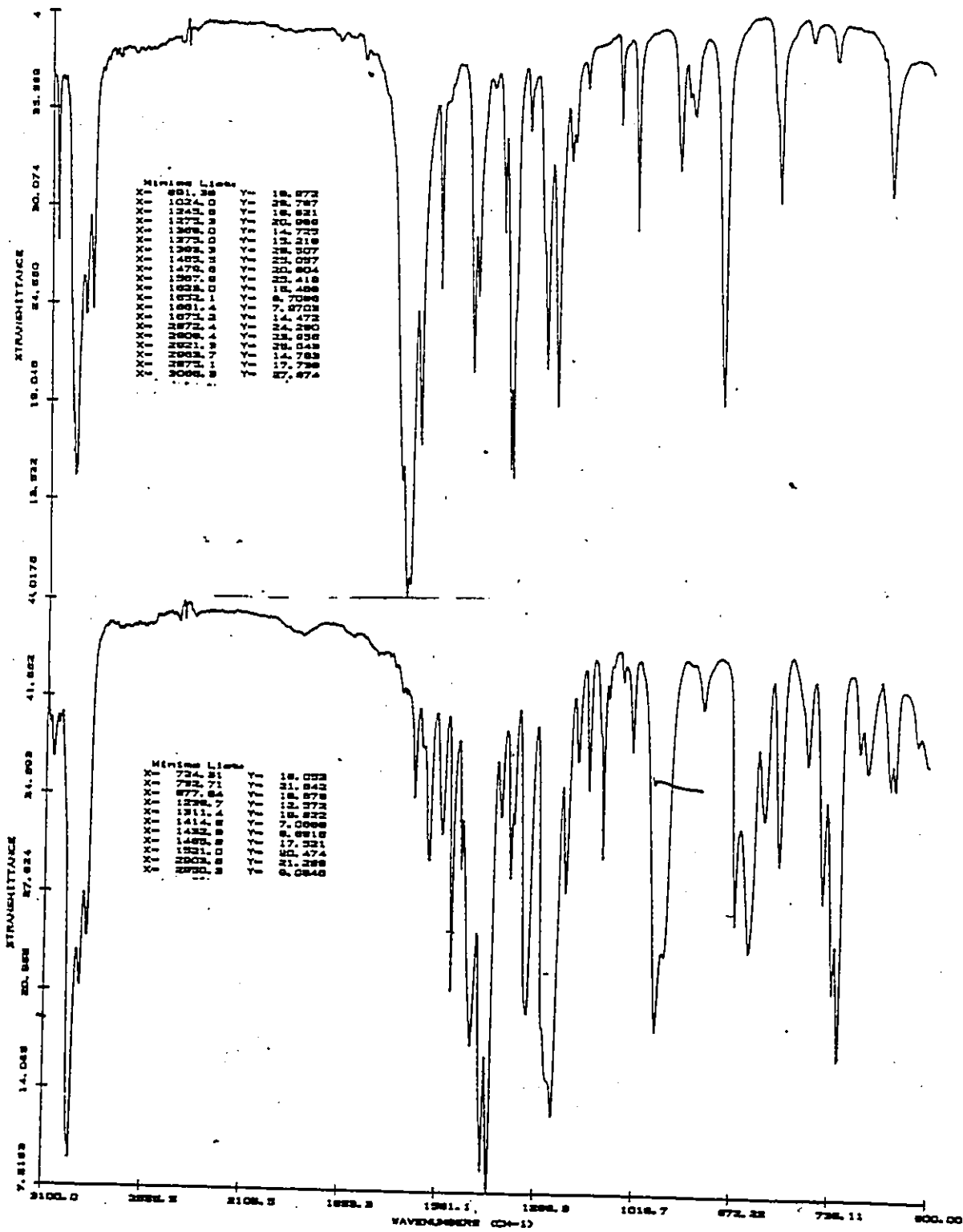


FIGURE 6.3

IR SPECTRUM OF (A) TBQ (B) (TBSQ)InCl₂.phen

A



The ESR spectra presented in Figs. 6.4-6.8 provide the most convincing evidence that the complexes being discussed in this chapter can correctly be formulated as orthobenzosemiquinones.

Unless otherwise stated, all spectra were run in degassed solvents in micromolar concentrations, at room temperature. All the ESR parameters are presented in Table 6.5.

(a) InX/PQ/tmen. A typical spectrum of this system in THF is presented in Fig. 6.4a, and in Fig.6.4b is shown a computer simulated spectrum based on the parameters in Table 6.5. Just like in the TBQ systems with InX we observe here a coupling of the unpaired electron with the ^{115}In nucleus and also coupling with the protons at positions 1,8 and 3,6. The electron density at positions 2,7 and 4,5 are apparently low and hence no coupling effect is observed from them. The value of the hyperfine constant for indium suggests that the unpaired electron is located mainly on the semiquinonato ligand. On this basis we propose the following structure for this compound.

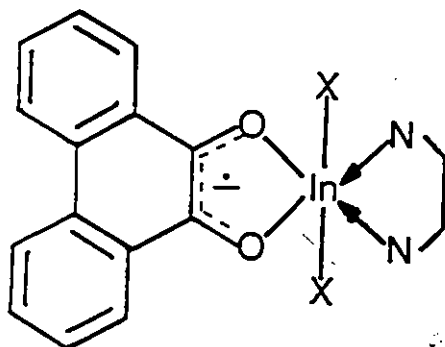


TABLE 6.5

ESR PARAMETERS OF In SEMIQUINONATE COMPLEXES ($G \approx 2.0039$)

Compound	Method	Solvent	A_{In}	A_H	A_{Other}
(TBSQ)InCl ₂ .2py	ii	Tol	10.72(In ⁺) 6.51(In ³⁺)	3.31 (C'-4)(a) 3.48(C'-4)(b)	-
(TBSQ)InBr ₂ .2py	ii	Tol	10.14(In ⁺) 6.33(In ³⁺)	3.19 (C'-4)(a) 3.53 (C'-4)(b)	-
(TBSQ)InCl ₂ .2py	v	THF	6.38	3.31 (C-4) 0.31 (C-5)	-
(TBSQ)InBr ₂ .2py	v	THF	5.13	3.85(C-4) 0.34 (C-5)	-
(TBSQ)InCl ₂ .tmen	i	Tol/CH ₂ Cl ₂	7.60	2.5 (C-4) 2.1 (C-6)	-
(TBSQ)InBr ₂ .tmen	i	Tol/CH ₂ Cl ₂	7.40	2.3 (C-4) 2.2 (C-6)	-
(TBSQ)InI ₂ .tmen	i	Tol/CH ₃ Cl ₂	7.10	2.3 (C-4) 2.1 (C-6)	-
(TBSQ)In(SePh) ₂ .2pic	iv	Tol	6.06	3.25 (C-4)	1.5 (Se)
(TBSQ)In(SPh) ₂ .2pic	iv	Tol	6.51	3.53 (C-4)	-
(PSQ)InCl.tmen	i	Tol	4.85	2.43 (H-1,8) 1.75 (H-3,6)	-
(PSQ)InBr.tmen	i	Tol	4.73	2.58 (H-1,8) 1.80 (H-3,6)	-
(PSQ)InBr.tmen	i	Tol	4.62	2.75 (H-1,8) 1.85 (H-3,6)	-
(TBSQ)In.2py	iii	Tol	10.44	3.40 (C-4)	-
(TBSQ)In.phen	iii	Tol/CH ₂ Cl ₂	8.74	2.30 (C-4) 2.17 (C-6)	-

(a) Hyperfine constant for In(I) complex and (b) for In(III) complex.

FIGURE 6.4

ESR SPECTRA OF $(\text{PSQ})\text{InCl}_2 \cdot \text{tmen}$ IN THF: (A) EXPERIMENTAL

(B) CALCULATED

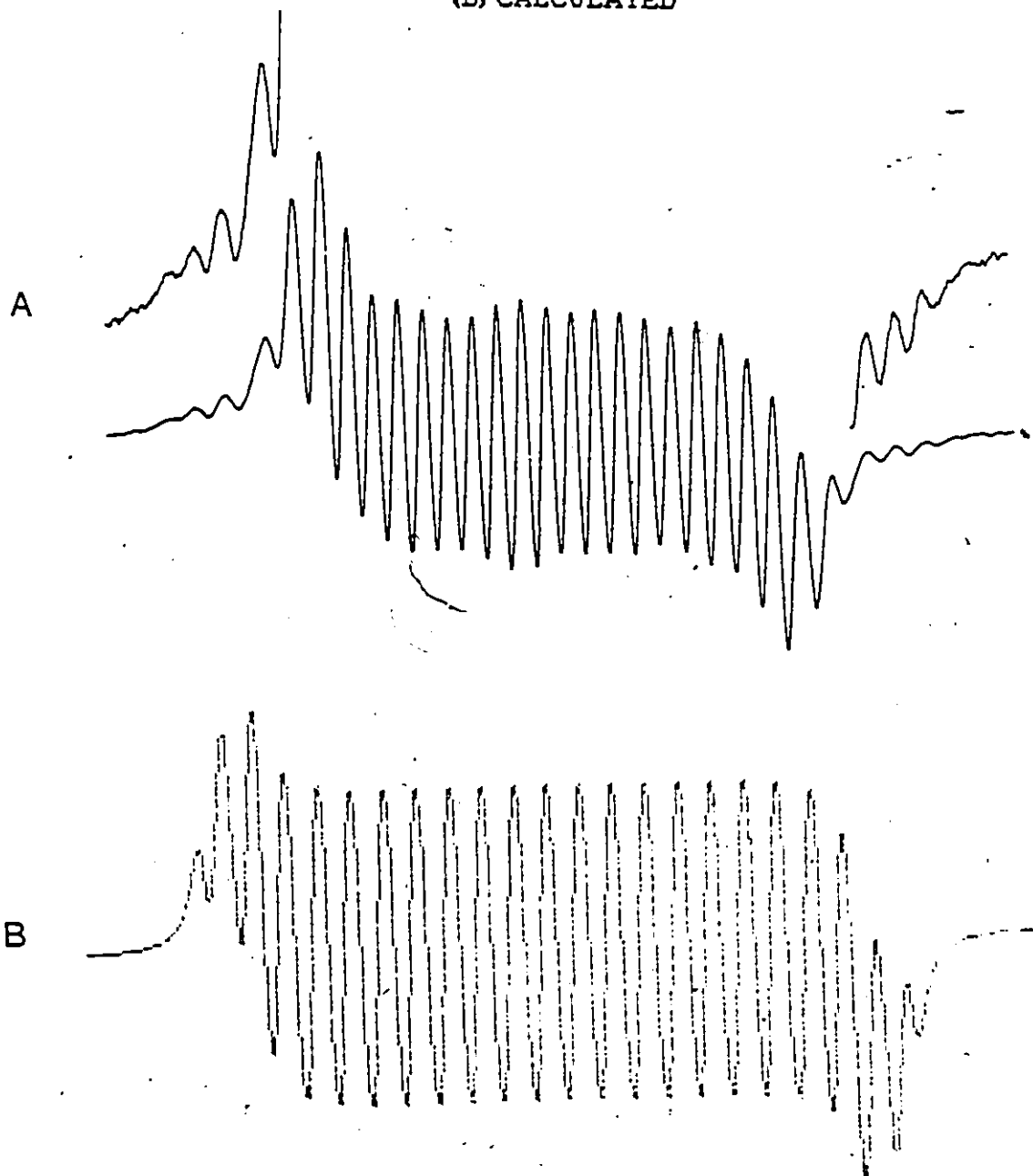
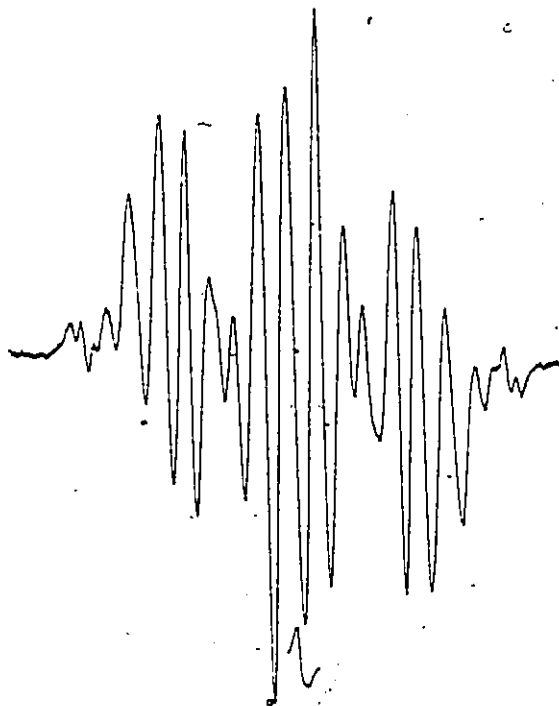


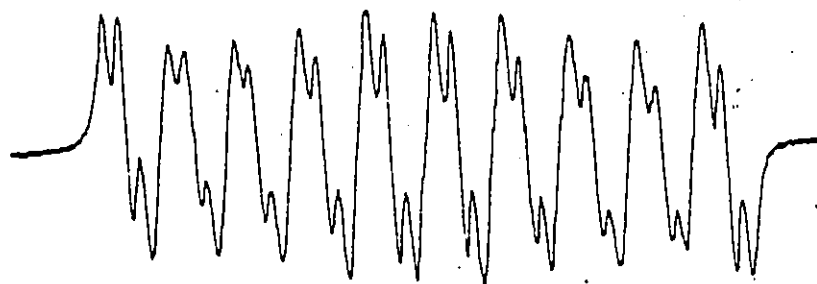
FIGURE 6.5

ESR SPECTRA OF $(\text{TBSQ})\text{InCl}_2 \cdot \text{tmen}$ (A) IN TOLUENE (B) IN CH_2Cl_2 (C) CALCULATED
SPECTRUM OF B.

A



B



C

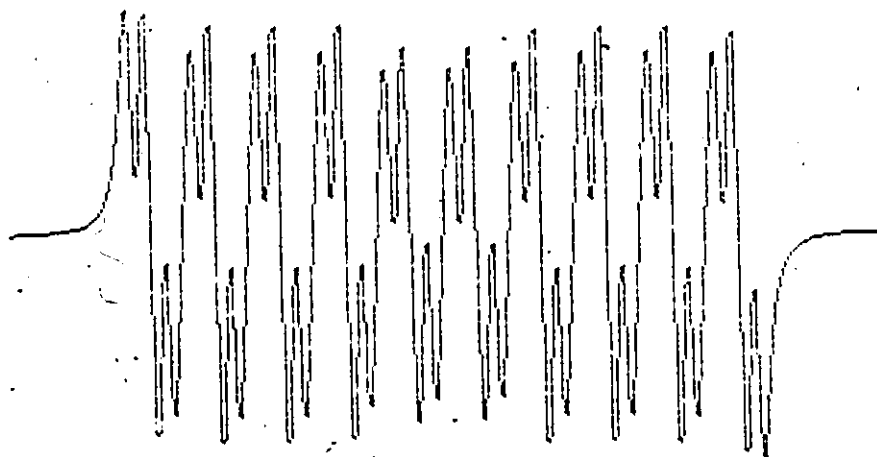


FIGURE 6.6

ESR SPECTRUM OF THE SYSTEM InCl/TBQ/Py IN TOLUENE (A) EXPERIMENTAL

(B) CALCULATED

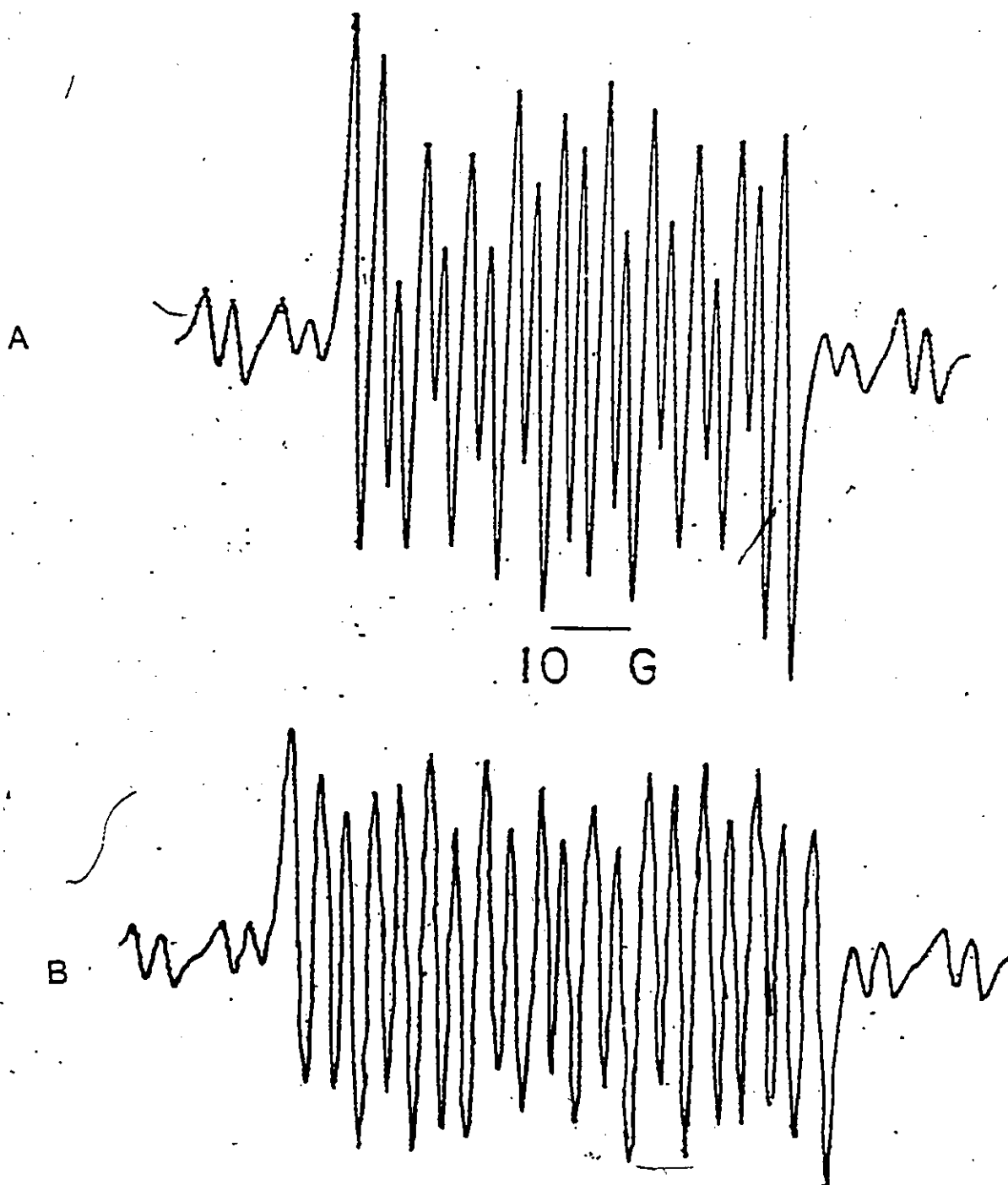


FIGURE 6.7

ESR SPECTRA OF $(\text{TBSQ})\text{InCl}_2 \cdot 2\text{py}$ IN THF (A) FIRST DERIVATIVE ON 100 G SCAN RANGE (B) EXPANDED PORTION OF THE RIGHT HAND SPECTRUM OF A (C) SECOND DERIVATIVE OF B

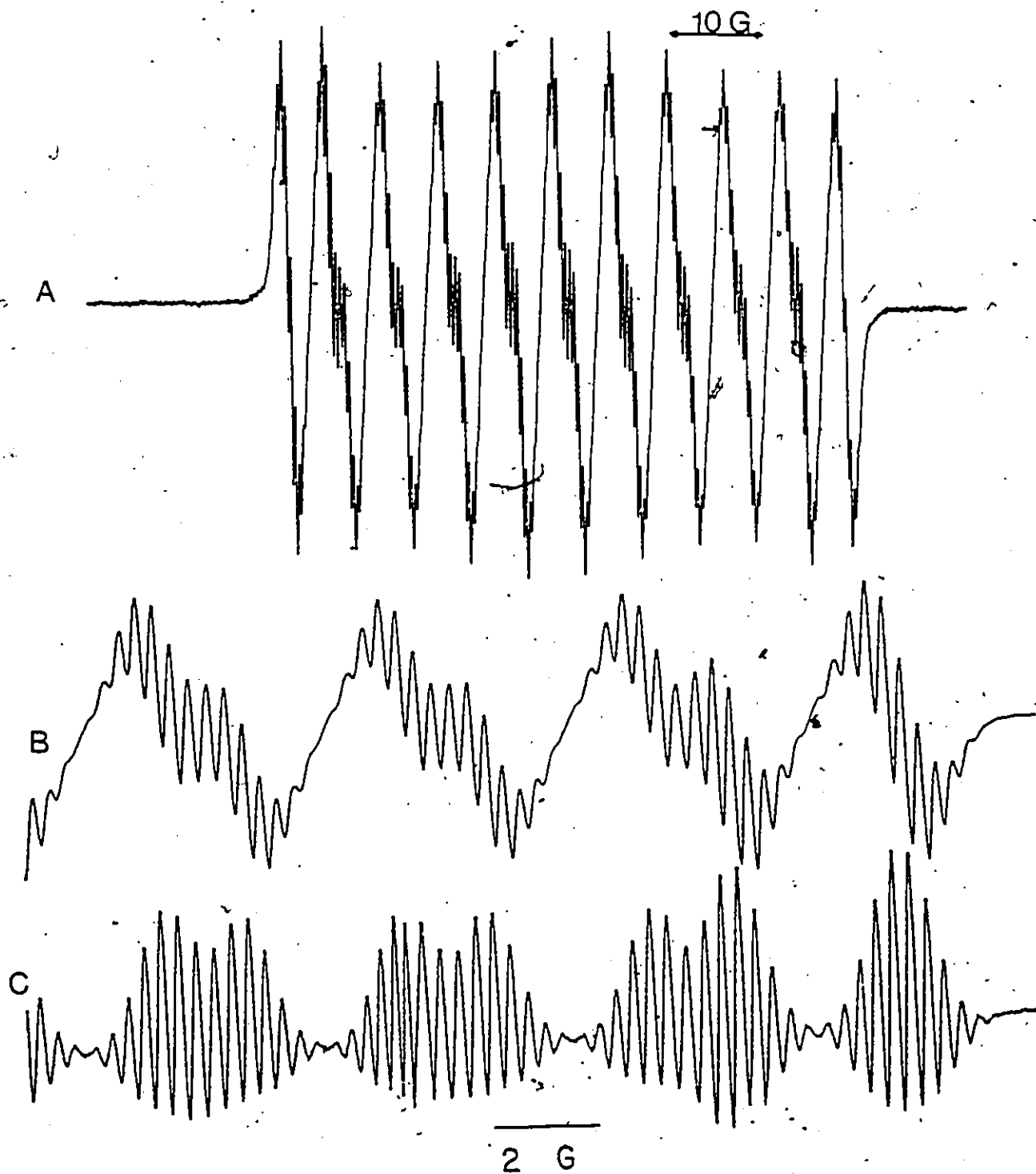
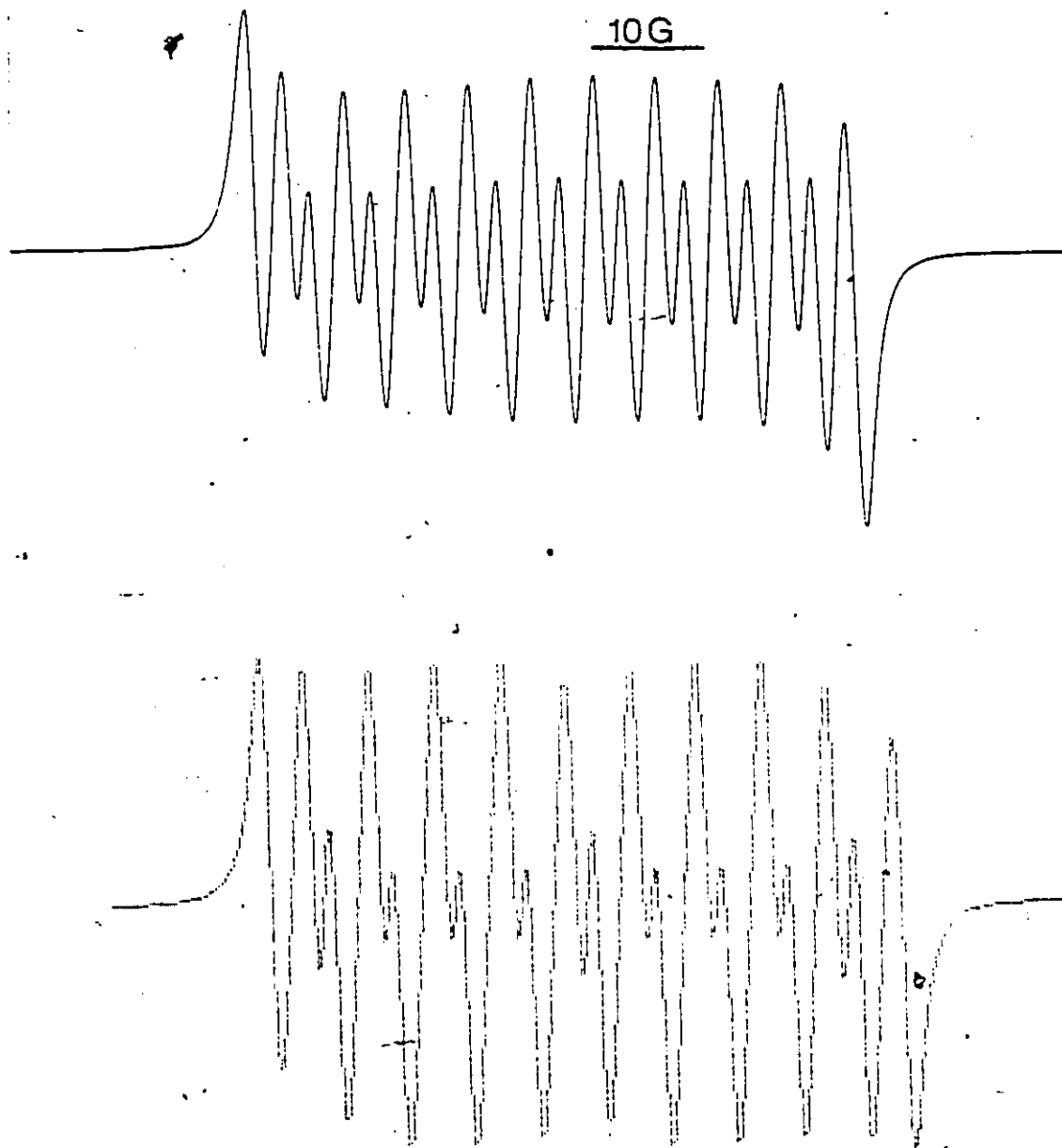
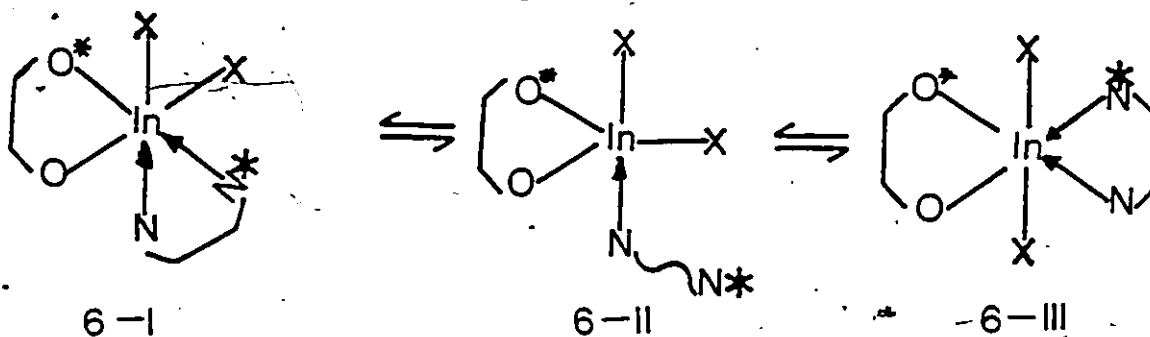


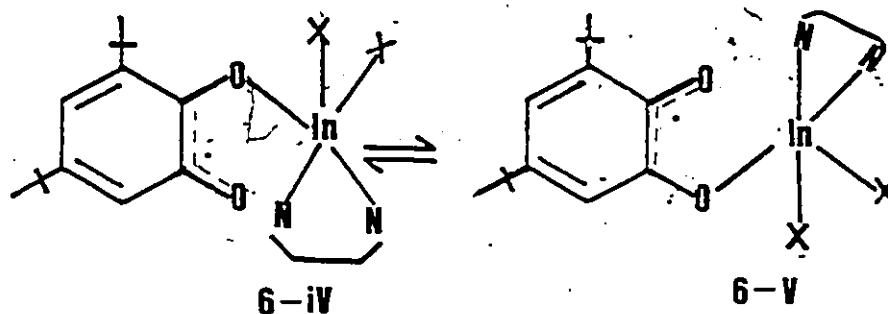
FIGURE 6.8

ESR SPECTRA OF (TBSQ)InCl₂.py IN TOLUENE (A) EXPERIMENTAL (B) CALCULATED

(b) InX/TBQ/tmen. The spectrum obtained in toluene from this reaction is presented in Fig. 6.5a. The best computer simulation was obtained by considering two equivalent nitrogens, two equivalent hydrogens with coupling constants of 21.32 G and 4.62 G respectively, in addition to an indium with a coupling constant of 8.27G. Addition of a few drops of methylene chloride to the above solution resulted in the spectrum in Fig. 6.5b and the computer simulated spectrum is presented in Fig. 6.5c. The coupling constants (see Table 6.5) for the two observable protons suggest that they are equivalent. This was considered improbable since the electron densities at each carbon in the semiquinonato ring are inequivalent. We offer the following explanations. In the scheme below, we consider a six coordinated indium atom (6-I and 6-III), with the stereochemistry around constantly changing. These changes occur partly due to the lability of the tmen ligand forming a five coordinate intermediate (6-II). In this scheme one nitrogen atom is considered directly opposite an oxygen atom (both in asterisks) and due to a possible internal rotation an equilibrium is established between 6-I and 6-III consequently causing the protons at positions 4 and 6 to become equivalent by symmetry. Hence the resultant spectrum



Another interpretation is by considering a process where the following conformers might exist in solution. (6-IV and 6-V)



where the semiquinone acts as a fluxional (IV \rightleftharpoons V) ligand with the formation of a five coordinate indium atom. Again the rate of exchange between these conformers may be such that the two protons in question become magnetically equivalent. A similar explanation has been offered in the ESR studies of reactions leading to the formation of organotin(IV) derivatives of 3,6-di-*t*-butyl-1,2 benzosemiquinone.¹⁵⁵

Variable temperature studies will be helpful in giving a better understanding of this system.

(c) InX/TBQ/py. The type of spectra, and hence the type of reaction which occurred with these reagents was dependent upon the type of solvent used. In toluene, the spectrum shown in Fig. 6.6a was observed, while Fig. 6.7a shows a spectrum run in THF.

In the toluene spectrum, we observe two species which were identified from their hyperfine coupling constants (see Table 6.5) as In(I) and In(III) semiquinonato complexes. The calculated spectrum based on the parameters in Table 6.5 is presented in Fig. 6.6b. A similar observation was made in Chapter 5 in the reaction of metallic indium with tetrahalogeno orthoquinone in the presence of iodine. The good fit of the simulated spectrum with the experimental

spectrum confirm the presence of both species in solution.

The spectrum in Fig. 6.7 was obtained by the above reaction in THF. An identical spectrum was also obtained by the reaction of indium trihalides with sodium benzosemiquinonate in toluene. The agreement between these two spectra supports the proposal that the reaction of InX with TBQ yields an indium (III) semiquinonate as the principal product.

From the spectrum we observe 11 components of the hyperfine structure. Considering only the splitting from the metal ($I = 9/2$) then ten lines should be observed due to interaction with one proton. However, the splitting constants of In and H are found to be reasonably close. (See Table 6.5.) This results in the superimposition of the two sets of lines and hence the observation of eleven lines. The value of the hyperfine constant for hydrogen in this work is found to be close to that of the hydrogen at the same position in free TBSQ,¹¹ which suggests that the unpaired electron is located largely on the ligand.

In the spectrum, a superhyperfine structure (Fig. 6.7a) is observed with a splitting constant of ca. 0.3 G. Following the work of Razuvaev *et al.*,¹⁴¹ we attributed the splitting to the tert-butyl protons in the 5-position. This assignment was found to be correct when such structures were observed with reactions of TBQ with both indium trichloride and tribromide. The splittings could then not have been caused by the halogens.

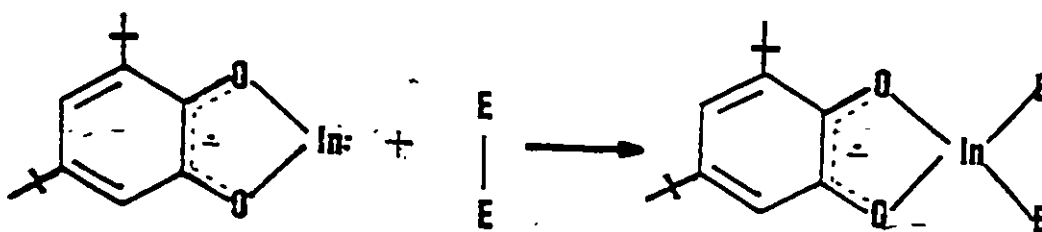
The expanded portion of the left side of the spectrum together with its second derivative spectrum are presented respectively in Figs 6.7B and 6.7c. The latter permitting the accurate counting of the number of lines generated by the splitting brought about by the 9 protons on the butyl group.

The interaction of the proton at positions 6 and of the tertiary butyl group in position 3 is apparently weaker than those at positions 4 and 5 and could not be identified from the spectrum.

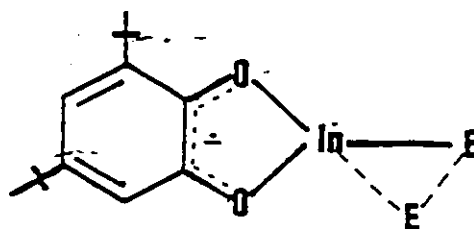
The dependence of the line width of the spectra obtained thus far on the properties of the solvent is exhibited in Fig. 6.8. This is a spectrum obtained by the reaction of indium trihalides with sodium benzoquinone in toluene. Here we see the eleven-line pattern as explained above. The supplementary hyperfine structure is not observed in this case due to line broadening.

(d) In/TBQ. As discussed earlier, this reaction yielded a product which has been formulated as an indium(I) semiquinone complex. The ESR parameters are presented in Table 6.5. The hyperfine constant for indium in this case is close to other values for complexes identified as indium(I) complexes in this chapter and Chapter 5. The spectrum obtained in methylene chloride exhibited the same properties as the InX/TBQ/tmen system in the same solvent. As far as the detailed description of the spectrum is concerned, the general description given in the InX/TBQ/tmen system holds, where a possible fluxional behaviour in the molecule allows the protons at positions 4 and 6 to become magnetically equivalent.

(e) In/TBQ/E₂ (E = I₂, Ph₂Se₂, Ph₂S₂). The refluxing of metallic indium with TBQ in the presence of equimolar quantities of I₂, Ph₂S₂ or Ph₂Se₂ successfully led to the isolation of the corresponding indium(III) semiquinones. The overall reaction can be considered as the oxidative insertion reaction indium(I) semiquinone into the E-E bond (E = I, S, Se).



A possible mechanism of this reaction could involve the initial transfer of an electron to E forming an intermediate



and a later transfer of the remaining electron to form the product. If this assumption is correct, then one might hope to use ESR spectroscopy to follow these successive electron transfers since the unpaired electron on the semiquinonate ring would be sensitive to changes occurring around the indium nucleus. Particularly attractive is the insertion into Ph_2Se_2 , since Se with $I = 1/2$ could interact with the unpaired electron to give additional splitting pattern to the splitting by indium as we observe in the present work. (See Table 6.5.) Such studies should elucidate the mechanisms of electron transfer reactions.

6.4 X-ray Studies

Attempts to grow suitable crystals for X-ray studies finally bore fruit when 4-methyl pyridine (γ -picoline) was used as the neutral donor ligand. The details on data collection and processing for the crystal structure determination are given in Chapter 1. Table 6.6 summarizes the crystal data and other parameters related to data collection and structural refinement.

TABLE 6.6

SUMMARY OF CRYSTAL DATA, INTENSITY COLLECTION, AND STRUCTURAL
REFINEMENT (3,5-BIS-T-BUTYL-1,2-BENZOSEMIQUINONE)InBr₂·(γ-Pic)₂·¹/₂DMF

Formula	InBr ₂ N _{2.5} O _{2.5} C _{27.5} H _{37.5}
cell constants	31.479(8), 10.941(4), 21.962(8)Å; 125.06(2) ^o
cell volume, Å ³	6191.5(3)
crystal system	monoclinic
space group	C2/c
mol wt	689.6
Z, F(000)	8, 2732
d _{calcd} :d _{measd} , g cm ⁻³	1.48, 1.51
cryst dimens, mm	0.15 x 0.18 x 0.30
abs coeff, μ, cm ⁻¹	32.45
min abs corr	1.675
max abs corr	2.015
2θ angle, deg	4-45 ^o
radiation	MoKα, λ = 0.71069Å
monochromator	highly oriented graphite
temp, °C	21
scan type	coupledθ (crystal)/2θ (counter)
scan width	K _{α1} -1 ^o to K _{α2} +1 ^o
scan speed, °min ⁻¹	variable, 2.02-4.88
bkgd time/scan time	0.5
total reflcns measd	4001 (th, +k, ±l)
unique data used	1697
no. of parameters	183

PAGE 180 IS OMITTED.

PAGE 180 NON INCLUS DANS LA PAGINATION.

$R = (\sum F_o - F_c) / \sum F_o $	0.0529
$R_\omega = [\sum \omega (F_o - F_c)^2 / \sum \omega F_o ^2]^{1/2}$	0.0547
$\Delta \rho_{\max} \cdot e^{\lambda-3}$	0.94
shift/error(max)	0.05

To guard against decomposition in air a single green crystal was sealed in a capillary tube. During the data collection, the intensity of the three monitor reflections decreased by approximately 15% and this was corrected by applying an appropriate scaling factor. The data were further corrected for Lorentz, polarization and for absorption effects. The systematic absences h,k,l , $h + k = 2n + 1$; hol , $l = 2n + 1$ indicated the space groups $C2/c$ or Cc . The former was used and assumed correct because of successful refinement of the structure. The structure was solved by the heavy atom method.

The position of the indium atom was obtained from a sharpened Patterson synthesis. The positions of the remaining non-hydrogen atoms were obtained from subsequent difference Fourier synthesis based on the coordinates of the indium atom, the structure was then refined by full matrix least-squares methods with In, Br, N and O(1) and O(2) being treated anisotropically, and all carbon atoms isotropically. Hydrogen atoms were included in idealized positions with isotropic thermal parameters which were assigned the same values for the appropriate thermal parameters of the bonded carbon atoms. At this stage a difference synthesis contained a few peaks of the order of $1-3 \text{ e}\text{\AA}^3$ in an empty region. It was apparent that some scattering material was present and the volume of the hole it occupied was apparently that of a dimethyl formamide molecule. These positions were included in further refinement as a disordered DMF molecule with nitrogen atom on a two fold axis. With isotropic vibration, U , for carbonyl C and O fixed at 0.20 \AA^2 (higher than that of N), the refinement converged (R 0.070 to 0.0529) with carbon and oxygen occupancies respectively at 52 and 35%. After six more cycles of refinement, convergence was achieved with the final $R = 0.0529$ and the final $R_w = 0.0547$ for 1697 unique "observed $|I| > 2 \sigma(I)$ " reflections.

Positional and thermal parameters are given in Table 6.7 bond distances and angles are listed in Table 6.8. Figure 6.9 shows the molecule with the atomic numbering scheme and Figure 6.10 gives the cell packing.

TABLE 6.7

FINAL FRACTIONAL COORDINATES AND ISOTROPIC THERMAL PARAMETERS (\AA^2)
 FOR NON-HYDROGEN ATOMS OF (3,5-BIS-T-BUTYL-
 1,2-BENZOSEMIQUINONE)InBr₂(γ -pic)₂^{1/2}/2DMF WITH STANDARD DEVIATIONS IN
 PARENTHESES

	X	Y	Z	U _{eq} /U
In	0.1274(1)	0.2189(1)	0.1434(1)	50.7(7)
Br(1)	0.1732(1)	0.2619(2)	0.2822(1)	78(1)
Br(2)	0.0326(1)	0.2747(2)	0.0869(1)	86(2)
O(1)	0.2019(3)	0.1625(9)	0.1613(5)	48(6)
O(2)	0.1063(4)	0.1616(9)	0.0333(5)	52(6)
N(1)	0.1435(5)	0.4097(11)	0.1181(7)	57(9)
N(2)	0.1161(5)	0.0147(11)	0.1586(7)	55(9)
C(1)	0.1869(6)	0.4742(14)	0.1689(9)	55(5)
C(2)	0.1951(6)	0.5931(15)	0.1561(9)	65(5)
C(3)	0.1595(6)	0.6495(15)	0.0908(9)	56(5)
C(4)	0.1161(6)	0.5869(15)	0.0406(9)	62(5)
C(5)	0.1094(6)	0.4697(16)	0.0540(10)	67(5)
C(6)	0.1692(7)	0.7803(16)	0.0785(10)	91(6)
C(7)	0.1515(7)	-0.0498(17)	0.2181(10)	71(5)
C(8)	0.1448(7)	-0.1702(17)	0.2287(10)	78(5)
C(9)	0.0976(6)	-0.2263(17)	0.1743(9)	69(5)
C(10)	0.0609(7)	-0.1601(17)	0.1132(10)	72(5)
C(11)	0.0720(6)	-0.0395(15)	0.1082(9)	63(5)
C(12)	0.0870(7)	-0.3559(18)	0.1840(11)	111(7)
C(13)	0.1440(5)	0.1240(12)	0.0318(7)	36(4)
C(14)	0.1393(6)	0.0816(13)	-0.0349(8)	49(4)
C(15)	0.1832(5)	0.0528(13)	-0.0282(8)	50(4)
C(16)	0.2348(5)	0.0579(13)	0.0377(8)	45(4)

C(17)	0.2401(5)	0.0939(12)	0.1030(8)	46(4)
C(18)	0.1965(5)	0.1274(13)	0.1018(8)	42(4)
C(19)	0.0842(6)	0.0753(15)	-0.1079(9)	63(5)
C(20)	-0.0512(6)	-0.0148(15)	-0.0979(9)	78(6)
C(21)	0.0579(6)	0.2003(16)	-0.1300(10)	86(6)
C(22)	0.0877(7)	0.0283(18)	-0.1712(10)	102(7)
C(23)	0.2796(6)	0.0280(14)	0.0338(9)	57(5)
C(24)	0.2803(6)	-0.1062(15)	0.0204(9)	81(6)
C(25)	0.2766(6)	0.0995(16)	-0.0278(9)	84(6)
C(26)	0.3314(6)	0.0602(17)	0.1050(9)	90(6)
N(3)	0.0 (0)	0.3868(31)	0.2500(0)	137(10)
C(27)	0.0464(16)	0.3185(39)	0.2922(23)	263(19)
C(28)	0.0008(29)	0.4726(47)	0.1979(35)	200(0)
O(3)	-0.0425(28)	0.4976(64)	0.1396(43)	200(0)

TABLE 6.8

INTERATOMIC DISTANCES (Å) AND ANGLES WITH ESD'S IN PARENTHESES FOR
 (3,5-DI-T-BUTYL-1,2-BENZOSEMIGUINONE)InBr₂·(ν-PIC)₂·¹/₂DMF

In-Br(1)	2.554(2)	Br(1)-In-Br(2)	-103.6(1)
In-Br(2)	2.561(2)	Br(1)-In-O (1)	91.3(3)
In-O (1)	2.23 (1)	Br(2)-In-O (1)	165.1(3)
In-O (2)	2.21 (1)	Br(1)-In-O (2)	165.8(3)
In-N (1)	2.30 (1)	Br(2)-In-O (2)	90.4(3)
In-N (2)	2.31 (1)	O (1)-In-O (2)	74.8(4)
O(1)-C(18)	1.27 (2)	Br(1)-In-N (1)	93.8(4)
O(2)-C(13)	1.26 (2)	Br(2)-In-N (1)	91.3(4)
N(1)-C (1)	1.36 (2)	O (1)-In-N (1)	86.7(5)
N(1)-C(5)	1.30 (2)	O (2)-In-N (1)	88.0(5)
N(2)-C(7)	1.34 (2)	Br(1)-In-N (2)	91.7(4)
N(2)-C(11)	1.34 (2)	Br(2)-In-N (2)	94.2(4)
O(1)-In-N(2)	86.2 (5)	O (2)-In-N (2)	84.9(5)
N(1)-In-N(2)	171.1(5)	In-O(1)-C(18)	113(1)
In-O(1)-C(13)	115(1)	In-N(1)-C(1)	122(1)
In-N(1)-C(5)	123(1)	C(1)-N(1)-C(5)	115(2)
In-N(2)-C(7)	124(1)	In-N(2)-C(11)	118(1)
C(7)-N(2)-C(11)	117(2)	C(2)-C(3)-C(6)	119(2)
C(4)-C(3)-C(6)	119(2)	C(8)-C(9)-C(12)	120(3)
C(10)-C(9)-C(12)	122(2)	O(2)-C(13)-C(14)	123(2)
O(2)-C(13)-C(18)	118(2)	C(15)-C(16)-C(23)	120(2)
C(7)-C(16)-C(23)	123(2)	O(1)-C(18)-C(13)	120(1)
O(1)-C(18)-C(17)	120(2)		

r-pic (C1-C5)
mean C-C 1.36 (4)

mean C-C-C 121 (3)

C(3)-C(6) 1.51(3)

r-pic (C7-C11)
mean C-C 1.39 (5)

mean C-C-C 120(4)

C(9)-C(12) 1.51(3)

Ring (C13-C18)
mean C-C 1.43(5)

mean C-C-C 120(4)

C(14)-C(19) 1.54(2)

C(16)-C(23) 1.53(3)

t-butyl group C19-C22
mean C-C 1.53(3)

mean C-C-C 110(3)

t-butyl group C23-C26
mean C-C 1.52(2)

mean C-C-C 110(2)

Esd's on mean values have been calculated from the scatter formula $\sigma = [\sum (d_i - \bar{d})^2 / N]^{1/2}$, where d_i is the i th and \bar{d} is the mean of N measurements.

FIGURE 6.9

ORTEP PLOT OF THE MOLECULE $(C_{14}H_{20}O_2)InBr_2 \cdot 2\gamma\text{-pic.} \cdot \frac{1}{2}DMF$

The atoms are drawn with 20% probability ellipsoids. Atoms with numbers only are carbon atoms.

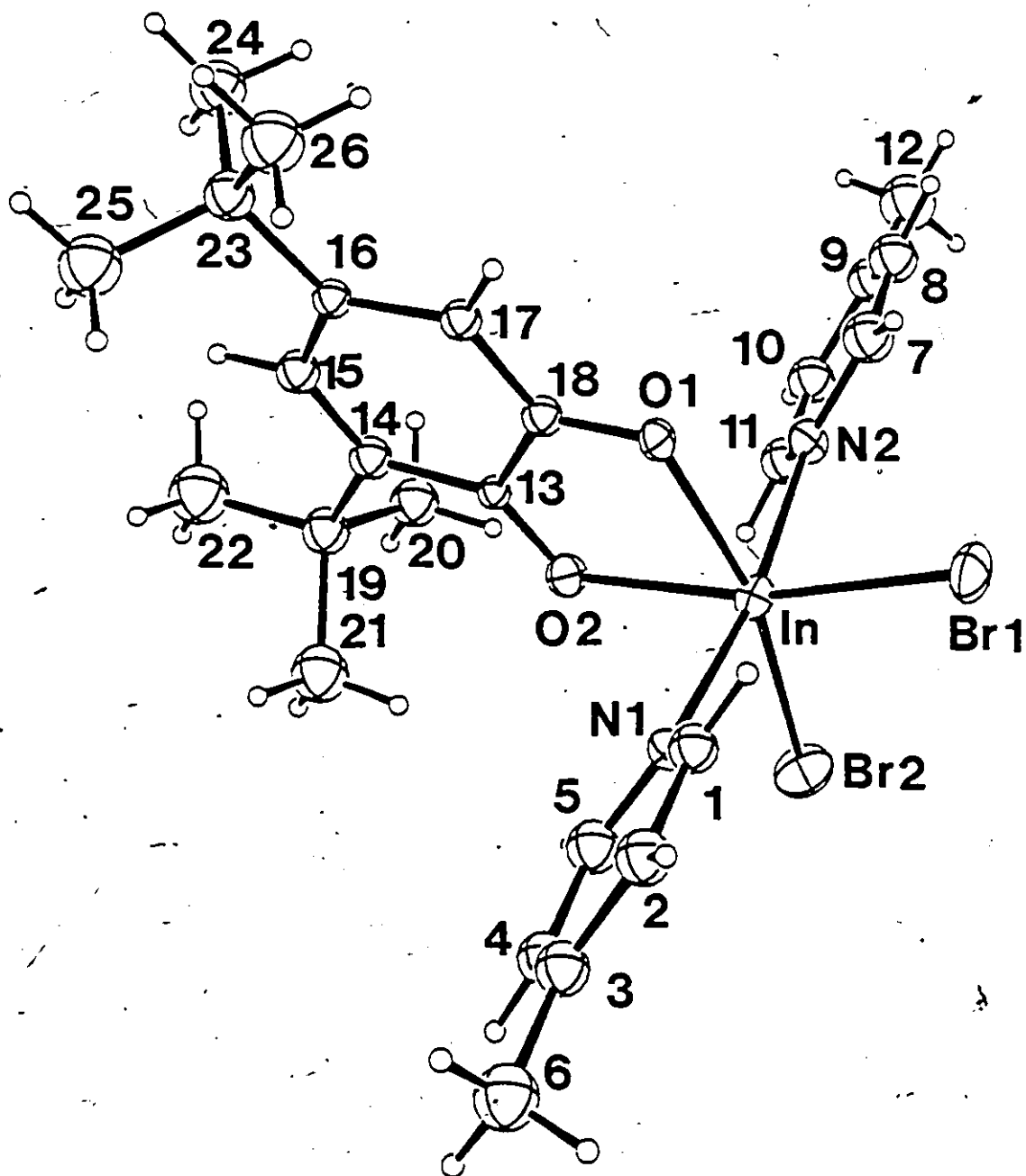


FIGURE 6.10

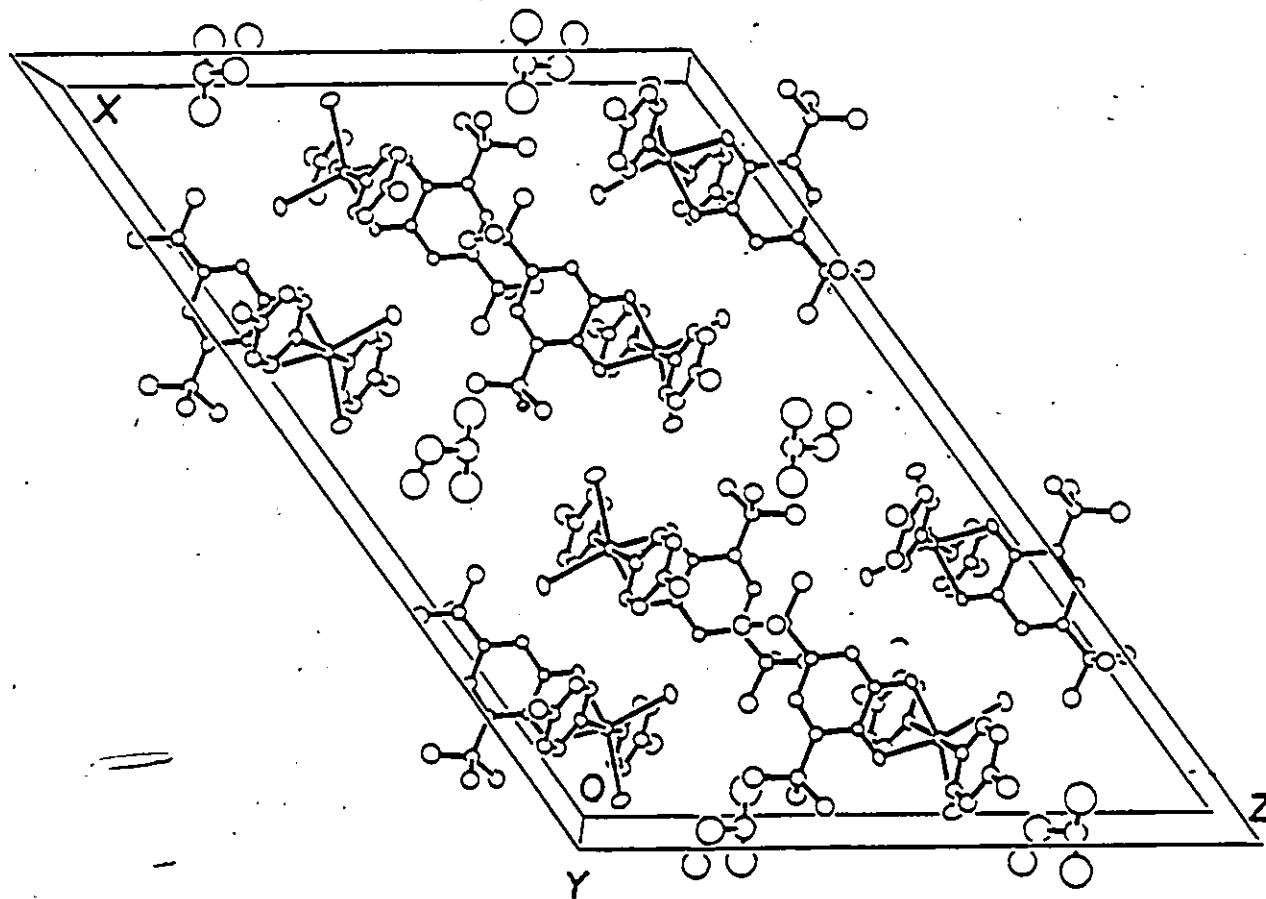
THE UNIT CELL PACKING OF $(C_{14}H_{20}O_2)InBr_2 \cdot 2\gamma\text{-pic.}^{\frac{1}{2}}/2\text{DMF}$ 

Table of structure factors and H atom coordinates are available as supplementary material.

6.4.1 Description and discussion of the structure

The structure of the compound in question contains a number of interesting features, some of which focus upon the manner of the bonding of the semiquinonate ligand. The overall structure of the compound is apparent in the drawing of the molecule (Fig. 6.9). The indium atom is essentially in an octahedral environment with the InO_2Br_2 kernel lying in the same plane and the two picoline ligands almost perpendicular to this plane. Description of the various features are discussed below.

Indium-picoline. The two picoline rings are identical within experimental error in terms of N-C bond distances, C-C bond distances, bond angles and planarity. The N-C and C-C bond distances reported in Table 6.8 are essentially identical to those for free picolines. The In-N Bond lengths of 2.30(1) and 2.31(1) Å are similar to values determined for $\text{Cl}_2\text{In}(\text{O}_2\text{CC}_6\text{H}_5)_2\text{py}$,²¹⁵ which are 2.250(5) and 2.299(4) Å.

For comparison of other features in the structure especially the In-N and In-O bond distances we shall consider the structure of $\text{Cl}_2\text{In}(\text{O}_2\text{CC}_6\text{H}_5)_2\text{py}$ and $\text{Cl}_2\text{In}(\text{acac})\text{bipy}$ ²¹⁶ considering the structure of the bromo-analogue is not known, furthermore, these are the closest in identities as far as our compound is concerned.

The In-N bond lengths of 2.30(1) and 2.31(1) Å can be compared with the values for the structures mentioned above where the In-N bond lengths trans to O are found to be 2.250(5) and 2.299(4) Å respectively and trans to chlorine 2.300(6) and 2.276(2) Å.

PAGE 190 IS OMITTED.

PAGE 190 NON INCLUS DANS LA PAGINATION.

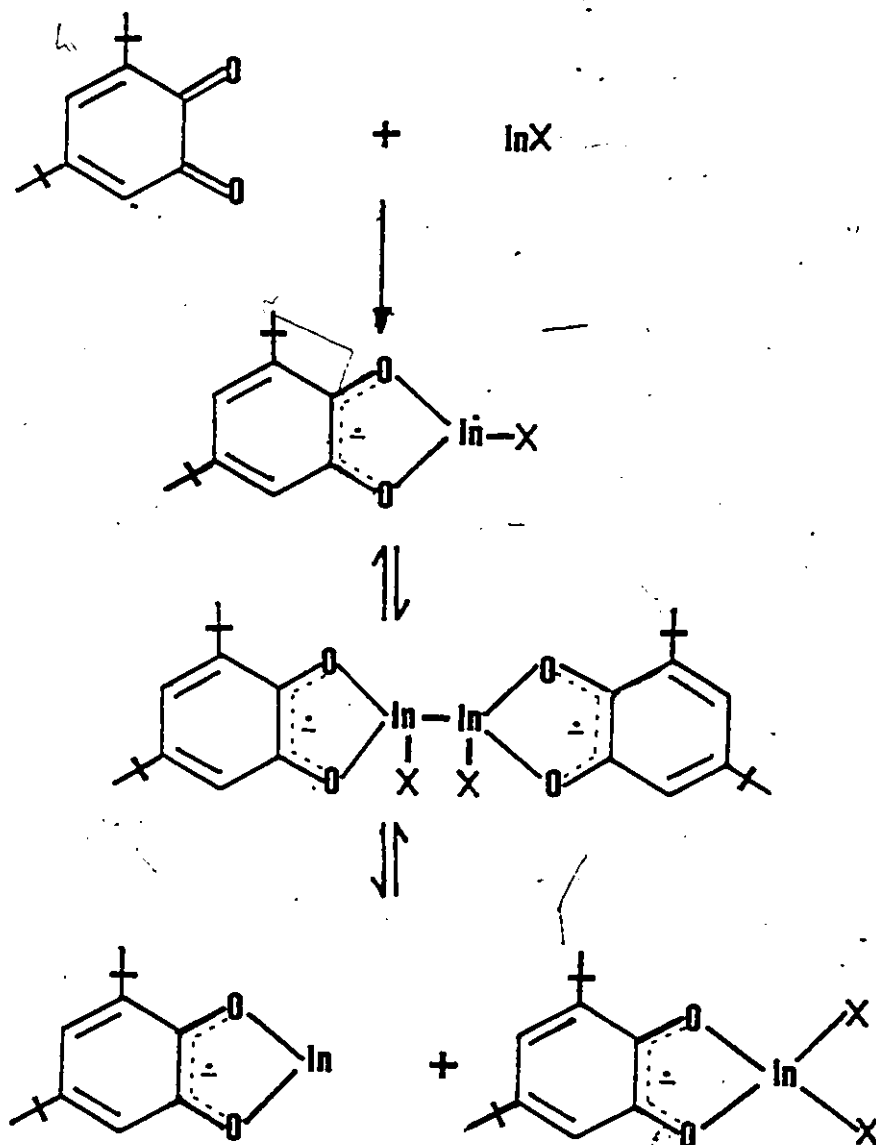
TABLE 6.9

CHELATE RING BOND LENGTHS(A) FOR SEMIQUINONE COMPLEXES CHARACTERIZED
CRYSTALLOGRAPHICALLY

COMPLEX	M-O	C-O	C-C	REFS.
Cr(TBSQ) ₃	1.933(5)	1.285(8)	1.433(9)	214
Ni(PSQ) ₂ ·2py	2.058(7)	1.272(11)	1.442(14)	221
Fe(PSQ) ₃	2.027(3)	1.283(5)	1.435(6)	222
In(TBSQ)Br ₂ ·2py	2.220(1)	1.265(2)	1.430(5)	This Work

6.4.2 Mechanism

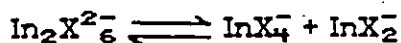
One can postulate a reaction scheme for the reactions of indium(I) halides with the orthoquinones as follows



This scheme, according to work presented in this chapter, explains observations made as far as analytical and spectroscopic results depict. The same mechanistic pathway was involved in the orthoquinone reactions with tin(II) halides.

The first step of this mechanism is the apparent formation of $(SQ')InX$, which would be a mononuclear indium(II) species. We, however, did not observe a spectrum which could be assigned to this structure which was in fact not surprising as no such molecules are known. (See Introduction.) Nor was any spectrum corresponding to the dimer recorded $[(SQ')(X)In]_2$ recorded, but as reported above the final solution obtained with Q = 3,5-di-tert-butyl-1,2-benzoquinone shows the presence of two indium containing compounds, and the ESR spectrum corresponds to the superimposition of the spectra of solvated $(SQ')In$ and $(SQ')InX_2$ prepared independently.

The disproportionation of the dimer $[(SQ')(X)In]_2$ is believed to involve halide ion transfer, with retention of the semiquinone radical ligand bonded to indium, following the mechanism proposed to explain both the process



and the interactions of In^I and In^{III} halides in solution. This equilibrium lies to the right, probably favoured by the presence of the bulky 3,5-di-tert-butyl-1,2-benzosemiquinone equally the relatively high reduction potential of this ligand inhibits conversion to the catechol form by internal electron transfer.

This chapter concludes our studies involving oxidative addition reactions of tin(II) and indium(I) halides with substituted orthoquinone. We have, established

U

a convenient route to the synthesis of stable catecholato and semiquinonato complexes. Spectroscopic and structural studies has helped in establishing a mechanism to explain the various steps involved in the formation of these complexes. We do not see this as the end of such studies, but the exploitation of these results should further the understanding of electron transfer processes involving Main Group elements.

CHAPTER 7

THE REACTIONS OF InX ($\text{X} = \text{Cl}, \text{Br}, \text{I}$) WITH SOME TRANSITION METAL COMPLEXES.

⁸⁰ THE CRYSTAL STRUCTURE OF $\text{In}^{3+}[\text{Ni}_3(\mu_3\text{-O})(\mu_3\text{-Cl})(\mu\text{-Cl})_3\text{tmen}_3]^{3-}$

7.1 Introduction

Bimetallic compounds containing transition metals directly bonded to main group metals are of current interest firstly because of hopes that novel and useful properties may be associated with these complexes, and secondly because bonds between dissimilar metals are often amenable to examination by spectrochemical techniques which cannot be applied to homonuclear derivatives. The second chapter of this thesis looked at one aspect of this subject. Again the driving force behind the present work was the use of solutions of indium monohalides in a mixture of aromatic organic solvent and a neutral donor base.

In the past reactions involving indium monohalides and transition metal compounds were carried out under vigorous conditions. The reaction, for example, between indium monobromide and $\text{Mn}_2(\text{CO})_{10}$ required that the reactants be heated in a sealed tube at 180° to obtain the desired $\text{BrIn}[\text{Mn}(\text{CO})_5]_2$.⁸⁰ Later reports showed that the products of indium monohalides with complexes like $[\pi\text{-C}_5\text{H}_5\text{Fe}(\text{CO})_2]_2$, Ph_3PAuCl , $\text{Cl}(\text{CO})\text{Rh}(\text{Ph}_3\text{P})_2$ and $(\text{R}_3\text{P})_2\text{PtCl}_2$ could be obtained by refluxing the reactants in dioxan.⁸¹

The research carried on in this chapter was undertaken primarily in the hope of establishing a more convenient synthetic route to some transition metal-indium containing compounds. Previous work from this laboratory involved studies with Co, Fe, and Mn compounds.¹⁰⁹ Since one of the principal goals of this research was to investigate the synthetic-usefulness of tmen/toluene solution of indium monohalides, the compounds metals used in this work were chosen

to be consistent with these objectives. The preliminary results obtained are interesting, and show the need for further work. In one case an attempt to recrystallize the product led to a rearranged product whose crystal structure was determined by X-ray diffraction methods.

7.2 Experimental

7.2.1 The Reaction of InX (X = Cl, Br, I) With Some Transition Metal Complexes

The standard procedure used in all these experiments involved stirring a suspension of equimolar amounts of InX (ca. 3 mmol) and the transition metal complex with a four-fold excess of tmen (2 mL, 13.2 mmol) in 50 mL of toluene. The temperature of the reaction was held steady at ca. -40°C for 2 h. Slowly the cold bath was removed, and stirring continued. As the solution warmed up, a precipitate formed and was collected by filtration, washed twice with 10 mL portions of benzene and dried *in vacuo*. The products obtained are listed in Table 7.1 and analytical data in Table 7.2.

7.3. Results and Discussion

7.3.1 Preparative

In the present work, using very mild synthetic conditions for the reasons discussed in Chapter 2, the general reaction of InX with transition metal halides is represented in eqn. 7.1.



The principal reaction products were formulated as 1:1 adducts, and others as rearrangement products based on the analytical and spectroscopic data discussed below.

TABLE 7.1

THE SYNTHESIS OF TRANSITION METAL-INDIUM COMPLEXES

Reactants(a)	Principal Product
(i) $(\text{Ph}_3\text{P})_2\text{NiCl}_2 + \text{InCl}$	$\text{ClNiInCl}_2 \cdot \text{tmen}$
(ii) $(\text{Ph}_3\text{P})_2\text{MCl}_2 + \text{InX}$ M = Pd, Pt	$(\text{Ph}_3\text{P})_2\text{MClIn(X)Cl}$
(iii) $(\text{CO})(\text{Ph}_3\text{P})_2\text{M}_2\text{Cl}_2 + \text{InX}$ M = Rh, Ir X = Cl, Br, I	$(\text{CO})(\text{Ph}_3\text{P})_2\text{M}_2\text{In(X)Cl}$
(iv) $\text{PhHgCl} + \text{InCl}$	$\text{ClHgInCl}_2 \cdot \text{tmen}$
(v) $\text{PhHgOAc} + \text{InCl}$	$\text{ClHgIn(HgOAc)}_2 \cdot \text{tmen}$

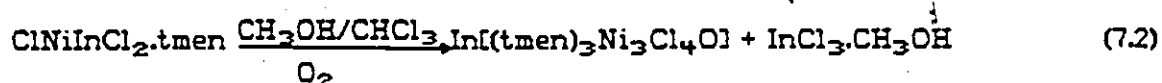
TABLE 7.2
ANALYTICAL DATA

Compound	Reaction ^(a) In	C	H	N	X=Cl, Br, I	
ClNiInCl ₂ .tmen	i	29.4(30.0)	19.8(18.2)	4.08(4.04)	6.79(7.07)	27.2(26.9)
(Ph ₃ P) ₂ PdCl(InCl ₂)	ii	13.6(13.5)	-	-	-	12.6(12.5)
(Ph ₃ P) ₂ PdClIn(Br)Cl	ii	12.7(12.8)	-	-	-	-
(Ph ₃ P) ₂ PdClIn(I)Cl	ii	12.1(12.2)	-	-	-	-
(Ph ₃ P) ₂ PtClInCl ₂	ii	12.3(12.2)	45.2(46.0)	3.56(3.22)	-	11.4(11.3)
(Ph ₃ P) ₂ PtClIn(Br)Cl	ii	11.7(11.7)	-	-	-	-
(Ph ₃ P) ₂ PtClIn(I)Cl	ii	11.3(11.1)	-	-	-	-
(CO)(Ph ₃ P) ₂ RhInCl ₂	iii	13.7(13.7)	53.9(52.9)	4.07(3.60)	-	12.7(12.7)
(CO)(Ph ₃ P) ₂ RhInBrCl	iii	13.1(13.0)	-	-	-	-
(CO)(Ph ₃ P) ₂ IrInCl ₂	iii	12.5(12.5)	-	-	-	11.5(11.5)
(CO)(Ph ₃ P) ₂ IrInBrCl	iii	11.7(11.8)	-	-	-	-
(CO)(Ph ₃ P) ₂ IrInICl	iii	11.2(11.2)	-	-	-	-
ClHgInCl ₂ .tmen	iv	21.2(21.3)	12.7(13.4)	2.74(2.99)	4.92(5.21)	19.8(19.8)
ClHgIn(HgOAc) ₂ .tmen	v	11.5(11.6)	11.6(12.2)	2.15(2.25)	2.56(2.84)	3.54(3.60)

(a) Reaction as described in Table 7.1.

The principal reaction products were formulated as 1:1 adducts, and others as rearrangement products based on the analytical and spectroscopic data discussed below.

(i) $(\text{Ph}_3\text{P})_2\text{NiCl}_2/\text{InCl}/\text{tmen}$. $(\text{Ph}_3\text{P})_2\text{NiCl}_2$ which was prepared by literature method²²³ reacted smoothly at low temperature (-40°C) with InCl forming a clear green solution. As the solution warmed up, a green precipitate formed and this analyzed as $\text{ClNiInCl}_2\cdot\text{tmen}$. Recrystallization of this compound in a 1:1 (v/v) mixture of $\text{CH}_3\text{OH}/\text{CHCl}_3$ resulted in light green solid. A single crystal X-ray study (see below) revealed that this substance had formed as the result of rearrangement of the primary product, possibly by this scheme.

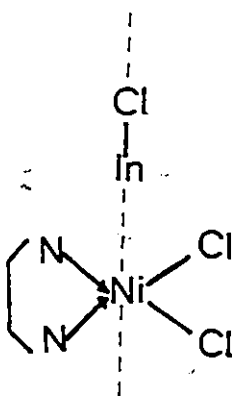


Atmospheric oxygen could have been an active participant, since recrystallization was carried out in an open flask.

The filtrate obtained after collecting the precipitate was evaporated to dryness to leave colourless crystals which were identified as Ph_3P by ^1H NMR (multiplets in the aromatic region in CD_3CN solution) and by i.r. (characteristic bands in the 3000 cm^{-1} region of $\nu(\text{C-H})$ (aromatics)) and two strong bands at 740 and 690 cm^{-1} (C-H out of plane vibration) confirming the presence of a monosubstituted aromatic ring and melting point of 82°C (literature value = 79°C).²²⁴

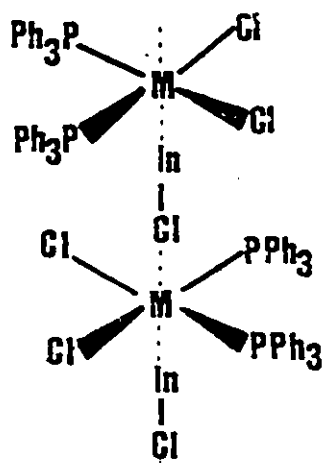
In the ir spectrum of $(\text{Ph}_3\text{P})_2\text{NiCl}_2$ bands occurring at 335 and 300 cm^{-1} were assigned to $\nu(\text{Ni-Cl})$ and a band 184 cm^{-1} to $\nu(\text{Ni-P})$ in good agreement with reported values.²²⁵ The precipitate obtained in the reaction of the nickel complex with InCl as noted above analyzed as $\text{ClNiInCl}_2\cdot\text{tmen}$. The far ir of the

precipitate revealed no bands assignable to a coordinated Ph_3P ligand. We instead, observed a strong C-H (alkyl) vibration at ca. 2900 cm^{-1} and another strong band at ca. 1430 cm^{-1} ($\nu(\text{C-N})$ of tmen) confirming the presence of a coordinated tmen. The broadness of a band centred at 280 cm^{-1} does not permit any definite assignment to $\nu(\text{M-Cl})$ ($\text{M} = \text{In, Ni}$). It is clear, though, that the original tetrahedral geometry around the nickel atom in the starting material has been lost since we did not observe the characteristic vibrations of a tetrahedral complex in the product. We as a result propose the following structure:



(ii) $(\text{Ph}_3\text{P})_2\text{MCl}_2/\text{InX}/\text{tmen}$ ($\text{M} = \text{Pd, Pt}$): This reaction appears to have followed a different route from that with NiCl_2 . The analytical data suggested a 1:1 adduct formation as $(\text{Ph}_3\text{P})_2\text{MCl}_2 \cdot \text{InCl}$, but ir spectroscopic data did not support the formulation of a M-In bonded complex. Unlike the nickel complex, these compounds were only slightly soluble in common organic solvents. The presence of the Ph_3P ligand was evident from the ^1H NMR spectrum of $\text{CDCl}_3/\text{CD}_3\text{OD}$ (1:1 v/v) solution since multiplets in the aromatic region were observed. The lack of resonance signals in the alkyl region of the spectrum confirmed the absence of the tmen ligand. The ir spectrum in the mid-region agreed with the ^1H NMR spectrum. The far ir spectra did not show any significant

changes to the $\nu(\text{M-Cl})$ of the precursors. Furthermore, no $\nu(\text{In-X})$ bands were observed. On this basis, we propose the structure



Such chain-like structures have been observed in some platinum and palladium complexes, examples of which are PtInCl_2 and Pd dimethylglyoximate. Salts such as $[\text{Pt}(\text{NH}_3)_4][\text{PtCl}_4]$, $[\text{Pd}(\text{NH}_3)_4][\text{Pd}(\text{SCN})_4]$ or $[\text{Cu}(\text{NH}_3)_4][\text{PtCl}_4]$ also have stacked cations and anions with stacks of metal atoms linked by halides.²¹⁶

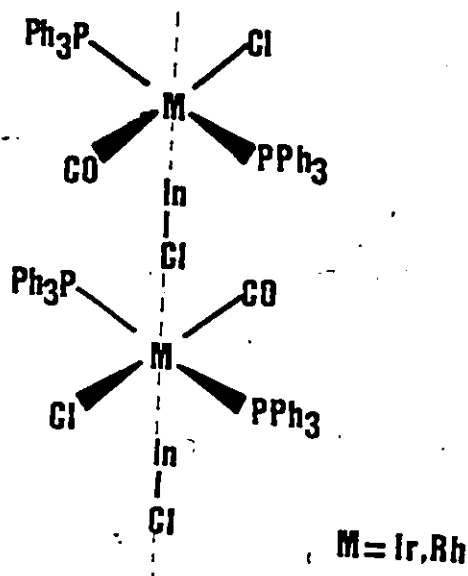
Unlike the nickel system, where tmen replaced Rh_3P on the nickel, no such ligand exchange occurred in the Pt or Pd systems. The preference for one ligand to the other on these metals can be argued on the basis of soft and hard acids. According to this "soft" and "hard" concept developed by Pearson,²²⁷ Pt^{2+} and Pd^{2+} can be classified as type b or "soft" metals, while Ni^{2+} , appears on the borderline between type b and type a metals.²²⁸ It has further been established that the relative co-ordinative affinity for type b metals forming complexes under comparable conditions with Group V atoms is $\text{N} \ll \text{P} > \text{As} > \text{Sb}$.²²⁸

(ii) Cl(CO)M(Ph₃P)₂/InX/tmen (M = Rh,Ir). Results obtained in this section were similar to those for the Pt or Pd systems. In this particular case, diagnostic use was made of the sharp $\nu(\text{C}\equiv\text{O})$ mode at ca. 1930 cm^{-1} in the starting material, changing to a broad band centred at 1950 cm^{-1} in the product. A discussion of the causes of its broadening is beyond the scope of this dissertation, but Kettle²²⁹ has discussed a similar effect on some carbonyl complexes, where he suggests that such broadening could be caused by long range dipole-dipole coupling. Such coupling appears likely in our complex (see proposed structure below). There is a report, though in the literature of the formation of $\text{CO}(\text{Ph}_3\text{P})_2\text{RhInCl}_2$ by the reaction of InCl with $\text{CO}(\text{Ph}_3\text{P})_2\text{RhCl}$ in dioxane⁸¹ but unfortunately no spectroscopic data are available to make comparisons with the present work. Camia *et al.*²³⁰ maintain on the basis of infrared spectroscopic evidence, that the product of the reaction between the isoelectronic SnCl_2 and $\text{Cl}(\text{CO})\text{Ir}(\text{Ph}_3\text{P})_2$ is a 5-coordinate complex with SnCl_2 coordinated to iridium rather than the expected compound $(\text{Ph}_3\text{P})_2(\text{CO})\text{IrSnCl}_3$. A successful iridium-tin bonded compound with the formula $(\text{COD})_2\text{IrSnCl}_3$ has been made²³¹ by the reaction of tin(II) chloride with a solution of sodium chloroiridate(III) in the presence of cyclo-octa-1,5-diene in glacial acetic acid



The crystal structure of this compound confirmed the iridium-tin bond.²³¹

The product of our reaction could be polymeric on the basis of its slight solubility and high melting point ($> 300^\circ\text{C}$). The following structure is therefore proposed:



RHgX/InCl/tmen ($X = Cl, OAc$). Reactions involving metal halides and organomercurials have been of interest because of their applications in the synthesis of organometallic compounds. Of particular interest and relevance to our work is the reaction of organomercuric halides with InX .²³² The reaction, presumably, takes place by the insertion of In^I into the Hg-X bond followed by the extrusion of mercury as in eqn. 7.4



The importance of donor solvents and light in such reactions has been established. To date there has been no report of compounds containing Hg-M bond ($M =$ Main Group III metal), although there a number of compounds reported with $M = Si$,²³³ Ge ,^{234,235} and Sn .²³⁶ The first Hg-Sn bonded compound was bis(triphenylstannyl)mercury, a bright yellow solid prepared by the reaction of triphenylstannane with di[bis(trimethylsilyl)amido]mercury in 2:1 mol ratio at room temperature.²³⁶

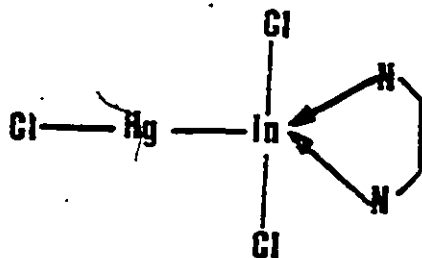


The product is much less stable than the silicon or germanium analogues. The crystal structure of the silicon analogue has been determined by Oliver and

his group thereby confirming the existence of the Si-Hg bond.²³³

The reaction between PhHgCl and InCl under the mild conditions of our reaction led to the isolation of Ph_2Hg from the filtrate and a greyish white precipitate which analyzed as a rearranged product, $\text{ClHgInCl}_2 \cdot \text{tmen}$. The Ph_2Hg was identified from melting point, ^1H NMR, ir and mass spectral data. The ^1H NMR in CD_3CN showed multiplets in the aromatic region of the spectrum, and was supported by the ir spectrum which had characteristic vibrational bands assignable to the in-plane and out-of-plane vibration of aromatic C-H. In addition a strong absorption band at 540 cm^{-1} was assigned to $\nu(\text{C-Hg})$. The mass spectrum in the field desorption mode had a cluster of peaks with the highest intensity peak at $m/e = 356$ (Ph_2Hg^+); a second cluster with the highest intensity peak at $m/e = 217$ was not identified. The compound melted sharply at 123°C (literature value for $\text{Ph}_2\text{Hg} = 125^\circ\text{C}$).²²⁴

The ir spectrum of the precipitate in the mid-region confirmed the presence of a coordinated tmen ligand with a C-H (alkyl) vibration at ca. 2900 cm^{-1} and strong C-N vibration at ca. 1420 cm^{-1} . Characteristic In-N vibrations were identified in the far region of the spectrum in the region between $380\text{--}500 \text{ cm}^{-1}$ (see Chapter 2). A broad band centred at 280 cm^{-1} was assigned to $\nu(\text{In-Cl})$. A band at 132 cm^{-1} was assigned as $\nu(\text{Hg-Cl})$. On this basis we propose the following structure for our compound.



The reaction with PhHgOAc also lead to the formation of Ph₂Hg which was identified as described above. The second product which precipitated out of the reaction analyzed as Hg₃(OAc)₂ InCl.tmen. The presence of the coordinated tmen ligand was identified by the presence of three bands in the 380-500 cm⁻¹ region of the ir spectrum. Based on work in Chapter 2 these bands were assigned to ν(In-N). The absence of a band at ca. 300 cm⁻¹ excluded the presence of ν(In-Cl). A band appearing at ca. 130 cm⁻¹ was tentatively assigned to ν(Hg-Cl). The presence of a coordinated acetato ligand was confirmed by strong stretching modes at 1460 and 1568 cm⁻¹. We were, however, in no position to determine to which metal the ligand was coordinated.

From the evidence available thus far, it is difficult to assign a structure for this product, and the amorphous nature as well as the low solubility of this product in common organic solvents hindered any attempt to grow single crystals to allow the determination of its structure by X-ray diffraction studies.

7.4 The crystal and molecular structure of In³⁺[Ni₃(μ₂-O)(μ₂-Cl)(μ-Cl)₃tmen₃]³⁻CHCl₃

Details of the procedure for data collection, processing and refinement of the structure are given in Chapter 1. Table 7.3 gives a summary of crystal data, intensity collection and structural refinement. The position of In was determined by a sharpened Patterson synthesis and subsequent difference maps revealed the remaining atoms. The structure was refined by full matrix least squares methods, with all non-hydrogen atoms being treated anisotropically. The refinement converged at R = 0.0640 and R_w = 0.0692, at which stage some peaks appeared in the difference map at plausible hydrogen atom locations. All hydrogen atoms were subsequently included in idealized positions with C-H = 0.95Å. Isotropic

TABLE 7.3

SUMMARY OF CRYSTAL DATA, INTENSITY COLLECTION, AND STRUCTURAL
REFINEMENT FOR $\text{In}^{2+}[\text{Ni}_3(\mu_3\text{-O})(\mu_3\text{-Cl})(\mu\text{-Cl})_3\text{men}_3]^{3-} \cdot \text{CHCl}_3$

cell constants	11.206(2), 11.839(4), 15.770(5) Å, 116.71(2), 95.39(2), 95.27(2)°
cell volume (Å ³)	1839.4(8)
crystal system	triclinic
space group	$\bar{P}1$
mol. wt.	910.4
Z, F(000)	2, 918
ρ_c , ρ_o (g cm ⁻³)	1.64, 1.60
abs coeff, μ (cm ⁻¹)	25.28
min abs corr	1.052
max abs corr	1.087
radiation	MoK α , $\lambda=0.71069$ Å
monochromator	highly oriented graphite
temp (°C)	20
2 θ angle (°)	4-45
scan type	coupled θ (crystal)/2 θ (counter)
scan width	$K_{\alpha_1} -1^\circ$ to $K_{\alpha_2} +1^\circ$
bkgd time/scan time	0.5
total reflcns measd	3256 ($\pm h, \pm k, \pm l$)
unique data used	2519 ($I > 3\sigma(I)$)
no. of parameters (NP)	239
$R = \frac{\sum F_o - F_c }{\sum F_o}$	0.0580

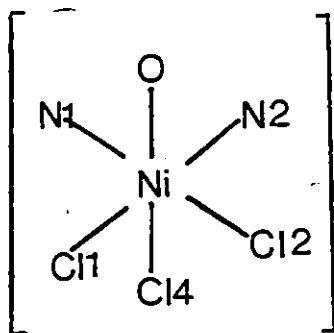
$R_v = \frac{\sum \omega (F_o - F_c)^2 / \sum \omega F_o ^2}{}^{1/2}$	0.0667
$\Delta \rho_{\max} (e \text{ \AA}^{-3})$	1.1
shift: error (max)	0.05

thermal parameters for all hydrogen atoms were assigned values $0.014 (\text{\AA}^2)$ greater than those for the appropriate (bonded) carbon atoms. After six more cycles of refinement, convergence was achieved with the final $R = 0.0580$ and the final $R_w = 0.0667$ for 2519 unique "observed" [$I > 3 \sigma(I)$] reflections.

Positional and thermal parameters are given in Table 7.4, and interatomic distances and angles are listed in Table 7.5. Tables of structure factors, anisotropic thermal parameters and hydrogen atom coordinates are available as supplementary data.

Figure 7.1 shows the molecule with the atomic numbering scheme, and Fig. 7.2 gives the cell packing; hydrogen atoms are excluded from Fig. 7.2 for the sake of clarity.

In order to assign charges to the indium and nickel atoms the following argument was used. A cross-section of one third of the anion is presented as follows:



Oxygen(B) being a triply bridging atom will then carry a charge of $-2/3$, the triply bridging chlorine atom (Cl_4) will have a charge of $-1/3$ and the two bridging chlorine atoms Cl_1 , Cl_2 then will have charges of $-1/2$ each. The total charge of these electronegative atoms is then

TABLE 7.4

FINAL FRACTIONAL COORDINATES AND ISOTROPIC THERMAL PARAMETERS FOR
 NON-HYDROGEN ATOMS OF $\text{InNi}_3(\mu_3\text{-O})(\mu_3\text{-Cl})(\mu\text{-Cl})_3\text{tmed}_3\cdot\text{CHCl}_3$ WITH
 STANDARD DEVIATIONS IN PARENTHESES

	x	y	z	$U_{\text{eq}}^a / \text{\AA}^2 \cdot 10^3$
In	0.4311(1)	0.3300(1)	0.2213(1)	62.8(7)
Ni(1)	0.2437(1)	0.7547(1)	0.4367(1)	39(1)
Ni(2)	0.0403(1)	0.5526(1)	0.2941(1)	38(1)
Ni(3)	0.2072(1)	0.7047(1)	0.2290(1)	42(1)
Cl(1)	0.0896(3)	0.6220(3)	0.4651(2)	48(2)
Cl(2)	0.3591(3)	0.8607(3)	0.3618(2)	54(2)
Cl(3)	0.0343(3)	0.5368(3)	0.1344(2)	61(2)
Cl(4)	0.0629(3)	0.7918(3)	0.3481(3)	74(3)
Cl(5)	0.3991(6)	-0.0475(5)	-0.1074(4)	144(4)
Cl(6)	0.1841(6)	0.0238(5)	-0.0272(4)	134(4)
Cl(7)	0.2974(6)	0.1729(5)	-0.1027(4)	140(4)
O	0.2241(6)	0.5985(6)	0.3021(4)	38(4)
N(1)	0.2435(10)	0.9225(8)	0.5708(7)	57(6)
N(2)	0.3956(8)	0.7214(8)	0.5089(6)	42(6)
N(11)	-0.1545(9)	0.5272(9)	0.2876(7)	57(7)
N(12)	0.0247(8)	0.3547(8)	0.2545(6)	49(6)
N(21)	0.3314(9)	0.6349(9)	0.1280(7)	52(7)
N(22)	0.1716(10)	0.8233(9)	0.1633(7)	61(7)

C	0.3240(15)	0.0816(14)	-0.0421(11)	89(5)
C(1)	0.2752(15)	1.0433(14)	0.5678(11)	89(5)
C(2)	0.1309(13)	0.9256(13)	0.6098(10)	75(4)
C(3)	0.3336(20)	0.9005(20)	0.6337(15)	133(7)
C(4)	0.4237(19)	0.8319(18)	0.6033(14)	127(7)
C(5)	0.5054(16)	0.7137(15)	0.4655(12)	97(5)
C(6)	0.3770(13)	0.6028(12)	0.5175(9)	70(4)
C(11)	-0.1936(14)	0.5833(13)	0.3804(10)	80(4)
C(12)	-0.2151(14)	0.5765(13)	0.2285(10)	82(4)
C(13)	-0.1869(17)	0.3835(15)	0.2330(12)	102(5)
C(14)	-0.1045(14)	0.3196(15)	0.2610(11)	89(5)
C(15)	0.1008(14)	0.3216(13)	0.3184(9)	75(4)
C(16)	0.0509(12)	0.2748(12)	0.1570(8)	65(4)
C(21)	0.2951(14)	0.4997(13)	0.0571(10)	76(4)
C(22)	0.4562(13)	0.6420(13)	0.1712(10)	73(4)
C(23)	0.3309(16)	0.7190(15)	0.0829(11)	94(5)
C(24)	0.2262(17)	0.7664(17)	0.0726(12)	112(6)
C(25)	0.2185(19)	0.9590(18)	0.2230(15)	135(7)
C(26)	0.0463(18)	0.8145(16)	0.1297(13)	109(6)

^a U_{eq} for atoms other than carbon is calculated from the refined anisotropic thermal parameters ($U_{eq} = \frac{1}{3} \sum_i \sum_j U_{ij} a_i^* a_j^* a_i \cdot a_j$). Carbon atoms are refined isotropically.

TABLE 7.5

SOME IMPORTANT INTERATOMIC DISTANCES (Å) AND ANGLES (°) FOR
 $\text{In}^{3+}[\text{Ni}_3(\mu_3\text{-O})(\mu_3\text{-Cl})(\mu\text{-Cl})_3\text{tmen}_3]^{3-} \cdot \text{CHCl}_3$ WITH STANDARD DEVIATION IN
 PARENTHESES

Ni(1)-Cl(4)	2.435(3)	Cl(1)-Ni(1)-Cl(2)	162.8(1)
Ni(1)-Cl(2)	2.442(3)	Cl(1)-Ni(1)-Cl(4)	83.1(1)
Ni(1)-Cl(4)	2.536(4)	Cl(2)-Ni(1)-Cl(4)	83.3(1)
Ni(1)-O	2.070(6)	Cl(1)-Ni(1)-O	83.8(2)
Ni(1)-N(1)	2.155(8)	Cl(2)-Ni(1)-O	83.2(2)
Ni(1)-N(2)	2.124(8)	Cl(4)-Ni(1)-O	78.0(2)
Ni(2)-Cl(1)	2.428(3)	Cl(1)-Ni(1)-N(1)	94.6(2)
Ni(2)-Cl(3)	2.435(3)	Cl(2)-Ni(1)-N(1)	97.0(2)
Ni(2)-Cl(4)	2.543(3)	Cl(4)-Ni(1)-N(1)	95.0(2)
Ni(2)-O	2.058(7)	O-Ni(1)-N(1)	173.0(3)
Ni(2)-N(11)	2.162(9)	Cl(1)-Ni(1)-N(2)	97.0(2)
Ni(2)-N(12)	2.121(8)	Cl(2)-Ni(1)-N(2)	96.5(2)
Ni(3)-Cl(2)	2.444(3)	Cl(4)-Ni(1)-N(2)	179.1(2)
Ni(3)-Cl(3)	2.452(3)	O-Ni(1)-N(2)	101.1(3)
Ni(3)-Cl(4)	2.518(3)	N(1)-Ni(1)-N(2)	85.8(3)
Ni(3)-O	2.062(6)	Cl(1)-Ni(2)-Cl(3)	163.4(1)
Ni(3)-N(21)	2.146(8)	Cl(1)-Ni(2)-Cl(4)	83.1(1)
Ni(3)-N(22)	2.146(8)	Cl(1)-Ni(2)-Cl(4)	83.1(1)
Ni(3)-N(22)	2.130(9)	Cl(3)-Ni(2)-Cl(4)	83.7(1)
Cl(5)-C	1.76(1)	Cl(1)-Ni(2)-O	84.2(2)
Cl(6)-C	1.73(2)	Cl(3)-Ni(2)-O	83.2(2)

C(7)-C	1.76(2)	Cl(4)-Ni(2)-O	78.1(2)
Cl(5)-C-Cl(6)	109.4(8)	Cl(1)-Ni(2)-N(11)	96.5(3)
Cl(5)-C-Cl(7)	111.9(8)	Cl(4)-Ni(2)-N(11)	95.2(3)
Cl(6)-C-Cl(7)	107.2(9)	O-Ni(2)-N(11)	173.1(3)
		Cl(1)-Ni(2)-N(12)	94.7(2)
		Cl(3)-Ni(2)-N(12)	177.8(3)
		O-Ni(2)-N(12)	101.3(3)
<u>mean ligands^a</u>		N(11)-Ni(2)-N(12)	85.6(3)
mean N-C	1.49(4)	Cl(2)-Ni(3)-Cl(3)	162.8(1)
mean C-C	1.37(3)	Cl(2)-Ni(3)-Cl(4)	83.6(1)
mean Ni-N-C	111(6)	Cl(3)-Ni(3)-Cl(4)	83.9(1)
mean C-N-C	108(4)	Cl(2)-Ni(3)-O	83.3(2)
mean N-C-C	116(5)	Cl(3)-Ni(3)-O	82.7(2)
		Cl(4)-Ni(3)-O	82.7(2)
		Cl(2)-Ni(3)-N(21)	95.7(3)
In...Cl(5) ^b	3.800	Cl(3)-Ni(3)-N(21)	97.0(3)
In...O	3.922	Cl(4)-Ni(3)-N(21)	178.7(2)
		O-Ni(3)-Ni(21)	102.4(3)
		Cl(2)-Ni(3)-N(22)	96.9(3)
		Cl(3)-Ni(3)-N(22)	95.8(3)
		Cl(4)-Ni(3)-N(22)	94.3(3)
		O-Ni(3)-N(22)	172.9(3)
		N(21)-Ni(3)-N(22)	84.7(3)
		Ni(1)-Cl(1)-Ni(2)	77.0(1)
		Ni(1)-Cl(2)-Ni(3)	76.8(1)
		Ni(2)-Cl(3)-Ni(3)	76.7(1)

Ni(1)-Cl(4)-Ni(2)	73.2(1)
Ni(4)-Cl(4)-Ni(3)	73.8(1)
Ni(2)-Cl(4)-Ni(3)	73.6(1)
Ni(1)-O-Ni(2)	94.4(3)
Ni(1)-O-Ni(3)	94.5(3)
Ni(2)-O-Ni(3)	94.8(3)

a Esd's on mean values have been calculated with the use of the Scatter formula $\sigma = [\sum(d_i - \bar{d})^2 / (N-1)]^{1/2}$, where d_i is the i th and \bar{d} is the mean of N equal measurements.

b Symmetry equivalent position is $1-x, -y, -z$.

FIGURE 7.1

ORTEP PLOT OF THE MOLECULE



The atoms are drawn with 20% probability ellipsoids. Atoms with numbers only are the carbon atoms.

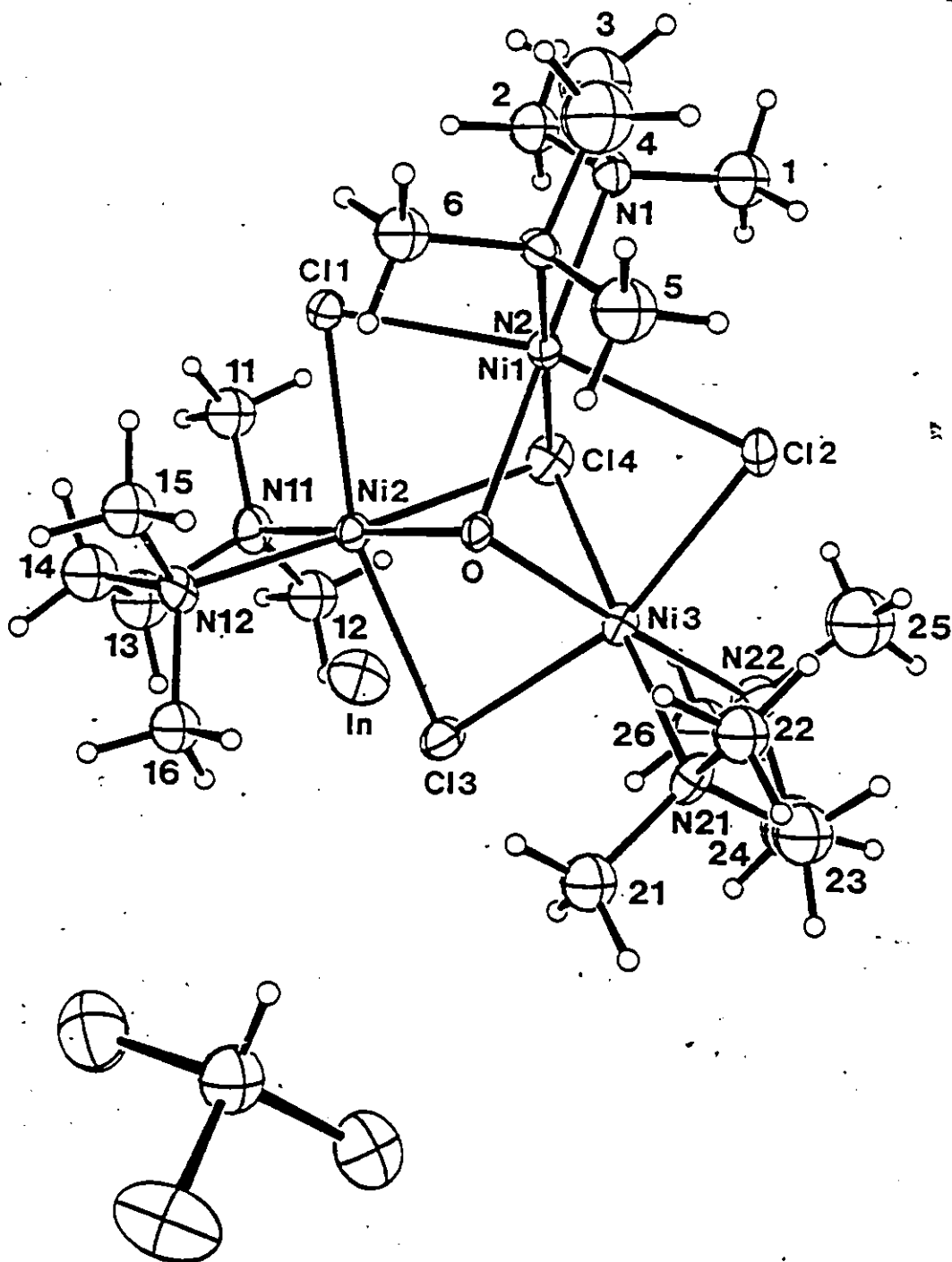
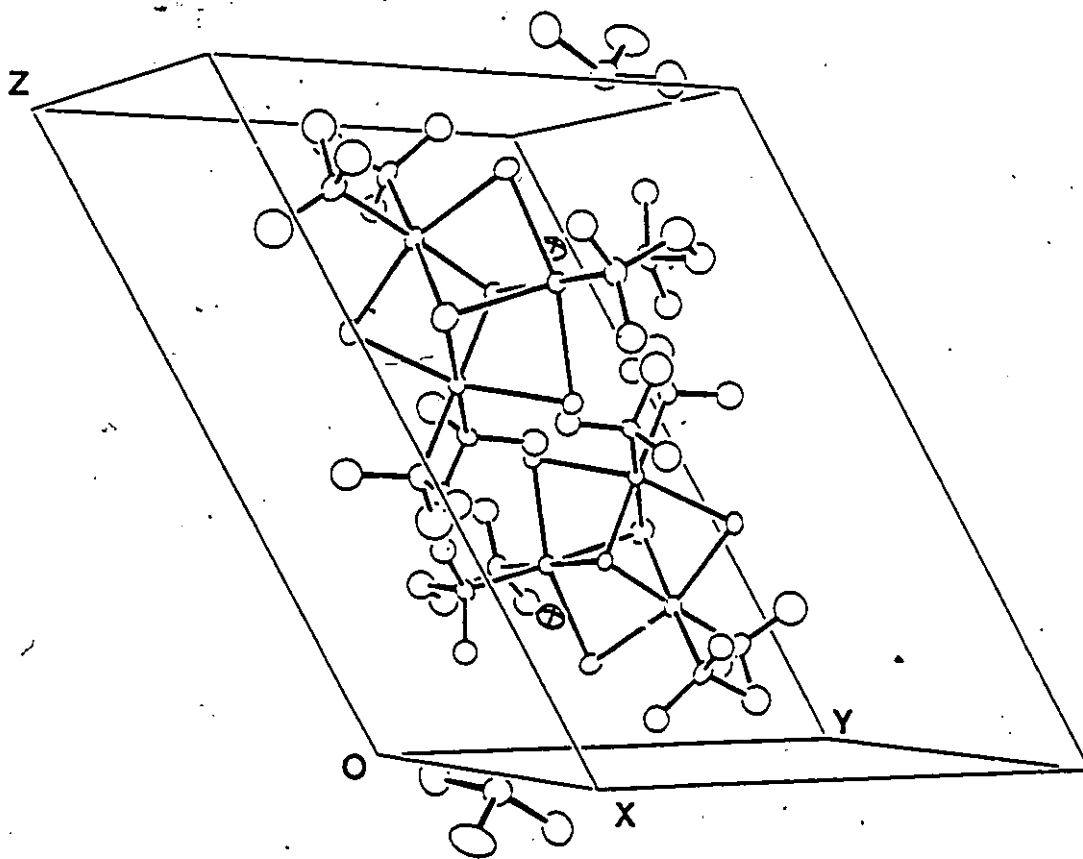


FIGURE 7.2

UNIT CELL CONTENTS OF THE MOLECULE



Hydrogen atoms are omitted for clarity. In cations are shown as ellipsoids with axes.



$$-2/3 - 1/3 - 1/2 - 1/2 = -2$$

Assigning a charge of +1 to the nickel atom then leaves one third of the anion a charge of -1. Consequently, the whole anion will then carry a charge of -3 making the indium atom a +3 ion, which will be an acceptable charge for the indium atom under our experimental condition. Alternatively, if one were to assume a charge of +1 to the indium, then the nickel atom will then, on the basis of the present argument, carry a charge of $5/3$ which is highly unlikely. If this argument is correct, then this structure is the first nickel(I) complex in an octahedral environment. Because of the uniqueness of this structure, it is impossible to make any comparisons involving bond lengths and bond angles. Compounds with bridging and capping electronegative atoms are known in the chemistry of Mo and W. For example, the crystal structure of $W_3O_3Cl_5(O_2CCH_3)(Pn_3)_3$,²³⁷ revealed the presence of a triply bridging chlorine atom to the tungsten atoms, and another example from this group is found in the $[Mo_3OCl_3(O_2CCH_3)_3(H_2O)_3]^{2+}$ ion which includes a triply bridging oxygen to the metal.²³⁸

In the present structure, the three nickel atoms of the anion form an equilateral triangle with average Ni ... Ni distance of 3.032(4) Å which is clearly a non-bonding distance since values in the range of 2.5 Å¹⁷ have been determined for Ni-Ni bonds.²³⁹ The Ni ... N ... Ni angle is 60.0(1)°, in good agreement with equilateral triangle formulation for the three nickel atoms. The Ni atoms are bridged by three Cl atoms with an average Ni-Cl distance of 2.439(6) Å and Ni-Cl-Ni angle of 76.8(2)°. A Ni-Cl bridging distance for the complex $[(NiCO)_4(C_3Cl_4)_2]_2$ has been found to be 2.238 Å.²³⁹ Both values are longer than the terminal Ni-Cl bond distance of 2.269 Å in the Ni(II) complex $(Me_3SiCH_2)(PMe)_2NiCl$. These comparisons should be treated semi-quantitatively since identical molecules are

not known. The triply bridging chlorine atom Cl(4) has an average distance of 2.532(10)Å which as expected is longer than the doubly bridging Ni-Cl distance. From the other side of the bridging Cl(4) is an oxygen atom which caps the Ni₃ triangle with an average Ni-O distance of 2.063(8)Å and O-Ni-O of 94.6(2)°. A Ni-O bond distance of 1.94Å has been determined for the cationic complex [Ni^{II}SO₂Me(PPh₂C₂H₄)₂PPh]⁺BPh₄⁻.²⁴¹ The sum of the ionic radii (Pauling) of Ni²⁺ and O²⁻ is 2.09Å, so a distance of 2.069Å found in our case seems to be acceptable although the formal charge of nickel is +1, and dictates a longer ionic radii.

The tmen ligand is bidentate to each Ni atom, with an average Ni-N distance of 2.140(10)Å. Each Ni atom, therefore, has a distorted octahedral geometry with axial Cl-Ni-Cl angles averaging 163.0(2)°, which is less than the idealized 180°. As a result the three octahedra share faces thus:

face O, Cl(1), Cl(4) common between Ni(1) and Ni(2)

face O, Cl(3), Cl(4) common between Ni(2) and Ni(3)

face O, Cl(2), Cl(4) common between Ni(1) and Ni(3)

and all the three octahedra share the edge O-Cl(4). This edge is coincident with the direction of an approximate three fold symmetry. The anion is bisected by three planes

plane 1 Cl(1), O, Cl(4), Ni(3), N(21), N(22)

plane 2 Cl(3), O, Cl(4), Ni(1), N(1), N(2)

plane 3 Cl(2), O, Cl(4), Ni(2), Ni(11), N(12)

Since these planes include the 3 fold axis O-Cl(4) and the interplanar angles being ~ 60°, this anion has approximate C₃ symmetry.

The short C-C and C-N interatomic distances found in the tmen ligands (see Table 7.5) require some additional comment. Previous studies on the tmen complexes of copper ($[\text{Cu}(\text{tmen})\text{Cl}_2]_2$,²⁴² $[\text{Cu}(\text{tmen})\text{OH}]_2\text{Br}_2$,²⁴³ $\text{Cu}(\text{NO}_3)_2 \cdot \text{tmen}$,²⁴⁴ $\text{Cu}(\text{ClC}_2\text{H}_2\text{O}_2)_2 \cdot \text{tmen}$,²⁴⁵ and in the sodium complex $\text{NaC}_5\text{H}_5 \cdot \text{tmen}$ ²⁴⁶ have reported C-C and C-N distances in the range 1.43-1.51Å. These values, although commonly observed, are short, particularly when compared to the normal value of a C-C distance of 1.54Å. There have been attempts²⁴⁷ to rationalize the causes of the shortening effect encountered in ethylenediamine (and related ligands) complexes, and has been concluded that these ligands are somewhat flexible and responsive to the demands of the system in which they find themselves. The distances measured in this work are in the range 1.37-1.50Å in good agreement with values determined for the complexes $[\text{Cu}(\text{tmen})\text{SO}_4(\text{OH}_2)_2] \cdot \text{H}_2\text{O}$ ²⁴⁸ and $\text{In}_2\text{Br}_3 \cdot 1.2\text{tmen}$.³⁸ In these complexes the measured angles about the N-C-C-N ligand backbone were 114.5 and 116.8° and 117 and 120° respectively. These values are considerably larger than the angles in the other tmen complexes listed above, which are within $\pm 2^\circ$ of the normal tetrahedral value of 109.5°. In this case, the shortening of the C-C distance was attributed to the severe distortion imposed on the backbone of the ligand. In keeping with this, we also observe that the angles C-N-C (108°) and N-C-C (116°) are also considerably different than the normal tetrahedral value, and therefore, it seems possible that similar arguments apply here.

Finally, the cation In^{3+} is isolated with only long range contact to one of the chlorine atoms of the solvent of crystallization CHCl_3 with a distance of 3.800Å.

In conclusion, we would like to emphasize the fact that results presented in this chapter are intended to be a prelude to an interesting synthetic approach

to new indium containing complexes. One important point to note though, is that insertion reactions as we have demonstrated, take place easily when the substrate involved contains only one M-X bond. It is our hope that these results will make a significant contribution to the studies of the reactivities of low oxidation state metal halides in Main Group Elements.

REFERENCES

1. Carty, A.J., Tuck, D.G., *Prog. Inorg. Chem.*, 19, 243 (1975).
2. Tuck, D.G., *MTP International Rev. Sci., Inorg. Chem., Series 2, Vol. 1* (M.F. Lappert, Ed.), 311 (1975).
3. Tuck, D.G., *Comprehensive Organometallic Chemistry, Vol. 1, Chapter 7* (E. Abel, F.G.A. Stone and G. Wilkinson, Ed.), Pergamon (1982).
4. Ingham, R.K., Rosenberg, S.D., Gilman, H., *Chem. Rev.* 60, 459 (1960).
5. Thiel, A., Luckman, H., *Z. Anorg. Allgem. Chem.*, 172, 353 (1928).
6. Klemm, W., Vogel, H.U.V., *Z. Anorg. Allgem. Chem.*, 219, 45 (1934).
7. Thiel, A., *Z. Anorg. Allgem. Chem.*, 172, 353 (1928).
8. Nilson, L.F., Petersen, O., *Z. Phys. Chem.*, 2 657 (1888).
9. van der Berg, J.M., *Acta Cryst.*, 20, 905 (1966).
10. Stephenson, N.C., Mellor, D.P., *Aust. J. Sci. Res.*, A3, 581 (1950).
11. Jones, R.E., Templeton, D.H., *Acta Cryst.*, 8 847, (1955).
12. Fischer, E.O., Hofmann, H.P., *Angew Chem.* 69, 635 (1957).
13. Tuck, D.G., Pofand, J.S. *J. Organomet. Chem.* 42, 307 (1972).
14. Abel, E.W. *Comprehensive Inorganic Chem. Vol. 2* (J.C. Bailar, H.J. Emeleus, R. Nyholm and A.F. Trotman-Dickenson, Ed.), Pergamon (1973).
15. Hsu, C.C., Geangel, R.A. *Inorg. Chem.*, 16, 2529 (1977).
16. Harrison, P.G., Zuckerman, J.J., *J. Amer. Chem. Soc.*, 92, 2577 (1970).
17. Hsu, C.C., Geangel, R.A., *Inorg. Chim. Acta*, 34, 241 (1979).

18. Kochetkova, A.P., Tronev, V.G., Gilyarov, V.N. Dokl. Akad. Nauk, 147, 1086 (1962).
19. Goggin, P.L., McColm, I.J., J. Inorg. Nucl. Chem. 28, 2501 (1966).
20. Contreras, J.G., Tuck, D.G. Chem. Comm., 1552 (1971).
21. Contreras, J.G., Tuck, D.G. Inorg. Chem., 11, 2967 (1972).
22. Habeeb, J.J., Tuck, D.G. Chem. Comm. 600 (1975).
23. Habeeb, J.J., Tuck, D.G. J. Chem. Soc., Dalton Trans., 639 (1976).
24. Peppe, C., Tuck, D.G. Victoriano, L. J. Chem. Soc., Dalton Trans., 2165 (1982).
25. Contreras, J.G., Tuck, D.G., Inorg. Chem. 12, 2596 (1973).
26. Habeeb, J.J., Tuck, D.G., J. Chem. Soc., Dalton Trans., (1975) 1815.
27. Aitken, J.K., Haley, J.B., Terrey, H., Trans. Faraday Soc., 32, 1617 (1936).
28. Klemm, W., Z. Anorg. Allg. Chem., 152, 252 (1926).
29. Thiel, A. Z. Anorg. Allg. Chem., 40, 280 (1904).
30. Thiel, A., Koelsch, H., Z. Anorg. Allg. Chem., 66, 288 (1910).
31. Walker, P.H.L., Kleinberg, J. Griswold, E., J. Inorg. Nucl. Chem., 19, 223 (1961).
32. Peretti, E.H. J. Amer. Chem. Soc., 78 5745 (1956).
33. Hannebohn, O., Klemm, W. Z. Anorg. Chem., 229, 337 (1936).
34. Goggin, P.L., McColm, I.J. J. Less-Common Metals, 11, 292 (1966).
35. Habeeb, J.J., Tuck, D.G., J. Chem. Soc. Dalton Trans. 243 (1973).
36. Sinclair, I., Worrall, L.J., Can. J. Chem., 60, 695 (1982).

37. Taylor, M.J., Tuck, D.G., Victoriano, L., *Can. J. Chem.* 60, 691 (1982).
38. Khan, M.A., Peppe, C., Tuck, D.G., *Can. J. Chem.* 62, 701 (1984).
39. Kochetkova, A.P., Gilyarov, O.N., *Zh. Neorg. Khim.*, 11, 1239 (1966).
40. Beck, H.P., *Z. Naturforsch.*, 39b, 310 (1984).
41. Khan, M.A., Tuck, D.G. *Inorg. Chim. Acta*, 97, 73 (1985).
42. Greenwood, N.N., *Adv. Inorg. Radiochem.*, 5, 91 (1963).
43. Beck, H.P., unpublished results.
44. Contreras, J.G., Poland, J.S., Tuck, D.G. *J. Chem. Soc., Dalton Trans.*, 922 (1973).
45. Freeland, B.H., Hencher, J.L., Tuck, D.G., Contreras, J.G., *Inorg. Chem.*, 15, 214 (1976).
46. McGarvey, B.R., Trudell, C.O., Tuck, D.G., Victoriano, L., *Inorg. Chem.*, 19, 3432 (1980).
47. Peppe, C., Tuck, D.G., *Can. J. Chem.* 62, 2793 (1984).
48. Cotton, F.A., Wilkinson, W., *Advanced Inorganic Chemistry A Comprehensive Text, Fourth Edition.* Wiley-Interscience 1237 (1980).
49. Cotton, J.D., Davidson, P.J., Lappert, M.F., *J. Chem. Soc., Dalton Trans.* 2275 (1976).
50. Schröer, U., Albert, H.J., Neumann, W.P., *J. Organomet. Chem.* 102, 291 (1975).
51. Messin, G., Janier, Dubry, J.L., *Inorg. Nucl. Chem. Lett.* 15, 409 (1979).
52. Bos, K.D., Bulten, E.J., Noltes, J.G., *J. Organomet. Chem.* 99, 397 (1975).

53. Veith, M., Reckkenwald, O., Humpfer, E., Z. Naturforsch. 33b, 14 (1978).
54. Cornwell, A.B., Harrison, P.G., Richards, J.A., J. Organomet. Chem. 108, 47 (1976).
55. Cornwell, A.B., Harrison, P.G., J. Chem. Soc. Dalton Trans 1608 (1976).
56. Cole, B.J., Cotton, J.D., McWilliam, D., J. Organomet. Chem. 64, 223 (1974).
57. Cornwell, A.B., Harrison, P.G. J. Chem. Soc. Dalton Trans 2017 (1975).
58. Harris, D.H., Lappert, M.F., Chem. Comm. 895 (1974).
59. Albert, H.J., Schröer, U., J. Organomet. Chem. 60, 16 (1973).
60. Bos, K.D., Bulten, E.J., Noltes, J.G., J. Organomet. Chem., 99, 397 (1975).
61. Gynane, M.J.S., Miles, S.J., Power, P.P., Chem. Comm. 256 (1976).
62. Gynane, M.J.S., Miles, S.J., Power, P.P., Carty, A.J., Taylor, N.J., J. Chem. Soc. Dalton Trans., 2009 (1977).
63. Gynane, M.J.S., Miles, S.J., Power, P.P., Chem. Comm. 192 (1978).
64. Glockling, F., McGregor, A., Schneider, M.L., Shearer, H.M.M., J. Inorg. Nucl. Chem., 32, 3101 (1970).
65. McArdle, P.A., Manning, A.R., J. Chem. Soc., D, 417 (1967).
66. Mason, R., Whimp, P.O., J. Chem. Soc. (A), 2709 (1969).
67. Olmstead, M.M., Benner, L.S., Hope, H., Balch, A.L., Inorg. Chim. Acta, 32, 193 (1979).
68. von Werner, K., Blank, H., Yasufuku, K., J. Organomet. Chem. 165, 187 (1979).
69. Waterworth, L.G., Worrall, I.J., Chem., Comm., 569 (1971).

70. Gynane, M.J.S., Worrall, I.J., *Inorg. Nucl. Chem. Lett.*, 8, 547 (1972).
71. Gynane, M.J.S., Waterworth, L.G., Worrall, I.J., *J. Organomet. Chem.*, 43, 257 (1972).
72. Waterworth, L.G., Worrall, I.J., *J. Organomet. Chem.*, 81, 23 (1974).
73. Poland, J.S., Tuck, D.G., *J. Organomet. Chem.* 42, 315 (1972).
74. Berniaz, A.F., Hunter, G., Tuck, D.G., *J. Chem. Soc. (A)* 3254 (1971).
75. Berniaz, A.F., Tuck, D.G., *J. Organomet. Chem.*, 51, 113 (1973).
76. Peppe, C., Tuck, D.G. *Can. J. Chem.*, 62, 2798 (1984).
77. Khan, M.A., Peppe, C., Tuck, D.G. *Acta Cryst.*, C39, 1339 (1983).
78. Patmore, D.J., Graham, W.A.G., *Chem. Comm.*, 591 (1965).
79. Patmore, D.J., Graham, W.A.G., *Inorg. Chem.*, 5, 1586 (1966).
80. Hoyano, J., Patmore, D.J., Graham, W.A.G., *Inorg. Nucl. Chem. Lett.*, 4, 201 (1968).
81. Hsieh, A.T.T., Mays, M.J., *Inorg. Nucl. Chem. Lett.*, 7, 223 (1971).
82. Leibenzeder, S. DBP 1141451, Dec. 20, 1962.
83. Carty, A.J., Tuck, D.G., *J. Chem. Soc., A*, 1081 (1966).
84. Freeland, B.H., Tuck, D.G., *Inorg. Chem.*, 15, 475 (1976).
85. Contreras, J.G., Ph.D. Thesis, Simon Fraser University (1974).
86. *International Tables for X-ray Crystallography*, J.A. Ibers, W.C. Hamilton, Eds., Kynoch Press, Birmingham, England, Vol. IV (1974).
87. Lewis, J., Nyholm, R.S. *Sci. Prog.*, 52, 447 (1964).


88. Vahrenkamp, H., *Angew. Chem., Int. Ed. Engl.*, 17, 379 (1978).
89. Baird, M.C., *Prog. Inorg. Chem.*, 9, 1 (1968).
90. Cotton, J.D. *Organometallic Chemistry*, ed. F.G.A. Stone and E.W. Abel, Chemical Society London Vol. 1-8 (1972-79).
91. Vyazankin, N.S., Razuvaev, G.A., Kruglaya, O.A., *Organomet. Chem. Rev. (A)*, 3, 323 (1968).
92. Gladfelter, W.L., Geoffroy, G.L., *Adv. Organomet. Chem.*, 18, 207 (1980).
93. Taylor, M.J. *Metal-to-Metal Bonded States of the Main Group Elements*. Academic Press (1975).
94. Muettterties, E.L., *Bull. Soc. Chim. Belg.*, 85, 451 (1976).
95. Smith, A.K., Basset, J.M., *J. Mol. Catal.*, 2, 229 (1979).
96. Pittman, Jr., C.U., Ryan, R.C., *Chemtech.*, 170 (1978).
97. Muettterties, E.L., *Bull. Soc. Chim. Belg.*, 84, 959 (1975).
98. Robinson, A.L., *Science*, 194, 1150 (1976).
99. Muettterties, E.L., Rhodin, T.H., Band, E., Brucker, C.F., Pretzer, W.R., *Chem. Rev.*, 79, 91 (1979).
100. Bailar, J.C., Tayim, H.A. *J. Amer. Chem. Soc.*, 77 2671 (1967).
101. Frankel, E.N., Emken, E.A., Itatani, H., Bailar, J.C. *J. Org. Chem.*, 32 1447 (1967).
102. Pietropaolo, R., Dolcetti, G., Giustiniani, M., Belluco, U., *Inorg. Chem.*, 9, 549 (1970).

103. Ugo, R., Cenini, S., Bonati, F., *Inorg. Chim. Acta* 1, 451 (1967).
104. Clark, H.C., Cotton, J.D., Tsai, J.H., *Inorg. Chem.*, 5, 1407 (1966).
105. Clark, H.C., Cotton, J.D., Tsai, J.H., *Inorg. Chem.*, 5, 1582 (1966).
106. Brooks, E.H., Glockling, F., *J. Chem. Soc., A*, 1241 (1966).
107. Shaw, C.F., Alfred, A.L., *Inorg. Chem.* 10, 1340 (1971).
108. Weibel, A.T., Oliver, J.P., *J. Amer. Chem. Soc.*, 94, 8590 (1972).
109. Peppe, C. Ph.D. Dissertation, University of Windsor, 1983.
110. Grimes, R.N., Rademaker, W.J., *J. Amer. Chem. Soc.*, 91, 6498 (1970).
111. Schmid, G. *Angew Chem., Int. Ed.* 9, 819 (1970).
112. Gilbert, K.G., Boocock, S.K., Shore, S.G. *Comprehensive Organometallic Chemistry*, Vol. 6, Chapter 41.1 E.W. Abel, F.G.A. Stone and G. Wilkinson, Ed.) Pergamon 1982.
113. Schmid, G., Nöth, H., *Z. Naturforsch. B*, 20 1008 (1965).
114. Nöth, H., Schmid, G., *J. Organomet. Chem.*, 5, 109 (1966).
115. Nöth, H., Hermannsdorfer, K.H., *Angew Chem., Int. Ed.* 3, 377 (1964).
116. Schmid, G., Petz, W., Arloth, W., Nöth, H., *Angew, Chem., Int. Ed.* 6, 696 (1967).
117. Carfy, A.J., Tuck, D.G. *J. Chem. Soc., A*, 1081 (1966).
118. Lin, C.S., Tuck, D.G., *Can. J. Chem.* 60, 699 (1982).
119. van der Kelen, G.P., van den Berghe, E.P., Verdonck, L. in A.S. Sawyer (Ed.) *Organotin Compounds*, Marcel Dekker, New York, 1971, Vol. 1, p. 118.
120. Poller, R.C. *Spectrochim. Acta*, 22, 935 (1966).

121. Drake, J.E., Hancher, J.L., Khasrou, L.N., Tuck, D.G., Victoriano, L., Inorg. Chem., 19, 34 (1980).
122. Einstein, F.W.B., Gilbert, M.M., Tuck, D.G., J. Chem. Soc., Dalton Trans., 248 (1973).
123. Cundy, C.S., Nöth, H., J. Organomet. Chem., 30, 135 (1970).
124. Burnham, R.A., Glockling, F., Stobart, S.R. J. Chem. Soc., Dalton Trans., 1991 (1972).
125. Evans, M.G., Trans. Faraday Soc., 42, 113 (1946).
126. Berliner, E., J. Amer. Chem. Soc., 68, 49 (1946).
127. Crowley, P.J., Haendler, H.M., Inorg. Chem., 1, 904 (1962).
128. Balch, A.L., J. Amer. Chem. Soc., 95, 2723 (1973).
129. Pierpont, C.G., Downs, H.H., Inorg. Chem., 14, 343 (1975).
130. Valentine, J.S., Valentine, Jr., D., J. Amer. Chem. Soc. 14, 343 (1975).
131. Sohn, Y.S., Balch, A.L., J. Amer. Chem. Soc., 93, 1290 (1971).
132. Cenini, S., Ugo, R., La Monica, G., J. Chem. Soc. A, 416 (1971).
133. La Monica, G., Navazio, G., Sandrini, P., Cenini, S., J. Organomet. Chem., 31, 89 (1972).
134. Barlex, D.M., Kemmitt, R.D.W., Littlecott, G.W., J. Organomet. Chem., 43, 225 (1972).
135. Sohn, Y.S., Balch, A.L., J. Amer. Chem. Soc., 94, 1144 (1972).
136. Balch, A.L., Sohn, Y.S., J. Organomet. Chem., 30, C31 (1971).

137. Rouschias, G., Wilkinson, G., J. Chem. Soc. A, 993 (1967).
138. Floriani, C., Fachinetti, G., Chem. Commun., 790 (1972).
139. Pierpont, C.G., Buchanan, R.M. Coord. Chem. Rev. 38, 45 (1981).
140. Razuvaev, G.A., Abakumov, G.A., Klimov, E.S., Dok. Akad. Nauk, SSSR 201, 624 (1971).
141. Razuvaev, G.A., Klimov, E.S., Dokl. Akad. Nauk, SSSR, 202, 827 (1972).
142. Abakumov, G.A., Gladyshev, N.S., Vyazankin, N.S.,
143. Razuvaev, G.A., Bayushkin, P. Ya., Muraev, V.A., J. Org. Chem., 64 327 (1974).
144. Shal'nova, K.G., Rachkova, O.F., Teplova, I.A., Razuvaev, G.A., Abakumov, G.A., Izv. Akad. Nauk SSSR, 2422 (1978).
145. Butters, Th., Scheffler, K., Stegmann, H.B., Weber, U., Winter, W., J. Organomet. Chem., 272, 351 (1984).
146. Dove, M.F.A., Hallett, J.G., J. Chem. Soc., A, 1204 (1969).
147. Knuutinen, J., Laatikainen, R., Paasivirta, J. Org. Magn. Resonance 14, 5 (1980).
148. Birchall, T., Johnson, J.P., J. Chem. Soc., Dalton Trans. 69 (1981).
149. Alcock, N.W., Tracy, V.L., Acta Cryst. B35, 80 (1979).
150. Ewings, P.F.R., Harrison, P.G., Morris, A., King, T.J. J. Chem. Soc., Dalton Trans., 1602 (1976).
151. Thompson, J.S., Calabrese, J.C., J. Amer. Chem. Soc., 108, 1902 (1986).
152. Pierpont, C.G., Downs, H.H., Inorg. Chem., 14 343 (1975).

153. Mochida, K., Kochi, J.K., Chen, K.S., Wan, J.K.S., J. Amer. Chem. Soc., 100, 2927 (1978).
154. Stegmann, H.B., Uber, W., Scheffler, K., Tetrahedron Letts., 31, 269(1977).
155. Davies, A. G., Hawari, J. A-A., J. Organomet. Chem., 251, 53 (1983).
156. Drago, R.S., Physical Methods In Chemistry (Saunders Golden Sunburst Series) Chapter 9 (1977).
157. Wertz, J.E., Bolton, J.R., ESR: Elementary Theory and Practical Applications (McGraw-Hill Inc.) (1972).
158. Gilbert, B.C., Essays In Chemistry (Ed. Bradley, J.N., Gillard, R.D., Hudson, R.F.) Academic Press, Vol. 4, page 61 (1972).
159. Castellano, S., Gunther, H., Ebersole, S., J. Phys. Chem., 69, 4166 (1965).
160. Dove, M.F.A., Hallet, J.G., J. Chem. Soc., A, 1204 (1969).
161. Morton, J.R., Preston, K.F.J., J. Magnet. Resonance, 30, 577 (1978).
162. Abragams, A., Bleaney, B., Electron Paramagnetic Resonance of Transition Metal Ions, Clarendon Press, Oxford, page 508 (1970).
163. Prokof'ev, A.I., Prokof'eva, T.I., Bubnov, N.N., Solodnikov, S.P., Belostotskaya, I.S., Ershov, V.V., Kabachnik, M.I., Dokl. Akad. Nauk. SSSR, 245, 1393 (1979).
164. Hudson, A., Lappert, M.F., Lednar, P.W., J. Chem. Soc., Dalton Trans., 2369 (1976).
165. Gynane, M.J.S., Harris, D.H., Lappert, M.F., Power, P.P., Riviere-Baudet, P., J. Chem. Soc. Dalton Trans., 272, 351 (1984).
166. Preupt, H., Haupt H.J., Huber, F., Z. Anorg. Allg. Chem., 396, 81 (1973).

167. Butters, T., Scheffler, K., Stegmann, H.B., weber, U., Winter, W., J. Orgnomet. Chem., 272, 351 (1984).
 168. Bokii, N.G., Zhakarova, G.N., Strutchkov, Yu.T., J. Struct. Chem. (Engl. Trans.), 11, 828 (1970).
 169. Lloyd, R.V., Rogers, M.T., J. Amer. Chem. Soc., 95, 2459 (1973).
 170. Rohrscheid, F., Balch, A.L., Holm, R.H., Inorg. Chem., 5, 9 (1966).
 171. Ryba, O., Pilar, J., Petranek, J., Coll. Czech. Chem Comm., 33, 26 (1968).
 172. Harrison, P.G., King, T.J., Richards, J.A., J. Chem. Soc., Dalton Trans., 1723, (1974).
 173. Sawyer, A.K., Organotin Compounds (Ed. Sawyer, A.K.), Marcell Dekker, New York, Vol. 3 (1972).
 174. Hencher, J.L., Khan, M.A., Said, F.F., Sieler, R., Tuck, D.G., Inorg. Chem., 21, 2787 (1982).
 175. Morgan, G.T., Drew, H.D.K., J. Chem. Soc., 119, 1058 (1921).
 176. Habeeb, J.J., Tuck, D.G., Inorg. Synth., 19, 257 (1979).
 177. Gribov, L.A., Zolotov, Yu.A., Noskova, N.P., Zh. Strukt. Khim., 9, 448 (1969).
 178. Noskova, M.P., Gribov, L.A., Zolotov, Yu.A., Zh. Strukt. Khim., 10, 474 (1969).
 179. Hester, R.E., Plane, R.A., Inorg. Chem., 3, 63 (1964).
 180. Holm, R.H., Cotton, F.A., J. Amer. Chem. Soc., 80, 5658 (1958).
 181. Smith, J.A.S., Thwaites, J.D., Disc. Faraday Soc., 34, 143 (1962).
 182. Carty, A.J., Tuck, D.G., Bullock, E., Can. J. Chem., 43, 2559 (1965).
- 

183. Smith, J.A.S., Wilkins, E.J., J. Chem. Soc., A, 1749 (1966).
184. Rodriguez, J.G., Cano, F.H., Garcia-Blanco, S., Cryst. Struct. Commun., 8 53 (1979).
185. Tuck, D.G., Pure Appl. Chem., 55, 1477 (1983).
186. Tuck, D.G., Yang, M.K., J. Chem. Soc., A, 3100 (1971).
187. Einstein, F.W.B., Hunter, G., Yang, M.K., Tuck, D.G., Chem. Comm., 423 (1968).
188. Einstein, F.W.B., Jones, R., Tuck, D.G., J. Chem. Soc., A, 3100 (1971).
189. Bevillard, P., Compt. Rend., 240, 1776 (1955).
190. Srivastava, T.N., Mohan, G., Z. Anorg. Allg. Chem., 379, 82 (1970).
191. Khan, M.A., Peppe, C., Tuck, D.G., J. Organomet. Chem., 280, 17 (1985).
192. Steevensz, R.S., Tuck, D.G., Meneima, H.A., Noltes, J.G., Can. J. Chem., 63, 755 (1985).
193. Khan, M.A., Steevensz, R.A., Tuck, D.G., Noltes, J.G., Corfield, P.W.R., Inorg. Chem., 19, 3407 (1980).
194. Harrowfield, J.McB., Pakawatchai, C., White, A.H., J. Chem. Soc., Dalton Trans., 1109 (1983).
195. Johnson, B.F.G., Walton, R.A., Inorg. Chem. 5, 49 (1966).
196. Patel, S.J., Sowerby, D.B., Tuck, D.G., J. Chem. Soc., A, 1187 (1967).
197. Nagakura, S., Kuboyama, A., J. Amer. Chem. Soc., 76, 1003 (1954).
198. Gynana, M.J.S., Worrall, L.J., J. Organomet. Chem., 81, 329 (1974).
199. Chao, L-C, Riecke, R.D., J. Organomet. Chem., 67, C64 (1974).

200. Mabrouk, H.E., Kumar, R.K., Tuck, D.G., J. Chem. Soc., Dalton Trans. (in press).
201. Cass, M.E., Gordon, N.R., Pierpont, C.G., Inorg. Chem., 25, 3962 (1986).
202. Wicklund, P.A., Brown, D.G., Inorg. Chem., 15, 396 (1976).
203. Carty, A.J., Tuck, D.G., J. Chem. Soc. A, 1081 (1966).
204. Walton, R.A., J. Chem. Soc., A, 61 (1969).
205. Contreras, J.G., Tuck, D.G., J. Chem. Soc., Dalton Trans., 1249 (1974).
206. Adams, D.M., Carty, A.J., Carty, P., Tuck, D.G., J. Chem. Soc., A, 162 (1968).
207. Greenwood, N.N., Prince, D.J., Straughan, J., J. Chem. Soc., A, 1694 (1968).
208. Nakamoto, K., Udovich, C., Takemoto, J., J. Amer. Chem. Soc., 92, 3973 (1970).
209. Evans, C.A., Taylor, M.J., J. Chem. Soc., A, 214 (1971).
210. Said, F.F., Tuck, D.G., Inorg. Chim. Acta., 59, 1 (1982).
211. Berry, R.S., J. Chem. Phys., 32, 933 (1960).
212. Felix, C.C., Sealy, R.C., J. Amer. Chem. Soc., 104, 1555 (1982).
213. Wicklund, P.A., Beckmann, L.S., Brown, D.G., Inorg. Chem., 15, 1996 (1976).
214. Sofen, S.R., Ware, D.C., Cooper, S.R., Raymond, K.N., Inorg. Chem., 18, 234 (1979).
215. Khan, M.A., Peppe, C., Tuck, D.G. Acta Cryst., C39, 1339, (1983).
216. Contreras, J.G., Einstein, F.W.B., Tuck, D.G., Can. J. Chem. 52, 3793 (1974).
217. Khan, M.A., Tuck, D.G., Acta Cryst., B37, 683 (1981).
218. Stevenson, D.P., Schomaker, V., J. Amer. Chem. Soc. 64, 2514 (1942).
219. Clark, G.R., Rickard, C.E.F., Taylor, M.J., Can. J. Chem., 64, 697 (1986).

220. Wignacourt, J.P., Lorriaux-Rubbens, A., Mairesse, G., Barbier, P., Wallart, F., *Spectrochim. Acta*, 36A, 403 (1980).
221. Lynch, M.W., Buchanan, R.M., Pierpont, C.G., Hendrickson, D.N., *Inorg. Chem.*
222. Buchanan, R.M., Kessel, S.C., Downs, H.H., Pierpont, C.G., Hendrickson, D.N., *J. Amer. Chem. Soc.*, 100, 7894 (1978).
223. Venanzi, L.M., *J. Chem. Soc.*, 719 (1958).
224. *Handbook of Chemistry and Physics*, 53rd Edition, CRC Press (1973).
225. Cárty, A.J., Boorman, P.M., *Inorg. Nucl.-Chem. Lett.*, 4, 101 (1968).
226. Cotton, F.A., Wilkinson, G., *Basic Inorganic Chemistry*, (John Wiley and Sons Inc.) (1976).
227. Pearson, R.G., *Chemistry in Britain*, 3, 103 (1967).
228. Pearson, R.G., *J. Amer. Chem. Soc.*, 85, 3533 (1963).
229. Kettle, S.F.A., *Topics in Current Chemistry* (Eds. Dewar, M.J.S., Hafner, K., Heilbronner, E., Ito, S., Lehn, J-M., Niedenzu, K., Schafer, K., Wittig, G.) No. 71, page 111, 1977.
230. Camia, M., Lachi, M.P., Benzoni, L., Zanzottara, C., Venturi, M.T., *Inorg. Chem.*, 9, 251 (1970).
231. Porta, P., Powell, H.M., Mawby, R.J., Venanzi, L.M., *J. Chem. Soc.*, A, 455 (1967).
232. Miller, S.B., Jelus, B.L., Brill, T.B., *J. Organomet. Chem.*, 96, 1 (1975).
233. Isley, W.H., Sadurski, E.A., Schaaf, T.F., Albright, M.J., Anderson, T.J., Glick, M.D., Oliver, J.P., *J. Organomet. Chem.*, 190, 257 (1980).
234. Bochkárev, M.N., Maiorova, L.P., Vyazankin, N.S., *J. Organomet. Chem.*, 55, 89, (1973).

235. Reutov, O.A., Bashilov, V.V., Sokolov, V.L., Makarenko, N.P., Maiorova, L.P., Razuvaev, G.A., Bochkarev, M.N., *J. Organomet. Chem.*, 131, 399 (1977).
236. Eaborn, C., Thompson, A.R., Walton, D.R.M., *Chem. Commun.*, 1051 (1968).
237. Cotton, F.A., Felthouse, T.R., Lay, D.G., *Inorg. Chem.*, 20, 2219 (1981).
238. Bino, A., Cotton, F.A., Dovi, Z. *Inorg. Chim. Acta*, 33, L133 (1979).
239. Posey, R.G., Khare, G.P., Frisch, P.D., *J. Amer. Chem. Soc.*, 99, 4863 (1977).
240. Jolly, P.W., *Comprehensive Organometallic Chemistry*, Vol. 6, Chapter 37.4, (Ed. Abel, E., Stone, F.G.A., Wilkinson, G.) Pergamon (1982).
241. Mealli, C., Peruzzini, M., Stoppioni, P., *J. Organomet. Chem.*, 192, 437, (1980).
242. Estes, E.D., Estes, W.E., Hatfield, W.E., Hodgson, D.J., *Inorg. Chem.*, 14, 106 (1975).
243. Mitchell, T.P., Bernard, W.H., Wasson, J.R., *Acta Cryst.*, B26, 2096 (1970).
244. Pavkovic, S.F., Miller, D., Brown, J.N., *Acta Cryst.*, B33, 2894 (1977).
245. Ahlgren, M., Hamalai, R., Turpeinen, U., *Acta Chem. Scand.*, A32, 57 (1978).
246. Aoyagi, T., Shearer, M.M., Wade, K., Whitehead, G., *J. Organomet. Chem.*, 175, 21 (1979).
247. Maslen, H.S., Waters, T.N., *Coord. Chem. Rev.*, 17, 137 (1975).
248. Balvich, J.N., Fivizzani, K.P., Pavkovic, S.F., Brown, J.N., *Inorg. Chem.*, 15, 71 (1976).

VITA AUCTORIS

THEODORE JAMES ALLOTEY ANNAH

Birth:

November 2, 1953
Accra, Ghana

Education:

1976-1983 Degree of Master of Science (With Honours)
Patrice Lumumba Peoples' Friendship University
Moscow, USSR

Teacher's Certificate
Translators Certificates - Russian/English

1983-1988 Degree of Doctor of Philosophy
University of Windsor
Windsor, Canada

Awards and Scholarships:

1986/87 and

1984/85 Redmond Memorial Bursary
University of Windsor
Windsor, Canada

1983-Present Natural Sciences and Engineering Research Council (through
Research Grant to Professor D.G. Tuck)

1983 Second place prize for competition on M.Sc. Thesis work

1982/1983 Rector's Honour Roll
Lumumba University
Moscow, USSR

1976-1983 Ghana Government Scholarship tenable at the Friendship
University, Moscow, USSR

Publications:

1. The insertion of indium(I) halides into the M-X bond of some Main Group Organometallic Halides, *J. Organomet. Chem.* **325**, 83 (1987).
2. The oxidation of stannous halides by tetra-halogeno-orthoquinones, and the crystal structure of Bis[2-dimethylamino)ethyl(dimethylammonium) tris(tetrachlorocatecholato)tin(IV), $(Me_2NC_2H_4NHMe_2)XSn(O_2C_6Cl_4)_3$, *Can. J. Chem.* **65**, 2670 (1987).

3. The direct electrochemical synthesis of metal-diphenylphosphido complexes, and the crystal structure of $\text{Cu}_4(\mu\text{-PPh}_2)_4(\text{dppm})_2$. Chem. Commun. (accepted for publication).
4. One-electron transfer processes in the reaction of stannous halides with substituted orthoquinones. J. Chem. Soc., Dalton Trans. (ready for submission).

Talks/Posters Presented to Professional Societies:

1. The insertion of indium(I) halides into the M-X bond of some Main Group organometallic halides. XVII Inorg. Discussion Weekend, University of Guelph, Guelph, Ontario (1984).
2. Oxidative addition reactions of indium(I) and tin(II) halides with orthoquinones. XIX Inorg. Discussion Weekend, McMaster University, Hamilton, Ontario (1986).
3. The direct electrochemical synthesis of metal-diphenylphosphido complexes and the crystal structure of $\text{Cu}_4(\mu\text{-PPh}_2)_4(\text{dppm})_2$. XX Inorg. Discussion Weekend, University of Windsor, Windsor, Ontario (1987).
4. Spectroscopic and Structural Studies of One-electron transfer in the reaction of indium(I) halides with 3,5-di-t-butyl 1,2-benzoquinone. XX Inorg. Discussion Weekend, University of Windsor, Windsor, Ontario (1987).